HIGH-LEVEL AB INITIO STUDIES OF AMINO ACID CONFORMATIONS, ROTAMERIZATIONS, AND TUNNELING DYNAMICS – THE INTRICATE BALANCE OF INTRAMOLECULAR FORCES

by

KEDAN HE

(Under the Direction of Wesley D. Allen)

ABSTRACT

The effects of intramolecular forces on molecular geometries, energies, and dynamics are presented for various molecular prototypes. High-accuracy relative energies of glycine and serine conformers and barriers for their conformational interconversions are computed via focal point analyses. Quantum tunneling is investigated within a reaction-path Hamiltonian model with transmission probabilities given by standard methods. The half-lives of the multiple interconversions among the eight glycine conformers show that conformer **IVn** has escaped detection due to fast rotational tunneling to the global minimum **Ip**. The complex conformational space of serine is investigated, and the relationship between intramolecular hydrogen bonds and conformational structures is examined. A total of 85 conformers of serine are located through an exhaustive conformational search with delicately balanced levels of theories. A general categorizing scheme based on the interactions between the amine and carboxylic acid groups is proposed. Finally, we show how the Coulomb operator within two-electron integrals can be split into long- and short-range pieces to unravel the correlation energy dependence on the electron-electron interaction distance within rigorous wave functions. This analysis seeks to place intra- and intermolecular dispersion on an equal footing and challenges common understandings of these phenomena.

INDEX WORDS: Amino acids conformational search, Isomerization Tunneling, Intramolecular Dispersion, Truncated Coulomb Integral

HIGH-LEVEL AB INITIO STUDIES OF AMINO ACID CONFORMATIONS, ROTAMERIZATIONS, AND TUNNELING DYNAMICS – THE INTRICATE BALANCE OF INTRAMOLECULAR FORCES

by

KEDAN HE

BA, Hainan University, China, May 2007

MS, University of Alabama in Huntsville, July 2009

A Dissertation Submitted to the Graduate Faculty of The University of Georgia in Partial Fulfillment of the Requirements for the Degree

DOCTOR OF PHILOSOPHY

ATHENS, GEORGIA

2015

© 2015

Kedan He

All Rights Reserved

HIGH-LEVEL AB INITIO STUDIES OF AMINO ACID CONFORMATIONS, ROTAMERIZATIONS, AND TUNNELING DYNAMICS – THE INTRICATE BALANCE OF INTRAMOLECULAR FORCES

by

KEDAN HE

Major Professor:	Wesley D. Allen
Committee:	Henry F. Schaefer
	Michael Duncan

Electronic Version Approved:

Julie Coffield
Interim Dean of the Graduate School
The University of Georgia
May 2015

DEDICATION

For my parents who have always trusted in me.

ACKNOWLEDGEMENTS

The journey towards completing my PhD program is not lonely, many individuals and organizations have lent their helping hands to me. First and foremost, I'd like to express my gratitude to Prof. Wesley D. Allen, my advisor who gave me this precious opportunity to join his research group. I also thank my committee members Prof. Henry F. Schaefer, Michael Duncan and other faculty members for their academic and moral support at the Chemistry Department of University and the Center for Computational Quantum Chemistry (CCQC). Likewise, I very much appreciate the friendship and understanding extended to me by the colleagues of my research group, CCQC, and the whole Chemistry Department. Finally, I would like to thank my parents and family, whose unfailing encouragement and support has always been deeply appreciated.

TABLE OF CONTENTS

Page

ACKNOWLEDGEMENTS……V

CHAPTER

1 THEORETICAL BACKGROUND……...……1

1.1 Computational Methods……...2

1.2 Weak Molecular Interactions…….....16

1.3 Dispersion Corrected Density Functional Theory…….....22

2 GLYCINE ISOMERIZATION VIA QUANTUM TUNNELING……...33

2.1 Introduction……...36

2.2 Computational Methods……...….41

2.3 Results and Discussion……..……43

2.4 Conclusion…….58

3 SYSTEMATIC SEARCH AND ANALYSIS OF THE CONFORMERS OF SERINE …….....33

3.1 Introduction……...64

3.2 Computational Methods……70

3.3 Results and Discussion……..75

3.4 Conclusion……...103

4 TRUNCATED COULOMB ANALYSIS……...109

4.1 Introduction……..111

4.2 Computational Methods……...116

4.3 Results and Discussion……120

4.4 Conclusion……...132

APPENDICES

A Supporting Information for Chapter 2……...135

B Supporting Information for Chapter 3……...154

C Supporting Information for Chapter 4……...205

CHAPTER 1

THEORETICAL BACKGROUND

1.1 Computational Methods

Ab initio quantum chemistry computations are based on the use of the 'first principles' Schrödinger equation and the fundamental physical constants. They employ the true molecular Hamiltonian, which accounts for all the interactions within the molecular system.

1.1.1 Self-Consistent Field Hartree-Fock (SCF-HF) Method

The time-dependent Schrödinger equation has the form

$$i\hbar\frac{\partial}{\partial t}\Psi = \hat{H}\Psi, \tag{1.1}$$

where Ψ is the wave function that describes the "state" of the system. The Hamiltonian operator $\hat{H}$ acts on the wave function to determine the energy of any given state.

Since the mass of any nucleus is much larger than that of the electron, the nuclei are assumed to be stationary relative to electronic motions, as embodied in the Born-Oppenheimer (BO) approximation.[1] The molecular wave function can be multiplicatively separated into electronic and nuclear components ($\Psi_{total} = \Psi_{el}\Psi_N$). The purely electronic nonrelativistic Hamiltonian in atomic units for a polyatomic molecule is presented in the form

$$\hat{H}_{el} = -\frac{1}{2}\sum_i \nabla_i^2 - \sum_i\sum_a \frac{Z_a}{r_{ia}} + \sum_i\sum_{i\geq j}\frac{1}{r_{ij}} + \sum_{a>b}\frac{Z_a Z_b}{r_{ab}}, \tag{1.2}$$

The first term is the kinetic energy operator of the electrons. The second and third term is the potential energy operator for electron-nuclear attraction and electron-electron repulsion. The fourth term is the nuclear-nuclear repulsion operator.

It can be shown[2] that if the interelectronic repulsions are treated as an average effect in HF approximation, the zeroth-order wave function is the product of one-electron spatial

function.[3] The one-electron spatial functions are referred to as molecular orbitals. Taking into account the electron spin and the Pauli exclusion principle leads to the zeroth-order wave function, which is the antisymmetrized slater determinant of molecular-spin orbitals, each molecular-spin orbital being a product of a spatial molecular orbital (MO) and a spin function. The Hartree-Fock self-consistent field (HF SCF)[4] wave function is the best variational trial function that has the form of a single antisymmetrized product of spin-orbitals. It is convenient for the MOs to be expressed as a linear combination of atomic basis functions. If the set of the basis functions is large enough, then the LCAO molecular orbitals are an accurate approximation to the exact HF MOs.

For a single electron, the average electron-electron repulsion can be expressed in terms of the Coulomb operator $\hat{J}$ and the exchange operator $\hat{K}$. If another electron occupies molecular orbital ϕ_j, the effects of these operators on an electron in orbital ϕ_i are

$$\hat{J}_j\left|\,\phi_i(1)\right\rangle = \left\langle\phi_j(2)\left|r_{12}^{-1}\right|\phi_j(2)\right\rangle\left|\phi_i(1)\right\rangle, \tag{1.3}$$

called the *Coulomb term*, which gives the average local potential at point 1 due to the charge distribution from the electron in orbital ϕ_j, and the *exchange term*

$$\hat{K}_j\left|\,\phi_i(1)\right\rangle = \left\langle\phi_j(2)\left|r_{12}^{-1}\right|\phi_i(2)\right\rangle\left|\phi_j(1)\right\rangle, \tag{1.4}$$

which arises from the antisymmetry requirement of the total wavefunction.

In terms of these Coulomb and exchange operators, the Hartree-Fock equations are compact. If we introduce the *Fock operator*, as

$$\hat{F} = \hat{H}^{core} + \sum_{j}^{occ}(\hat{J}_j - \hat{K}_j), \tag{1.5}$$

where

$$\hat{H}^{core} = -\frac{1}{2}\sum_i \nabla_i^2 - \sum_i \sum_a \frac{Z_a}{r_{ia}}, \tag{1.6}$$

then the Hartree-Fock equations are just

$$\hat{F}\phi_j = \varepsilon_j \phi_j. \tag{1.7}$$

1.1.2 Coupled-Cluster Theory and Electron Correlation

It is widely accepted that the coupled cluster ansatz, first introduced to electronic structure by Čížek and Paldus[5-6] is the best means for highly accurate treatments of electron correlation.

In coupled cluster theory, the final wave function is parameterized by an exponential operator as

$$|\Psi\rangle = e^{\hat{T}}|\Phi_0\rangle, \tag{1.8a}$$

where $\hat{T}$ is an excitation operator which, when acting on the reference function $|\Phi\rangle$, produces a linear combination of excited determinants that is commonly a solution to the Hartree-Fock equations.[7] The singly and doubly excited determinants Φ_i^a and Φ_{ij}^{ab} are produced when $\hat{T}_1$ and $\hat{T}_2$ act on Φ_0, respectively.[7]

$$\hat{T}_1\Phi_0 = \sum_i^{occ}\sum_a^{vir} t_i^a \, \Phi_i^a, \tag{1.8b}$$

$$\hat{T}_2\Phi_0 = \sum_{i<j}^{occ}\sum_{a<b}^{vir} t_{ij}^{ab} \, \Phi_{ij}^{ab}, \tag{1.8c}$$

Having defined the functional form of the wavefunction, we need to specify $\hat{T}$. In coupled cluster with single and double excitations (CCSD), we define

$$\hat{T} = \hat{T}_1 + \hat{T}_2, \tag{1.9}$$

and all single excitations from the reference determinant are effected by $\hat{T}_1$, with double excitations introduced through the $\hat{T}_2$ operator. The commutative nature of the individual excitation operators allows us to employ the power series expansion of the exponential operator. Thus we can write the CCSD wavefunction as

$$e^{\hat{T}_1+\hat{T}_2}\,|\Phi\rangle = \left(1 + \hat{T}_1 + \hat{T}_2 + \frac{\left(\hat{T}_1 + \hat{T}_2\right)^2}{2!} + \frac{\left(\hat{T}_1 + \hat{T}_2\right)^3}{3!} + \cdots\right)|\Phi\rangle. \qquad (1.10)$$

Terms such as ${\hat{T}_1}^3$ and $\hat{T}_2\hat{T}_1$ correspond to triple excitations; likewise, the ${\hat{T}_2}^2$, ${\hat{T}_1}^4$ and $\hat{T}_2{\hat{T}_1}^2$ entities are quadruple excitation operators. The product terms in the wavefunction introduce higher-order excitation character even if a direct excitation operator of a given order is not present. The appearance of these higher-level operators is the main reason for the efficacy of the coupled cluster approach. The coupled nature of the equations makes them amenable only to iterative solution.

The main drawback to such an approach is the immense computational time required for large systems. Choosing the cluster operator $\hat{T}$ such that

$$\hat{T} = \hat{T}_1 + \hat{T}_2 + \hat{T}_3, \qquad (1.11)$$

defines coupled cluster theory complete through single, double and triple excitations (CCSDT). This is an extension to CCSD, but has even more unfavorable scaling. However, by performing a CCSD computation and then applying perturbation theory to account for $\hat{T}_3$ terms, the popular CCSD(T) model is obtained.[8] This powerful method is commonly referred to as the "gold standard" of quantum chemistry due to its efficiency and high accuracy. A single CCSD(T) computation with a reasonable basis set will usually deliver 1-2 kcal mol^{-1} accuracy for relative energies.

The application of these methods, however, requires careful thought. The complete

basis set limit of a Hartree-Fock calculation, which neglects electron correlation, is not likely to be very accurate, just as a highly correlated wavefunction computed with a small basis set will be unreliable. In order to compute energies to high accuracy, we have to combine these two extremes, which we achieve through focal point analyses.

1.1.3 Focal Point Analysis (FPA)

1.1.3.1 Basis set extrapolation

The necessity of constructing wavefunctions in a one-particle basis set introduces basis set truncation error. In Hartree-Fock theory, the wavefunction is written as an antisymmetrized product of one-electron functions and each electron moves in the average field produced by all other electrons. The one-particle nature of this wavefunction is highly suitable for description with a one-particle basis set because no electron-electron cusps are present, and thus Hartree-Fock is relatively insensitive to the choice of basis set.

Feller demonstrated[9] that the Hartree-Fock energy exhibits an effective exponential dependence on the maximum angular momentum in the basis set, as long as the basis set is correctly balanced. Dunning has constructed a family of such basis sets that are now ubiquitous in quantum chemistry, for example cc-pV*X*Z, where *X* is the "cardinal number" of the basis set, i.e. the number of functions used to describe the valence electrons of each atom. The name "correlation-consistent (cc-)" refers to the property that all contracted Gaussian functions (CGFs) contributing similar amounts to the electron correlation energy included. For the Hartree-Fock energy, the energy for a given cardinal number, *E(X)*, can be expressed as

$$E(X) = A + Be^{-CX}, \tag{1.12}$$

where A, B and C are parameters to be determined by fitting to three energy computations with different basis sets. Given that e^{-CX} becomes zero as $X \rightarrow \infty$, the asymptote of this expression yields the complete basis set (CBS) limit:

$$E(\infty) = \lim_{X \rightarrow \infty} E(X) = A. \tag{1.13}$$

Correlated computations pose a larger problem, however. Here we are trying to model electrons avoiding each other, which is necessarily a two-body phenomenon. There is a rapid decay in the wavefunction, known as the Coulomb hole, as two electrons approach each other, forming a cusp at the coalescence point of the two electrons. This feature of correlated wavefunctions is very difficult to model with a one-particle basis set; hence correlated wavefunctions exhibit significantly more basis set dependence than those devoid of this many-body effect. Using the same Dunning basis set, Helgaker and co-workers have shown[10] that extrapolation can be performed upon correlation energies, via the form

$$E_{corr}(X) = a + bX^{-3}, \tag{1.14}$$

leading to the simple expression for the CBS correlation energy:

$$E_{corr}(\infty) = \lim_{X \rightarrow \infty} E_{corr}(X) = a. \tag{1.15}$$

A more rigorous and efficient route to removing the basis set error from correlated wavefunctions is through explicitly correlated methods. These methods are similar to conventional coupled cluster and perturbation theories, but have two-electron terms appended to the conventional products of one-electron functions. These additional terms were originally chosen to be germinal over the interelectronic distance operator r_{12} and are therefore commonly called R12 methods.

1.1.3.2 The Focal Point Approach

The focal point analysis of Allen and co-workers aims to eliminate errors arising from both inexact correlation treatment and basis set truncation.[11] Focal point analyses yield accurate relative energies, however key assumptions must be introduced to make the approach tractable.

First, the geometries of the individual species are optimized at a high level of theory. Around the equilibrium geometry on the "exact" potential energy surface, the energy is approximately quadratic with respect to small displacements. Small errors in the equilibrium geometry will lead to small errors in the absolute energies, which in turn will be largely canceled when calculating relative energies. For this reason, no re-optimization of the geometry is performed as part of the focal point analysis.

Having chosen the reference geometires, a hierarchical series of single point energies are computed, increasing the basis set and the correlation treatment as far as the system size permits. Coupled cluster theory with x-fold excitations included is exact for an x electron system, within a given one-electron basis. This crucial property combined with the advantages discussed above makes it the method of choice to define the correlation hierarchy in the focal point regime. The resulting energies are extrapolated to compute the CBS limit for those excitation levels where, at least, the basis sets cc-pVTZ and cc-pVQZ can be used. For CCSDT and higher theories, it is often the case that calculations with the cc-pVTZ and cc-pVQZ basis sets are prohibitively expensive, and here a different approximation is introduced.

For each theory that is too expensive to be evaluated with a large basis set, the difference in the energy computed by that theory and the energy emanating from highest

level for which extrapolation is performed is assumed to be independent of basis set. This defines the additivity approximation, whereby the difference between two correlation treatments is computed in a small basis and appended to the energy difference computed at the lower level in the complete basis set limit. As a concrete example, consider the case where CCSD(T) energies can be computed using large basis sets and extrapolated, but only cc-pVDZ computations are tractable for CCSDT. Here the complete basis set limit CCSDT energy for CCSDT would be approximated in the focal point regime as

$$E_{CCSDT}^{\infty} \approx E_{CCSD(T)}^{\infty} + E_{CCSDT}^{cc-pVDZ} - E_{CCSD(T)}^{cc-pVDZ}. \quad (1.16)$$

The physical justification for making the approximation is that the Coulomb hole that introduces the strong basis set sensitivity to the energy is primarily a two-body effect. The wavefunction is non-zero at the coalescence point of two electrons with opposite spin since the Pauli Exclusion Principle is not violated. Therefore, it is important to model the two-body terms accurately to describe the Coulomb hole, since there is a non-zero contribution to the energy in vicinity of the electron-electron coalescence point. Now considering the difference between CCSDT and CCSD(T), the two-body terms are cancelled by the subtraction, as both CCSDT and CCSD(T) contain them. The energetic contribution of the remaining terms is small so the basis set dependence is also small.

We have already noted that an equation analogous to (1.18) defines the final focal point energy but, despite this simple form, a large table showing all of the energies computed at lower levels of theory is usually reported. For example, the CCSD/cc-pVTZ energy will be tabulated, but will have no bearing on the final focal point energy; these intermediate results are useful for monitoring convergence with respect to level of theory and thus afford an estimate of the error bars. This feature sets the focal point analysis

apart from related high accuracy extrapolation procedures, such as HEAT[12-13] and the W*n* family of methods.[14-15] The energy differences could be clearly visualized in a focal point table. Inspecting the difference in relative energies predicted by the highest levels of theory is a good indicator of how close to the exact non-relativistic Born-Oppenheimer energy the final result is. Even if the absolute energies from a focal point analysis are not exact, the relative energies are very accurate, as they benefit from a large degree of error cancellation.

1.1.3.3 Auxiliary Corrections

The Born-Oppenheimer approximation, [1] an adiabatic approximation whereby the timescale of electronic motion is assumed to be much shorter than that of the nuclei, is justified by considering the large ratio of the nuclear mass to the electronic mass. Commonly, the diagonal Born-Oppenheimer correction (DBOC)[16-18] is computed. This is the first-order correction to the clamped nucleus approximation that can be important in the pursuit of "subchemical accuracy" (*ca*. 0.1 kcal mol^{-1}). The DBOC retains the concept of the potential energy surface – something that is missing in the absence of the adiabatic approximation; however, a mass-dependence is introduced, meaning that isotopically substituted molecules have distinct potential energy surfaces.

1.1.4 Potential Energy Surface

Finding the equilibrium geometry of a molecule is one of the major goals of theoretical computations. The equilibrium geometry of a molecule represents the arrangement of the atomic nuclei that minimizes the total molecular energy, including the internuclear repulsions. The task of finding the equilibrium geometry becomes more challenging as

the molecular size increases. The problem is aggravated by the fact that polyatomic molecules have very many degrees of freedom, and often several different atomic arrangements may result in a similar molecular energy, which poses very stringent requirements on the accuracy of energy computations.

1.1.4.1 Geometry Optimizations

The geometrical structure of a (nonlinear) molecule is uniquely determined by defining *3N−6* independent internal coordinates, where *N* stands for the number of atoms in the molecule. As mentioned in the preceding section, the energy of a molecule depends on the atomic configuration. The minima on this surface correspond to stable equilibrium structures of the molecule. The lowest-energy minimum is referred to as the global minimum. The other minima are simply local minima. There are also points on the PES corresponding to minima for *3N−7* coordinates, and to a maximum for one coordinate. Such points are referred to as saddle points, which correspond to transition states for chemical reactions. The calculation of the energy at a fixed conformation is called a single-point energy calculation.

The set of the dihedral angles about all bonds in a molecule defines its conformation. The conformation corresponding to an energy minimum (local or global) is termed a conformer. The larger the molecule, the more conformers it is likely to have. That is why the prediction of molecular conformers is one of the major goals of the theoretical computations.

1.1.4.2 Conformational Search

A geometry optimization or energy minimization is the procedure of finding the molecular conformation corresponding to an energy minimum in vicinity of some

initially defined molecular geometry (conformation). From the viewpoint of mathematics, this is the problem of the multidimensional optimization. There exist various algorithms to handle the problem. Most nonlinear optimization algorithms are based on a local quadratic approximation of the potential energy surface.[19-22] Newton and quasi-Newton methods with an approximate hessian are the most widely used procedures for optimizing equilibrium geometries and can also be used effectively to find transitions states.[19-23] To find different molecular conformers, one has to probe different starting geometries, and search for the local energy minimum. The problem is aggravated in molecules with many internal degrees of freedom, which may have many different conformers. The finding of the global energy minimum is not a trivial task, and in general, this problem has not been solved yet. The guess of the starting conformation in the vicinity of which the global energy minimum is expected might be misleading since often it may happen that the most stable conformer is rather unconventional.

1.1.5 Molecular Vibrational Frequencies

1.1.5.1 Harmonic Vibrational Frequencies

The conformational search and the geometry optimization of a molecule provide the total electronic energy of this molecule. Since, however, atomic nuclei are never at rest but perform small oscillations about their equilibrium positions, it is of importance to calculate also the molecular vibrational frequencies. As part of this study, we will compute fundamental vibrational frequencies. In one instance our motive will be to provide values for spectroscopic characterization, and another study will require accurate zero-point vibrational energies.

The most common method for computing characteristic frequencies is to invoke the normal mode or multidimensional harmonic oscillator approximation, under which the potential energy surface is assumed to be quadratic to all coordinates around the equilibrium (stationary) point. The energy of a harmonic oscillator E_{vib} in N-dimensions is

$$E_{vib} = \left[(n_1 + \cdots + n_N) + \frac{N}{2}\right] h\nu, \tag{1.17}$$

where n_i stands for the vibrational quantum number in dimension *i* that can take on values from 0 to infinity, and ν is the vibrational frequency. For a *N*-atomic molecule there are *3N−6* vibrational modes if the molecule is not planar, and *3N−5* for linear molecules. The sum of all the ground-state vibrational energies yields the so-called zero-point vibrational energy (ZPVE). This is the lowest energy level a molecule can occupy for a certain conformer. In practice, the fundamental vibrational frequencies of a *N*-atomic molecule are determined by diagonalizing the mass-weighted quadratic force-constant matrix,

$$H_{ij} = \frac{1}{\sqrt{m_i m_j}} \left(\frac{\partial^2 V}{\partial x_i \partial x_j}\right)_e . \tag{1.18}$$

The advantage of doing so is that only second derivatives of the energy with respect to nuclear displacements are required; analytic formulae for the solution of these exist for all common levels of theory, although they are seldom implemented for coupled cluster theory due to the high complexity of the equations. The harmonic potential typically overestimates the curvature, resulting in frequencies that are consistently too high. Realizing this, Scott and Radom[24] among many others performed a systematic study of harmonic frequencies and compared them to experimental values, resulting in some

recommended scale factors for various levels of theory that will give good approximations to fundamental frequencies from harmonic frequencies.

1.1.5.2 Anharmonic Vibrational Frequencies

Perturbation theory offers a viable route to computing fundamental frequencies beyond the harmonic approximation. In vibrational perturbation theory, the zeroth-order Hamiltonian is chosen to be the harmonic oscillator rigid rotor Hamiltonian. Second-order vibrational perturbation theory (VPT2) then introduces the anharmonic (cubic and quartic) potential terms, as well as anharmonic kinetic energy terms, including Coriolis effects and centrifugal distortion, as a perturbation. The important point to note here is the implicit assumption that the harmonic oscillator provides a faithful representation; if this is not true, such as in many weakly-bound systems, perturbation theory breaks down.

The fundamental vibrational frequency ν_r is given by VPT2 theory as

$$\nu_r = \omega_r + 2\chi_{\mathrm{rr}} + \frac{1}{2}\sum_{s\neq r}\chi_{\mathrm{rs}}. \tag{1.19}$$

The general expression for anharmonic constants χ_{rs} is

$$\chi_{rr} = \frac{1}{16}\phi_{rrrr} - \sum_{s}\frac{\phi_{rrs}^2(8\omega_r^2 - 3\omega_s^2)}{16\omega_s(4\omega_r^2 - \omega_{sarv}^2)}, \tag{1.20}$$

and the off-diagonal term χ_{rs} term is given by

$$\chi_{rs} = \frac{1}{4}\phi_{rrss} - \frac{1}{4}\sum_{t}\frac{\phi_{rrr}\phi_{tss}}{\omega_t} - \frac{\frac{1}{2}\sum_t \phi_{rst}^2\,\omega_t(\omega_t^2 - \omega_r^2 - \omega_s^2)}{\Delta_{rst}}$$

$$+ \left[A_e\left(\zeta_{r,s}^{(a)}\right)^2 + B_e\left(\zeta_{r,s}^{(b)}\right)^2 + C_e\left(\zeta_{r,s}^{(c)}\right)^2\right]\left(\frac{\omega_r}{\omega_s} + \frac{\omega_s}{\omega_r}\right), \tag{1.21}$$

where

$$\Delta_{rst} = (\omega_r + \omega_s + \omega_t)(\omega_r + \omega_s - \omega_t)(\omega_r - \omega_s + \omega_t)(\omega_r - \omega_s - \omega_t), \tag{1.22}$$

The rotational constants A_e, B_e, and C_e are the equilibrium rotational constants associated with the principal rotational axes, a, b, and c, respectively. $\zeta_{r,s}^{(a)}$ is the Coriolis zeta constant that couples normal coordinates through rotation about the a axis.

Another potential pitfall occurs when Fermi resonance occurs. This happens when a combination or overtone band has nearly the same frequency as a fundamental, subject to symmetry restrictions.

1.1.5.3 Zero-Point energy correction

Having derived the anharmonicity constants χ_{rs}, the vibrational energy levels of an asymmetric top molecule are given by

$$G(\mathbf{v}) = G_0 + \sum_{\mathrm{r}} \omega_{\mathrm{r}}(\mathrm{v_r} + \frac{1}{2}) + \sum_{\mathrm{r}\geq\mathrm{s}} \chi_{\mathrm{rs}} \left(\mathrm{v_r} + \frac{1}{2}\right)\left(\mathrm{v_s} + \frac{1}{2}\right) + \cdots, \qquad (1.23)$$

from which we neglect the higher terms within the VPT2 framework. The complete VPT2 expression for the zero-point vibrational energy is[25]

$$ZPVE = \sum_{\mathrm{r}} \frac{\omega_{\mathrm{r}}}{2} - \frac{1}{32}\sum_{rst} \frac{\phi_{rrt}\phi_{tss}}{\omega_{\mathrm{t}}} - \frac{1}{48}\sum_{rst} \frac{\phi_{rst}^2}{\omega_{\mathrm{r}} + \omega_{\mathrm{s}} + \omega_{\mathrm{t}}} + \frac{1}{32}\sum_{rs} \phi_{rrss} + Z_{kinetic} \qquad (1.24)$$

where the kinetic energy term ($Z_{kinetic}$) is dependent on the molecular type.

1.2 Weak Molecular Interactions

In isolated molecules the negatively charged electron shell shields the positively charged molecular core, thus yielding a neutral system. When molecules are close to one another, however, their electron shells experience not only the influence of their own positive cores but also the presence of the electron shells of the surrounding molecules. This brings about a deformation and redistribution of the electronic charge within the molecules, leading to an incomplete shielding of the positive cores and respectively, to the appearance of locally charged molecular species. Nonbonding weak molecular interactions are two types: attractive and repulsive. Attractive weak molecular interactions are classified as electrostatic, inductive, and dispersion. Repulsive interactions stem from the Pauli exclusion principle.

1.2.1 Attractive and Repulsive Molecular Interactions

Static charge distributions can be expanded in a series of multipole moments. Thus two molecules, A and B, interact with each other through the static multipole moments of their charge distribution, the resulting interaction energy being designated as E_{el}. The electrostatic energy can be presented in the following way:

$$E_{el} = \frac{q_A q_B}{r} + \frac{q_A|\mu_B|}{r^{\,2}} + \frac{q_B|\mu_A|}{r^2} + \frac{\mu_A \cdot \mu_B}{r^3} + \frac{q_A Q_B}{r^3} + \frac{q_B Q_A}{r^3} + \frac{\mu_A \cdot Q_B}{r^4} + \frac{\mu_B \cdot Q_A}{r^4} + \frac{Q_A \cdot Q_B}{r^5} + \cdots, \tag{1.25}$$

where q, μ, Q, and r stand for the electric charge, electric dipole moment, electric quadrupole moment, and the distance of the second particle relative to the first one, respectively. The interaction energy E_{el} also depends on the mutual orientation of the multipoles, hence in natural systems the molecules are oriented such as to minimize the

total electrostatic energy. The magnitude of the higher-order terms in the multipole expansion dwindles down very rapidly with the intermolecular distance, and for this reason the interaction energy can be described fairly accurately only by retaining the first nonvanishing terms in the multipole series. Some molecules, due to symmetries, do not have low-rank permanent multipoles, and hence necessitate the inclusion of higher-order terms. There exist some molecular systems, e.g., complexes between rare gas atoms that do not have permanent multipoles at all, for which electrostatic interactions do not come to the scene.

Dispersion interactions are attractive intermolecular interactions that derive from the mutual polarization of the instantaneous electron density distributions of two monomers, A and B. Such forces were for the first time rationalized and described by London,[26] and hence are also called London interactions. The potential energy of such an interaction, E_{disp}, can be cast in the form

$$E_{disp} = -\frac{C_6}{r^6} - \frac{C_8}{r^8} - \frac{C_{10}}{r^{10}} - \cdots, \tag{1.26}$$

in which C_6, C_8, C_{10}, etc. are empirical constants, and r is the inter-monomer distance. Dispersion is the weakest among the attractive interactions, but this interaction gains importance in nonpolar molecular complexes where it gives rise to the only binding force. Hence, it is paramount in large molecules with large polarizability, and in complexes containing a noble-gas atom, as will be shown in this work.

The only repulsive intermolecular interaction arising when two molecules, A and B, are close to each other stems from the *exchange* interaction, a manifestation of the fundamental Pauli exclusion principle, which precludes the penetration of electrons from one of the molecular moieties into the occupied orbitals of the other one. The resulting

energy, E_{exch} has been mathematically formulated by Heitler and London[26-28] through an exponential or inverse power law:

$$E_{exch} = \frac{A}{r^n}, \tag{1.27}$$

In Eq. 1.27 *A* is an empirical constant, and the power *n* ranges between 10 and 20. The inverse-power law describes the exchange repulsion in cases of very small separation distances between the two molecules, A and B.

1.2.2 The Concept of Weak Molecular Bindings

Weak molecular interactions are usually not isolated but co-exist and act cooperatively. The net effect of the concurring weak interactions is a result of a delicate balance between them, ultimately leading to the formation of a weak noncovalent bond whose nature, however, is different from the nature of chemical bonds altogether. Its strength is typically from one to two orders of magnitude weaker compared to chemical bonds, depending on the nature of the particular molecular system and the weak interactions involved.

Due to the balance between the attractive and repulsive potentials, in most cases, there exists an equilibrium interatomic distance, r_0, at which the net interaction energy has a minimum. It may happen, however, that the attractive potential cannot make up for the action of the repulsive potential at any point, thus leading to a nonbonding potential with no minimum. In this case no weak bond can be formed. It is important, however, to point out that for a bond to be formed, not only must the potential have a minimum, but also the zero-point vibrational level must be below the dissociation energy.

1.2.3 Classification of Weak Molecular Bonds

While there are no rigorous boundaries between different types of weak molecular bonds, a general classification can be made according to the nature of the interactions involved, bond energies, and bond lengths.

1.2.3.1 Hydrogen Bonds

Hydrogen bonds are one of the most abundant and important types of weak molecular interactions in nature. Hydrogen bonds have the general motif X-H···Y, where the X-H group is a *proton donor,* and Y is a *proton acceptor*. Usually, X is an electronegative atom (O, N, Cl, F, etc.), and Y is most typically either an atom possessing a lone electron pair or it is a π-electron system, which has an excess of π-electron density. Once recently was the importance of another specific type of hydrogen bond realized: C-H···Y hydrogen bonds,[29-33] which play an important role in the stabilization of molecular structures in biochemical systems. Usually, Y is an electronegative atom or a π system. Such C-H···Y interactions are much weaker than conventional hydrogen bonds, and with respect to binding energy they are at the borderline between hydrogen bonds and dispersion interactions.

The most significant features and properties of hydrogen bonds are:

(1) Hydrogen bonds are stabilized by a subtle interplay between electrostatic, induction, and dispersion interactions. The most important contribution, however, is the electrostatic one, realized mainly though dipole-charge and dipole-dipole coupling.

(2) Hydrogen bonds provide a typical example of a two-body interaction. Due to the electrostatic attraction, the H-bond length is shorter than the sum of the van der Waals radii of the two atoms, X and Y.

(3) Hydrogen bonds are strongly directional, i.e., the three atoms, X, H, and Y, nearly lie along a straight line.

(4) Typical H-bond lengths range between 2 and 3 Å.

(5) The energy of H-bonds varies between 2 and 20 kcal mol^{-1}, depending on the nature of X and Y atoms. Some H-bonds render themselves at the brink of chemical bonds.

1.2.3.2 Dispersion Interactions

Dispersion bonds are formed when the interacting moieties do not have no permanent charges or low-rank multipoles, and hence only the dispersion term in the attractive potential is accounted for. Dispersion bonds lack directionality and help stabilize complexes of nonpolar species.

1.2.3.3 Charge-Transfer Bonds

Charge-transfer (CT) bonds emerge when one of the bonded moieties is a good electron donor, and the other one has high electron affinity. Donors exhibit higher-lying occupied orbitals designated as n, σ, and π, respectively, and acceptors have vacant orbitals labeled as n^*, σ^*, and π^*, respectively. The strongest of the so-formed CT complexes are the ones of *n-n* type.

1.2.3.4 Other Weak Molecular Bindings

Q*uadrupole-quadrupole* binding occurs in systems containing benzene rings. These interactions determine the T-shape structure of the benzene dimer, and play an important role for the stabilization of secondary and tertiary structures of macromolecules.

Ion-mediated bonds stem from the presence of metallic cations, which have high electron affinity, and hence form polar bonds on the basis of multipole interactions.

Hydrophobic interactions are a special class of interactions representing associations of nonpolar groups in polar solvents. It has been found[34-36] that the change of the enthalpy is almost vanishing, and the driving force for the reorganization of the molecules in a solution is the entropy.

1.2.4 Intramolecular Forces

Weak interactions and weak bonds can be *intramolecular* or *intermolecular*. Intramolecular weak bonds play an important role for the stabilization of molecular structures, in particular, those that have many internal degrees of freedom and can assume different conformations. The most abundant intramolecular bonds are the hydrogen ones, though quadrupole-quadrupole bonds are also observed. The effect of intramolecular bonds to the amino acid conformational space is examined for the amino acids glycine and serine in Chap. 2 and Chap. 3, respectively. Intermolecular bonds are responsible for the formation of noncovalent complexes. A qualitative analysis of both intramolecular and intermolecular dispersion dominated systems is presented in Chap. 4.

1.3 Dispersion Corrected DFT

1.2.1 Density-Functional Theory

Density-functional theory (DFT) differs from wave function methods by using the electron density $n(\mathbf{r})$ as the central quantity. An important advantage of using the electron density over the wave function is the much reduced dimensionality. Regardless of how many electrons one has in the system, the density is always three-dimensional. This enables DFT to readily be applied to much larger systems. Partly for this reason, DFT has become the most widely used electronic structure approach today, particularly in condensed-matter physics.

First, the electron density is defined as

$$n(\mathbf{r}) = N \int \cdots \int |\Psi(\mathbf{x}_1, \mathbf{x}_2, \cdots, \mathbf{x}_N)|^2 d\sigma_1 d\,\mathbf{x}_2 \cdots d\mathbf{x}_N, \tag{1.28}$$

where $\{\mathbf{x}_i\}$ represents both spatial and spin coordinates, σ is the electronic spin. The electron density $n(\mathbf{r})$ determines the probability of finding any of the *N* electrons within the volume $\mathbf{r}$ but with arbitrary spin σ while the other *N*–1 electrons have arbitrary positions and spin in the state represented by Ψ. This $n(\mathbf{r})$ is a nonnegative simple function that integrates to the total number of electrons,

$$N = \int n(\mathbf{r}) d\mathbf{r}. \tag{1.29}$$

In 1964, Hohenberg and Kohn derived the fundamentals of density-functional theory, allowing one to express the electronic Hamiltonian as a functional of $n(\mathbf{r})$.[37-39] This approach relies on two theorems: (1) there exists a one-to-one correspondence between external potential $v(\mathbf{r})$ and the electron density $n(\mathbf{r})$; and (2) the ground-state electron

density can be found by using a variational principle. For a given $v(\mathbf{r})$ we can write the energy E_v as a function of the electron density $n(\mathbf{r})$:

$$E_v\,[n] = T[n] + V_{ne}[n] + V_{ee}[n] = \int n(\mathbf{r})v(\mathbf{r})d\,\mathbf{r} + F_{HK}[n], \tag{1.30}$$

where

$$F_{HK}[n] = T[n] + V_{ee}[n]. \tag{1.31}$$

In 1965, Kohn and Sham published a paper which transformed density-functional theory into a practical electronic structure theory.[40] They re-introduced the idea of non-interacting electrons moving in an effective field, similar to the Hartree-Fock approach. The functional form of $F_{HK}[n(\mathbf{r})]$ is written as a sum of the kinetic energy of non-interacting electrons (T_s), the Hartree energy ($E^{Hartree}$), and the exchange-correlation energy (E_{xc}) that contains all the many-body quantum effects. So the energy functional obtained in the previous section now becomes,

$$\begin{aligned} E[n] &= \int n(\mathbf{r})v(\mathbf{r})d\,\mathbf{r} + F_{HK}[n(\mathbf{r})] \\ &= \int n(\mathbf{r})v(\mathbf{r})d\,\mathbf{r} + T_s[n(\mathbf{r})] + E^{Hartree}[n(\mathbf{r})] + E_{xc}[n(\mathbf{r})]. \end{aligned} \tag{1.32}$$

The next step is to define an effective potential in terms of functional derivatives (δ),

$$\begin{aligned} V^{eff} &= \frac{\delta\{\int n(\mathbf{r})v(\mathbf{r})d\,\mathbf{r} + E^{Hartree}[n(\mathbf{r})] + E_{xc}[n(\mathbf{r})]\}}{\delta n(\mathbf{r})} \\ &= v(\mathbf{r}) + \int \frac{n(\mathbf{r}')}{|\mathbf{r} - \mathbf{r}'|}d\mathbf{r}' + v_{xc}(\mathbf{r}), \end{aligned} \tag{1.33}$$

where $v_{xc}(\mathbf{r})$ is the exchange-correlation potential defined as:

$$v_{xc}(\mathbf{r}) = \frac{\delta E_{xc}[n(\mathbf{r})]}{\delta n(\mathbf{r})}. \tag{1.34}$$

This leads to the central equation in Kohn-Sham DFT, an one-electron Schrödinger-like equation expressed as:

$$\left[-\frac{1}{2}\nabla^2 + V^{eff}\right]\phi_i = \epsilon_i\phi_i. \tag{1.35}$$

Here $\{\phi_i\}$ denotes the set of Kohn-Sham one-electron orbitals, and the electron density is defined as

$$n(\mathbf{r}) = \sum_{i=1}^{N} |\phi_i(\mathbf{r})|^2. \tag{1.36}$$

The ϵ_i's are the energies of the Kohn-Sham one-electron orbitals. Clearly this is a Hartree-Fock-like single particle equation which needs to be solved iteratively. Finally, the total energy can be determined from the resulting density through

$$E = \sum_{i=1}^{N} \epsilon_i - \frac{1}{2}\iint \frac{n(\mathbf{r})n(\mathbf{r}')}{|\mathbf{r}-\mathbf{r}'|} + E_{xc}[n] - \int v_{xc}(\mathbf{r})n(\mathbf{r})d\mathbf{r}. \tag{1.37}$$

Note that the V^{eff} depends on $n(\mathbf{r})$ through Eq. (1.36), so the Kohn-Sham equation must be solved self-consistently. The general procedure is to begin with an initial guess of the electron density, construct the V^{eff} from Eq. (1.33), and then get the Kohn-Sham orbitals. Based on these orbitals, a new density is obtained from Eq. (1.36) and the process repeated until convergence is achieved. Finally, the total energy will be calculated from Eq. (1.37) with the final electron density.

E_{xc} includes the non-classical aspects of the electron-electron interaction, along with the component of the kinetic energy of the real system differing from the fictitious non-interacting system.

1.3.2 Exchange-Correlation Functionals

The exact form of E_{xc} is not known and may never be known. By now there is an almost endless list of approximate functionals with varying levels of complexity. Perdew proposed the "Jacob's ladder" as a way to categorize the many and varied E_{xc} functionals.[41] In this scheme functionals are grouped according to their complexity on rungs of a ladder which lead from the Hartree approximation to the exact exchange-correlation functional. Furthermore, functionals can be categorized into *non-empirical* and *empirical*.

(1) The local-density approximation (LDA)

In this approach a real inhomogeneous system is divided into infinitesimal volumes, and the electron density in each of the volumes is taken to be constant. The exchange-correlation energy for the density within each volume is then assumed to be the exchange-correlation energy obtained from the uniform electron gas for that density. Thus, the total exchange-correlation energy of the system can be written as

$$E_{xc}^{LDA}[n] = \int n(\mathbf{r})\, \epsilon_{xc}^{unif}\big(n(\mathbf{r})\big) d\mathbf{r}, \tag{1.38}$$

where ϵ_{xc}^{unif} is the exchange-correlation energy per particle of the interacting uniform electron gas of density $n(\mathbf{r})$. The correlation energy is generally obtained by fitting to the many-body free electron gas data obtained from rigorous quantum mechanical computations.

The LDA is valid only for slowly varying densities, and it performs poorly for weakly bonded systems, such as vdW and H-bonded systems. Also, long-range vdW interactions are completely missing in LDA.

(2) The generalized gradient approximation (GGA)

In order to improve upon the uniform density approximation, the gradient of the density ($\nabla n(\mathbf{r})$) needs to be included. If the exchange-correlation energy is assumed to be a general function of $n(\mathbf{r})$ and ($\nabla n(\mathbf{r})$), then

$$E_{xc}^{GGA}[n] = \int f^{GGA}\big(n(\mathbf{r}), \nabla n(\mathbf{r})\big) d\mathbf{r}, \tag{1.39}$$

which constitutes a GGA approach.

GGAs are "semi-local" and can yield better results than LDAs, especially for covalent bonds and weakly bonded systems. Some of the popular GGAs for treating hydrogen bonds are PBE,[42] BLYP,[43] PW91,[44] and BP86.[45]

(3) Meta-GGAs

The third-generation functionals contain the Laplacian of the density, $\nabla^2 n(\mathbf{r})$, and/or kinetic energy densities, $\tau_\sigma(n) = 1/2 \sum_i \left|\nabla_{\varphi i}(n)\right|^2$, as additional degrees of freedom. In gas-phase studies of molecular properties, meta-GGAs such as the TPSS[46] functional have been shown to offer improved performance over LDAs and GGAs.[47-50]

(4) Hybrid functionals

These fourth-generation functionals add "exact exchange" computed from the Hartree-Fock functional to some conventional treatment of DFT exchange and correlation. Most widely used is the B3LYP[51-53] functional, which employs three parameters (a_1 - a_3) to control the mixing of the HF exchange and density functional exchange and correlation. B3LYP has the following form:

$$E_{xc}^{B3LYP} = E_{xc}^{LDA} + a_1(E_x^{HF} - E_x^{LDA}) + a_2 \Delta E_x^{GGA} + a_3 \Delta E_c^{GGA}. \tag{1.40}$$

Beyond these few rungs of Jacob's ladder, there are other *xc* functionals of increasing complexity. However, adding complexity by climbing higher on Jacob's ladder or by

obeying more and more constraints[54] does not necessarily bring improved performance in total energies.

1.3.3 Dispersion-Corrected DFT

Dispersion interactions can be empirically defined as the attractive part of the van der Waals (vdW)-type interaction potential between atoms and molecules that are not directly bonded to each other. The terms "dispersion" and "vdW" are often used synonymously. Especially for the chemistry and physics of large systems, e.g., in bio-or nanoarchitectures, inclusion of these interactions in theoretical simulations is indispensable in order to reach chemical accuracy. Dispersion effects are due to omnipresent electron correlations, and they also influence the accuracy of theoretical (reaction) thermodynamics.

It is now clear that almost all gradient-corrected density functionals are unable to describe dispersive interactions.[55-58] At short electron-electron distance, the standard functionals describe the corresponding effects rather well because of their deep relation to the corresponding electron density changes. Electron correlations in the medium-range are difficult to classify and often have the typical wave function signatures of dispersion-type interactions.[59] Thus, any DFT approach including dispersion is faced with the problem of merging in a seamless fashion the short- and long-range asymptotic regions that are fairly well understood separately.

The currently used dispersion corrections can be grouped into a few classes. In the nonlocal, nonempirical DF (also called vdW-DF) method,[60] standard exchange and correlation components of LDA or GGA type are used for the short-ranged parts and E_c^{NL}

represents the nonlocal term describing the dispersion energy. This term also contributes at short electron-electron distance to the correlation in the form of a double-space integral

$$E_c^{NL} = \frac{1}{2}\iint n(\mathbf{r})\phi(\mathbf{r},\mathbf{r}')n(\mathbf{r}')d\mathbf{r}d\mathbf{r}'. \quad (1.41)$$

The different variants of vdW-DF that are currently on the market only differ in the choice of the nonlocal correlation kernel $\phi(\mathbf{r},\mathbf{r}')$. The biggest advantage of vdW-DF methods is that dispersion effects are naturally included via the charge density so that the charge-transfer dependence of dispersion is automatically included in a physically sound manner. What is currently not known is whether double-counting effects of correlation at short range are present in the mentioned vdW-DFs. These functionals have not been tested so far on intramolecular or thermochemical problems.

The Tao-Perdew-Staroverov-Scuseria (TPSS) and TPSS hybrid (TPSSh) functionals[48] produce vdW bonds in 10 rare-gas dimers with $Z \leq 36$ and correct the overbinding of the local spin density approximation,[61] but the binding energy curves have an incorrect asymptotic behavior for large internuclear separation.[62] Some highly parameterized meta-GGAs incorporate kinetic energy density and partially account for dispersion effects. The M06-2X functional[63] is probably the most accurate functional not containing an *a posteriori* dispersion correction that gives good results for the S22 set as well as stacked aromatic structures.[64] But numerical instability in the power series expansion might lead to artificial vdW minima and 'noisy' potential energy curves.[65] Modern highly parameterized DFs can 'emulate' medium-range, nonlocal dispersion effects rather accurately by semilocal exchange-correlation potentials. However, asymptotically, the dispersion energy in these approaches is zero and, therefore, they cannot be recommended for extended systems in which long-range contributions are important.

The semiclassical corrections (DFT-D) add an empirical potential of the form C_6R^{-6} to the usual DFT energy, where R is an interatomic distance and C_6 is the corresponding dispersion coefficient.[66-67] The general form for the dispersion energy (which is simply added to the Kohn-Sham DFT energy) is

$$E_{disp}^{DFT-D} = -\sum_{AB}\sum_{n=6,8,10} s_n \frac{C_n^{AB}}{R_{AB}^n} f_{damp}(R_{AB}), \tag{1.42}$$

where the sum is over all atom pairs in the system, C_n^{AB} denotes the averaged (isotropic) *n*th-order dispersion coefficient (order *n*=6, 8, 10,…) for atom pair AB, and R_{AB} is their internuclear distance. Global (DF-dependent) scaling factors s_n are typically used to adjust the correction to the repulsive behavior of the chosen DF.[68] The higher C_n terms can be used to adapt the potential specifically to the chosen DF in the mid-range region. But the question of how many higher-order terms are necessary is not completely clear at present.[66, 69-71] Damping functions f_{damp} are used in order to avoid near singularities for small R and double-counting effects of correlation at intermediate distances, which determine the range of the dispersion correction.[72] A fundamental difference between the existing damping approaches is their behavior for small R. Advantages of DFT-D3[66] are: (1) it can easily be coupled with any standard DF without any significant loss of accuracy; (2) it easily allows the calculation of energy gradients for efficient geometry optimization; and (3) the total dispersion energy is simply attributed to contributions from individual atom pairs, parts of a molecule, or for a particular distance range.

Reference

1. Born, M.; Oppenheimer, R., *Ann. Phys.* **1927,** *389*, 457-484.
2. Davydov, A., *Quantum Mechanics*. Pergamon Press: Oxford, 1965.
3. Levine, I. N.; Learning, P., *Quantum chemistry*. Pearson Prentice Hall Upper Saddle River, NJ: 2009; Vol. 6.
4. Hartree, D. R. Proc. Cambridge Philos. Soc., **1928**,89-110.
5. Čížek, J., *J. Chem. Phys.* **1966,** *45*, 4256-4266.
6. Čížek, J.; Paldus, J., *Int. J. Quant. Chem.* **1971,** *5*, 359-379.
7. Crawford, T. D.; Schaefer, H., *Rev. Comput. Chem.* **2000,** *14*, 33-136.
8. Raghavachari, K.; Trucks, G. W.; Pople, J. A.; Head-Gordon, M., *Chem. Phys. Lett.* **1989,** *157*, 479-483.
9. Feller, D., *J. Chem. Phys.* **1992,** *96*, 6104-6114.
10. Helgaker, T.; Klopper, W.; Koch, H.; Noga, J., *J. Chem. Phys.* **1997,** *106*, 9639-9646.
11. Wilke, J. J.; Allen, W. D.; Schaefer, H. F., *J. Chem. Phys.* **2008,** *128*, 74308-74500.
12. Bomble, Y. J.; Vázquez, J.; Kállay, M.; Michauk, C.; Szalay, P. G.; Császár, A. G.; Gauss, J.; Stanton, J. F., *J. Chem. Phys.* **2006,** *125*, 064108.
13. Tajti, A.; Szalay, P. G.; Császár, A. G.; Kállay, M.; Gauss, J.; Valeev, E. F.; Flowers, B. A.; Vázquez, J.; Stanton, J. F., *J. Chem. Phys.* **2004,** *121*, 11599-11613. See footnote 69 for the G_0 expression of asymmetric tops.
14. Martin, J. M.; de Oliveira, G., *J. Chem. Phys.* **1999,** *111*, 1843-1856.
15. Boese, A. D.; Oren, M.; Atasoylu, O.; Martin, J. M.; Kállay, M.; Gauss, J., *J. Chem. Phys.* **2004,** *120*, 4129-4141.
16. Handy, N. C.; Yamaguchi, Y.; Schaefer III, H. F., *J. Chem. Phys.* **1986,** *84*, 4481-4484.
17. Sellers, H.; Pulay, P., *Chem. Phys. Lett.* **1984,** *103*, 463-465.
18. Valeev, E. F.; Sherrill, C. D., *J. Chem. Phys.* **2003,** *118*, 3921-3927.
19. Gill, P. E.; Murray, W.; Wright, M. H., *Practical optimization*. Academic press London, 1981; Vol. 5.
20. Dennis, J. E.; Schnabel, R. B., *Numerical methods for nonlinear equations and unconstrained optimization*. Prentice-Hall: NJ, 1983; Vol. 16.
21. Scales, L., *Introduction to non-linear optimization*. Springer-Verlag Inc.: New York, 1985.
22. Fletcher, R., *Practical methods of optimization*. John Wiley & Sons: Chichester, 2013.
23. Schlegel, H. B., *WIREs Comput Mol Sci* **2011,** *1*, 790-809.
24. Pople, J. A.; Scott, A. P.; Wong, M. W.; Radom, L., *Isr. J. Chem.* **1993,** *33*, 345-350.
25. Schuurman, M. S.; Allen, W. D.; Schaefer, H. F., *J. Comput. Chem.* **2005,** *26*, 1106-1112.
26. London, F., *Z. Phys* **1930,** *63*, 245.
27. Maitland, G.; Rigby, M.; Smith, E.; Wakeham, W.; Henderson, D., *Intermolecular forces: their origin and determination*. 2nd ed ed.; Clarendon Press: Oxford, 2008; Vol. 36, p 57-58.

28. Heitler, W.; London, F., *Z. Phys.* **1927,** *44*, 455-472.
29. Carrasquillo, E.; Zwier, T. S.; Levy, D. H., *J. Chem. Phys.* **1985,** *83*, 4990-4999.
30. Nishio, M.; Hirota, M.; Umezawa, Y., *The CH/π interaction: evidence, nature, and consequences*. John Wiley & Sons: New York, 1998; Vol. 21.
31. Djafari, S.; Barth, H.-D.; Buchhold, K.; Brutschy, B., *J. Chem. Phys.* **1997,** *107*, 10573-10581.
32. Fujii, A.; Morita, S.-i.; Miyazaki, M.; Ebata, T.; Mikami, N., *J. Phys. Chem. A* **2004,** *108*, 2652-2658.
33. Chervenkov, S.; Wang, P.; Braun, J. E.; Chakraborty, T.; Neusser, H. J., *Phys. Chem. Chem. Phys.* **2007,** *9*, 837-845.
34. Müller-Dethlefs, K.; Hobza, P., *Chem. Rev.* **2000,** *100*, 143-168.
35. Kauzmann, W., *Adv. Prot. Chem.* **1959,** *14*, 1-63.
36. Chandler, D., *Nature* **2005,** *437*, 640-647.
37. Hohenberg, P.; Kohn, W., *Phys. Rev.* **1964,** *136*, B864.
38. Hellmann, H., *Z. Phys.* **1933,** *85*, 180-190.
39. Feynman, R. P., *Phys. Rev.* **1939,** *56*, 340.
40. Kohn, W.; Sham, L. J., *Phys. Rev.* **1965,** *140*, A1133.
41. Perdew, J. P.; Schmidt, K.; Dreizler, M. R.; Gross, E. K. U., *Density functional theory and its application to materials*. AIP Press: New York, 2001; p 1-20.
42. Perdew, J. P.; Burke, K.; Ernzerhof, M., *Phys. Rev. Lett.* **1996,** *77*, 3865.
43. Lee, C.; Yang, W.; Parr, R. G., *Phys. Rev. B* **1988,** *37*, 785.
44. Perdew, J. P.; Ziesche, P.; Eschrig, H., *Electronic structure of solids' 91*. Akademie Verlag: Berlin, 1991; Vol. 11.
45. Perdew, J. P., *Phys. Rev. B* **1986,** *33*, 8822.
46. Tao, J.; Perdew, J. P.; Staroverov, V. N.; Scuseria, G. E., *Phys. Rev. Lett.* **2003,** *91*, 146401.
47. Csonka, G. I.; Perdew, J. P.; Ruzsinszky, A.; Philipsen, P. H.; Lebègue, S.; Paier, J.; Vydrov, O. A.; Ángyán, J. G., *Phys. Rev. B* **2009,** *79*, 155107.
48. Staroverov, V. N.; Scuseria, G. E.; Tao, J.; Perdew, J. P., *J. Chem. Phys.* **2003,** *119*, 12129-12137.
49. Zhao, Y.; Truhlar, D. G., *J. Chem. Theory Comput.* **2005,** *1*, 415-432.
50. Zhao, Y.; Truhlar, D. G., *J. Phys. Chem. A* **2005,** *109*, 5656-5667.
51. Becke, A. D., *J. Chem. Phys.* **1993,** *98*, 5648-5652.
52. Vosko, S.; Wilk, L.; Nusair, M., *Can. J. Phys.* **1980,** *58*, 1200-1211.
53. Stephens, P.; Devlin, F.; Chabalowski, C.; Frisch, M. J., *J. Phys. Chem.* **1994,** *98*, 11623-11627.
54. Staroverov, V. N.; Scuseria, G. E.; Tao, J.; Perdew, J. P., *Phys. Rev. B* **2004,** *69*, 075102.
55. Kristyán, S.; Pulay, P., *Chem. Phys. Lett.* **1994,** *229*, 175-180.
56. Hobza, P.; Reschel, T., *J. Comput. Chem.* **1995,** *16*, 1315-1325.
57. Pérez-Jordá, J.; Becke, A. D., *Chem. Phys. Lett.* **1995,** *233*, 134-137.
58. Pérez-Jordá, J. M.; San-Fabián, E.; Pérez-Jiménez, A. J., *J. Chem. Phys.* **1999,** *110*, 1916-1920.
59. Grimme, S., *Angew. Chem., Int. Ed.* **2006,** *45*, 4460-4464.
60. Dion, M.; Rydberg, H.; Schröder, E.; Langreth, D. C.; Lundqvist, B. I., *Phys. Rev. Lett.* **2004,** *92*, 246401.

61. Tao, J.; Perdew, J. P., *J. Chem. Phys.* **2005,** *122*, 114102.
62. Ruzsinszky, A.; Perdew, J. P.; Csonka, G. I., *J. Phys. Chem. A* **2005,** *109*, 11015-11021.
63. Zhao, Y.; Schultz, N. E.; Truhlar, D. G., *J. Chem. Theory Comput.* **2006,** *2*, 364-382.
64. Zhao, Y.; Truhlar, D. G., *J. Phys. Chem. C* **2008,** *112*, 4061-4067.
65. Hohenstein, E. G.; Chill, S. T.; Sherrill, C. D., *J. Chem. Theory Comput.* **2008,** *4*, 1996-2000.
66. Grimme, S.; Antony, J.; Ehrlich, S.; Krieg, H., *J. Chem. Phys.* **2010,** *132*, 154104.
67. von Lilienfeld, O. A.; Tkatchenko, A., *J. Chem. Phys.* **2010,** *132*, 234109.
68. Grimme, S., *J. Comput. Chem.* **2004,** *25*, 1463-1473.
69. Kannemann, F. O.; Becke, A. D., *J. Chem. Theory Comput.* **2010,** *6*, 1081-1088.
70. Steinmann, S. N.; Csonka, G.; Corminboeuf, C., *J. Chem. Theory Comput.* **2009,** *5*, 2950-2958.
71. Steinmann, S. N.; Corminboeuf, C., *J. Chem. Theory Comput.* **2010,** *6*, 1990-2001.
72. Liu, Y.; Goddard, W. A. I., *Mat. Trans.* **2009,** *50*, 1664-1670.

CHAPTER 2

GLYCINE ISOMERIZATION VIA QUANTUM TUNNELING[*]

[*] He, K; Allen, W. D. To be submitted to *Journal of Chemical Theory and Computation*

Abstract

The glycine conformer **IIIp** has been repeatedly observed in low-temperature matrix isolation infrared (MI-IR) experiments despite its low barrier for isomerization to the global minimum **Ip**; however, the lower-lying **IVn** conformer has yet to be conclusively detected. The elusiveness of **IVn** has been attributed to the **IVn** → **Ip** interconversion. Conformer **VIp** has been prepared in low-temperature matrices by near-infrared (NIR) laser irradiation of the first OH stretching overtone of conformer **Ip**, and **VIp** was found to convert back to **Ip** by hydrogen-atom tunneling. High-level *ab initio* electronic structure computations, including extrapolations to the complete basis set (CBS) limit have been executed here to obtain highly precise relative energies for all conformers of glycine (**Gly**). An uncertainty of 0.03 kcal mol^{-1} for relative energies has been reached. The same FPA scheme was utilized to compute barrier heights for tunneling relaxation paths of the glycine conformers. These processes include interconversion through rotation about the C–O bond (**VIp** → **Ip**, **VIIIn** → **IVn**, and **VIIp** → **IIIp**), N–C bond (**IVn** → **Ip** and **Vn** → **IIIp**), and C–C bond (**IIIp** → **Ip**). Final potential energy curves for glycine interconversions were computed from MP2/cc-pVTZ reaction paths and high-quality AE-CCSD(T)/cc-pCVTZ energy points. The quantum tunneling dynamics was treated within a reaction-path Hamiltonian model with transmission probabilities given by the standard WKB (Wentzel-Kramers-Brillouin) formula in terms of barrier penetration integrals, which were computed numerically from our electronic structure data. The

tunneling lifetime is obtained by ascribing a 'collision' energy equivalent to the zero-point vibrational energy (ZPVE) of the reaction mode, evaluating the WKB transmission coefficient at this energy, and multiplying by the classical rate at which the reactant hits the barrier.

The **VIp** → **Ip** tunneling half-life of glycine was computed to be 1.68 s, in excellent agreement with the extrapolated half-life of 2.8 ± 1 s in Xe matrices from the MI-IR experiments. The FPA barrier heights for the **IIIp** → **Ip** and the **IVn** → **Ip** interconversions are 0.83 and 3.18 kcal mol^{-1}, respectively. Despite the much smaller barrier, the **IIIp** → **Ip** interconversion has a much longer tunneling half-life (25 h). The elusiveness of **IVn** should be attributed to the rapid tunneling isomerization to **Ip**, with a predicted half-life of 6.16×10^{-8} s.

2.1 Introduction

As probably the most studied biologically important molecule, there are questions still open concerning glycine's conformational distribution and dynamics. Numerous theoretical studies have worked to establish the relative energies of the glycine conformers and the barriers for their interconversion.[1-3] The structures of the eight existing conformers are presented in Figure 2.1 using conformational labels of both Balabin[4] and Császár[5] and subsequent studies.[6] The relative energies with thermal corrections[4-7] imply that at least four conformers should be present in detectable amounts in the gas phase in the 358-438 K temperature range. The expected abundance is roughly 60% for the lowest-energy conformer (**Ip**), and 10-20% for the next three conformers each (**IIn**, **IVn**, and **IIIp**).[7]

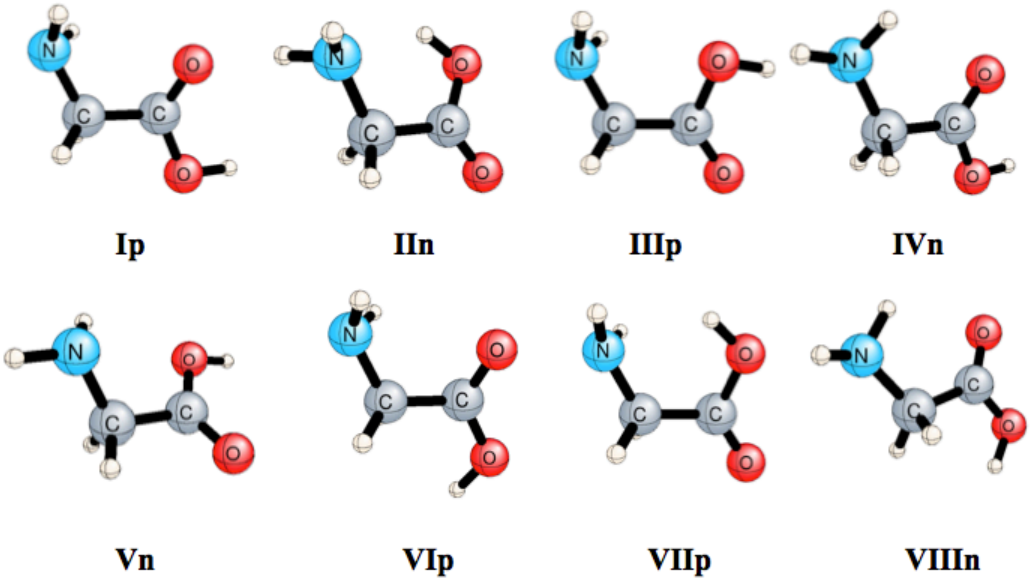


Figure 2.1 Structures of glycine conformers

The numbering of the conformers (I–VIII) reflects the increasing relative energies of the respective "planar" forms of glycine obtained from MP2/6-311++G** geometry optimizations.[8]

Early microwave (MW) spectroscopic studies identified only conformer **IIn.**[9-12] Due to its small dipole moment the observation of the lowest-energy **Ip** conformer using MW spectroscopy was more challenging, but it was identified only a few years later.[13] The other two low-energy conformers (**IVn** and **IIIp**) were not identified in the gas phase even in the latest MW experiments.[14-16] The absence of spectral signatures these two conformers was explained by conformational cooling to the **Ip** form via low-energy interconversion barriers in the free jet expansion, and by the small dipole moment of **IIIp**.[17]

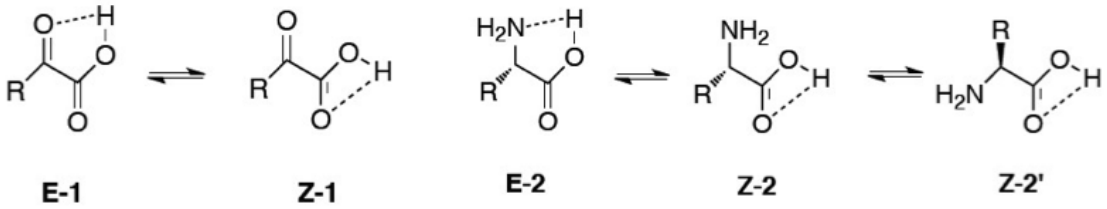
The structural parameters and conformational distribution of glycine were also studied using gas-phase electron diffraction[18] (GED). Conformer **Ip** was shown to be the most stable form by this method as well. In addition the abundances of the other conformers were observed to be about 24% at 492 K. As electron diffraction can only give the position of non-hydrogen atoms and cannot differentiate between arrangements of hydrogen atoms, it was only supposed that the minor components are a mixture of **IIn** and **IIIp** conformers.

The first matrix-isolation IR studies identified the **Ip** and **IIn** conformers of glycine.[19-20] Later matrix-isolation studies showed that the **IIIp** conformer can also be trapped in the matrix if the sample is deposited below 13 K.[21-27] The **IIIp** conformer can be converted to the **Ip** conformer by annealing the Ar matrix at 20-35 K,[21, 27] while the relative ratio of the **IIIp** conformer can be increased by the UV irradiation of the matrix.[23-24] The same three conformers were observed in the IR spectrum of glycine in He droplets.[25] In none of these studies was the fourth low-energy conformer (**IVn**) identified.

In order to understand the cause of the missing conformers in the MW, MI-IR and He droplet measurements, Miller et al.[7, 28] investigated the interconversion barriers and the collision-induced conformational change in glycine using quantum dynamical computations. They concluded that the **IVn → Ip** and the **IIIp →Ip** barrier heights are almost equal. Although they found that the **IVn → Ip** conversion process involves both classical and hydrogen-tunneling effects, while for the **IIIp → Ip** conversion only classical effects contribute, their calculations presented little indication that the **IVn → Ip** occurs more readily than the **IIIp → Ip** conversion process. They have also noted that according to earlier computations,[29] the C=O, N–H and O–H stretching regions of the IR spectra of conformers **IVn** and **Ip** are almost identical, while the C–H stretching of **IVn** is predicted to be much better resolved from the other free low-energy conformers. Based on this theoretical prediction, Linder et al.[30] tentatively assigned a weak shoulder at 2868 cm^{-1} in the 520 K gas-phase FT-IR spectrum to conformer **IVn**. Balabin also identified this conformer by jet-cooled Raman spectroscopy at short distance from the nozzle.[31] Increasing the distance between the observation point and the nozzle outlet, the intensity of the bands assigned to **IVn** dropped rapidly. Interestingly, he observed only conformers **Ip**, **IIn**, and **IVn** were observed. In a very recent study the same author concluded that very likely four conformers are present in the gas phase, but the signature of **IIIp** was seen only by decomposition of a broad, unresolved band and by comparison the relative intensities of the bands in the Raman spectra measured at 380 K in the gas phase and at low temperature in the jet expansion.[32]

Schreiner and co-workers[33] have shown that α-keto carboxylic acid **(E)-1** (R=Phenyl) undergoes tunneling isomerization to **(Z)-1** (R=Phenyl) in matrix-isolation studies

(Figure 2.2). The structure of amino acid conformers bears a similarity to that of α-keto carboxylic acids because the Lewis-basic keto group of **1** simply replaces the Lewis-basic amino group. Despite reports on the tunneling isomerization of formic as well as acetic acid, the amino acids have not been examined regarding their conformational isomerization due to tunneling until very recently.[34-36]



R=H, CH_3, aryl, cyclopropyl

Figure 2.2 Isomerization scheme for α-keto carboxylic acids and α-amino acids

Structures are shown for α-Keto carboxylic acids (**1**) in their *E* and *Z* forms (referring to the C–O bond rotation; *E* forms generally are energetically preferred) and the analogy to α-amino acids (**2**).

Tarczay et al.[34-36] attempted the preparation of higher-energy amino acid conformers in cryogenic matrices by narrow band near-infrared (NIR) and ultraviolet (UV) laser irradiation. Broad-band UV irradiation could be used to change the conformer ratio of glycine in the matrix.[23] Varying the wavelength of narrow-band UV laser irradiation was expected to give more flexibility in changing the conformer ratios, i.e. irradiation at different wavelengths can result in different conformers and different ratios. Narrow-band NIR irradiation (produced either by a laser source or by filtering a broad-band source) was successfully applied for example to induce *cis-trans* isomerization in carboxylic acids,[36-41] as well as rotamerization of the hydroxyl group of allyl alcohol,[42] 1-

propanol,[43] cytosine,[44-45] and hydroxyacetone[46] in low-temperature matrices by the excitation of the first overtone or a combination band of the OH stretching mode of a selected conformer. On the basis of molecular dynamics simulations,[47-48] it has been shown that the energy from the first excited OH stretching state of glycine flows into five other vibrational modes on the picosecond time scale. Kr and N_2 matrices were also used besides Ar, because in Kr matrixes NIR irradiation can more efficiently induce conformational change than in Ar matrixes,[35] whereas in N_2 matrices the lifetime of short-lived higher energy conformers can be longer than in Ar and Kr matrixes.[35-36, 49] The tunneling at 12 K of **Gly-VIp → Gly-Ip** and **Ala-VI → Ala-I** (alanine) were reported with observed half-lives of 2.8–4.4 s and 2.8–5.7 s in Ar.

The purpose of the present study is to provide high accuracy relative energies of glycine conformers, as well as the barrier heights of the rotational isomerizations. A search for transition states of all possible interconversions to the lowest-four glycine conformers has been executed, with an emphasis on the two interconversion processes **IIIp → Ip** and **IVn → Ip**, two rotamerization processes with similar barrier heights. Based on the experimental evidence that glycine **IVn** conformer is extremely elusive even under low-temperature matrix-isolation IR experiments, combined with our theoretical prediction that this conformer is likely converted to the lower energy conformer **Ip** by fast rotational tunneling, the elusiveness of **IVn** conformer is explained.

2.2 Computational Methods

2.2.1 Geometry Optimizations and FPA Energies

The geometry optimization of the eight glycine conformers was performed at the MP2/cc-pVTZ level, and a search of the transition states (**TS**) was carried out at the same level of theory by rotating all heavy-tom bonds (C–C, C–O, N–C). Both ground states and transition states were further optimized at the MP2/aug-cc-pVTZ level and subject to focal point analyses (See section 1.1.3) to determine highly accurate relative energies and interconversion barrier heights. Auxiliary corrections including ZPVE were obtained via MP2/cc-pVTZ with anharmonicities were computed at MP2/6-31G*. Core electron corrections were computed at MP2/aug-cc-pCVTZ level.

2.2.2 Tunneling Analysis

Intrinsic reaction paths (IRP) were obtained at MP2/cc-pVTZ with CCSD(T)/cc-pCVTZ single-point energies superimposed. The vibrational frequencies were computed at MP2/cc-pVTZ with anharmonicities obtained at MP2/6-31G*. The ZPVE corrections along the IRP were obtained using the unified internal projection scheme implemented in the INTDER 2005 program.[50] The final energy profiles consist of the high-level energy points and the ZPVE corrections along the reaction curve. A Fourier fit of the overall energy points was employed to express the potential energy (*V*) in terms of the arc length *s* in mass-weighted Cartesian coordinates along the IRP, as well as to construct a smooth curve connecting the two minima and the transition state. Tunneling probabilities $\kappa(\varepsilon)$ were evaluated by numerically computing one-dimensional barrier penetration integrals $\theta(\varepsilon)$ along the IRP and invoking the WKB (Wentzel-Kramers-Brillouin) formula

$$\kappa(\varepsilon) = \frac{1}{1 + e^{2\theta(\varepsilon)}}, \tag{2.1}$$

in which

$$\theta(\varepsilon) = \int_{s_1}^{s_2} \sqrt{2[V(s) - \varepsilon]ds}, \tag{2.2}$$

where ε is the collision energy, s_1 and s_2 are the classical turning points where the $V(s) = \varepsilon$, and atomic units are assumed throughout. The collision energy (ε) was equated to the ZPVE of the reaction mode $(\omega_i/2)$, because at 11 K virtually all molecules reside in the ground vibrational state. The tunneling half-life of deuterated glycine **VIp → Ip** and **IVn → Ip** are also reported. The quantum chemistry packages MOLPRO (2010.1),[51] CFour (v1.0),[52] GAMESS,[53] MPQC (2.3),[54] and QChem (4.0)[55-56] were used in this study.

2.3 Results and Discussion

2.3.1 Geometries and Relative Energies

The amine and carboxyl group in glycine can both contribute as donor or acceptor when forming a hydrogen bond. Four types of hydrogen bonds can occur: type **a**, carboxyl hydrogen acting as proton-donor bonding with carbonyl oxygen and adapting a *cis* conformation; **b**, COOH group in the *trans* conformation and acting as a proton donor to the amine nitrogen; **c**, NH_2 group acting as proton donor to the carboxylic oxygen; **d**, NH_2 group acting as proton donor to the carbonyl oxygen. Glycine conformers can be categorized into four classes based on the different preference and combination of the four types of hydrogen bonds: **ad**, **ac**, **b**, and **d**. When COOH is in the *cis* conformation, the carboxylic hydrogen is already involved in hydrogen bonding with the carbonyl oxygen, whereas the NH_2 is most likely forming a hydrogen bond with either the carbonyl (**d** type) or carboxylic (**c** type) oxygen simultaneously (**ad**: **Ip**, **IVn**; **ac**: **IIIp**, **Vn**). When COOH is in the *trans* conformation, either **b** or **d** type hydrogen bond is present (**b**: **IIn**, **VIIp**; **d**: **VIp**, **VIIIn**).

The results of our FPA relative energies, as well as single-point energies computed at the reference geometry obtained at each level of theory can be found in Table 2.1. The energy ordering is nearly identical with the labeling in all cases, except that **IIIp** is lower lying than **IVn** at MP2/6-31G* (see Table 2.2). The mean absolute deviation of MP2/aug-cc-pVTZ values from CCSD(T)/CBS is only 0.36 kJ mol^{-1}. Thus, MP2/aug-cc-pVTZ performs even better than the CCSD/cc-pVTZ level, demonstrating the importance of diffuse functions when pin-pointing the energetics of the conformers. The main

difference between MP2/aug-cc-pVTZ from CCSD(T)/CBS comes from **IIn** (1.49 kJ mol^{-1}), which is the one showing the largest MP2 correlation correction (See Table 2.2).

Table 2.1 Focal Point Analyses for the Relative Energies of the Glycine Conformers[a]

	Basis[a]	**Ip**	**IIn**	**IVn**	**IIIp**	**Vn**	**VIp**	**VIIp**	**VIIIn**
ΔE_e(RHF)	ADZ	0.00	3.41	1.64	2.12	2.84	5.73	7.98	7.51
	ATZ	0.00	3.29	1.56	2.12	2.85	5.63	7.66	7.29
	AQZ	0.00	3.29	1.56	2.13	2.86	5.60	7.63	7.25
	A5Z	0.00	3.30	1.56	2.13	2.86	5.61	7.63	7.25
	CBS	0.00	3.31	1.55	2.14	2.86	5.61	7.64	7.25
δ[MP2]	ADZ	+0.00	−2.88	−0.37	−0.53	−0.41	−0.86	−1.91	−1.22
	ATZ	+0.00	−2.96	−0.41	−0.49	−0.34	−0.76	−1.90	−1.22
	AQZ	+0.00	−2.96	−0.42	−0.48	−0.30	−0.73	−1.90	−1.20
	A5Z	+0.00	−2.95	−0.41	−0.47	−0.29	−0.71	−1.90	1.18
	CBS	+0.00	−2.93	−0.40	−0.46	−0.27	−0.69	−1.90	1.15
δ[CCSD]	ADZ	+0.00	+0.69	+0.10	+0.15	+0.05	−0.04	+0.43	+0.07
	ATZ	+0.00	+0.75	+0.12	+0.15	+0.07	+0.02	+0.50	+0.15
	AQZ	+0.00	+0.78	+0.13	+0.16	+0.08	+0.04	+0.52	+0.17
δ[CCSD(T)]	ADZ	+0.00	−0.43	−0.02	−0.09	−0.02	−0.13	−0.31	−0.15
	ATZ	+0.00	−0.47	−0.03	−0.09	−0.01	−0.13	−0.35	−0.17
	AQZ	+0.00	−0.48	−0.03	−0.09	−0.01	−0.14	−0.36	−0.18
ΔE_e(CCSD(T)/CBS)		0.00	0.68	1.25	1.75	2.65	4.82	5.91	6.90
Core Correction		+0.00	+0.00	−0.01	+0.02	+0.03	+0.03	−0.02	+0.01
Harmonic ZPVE		+0.00	+0.41	+0.02	+0.05	+0.05	−0.15	−0.09	−0.19
Anharm ZPVE		+0.00	−0.08	−0.04	+0.1	−0.03	+0.00	−0.14	−0.07
ΔE_0(FPA)		**0.00**	**1.01**	**1.22**	**1.83**	**2.70**	**4.70**	**5.66**	**5.84**

[a]All values given in kcal mol^{-1}. Basis set abbreviations: A*n*Z = aug-cc-pV*n*Z, *n*= D, T, Q, 5. ΔE_e denotes a vibrationless relative energy between conformers. δ denotes an increment with respect to the preceding level of theory in the hierarchy RHF → MP2 → CCSD → CCSD(T). Δ(core)= core electron correlation corrections; Δ(ZPVE, harm)= relative energy change due to harmonic ZPVE; δ(anharm) = anharmonicity correction to Δ(ZPVE, harm). ΔE_0(FPA) = ΔE_e(RHF,CBS) + δ(MP2,CBS) + δ(CCSD,ATZ) + δ(CCSD(T),ATZ) + Δ(core) + Δ(ZPVE, harm) + δ(anharm).

The RHF relative energies are converged to within 0.01 kcal mol^{-1} with the aug-cc-pV5Z basis. Similarly, the MP2/aug-cc-pV5Z correlation increments match the extrapolated values within 0.03 kcal mol^{-1} for all conformers. For the coupled-cluster increments, the aug-cc-pVQZ result matches the aug-cc-pVTZ result within 0.03 kcal mol^{-1}. Corrections due to quadruple and higher excitations are estimated to be 0.01 kcal

mol^{-1} at most. Zero-point vibrational corrections are generally insensitive to the level of theory and should not be greater than 0.02 kcal mol^{-1}. In summary, we estimate a standard error of 0.03 kcal mol^{-1} for our predicted conformational energies.

Table 2.2 Comparison of Conformational Energies of Glycine (kJ mol^{-1}) for Different Levels of Theory Without Zero-Point Vibrational Correction and Core Correction

	CCSD(T)/CBS	MP2/6-31G*	MP2/TZ	MP2/ATZ	CCSD/TZ
Ip	0.00	0.00	0.00	0.00	0.00
IIn	2.85	5.00	1.57	1.35	4.35
IVn	5.23	8.68	5.92	4.78	6.08
IIIp	7.32	6.82	6.79	6.85	7.53
Vn	11.09	12.99	11.91	10.52	12.03
VIp	20.17	27.15	21.24	20.39	21.66
VIIp	24.73	34.79	25.43	24.12	27.00
VIIIn	25.48	37.06	27.51	25.39	28.17
MAD		3.81	0.78	0.36	0.74
Max(AD)		11.58	2.03	1.49	2.69

CCSD(T)/CBS denotes the extrapolated value from the focal point analysis based on geometry optimized at MP2/aug-cc-pVTZ level. TZ=cc-pVTZ, ATZ=aug-cc-pVTZ. All single point energies were computed at the geometry optimized at each level of theory.

2.3.2 Interconversion Pathways and Barriers

It is well known that molecules in higher rotational energy states collisionally relax with high efficiency to lower rotational energies in free-jet expansions. The relaxation of higher energy conformers in cases of simple hindered internal rotations has been used to explain why some conformers (**IIIp** and **IVn**), predicted by *ab initio* computations to be low in energy, are not detected in jet spectroscopy. For jets of argon operating at room temperature, Ruoff et al.[17] found that when the barrier to internal rotation was less than ≈ 1.2 kcal mol^{-1}, relaxation to a lower energy conformer occurred, but with higher barriers the abundances of the conformers were "frozen" at the temperature prior to expansion.

The main processes involved in interconversions of conformers of glycine are the $Z \rightarrow E$ conversion of the carboxyl group, the rotation of the NH_2 group around the N–C bond, and the rotation of the carboxyl group around the C–C bond. Within each class of conformers (**ac**, **ad**, **b**, and **d**), the structures differ by the orientation of the NH_2 group (e.g. **IVn** → **Ip**). The rotation of the amino group from staggered through eclipsed conformations of methylamine involves a barrier of ≈ 2.6 kcal mol^{-1}. It is evident that the $Z \rightarrow E$ transformation for formic acid requires the surmounting of a larger barrier of about 8.6 kcal mol^{-1}. Godfrey et al.[57] suggested that the critical height for glycine conformers in the heated argon-seeded jet is ≈ 2.3 kcal mol^{-1}. Hence the probabilities of interconversions that overcome the rotational barrier could be estimated once highly accurate barrier heights are obtained.

A complete search of the transition states for the relaxation to the lowest four conformers (**Ip**, **IIn**, **IIIp**, and **IVn**) was completed with the rotamerization barrier height pin-pointed via the FPA method (see Appendix Table A.5). Those interconversion paths

via rotation about the N–C, C–C, and C–O bonds were presented in Table 2.4 with an emphasis on the **IIIp** → **Ip**, **IVn** → **Ip**, and **VIp** → **Ip** cases.

Let us first consider conformer **IIIp**. Figure 2.3 shows that the pathway between **IIIp** and **Ip** is very flat with a barrier height of 0.83 kJ mol^{-1}. This is low enough for a full relaxation of **IIIp** to **Ip** as observed in the heated jet spectroscopy experiment.[15, 57] However, **IIIp** cannot relax to **IIn** because the barrier separating these two is very high (14.3 kcal mol^{-1}),[57] which is not surprising because the interconversion involves not only the rotation of the COOH group, but also the transformation of it from *cis* to *trans* configuration. Conformer **IIn** is slightly less stable than **Ip**, but relaxation of **IIn** to **Ip** is excluded in this study. From the experimental observation[15] it is clear that **IIn** does not relax efficiently to **Ip** because appreciable proportions of **IIn** are detected by jet spectroscopy, also due to the high conformational barrier.

The rotation of the –COOH group about the C–C bond (**IIIp** → **Ip**) has the lowest barrier height (0.83 kcal mol^{-1}). The barrier height for the rotation of the $–NH_2$ group about the N–C bond is slightly higher than the predicted critical height. Hence in room temperature free-jet spectroscopy experiments, **IVn** and **Vn** could easily interconvert to **Ip** and **IIIp** with barrier heights of 3.18 and 3.07 kcal mol^{-1}, respectively. The interconversions involve the rotation of the –OH group about C–O bond have an average barrier height of 6.8 kcal mol^{-1}. The interconversions of **IVn** and **Vn** to **IIn** are not followed in the jet because this involves a rotation of the HOCO angle from 0° to 180°, as well as rotation about the C–C and N–C bonds, resulting in a very high barrier around 12 kcal mol^{-1} (see Appendix Table A.5).

The inert-gas matrix environment hinders the rotation of the molecules studied, and for samples deposited at temperature below 13 K, additional bands corresponding to **IIIp** appear in the IR spectra of matrix-isolated glycine.[58-59] However, a temperature of 20 K was high enough for conformer **IIIp** to interconvert to the lower energy conformer **Ip**. Thus is not unreasonable to assume that under the same low-temperature matrix conditions, **IVn** should also be detectable with a higher barrier to **Ip**. But the fact is that in none of these MI-IR studies was **IVn** identified. [27, 58-59]

Table 2.3 Focal-point Analysis of Barrier Heights for Glycine Interconversions

		C–C	N–C	C–O	N–C	C–O	C–O
	Basis	IIIp → Ip	IVn → Ip	VIp → Ip	Vn → IIIp	VIIp → IIIp	VIIIn → IVn
ΔE_e(RHF)	ADZ	0.89	4.23	6.40	4.27	6.79	6.50
	ATZ	0.86	3.81	6.43	3.78	7.01	6.57
	AQZ	0.87	3.75	6.47	3.71	7.06	6.62
	A5Z	0.87	3.75	6.48	3.71	7.06	6.62
	CBS	0.87	3.75	6.48	3.71	7.06	6.62
δ[MP2]	ADZ	–0.38	+0.33	+1.04	+0.41	+1.65	+1.04
	ATZ	–0.25	+0.42	+1.03	+0.57	+1.76	+1.04
	AQZ	–0.24	+0.30	+1.07	+0.42	+1.84	+1.07
	A5Z	–0.24	+0.25	+1.08	+0.37	+1.87	+1.09
	CBS	–0.24	+0.20	+1.10	+0.32	+1.91	+1.11
δ[CCSD]	ADZ	+0.02	+0.26	–0.48	+0.27	–0.93	–0.50
	ATZ	+0.07	+0.23	–0.48	+0.23	–0.90	–0.49
	AQZ	+0.09	+0.21	–0.47	+0.21	–0.89	–0.49
δ[CCSD(T)]	ADZ	–0.10	+0.14	+0.19	+0.12	+0.30	+0.20
	ATZ	–0.09	+0.13	+0.20	+0.12	+0.34	+0.22
	AQZ	–0.09	+0.13	+0.21	+0.12	+0.34	+0.22
ΔE_e(CCSD(T)/CBS)		0.63	4.29	7.31	4.36	8.42	7.47
Δ(core)		+0.02	–0.12	+0.02	–0.16	+0.09	+0.05
Δ(ZPVE, harm)		+0.18	–1.00	–1.00	–1.13	–0.96	–1.07
ΔE_0(FPA)		0.83	3.18	6.33	3.07	7.55	6.45

[a]All values given in kJ mol^{-1}. Basis set abbreviations: A*n*Z = aug-cc-pV*n*Z, *n*= D, T, Q, 5. ΔE_e denotes a vibrationless relative energy between conformers. δ denotes an increment with respect to the preceding level of theory in the hierarchy RHF → MP2 → CCSD → CCSD(T). Δ(core)= core electron correlation corrections; Δ(ZPVE, harm)= relative energy change due to harmonic ZPVE; δ(anharm) = anharmonicity correction to Δ(ZPVE, harm). ΔE_0(FPA) = ΔE_e(RHF,CBS) + δ(MP2,CBS) + δ(CCSD,ATZ) + δ(CCSD(T),ATZ) + Δ(core) + Δ(ZPVE, harm).

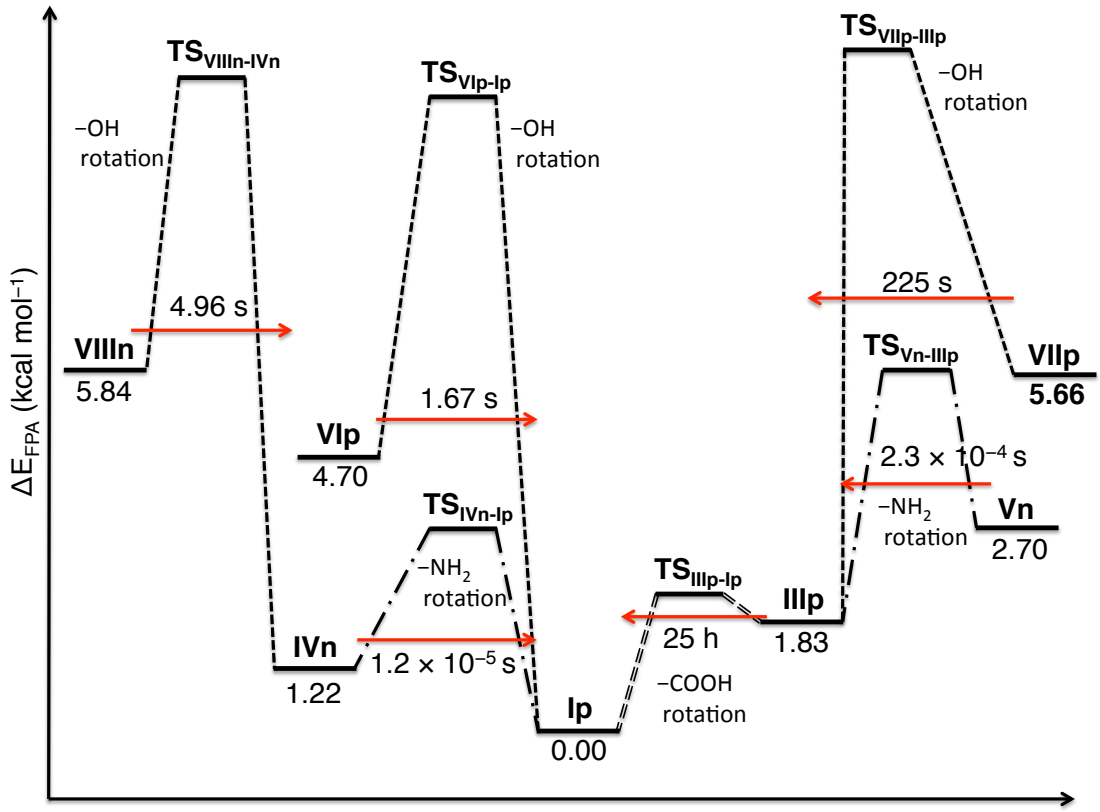


Figure 2.3 FPA relative energies (kcal mol^{-1}) and tunneling half-lives for glycine conformers

Rotation of the –OH group about the C–O bond: **VIIIn** → **IVn**, **VIIp** → **IIIp**, **VIp** → Ip; rotation of the –NH_2 group about the N–C bond: **IVn** → **Ip**, **Vn** → **Ip**; rotation of the –COOH group about the C–C bond: **IIIp** → **Ip**.

2.3.3 Tunneling Analysis

The quantum dynamical computations of Miller et. al's[28] give the dependence of matrix-induced (Ar, Ne, and He) interconversion probability on the collision energy of the **IIIp** → **Ip** and **IVn** → **Ip** interconversions. For collision energies in excess of the torsional barrier, neither **IIIp** → **Ip** nor **IVn** → **Ip** interconversion appears to be favored. However, the calculated **IIIp** → **Ip** probabilities appear to be sensitive to whether the collision energy is higher or lower than the torsional potential-energy barrier, whereas the **IVn** → **Ip** interconversion probabilities are not. Since **IIIp** → **Ip** interconversion corresponds to rotation about the C–C bond, it is likely that it proceeds via a classical mechanism. On the other hand, substantial He-induced interconversion is calculated at collision energies below that of the interconversion barrier for the bare glycine molecule. No classical mechanism exists for this interconversion process, since the energy of the He atom is insufficient to knock conformer **IVn** over the barrier and the interaction potential He atom is unable to lower the barrier. All the interconversion probability observed in this low-energy regime must therefore arise from quantum effects. Hence it is not unreasonable to assume that **IVn** → **Ip** interconversion is at least partially due to quantum tunneling.

Tunneling analysis was performed for all interconversions from the higher-energy conformer to the three lowest-energy (**Ip**, **IIn**, **IVn** and **IIIp**) conformers (see Appendix Table A.7). We first focus on the two important interconversions of special interest, in the hope that tunneling analysis will provide extra evidence to elucidate the mechanism of the **IIIp** → **Ip** and **IVn** → **Ip** interconversions. The predicted tunneling half-lives of the **IIIp** → **Ip** and **IVn** → **Ip** interconversion are 25 h and 1.2×10^{-5} second, respectively (see

Figure 2.3). The long tunneling half-life for **IIIp** → **Ip** should be due to the low collision energy (0.05 kcal mol^{-1}) (see Appendix Table A.7). On the other hand, **IVn** → **Ip** interconversion is obviously mainly dominated by a quantum effect, as demonstrated by the very small half-life, indicating that this is an almost instantaneously process on the time scale of the experiments.

Other interconversions predicted to have fast tunneling are: **VIp** → **Ip**, **VIIp** → **IIIp**, and **VIIIn** → **IVn** about the C–O bond rotation; aw well as **Vn** → **IIIp** about the N–C bond rotation. Among those interconversions, **VIp** → **Ip** is the most promising to be detectable in experiment, due to the fact that **Ip** is the global minimum, thus with the highest abundance.

Tarczay et al.[35-36] prepared glycine and glycine-N,N,O-d_3 in low-temperature Ar, Kr, Xe, and N_2 matrices by NIR laser irradiation of the first OH stretching overtone of conformer **Ip**. In order to determine the decaying lifetime, scans as short as possible were recorded, i.e., single scans were recorded with 3.8 s repetition rate. A clearly noticeable band at 1256.6 cm^{-1} was observed in the spectra recorded during the irradiation, but completely missing from the spectra recorded in a few minutes after switching off the laser. This is very close to the predicted –OH bending mode at 1258 and 1267 cm^{-1} of conformer **VIp** and **VIIIn**, respectively. This band is assigned to the **VIp** conformer because it differs from **Ip** only in the *cis-trans* structure of the carboxyl group. Conformer **VIp** was found to convert back to **Ip** in the dark by rotational tunneling. The observed half-lives of **VIp** in Ar matrices were 4.4 ± 1 s. This result is in correspondence with the observation for the *cis-trans* conversion of formic and acetic acids. This is also in excellent agreement with our theoretical predicted half-life of 1.67 s. To further

support our prediction, the computation of **VIp**-$d_3 \rightarrow$ **Ip**-d_3 is on the order of hours, which is also in good qualitative agreement with experiment for the isotopologues. (see Table 2.4.3)

Besides the OH stretching overtone, the NH stretching overtone band of **Ip** was also irradiated. Increases of bands that might be assigned to **IVn** were not observed. This is not an unexpected outcome according to our theoretical prediction, since the decaying half-life from higher-energy **IVn** to **Ip** was predicted to be on the order of nanoseconds, much too small for detection under experimental conditions (single scan at 3.6 s repetition). We also carried out the tunneling analysis for **IVn**-d_3 → **Ip**-d_3, and the corresponding half-life indeed increased, but it is still too fast to be identifiable (see Table 2.4.2).

Table 2.4.1 Important Tunneling Parameters for the Interconversion **IIIp → Ip**

IIIp → Ip	**IIIp-d_3 → Ip-d_3**
Collision energy (ε) = 0.05 kcal mol^{-1}	Collision energy (ε) = 0.02 kcal mol^{-1}
Collision frequency (ω_0) = 16 cm^{-1}	Collision frequency (ω_0) =16
Barrier[a] = 0.77 kcal mol^{-1}	Barrier[a] =0.77 kcal mol^{-1}
Turning points (s_1, s_2) = (–9.52, 3.62) au	Turning points (s_1, s_2) = (–10.21, 3.88) au
Effective penetration integral (θ) = 19	Effective penetration integral (θ) = 21
Transmission probability (κ) = 1.57×10^{-17}	Transmission probability (κ) = 1.10×10^{-18}
Half-life τ = 25 h	Half-life τ = 356 h

[a]The effective barriers for tunneling differ from the FPA value and from one another because one specific frequency corresponding to the reaction mode has been projected out at all points along the IRP.

Table 2.4.2 Important Tunneling Parameters for the Interconversion **IVn → Ip**

IVn → Ip	**IVn-d_3 → Ip-d_3**
Collision energy (ε) = 0.28 kcal mol^{-1}	Collision energy (ε) = 0.23 kcal mol^{-1}
Collision frequency (ω_0) = 196 cm^{-1}	Collision frequency (ω_0) =163
Barrier[a] = 3.85 kcal mol^{-1}	Barrier[a] =5.10 kcal mol^{-1} cm^{-1}
Turning points (s_1, s_2) = (–1.03, 0.96) au	Turning points (s_1, s_2) = (–1.86, 1.73) au
Effective penetration integral (θ) = 6.58	Effective penetration integral (θ) = 13
Transmission probability (κ) = 1.92×10^{-6}	Transmission probability (κ) = 1.36×10^{-11}
Half-life τ = 6.16×10^{-8} s	Half-life τ = 1.7×10^{-4} s

[a]The effective barriers for tunneling differ from the FPA value and from one another because one specific frequency corresponding to the reaction mode has been projected out at all points along the IRP.

Table 2.4.3 Important Tunneling Parameters for the Interconversion **VIp → Ip**

VIp → Ip	**VIp-d_3 → Ip-d_3**
Collision energy (ε) = 0.66 kcal mol^{-1}	Collision energy (ε) = 0.51kcal mol^{-1}
Collision frequency (ω_0) =463 cm^{-1}	Collision frequency (ω_0) = 355 cm^{-1}
Barrier[a] = 7.05 kcal mol^{-1}	Barrier[a] = 7.38 kcal mol^{-1}
Turning points (s_1, s_2) = (–1.93, 1.44)	Turning points (s_1, s_2) =(–2.69, 2.03)
Effective penetration integral (θ) = 14.95	Effective penetration integral (θ) =21.67
Transmission probability (κ) = 1.04×10^{-13}	Transmission probability (κ) =1.51×10^{-19}
Half-life τ = 0.48 s	Half-life τ = 120 h

[a]The effective barriers for tunneling differ from the FPA value and from one another because one specific frequency corresponding to the reaction mode has been projected out at all points along the IRP.

2.3.4 Vibrational Frequencies

IR spectroscopy could be a very suitable tool to investigate glycine conformational structures, since the IR spectra are very sensitive to the intramolecular H-bonding. Table 2.5 shows the most characteristic vibrational fundamentals of eight glycine conformers. Proper (red-shifting) hydrogen bonds weaken the covalent X-H bond, thus leading to its elongation, and respectively, to a red shift of the X-H stretching vibrations. The nature of this effect has been explained on the basis of bond orbital analysis.[60-61] It shows that a charge transfer takes place from the lone electron pair or the π-electron system of the proton acceptor to the antibonding orbitals of the proton donor. This leads to an increase of the electron density in the antibonding orbitals, which causes the weakening of the X-H chemical bond, and to its elongation. As it is seen in the molecular structures of the glycine conformers in Figure 2.1, they differ in the intramolecular H-bonds: bifurcated $NH_2 \cdots O{=}C$ H-bond in conformer **Ip** and **IVn**, $N \cdots H{-}O$ H-bond in conformer **IIn,** and bifurcated $NH_2 \cdots O{-}C$ H-bond in conformer **IIIp**.

Matrix isolation studies are affected by the so-called matrix shift, which is less pronounced for Ne than for Ar, due to the weaker interaction. One step further in the direction of nonperturbed gas-phase spectra would require the incorporation of the glycine molecule in a helium matrix, a technique hampered by serious experimental difficulties. It is possible to embed molecules in large liquid helium clusters and to carry out spectroscopy experiments. The helium clusters provide an ultracold (T_{He} = 0.4 K) and only weakly interacting environment, i.e., an almost ideal but liquid "nanomatrix". The spectra obtained for glycine trapped in helium clusters are compared with recent matrix measurements. The comparison of the results obtained with the different experimental

techniques provides consistent spectral assignments of the measured vibrational bands to specific conformers. The correlation of the measured matrix-induced frequency shifts with the critical temperature of the matrix material enables us to estimate the vibrational frequencies expected for the free gas phase. This extrapolated experimental result will be more suitable to compare with *ab initio* computations.

The O–H stretching vibration is very sensitive to hydrogen-bonding interactions, resulting in a large red-shift of the conformer **IIn** with respect to that of conformer **Ip**. In contrast, the line separation between the O–H vibrations of conformer **Ip** and **IIIp** is expected to be rather small (~2–3 cm^{-1}). Huisken et al.[25, 29] reported the estimated positions of the gas-phase O–H stretching absorption bands by extrapolating the experimental data plotted as a function of the square root of the critical temperature of the matrix material.

Because the –OH group is involved in the same intramolecular hydrogen bonds of both conformer **Ip** and conformer **IVn** (type **ad**), it may be very difficult to differentiate between the two conformers using this absorption band alone. There is no unique indication of conformer **IVn** in the –OH and –NH stretching regions above 3200 cm^{-1}. Similarly, in the C=O stretching region around 1800 cm^{-1}, the small calculated differences might be difficult to resolve experimentally. However, we do find at least one clear peak that uniquely corresponds to conformer **IVn**. It is the –CH2 stretching frequency at 2884 cm^{-1}. No fundamental absorption band from any other conformer (except for **Vn**) occurs within 75 cm^{-1} of this peak.

Table 2.5 Anharmonic Vibrational Fundamentals Glycine Conformers[a]

	ad		**ac**		**b**		**d**	
	Cis COOH, NH_2···O=C		*Cis* COOH, NH_2···CO(O)H		*Trans* COOH, OH··· NH_2		*Trans* COOH, NH_2···O=C	
	Ip	**IVn**	**IIIp**	**Vn**	**IIn**	**VIIp**	**VIp**	**VIIIn**
ν(O–H)sc	3584(75)	3586(81)	3577(79)	3586(81)	3255(292)	3546(96)	3640(60)	3641(63)
$\nu^{as}(NH_2)$	3446(7)	3469(13)	3462(7)	3464(8)	3482(18)	3536(16)	3443(9)	3469(17)
$\nu^{s}(NH_2)$	3363(4)	3385(6)	3418(3)	3397(2)	3417(1)	3444(11)	3361(5)	3378(12)
$\nu^{as}(CH_2)$	2999(4)		3015(3)		3019(5)	3013(2)	2973(8)	2932(22)
$\nu^{s}(CH_2)$	2985(14)		2970(12)		2970(10)	2992(9)	2935(22)	2900(39)
$\nu(O–H)_1$		2983(10)		3028(6)				
$\nu(O–H)_2$		2884(34)		2863(39)				
ν(C=O)	1792(231)	1801(223)	1794(231)	1801(238)	1820(283)	1819(221)	1821(187)	1822(180)
$\varrho_s(NH_2)$	1621(17)	1555(55)	1602(26)	1559(33)	1630(33)	1609(22)	1623(20)	1570(55)
$\varrho_s(CH_2)$	1439(13)	1467(11)	1440(2)	1468(3)	1439(5)	1431(4)	1468(7)	1473(8)
δ(COH)	1280(16)	1316(36)	1130(204)	1337(44)	1389(374)	1324(283)	1258(338)	1267(353)
ν(N–C)	1146(60)	1102(41)	1127(22)	1118(138)	1069(10)	1090(11)	1151(5)	1103(17)
ν(C–O)	1108(224)	1128(205)	801(70)	827(27)	1212(18)	1213(5)	1123(27)	1143(7)
$\varrho_w(NH_2)$	904(132)	819(160)	878(159)	827(118)	912(63)	888(4)	907(181)	818(154)
ϱ_t(COH)	628(89)	639(78)	660(102)	578(64)	827(82)	617(24)	444(79)	449(69)
δ(CCO)	462(31)	469(13)	609(51)	452(5)	701(7)	520(132)	465(1)	471(25)
δ(CC=O)	636(7)	633(38)	489(12)	543(29)	506(22)	489(3)	630(14)	629(8)
δ(CCN)+ δ(CCO)			257(3)	277(15)	312(20)	270(21)		
δ(CCN)+ δ(CC=O)	261(9)	268(1)					265(27)	295(12)
$\varrho_t(NH_2)$	206(45)	166(51)	262(44)	231(31)	241(16)	388(85)	194(57)	116(45)

[a] All frequencies in cm^{-1}; double-harmonic infrared intensities in km mol^{-1} given in parentheses. Harmonic frequencies and intensities were computed at the MP2/cc-pVTZ level. Anharmonic corrections were computed using MP2/6-31G*.

ν(O–H)sc: Stretching of the side chain O–H bond; ν(O–H)bb: Stretching of the back-bone COOH group O–H bond;

$\nu^{as}(NH_2)$: Asymmetric NH_2 stretching, $\nu^{s}(NH_2)$: Symmetric NH_2 stretching; δ(COH): bending of the side chain or back bone COH group; ν(C–O)sc: Stretching of the side chain C–O bond; ν(C–O)bb: Stretching of the back bone COOH group C–O bond; $\varrho_{w,}$ ϱ_t: wagging and twisting modes.

3. Conclusion

Our FPA computations gave a glycine isomerization barrier for **IVn** → **Ip** of 3.18 kcal mol^{-1}, which cannot be overcome thermally at 11 K. In contrast, **IIIp** → **Ip** exhibits an extremely low barrier height of 0.63 kcal mol^{-1} (CCSD(T)/CBS), which can be crossed classically even at 12 K. The fast tunneling of **IVn** → **Ip** can be rationalized by the small width of the barrier at energy ε, despite its higher barrier compared to that of **IIIp** → **Ip**. The predicted τ (half-life) also suggests an alternative explanation of the elusiveness the conformer **IVn**. Despite the higher barrier of **IVn** → **Ip** compared to that of **IIIp** → **Ip**, **IVn** tunnels to the global minimum **Ip**. Because of this almost instantaneous process, **IVn** disappears much too fast to be measured using current experimental setups.

References:

1. Vishveshwara, S.; Pople, J. A., *J. Am. Chem. Soc.* **1977,** *99*, 2422-2426.
2. Ramek, M.; KW Cheng, V.; Frey, R. F.; Newton, S. Q.; Schäfer, L., *J. Mol. Struct.-THEOCHEM* **1991,** *235*, 1-10.
3. Jensen, J. H.; Gordon, M. S., *J. Am. Chem. Soc.* **1991,** *113*, 7917-7924.
4. Balabin, R. M., *Chem. Phys. Lett.* **2009,** *479*, 195-200.
5. Császár, A. G., *J. Am. Chem. Soc.* **1992,** *114*, 9568.
6. Kasalova, V.; Allen, W. D.; Schaefer, H. F., III; Czinki, E.; Császár, A. G., *J. Comput. Chem.* **2007,** *28*, 1373-83.
7. Miller, I. I. I.; F., T.; Clary, D. C., *Phys. Chem. Chem. Phys.* **2004,** *6*, 2563.
8. Császár, A. G., *J. Am. Chem. Soc.* **1992,** *114*, 9568-9575.
9. Brown, R. D.; Godfrey, P. D.; Storey, J. W.; Bassez, M.-P., *J. Chem. Soc., Chem. Commun.* **1978,** 547-548.
10. R. D. Suenram, F. J. L., *J. Mol. Spectrosc.* **1978,** *72*, 372-382.The observed spectrum can be attributed to the hydrogen bonded conformation, III.
11. Sellers, H. L.; Schafer, L., *J. Am. Chem. Soc.* **1978,** *100*, 7728-7729.
12. Schaefer, L.; Sellers, H.; Lovas, F.; Suenram, R., *J. Am. Chem. Soc.* **1980,** *102*, 6566-6568.
13. Suenram, R.; Lovas, F., *J. Am. Chem. Soc.* **1980,** *102*, 7180-7184.
14. Lovas, F.; Kawashima, Y.; Grabow, J.-U.; Suenram, R.; Fraser, G.; Hirota, E., *Astrophys. J. Lett.* **1995,** *455*, L201.
15. Godfrey, P. D.; Brown, R. D., *J. Am. Chem. Soc.* **1995,** *117*, 2019-2023.
16. McGlone, S.; Elmes, P.; Brown, R.; Godfrey, P., *J. Mol. Struct.* **1999,** *485*, 225-238.
17. Ruoff, R.; Klots, T.; Emilsson, T.; Gutowsky, H., *J. Chem. Phys.* **1990,** *93*, 3142-3150.
18. Iijima, K.; Tanaka, K.; Onuma, S., *J. Mol. Struct.* **1991,** *246*, 257-266.
19. Grenie, Y.; Lassegues, J. C.; Garrigou‐Lagrange, C., *J. Chem. Phys.* **1970,** *53*, 2980-2982.
20. Grenie, Y.; Garrigou-Lagrange, C., *J. Mol. Spectrosc.* **1972,** *41*, 240-248.
21. Reva, I. D.; Plokhotnichenko, A. M.; Stepanian, S. G.; Ivanov, A. Y.; Radchenko, E. D.; Sheina, G. G.; Blagoi, Y. P., *Chem. Phys. Lett.* **1995,** *232*, 141-148.
22. Stepanian, S. G.; Reva, I. D.; Radchenko, E. D.; Rosado, M. T. S.; Duarte, M.; Fausto, R.; Adamowicz, L., *J. Phys. Chem. A* **1998,** *102*, 1041-1054.
23. Ivanov, A. Y.; Plokhotnichenko, A.; Izvekov, V.; Sheina, G.; Blagoi, Y. P., *J. Mol. Struct.* **1997,** *408*, 459-462.
24. Ivanov, A. Y.; Sheina, G.; Blagoi, Y. P., *Spectrochim. Acta, Part A* **1998,** *55*, 219-228.
25. Huisken, F.; Werhahn, O.; Ivanov, A. Y.; Krasnokutski, S., *J. Chem. Phys.* **1999,** *111*, 2978.
26. Ramaekers, R.; Pajak, J.; Lambie, B.; Maes, G., *J. Chem. Phys.* **2004,** *120*, 4182.
27. Espinoza, C.; Szczepanski, J.; Vala, M.; Polfer, N. C., *J. Phys. Chem. A* **2010,** *114*, 5919-5927.
28. Miller III, T. F.; Clary, D. C.; Meijer, A. J., *J. Chem. Phys.* **2005,** *122*, 244323.

29. Bludský, O.; Chocholoušová, J.; Vacek, J.; Huisken, F.; Hobza, P., *J. Chem. Phys.* **2000,** *113*, 4629.
30. Linder, R.; Seefeld, K.; Vavra, A.; Kleinermanns, K., *Chem. Phys. Lett.* **2008,** *453*, 1-6.
31. Balabin, R. M., *J. Phys. Chem. Lett.* **2010,** *1*, 20-23.Lowest two plus IVn identification.
32. Balabin, R. M., *Phys. Chem. Chem. Phys.* **2012,** *14*, 99-103.
33. Schreiner, P. R.; Reisenauer, H. P.; Ley, D.; Gerbig, D.; Wu, C. H.; Allen, W. D., *Science* **2011,** *332*, 1300-3.
34. Bazsó, G.; Najbauer, E. E.; Magyarfalvi, G.; Tarczay, G., *J. Phys. Chem. A* **2013,** *117*, 1952-1962.
35. Bazsó, G.; Magyarfalvi, G.; Tarczay, G., *J. Mol. Struct.* **2012,** *1025*, 33-42.
36. Bazsó, G.; Góbi, S.; Tarczay, G., *J. Phys. Chem.* **2012,** *116*, 10539-10547.
37. Pettersson, M.; Lundell, J.; Khriachtchev, L.; Räsänen, M., *J. Am. Chem. Soc.* **1997,** *119*, 11715-11716.
38. Reva, I. D.; Jarmelo, S.; Lapinski, L.; Fausto, R., *J. Phys. Chem. A* **2004,** *108*, 6982-6989.
39. Maçôas, E. M.; Khriachtchev, L.; Pettersson, M.; Fausto, R.; Räsänen, M., *Phys. Chem. Chem. Phys.* **2005,** *7*, 743-749.
40. Maçôas, E. M.; Khriachtchev, L.; Pettersson, M.; Fausto, R.; Räsänen, M., *J. Phys. Chem. A* **2005,** *109*, 3617-3625.
41. Marushkevich, K.; Siltanen, M.; Räsänen, M.; Halonen, L.; Khriachtchev, L., *J. Phys. Chem. Lett.* **2011,** *2*, 695-699.
42. Aspiala, A.; Lotta, T.; Murto, J.; Räsänen, M., *J. Chem. Phys.* **1983,** *79*, 4183-4192.
43. Wassermann, T. N.; Suhm, M. A.; Roubin, P.; Coussan, S., *J. Mol. Struct.* **2012,** *1025*, 20-32.
44. Lapinski, L.; Nowak, M. J.; Reva, I.; Rostkowska, H.; Fausto, R., *Phys. Chem. Chem. Phys.* **2010,** *12*, 9615-9618.
45. Reva, I.; Nowak, M. J.; Lapinski, L.; Fausto, R., *J. Chem. Phys.* **2012,** *136*, 064511.
46. Sharma, A.; Reva, I.; Fausto, R., *J. Am. Chem. Soc.* **2009,** *131*, 8752-8753.
47. Shmilovits-Ofir, M.; Gerber, R. B., *J. Am. Chem. Soc.* **2011,** *133*, 16510-16517.
48. BennyáGerber, R., *Phys. Chem. Chem. Phys.* **2011,** *13*, 8715-8722.
49. Bazso, G.; Najbauer, E. E.; Magyarfalvi, G.; Tarczay, G., *J. Phys. Chem. A* **2013,** *117*, 1952-62.
50. INTDER2005 is a general program developed by Wesley D. Allen and co-workers which performs various vibrational analyses and higher-order nonlinear transformations among force field representations.
51. Werner, H.-J.; Knowles, P. J.; Knizia, G.; Manby, F. R.; Schütz, M.; Celani, P.; Korona, T.; Lindh, R.; Mitrushenkov, A.; Rauhut, G.; Shamasundar, K. R.; Adler, T. B.; Amos, R. D.; Bernhardsson, A.; Berning, A.; Cooper, D. L.; Deegan, M. J. O.; Dobbyn, A. J.; Eckert, F.; Goll, E.; Hampel, C.; Hesselmann, A.; Hetzer, G.; Hrenar, T.; Jansen, G.; Köppl, C.; Liu, Y.; Lloyd, A. W.; Mata, R. A.; May, A. J.; McNicholas, S. J.; Meyer, W.; Mura, M. E.; Nicklaß, A.; O'Neill, D. P.; Palmieri, P.; Peng, D.; Pflüger, K.; Pitzer, R.;

Reiher, M.; Shiozaki, T.; Stoll, H.; Stone, A. J.; Tarroni, R.; Thorsteinsson, ; Wang, T. M., *MOLPRO*, version 2006.1; 2006. Version 2010.1.
52. Stanton, J.F.; Gauss, J.; Harding, M.E.; Szalay, P.G.; with contributions from Auer, A. A.; Bartlett, R. J.; Benedikt, U.; Berger, C.; Bernholdt , D. E.; Bomble, Y. J.; Cheng, L.; Christiansen, O.; Heckert, M.; Heun, O.; Huber, C.; Jagau, T.-C.; Jonsson, D.; Jusélius, J.; Klein, K.; Lauderdale, W. J.; Matthews, D. A.; Metzroth, T.; Mück, L. A.; O'Neill, D. P.; D.R. Price, E. Prochnow, C. Puzzarini, K. Ruud, F. Schiffmann, W. Schwalbach, C. Simmons, S. Stopkowicz, A. Tajti, J. Vázquez, F. Wang, J.D. Watts and the integral packages MOLECULE (J. Almlöf and P.R. Taylor), PROPS (P.R. Taylor), ABACUS (T. Helgaker, H.J. Aa. Jensen, P. Jørgensen, and J. Olsen), and ECP routines by A. V. Mitin and C. van Wüllen. *CFOUR*, For the current version, see http://www.cfour.de. 2008.
53. Schmidt, M. W.; Baldridge, K. K.; Boatz, J. A.; Elbert, S. T.; Gordon, M. S.; Jensen, J. H.; Koseki, S.; Matsunaga, N.; Nguyen, K. A.; Su, S., *J. Comput. Chem.* **1993,** *14*, 1347-1363.
54. Janssen, C. L.; Nielsen, I. B.; Leininger, M. L.; Valeev, E. F.; Kenny, J. P.; Seidl, E. T., *The Massively Parallel Quantum Chemistry Program (MPQC),* Version 2.3.1; Sandia National Laboratories, Livermore, CA, USA, 2008.
55. Shao, Y.; Molnar, L. F.; Jung, Y.; Kussmann, J.; Ochsenfeld, C.; Brown, S. T.; Gilbert, A. T.; Slipchenko, L. V.; Levchenko, S. V.; O'Neill, D. P., *Phys. Chem. Chem. Phys.* **2006,** *8*, 3172-3191.
56. Krylov, A. I.; Gill, P. M., *WIREs Comput. Mol. Sci.* **2013,** *3*, 317-326.
57. Godfrey, P. D.; Brown, R. D.; Rodgers, F. M., *J. Mol. Struct.* **1996,** *376*, 65-81.
58. Reva;, I. D.; Blagoi, Y. P., *Chem. Phys. Lett.* **1994,** *232*, 141-148.
59. Stepanian, S.; Reva, I.; Radchenko, E.; Rosado, M.; Duarte, M.; Fausto, R.; Adamowicz, L., *J. Phys. Chem. A* **1998,** *102*, 1041-1054.
60. Müller-Dethlefs, K.; Hobza, P., *Chem. Rev.* **2000,** *100*, 143-168.
61. Reed, A. E.; Curtiss, L. A.; Weinhold, F., *Chem. Rev.* **1988,** *88*, 899-926.

CHAPTER 3

SYSTEMATIC SEARCH AND ANALYSIS OF THE CONFORMERS OF SERINE*

* He, K; Allen, W. D. To be submitted to *Journal of Chemical Theory and Computation*

Abstract

The numerous conformers of the neutral form of the natural amino acid serine (**Ser**) have been investigated by systematic computations with reliable electronic wave function methods. A total of 85 unique conformers were located using the MP2/cc-pVTZ level of theory. The lowest twelve conformers of serine fall within a 8 kJ mol^{-1} window, and for these species geometric structures, precise relative energies, equilibrium and vibrationally averaged rotational constants, quartic and sextic centrifugal distortion constants, dipole moments, ^{14}N nuclear quadrupole coupling constants, anharmonic vibrational frequencies, and infrared intensities were determined. The relative energies were refined through composite focal-point analyses (FPA) employing basis set as large as aug-cc-pV5Z and correlation treatments as extensive as CCSD(T). The vibrationally averaged rotational constants computed in this study agree well with Fourier-transform microwave spectroscopy results available for seven conformers. The lowest nine serine conformers computed here match those identified in matrix isolation experiments, each species being distinguishable by its intramolecular hydrogen-bonding pattern.

3.1 Introduction

Of the molecules delivered to the early Earth,[1] the amino acids have tremendous chemical, and biological significance as building blocks of proteins, enzymes, and peptides. Serine (**Ser**) is a proteinogenic α-amino acid containing a $–CH_2OH$ side chain (Figure 3.1). The intrinsic conformational properties of such building blocks largely determine the functional specificity of proteins and polypeptides.[2] Detailed conformational studies of natural amino acids are also important to the search for prebiotic molecules.[3-6] Bada et al.[7] found traces of serine in meteorites, and quantum chemical computations showed that serine formation is possible in interstellar space.[8]

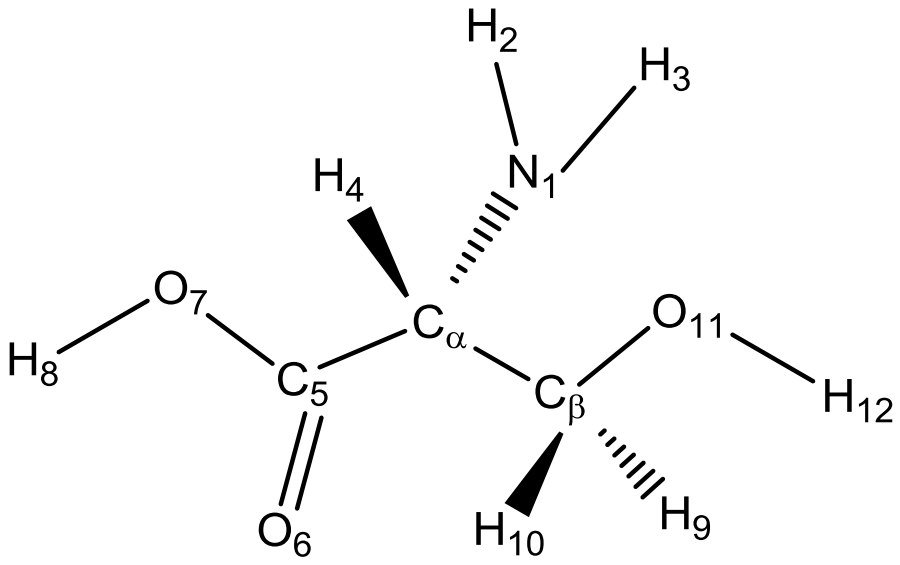


Figure 3.1. Atomic Labeling Scheme for Serine

The multiple internal rotational degrees of freedom of amino acids lead to a large number of low-energy conformers. It is obvious that hydrogen bonding (H-bond) patterns play a key role in determining the conformational energies and harmonic vibrational

frequencies. The intrinsic structural preferences of amino acids can be revealed only when they are studied as free species in the gas phase.

Several research groups have reported theoretical studies on the conformational space of neutral amino acids.[9-15] Gronert and O'Hair[12] first conducted a comprehensive conformer search for serine, starting with a set of 324 trial structures generated by systematic rotations around the five internal rotation axes, optimizing geometries with the semiempirical AM1 method, and then refining the structures at the HF/6-31G* level. Fifty-one conformers were identified with relative energies smaller than 50 kJ mol^{-1}. However, the same procedure based on AM1 screening failed to locate one of the key conformers of alanine because the corresponding surface for interaction of the amino hydrogens with the sp^3 carboxylic oxygen is very flat. Thus, a successful search for the complete set of amino acid conformers needs to meet two requirements: 1) the full ensemble of possible starting configurations needs to be sampled with a reliable screening procedure and 2) a high-level theoretical method should be applied for final characterization of conformations.

Miao and co-workers[14] revisited the conformers of serine by starting with the earlier set[12] of initial structures, optimizing geometries with B3LYP/6-31G*, and refining the structures at the B3LYP/6-311+G** level of theory. Serine was found to exhibit 74 unique conformers. Even though the necessity of considering the full ensemble of possible conformations was pointed out, the incompleteness of the set of initial structures resulted in a loss of several conformers, as shown below.

The polar –OH group on the side chain of serine introduces two additional rotors compared to alanine. This seemly small change dramatically increases the number of

possible conformers.[12,14-15] The presence of three H-bond donors and four H-bond acceptors in serine allows for the existence of twelve distinct types of H-bonds, as depicted in Figure 2 of ref 16.[16] These types include a) bifurcated H-bonds between $–NH_2$ and –COOH, similar to those found in the most stable conformers of glycine[17] (**Gly**) and alanine[18] (**Ala**); b) simple adducts of N–H donors with oxygen acceptors within the side-chain O–H or carboxylic acid group; c) side-chain O–H interactions with nitrogen or the –COOH oxygens; and d) O–H donations to C=O, side-chain O–H, or NH_2.[19] Cysteine (**Cys**) is only one atom different from serine, and thus the conformational possibilities of the latter can be discerned from previous studies of the former.[16]

Serine might be expected to exhibit the same conformers as cysteine, but the intramolecular interactions in cysteine involving the side chain $–CH_2SH$ are expected to be weaker than those of $–CH_2OH$ in serine, thus reducing or eliminating barriers separating the cysteine conformers with different polar side chain orientations. Hence serine is expected to exhibit more distinct conformers than cysteine. Cysteine exhibits 71 unique conformers and 11 conformers within 10 kJ mol^{-1} of the global minimum.[16]

It has long been recognized that correlation energy plays an essential role in the stabilization of amino acid conformers.[12,17-24] Møller-Plesset theory and coupled cluster methods are the usual post-Hartree-Fock treatments of correlation effects. Other less computationally demanding approaches involve density functional theory (DFT). Several DFT methods including dispersion effects have been introduced in order to provide a more confident description of noncovalent interactions.[20-25] In general, B3LYP with or without dispersion corrections performs well for geometries and zero-point vibrational corrections of amino acids, but inclusion of correlation via high-level wave function

methods is necessary for accurate conformational energies. Definitive energies with an accuracy of at least 0.5 kJ mol^{-1} requires treatments through the CCSD(T) level of theory.[16]

To the best of our knowledge, very few spectroscopic studies of serine have been published.[15,26-27] Microwave spectroscopy has the potential to distinguish unambiguously between different conformational structures; however, amino acids are solids with high melting points and low vapor pressures, and consequently they are refractory to gas-phase investigations. Microwave studies of natural amino acids started in the late 1970s with the work of Suenram[20, 28-29] and Godfrey[30-32] on glycine and alanine. Such studies were restricted for a long time by the difficulties of bringing the compounds into the gas phase, because of quick decomposition under classical vaporization methods which relied on heat. Recent improvements such as the use of picosecond pulse lasers, new ablation nozzles, and extension of the range of the spectrometers to low frequency have notably advanced the experimental techniques.[26,33-42] The combination of laser ablation with Fourier transform microwave spectroscopy in supersonic jets (LA-MB-FTMW) has made possible the gas-phase study of solid biomolecules with high melting points.[26,33] In these experiments, solids are efficiently vaporized by a high-energy laser pulse, supersonically expanded into an evacuated Fabry-Perot cavity, and characterized by their rotational spectra. The cooling afforded by the supersonic expansion in the vacuum chamber greatly simplifies the spectrum of the analyte and enables the characterization of the most abundant conformers.

Numerous studies by Alonso and co-workers have applied the LA-MB-FTMW method to explore the structural behavior of amino acids: alanine,[33] valine,[31] leucine,[36] serine,[26]

isoleucine,[35] proline,[37] 4-hydroxyproline,[38] phenylglycine,[42] sarcosine,[41] and N,N-dimethylglycine,[40] as well as β-alanine.[39] In the supersonic expansions the simplest α-amino acids exhibit two dominant conformers stabilized by either a N···H–O hydrogen bond or a bifurcated N–H···O=C hydrogen bond with a *cis*-COOH interaction. Analysis of the LA-MB-FTMW spectra of serine[26] finally identified seven conformers.

Matrix isolation within a rigid cage of inert atoms is a powerful tool to simulate the gas phase because environmental interactions are largely excluded. Because the rigid matrix prevents molecular rotation, rotational fine structure does not complicate the spectrum. Matrix isolation infrared spectroscopy has been used to study the amino acids glycine,[21] alanine,[22,] valine,[23] proline,[24] leucine,[43] and L-isoserine,[44] as well as N-acetylated amino acids.[45-48] In addition, the conformational behavior of neutral serine was investigated in low-temperature Ar matrices.[15,27] The combination of B3LYP/6-311++G** computations with experimental matrix FT-IR results demonstrated the presence of nine different conformers of serine.[15] The C=O, O–H, and N–H stretching as well as O–H bending vibrational modes allow the conformations with different intramolecular H-bond patterns to be distinguished. Analysis of the experimental IR spectra in consideration of the coexistence of different types of conformers was significantly facilitated by observing the effects of UV irradiation and annealing of the solid argon matrix. Recently a series of studies reported the observation of short-lived conformers of glycine,[49] alanine,[50] β-alanine,[51] and cysteine[52] by matrix-isolation IR spectroscopy combined with near-infrared laser irradiation (NIR).

Equilibrium structures and accurate relative energies, obtained within the focal-point analysis (FPA) approach,[53-58] are available for the amino acids glycine,[17,19,59] alanine, [18,59]

threonine,[60] proline,[61,62] and cysteine.[16] In this study we perform an exhaustive search of serine conformers and use a correlated wave function method with a high-quality basis set (MP2/cc-pVTZ) to locate 85 unique conformers. Definitive FPA relative energy computations are executed for the twelve conformers of lowest energy. The influence of hydrogen bonds upon the relative stability of the conformations is discussed. Copious spectroscopic molecular parameters related to the vibrational and rotational spectra of the most important conformers of serine are also reported.

3.2. Computational Methods

Electronic wave functions were determined by the restricted Hartree-Fock[63] (RHF) method, second Møller-Plesset perturbation theory[64] (MP2), and coupled cluster (CC)[65-66] methods including all single and double excitations (CCSD)[67] as well as perturbative contributions from connected triple excitations [CCSD(T)].[68] The T_1 diagnostic values of coupled cluster theory[69-70] for the different conformers lie in the range (0.014, 0.015), and the maximum T_2 amplitudes do not exceed 0.05, showing that single-reference electron correlation methods are most suitable for describing serine. The 6-31G* basis set[71] was used for initial screening of the conformers with RHF. Structures were then reinvestigated using the cc-pVTZ (correlation-consistent, polarized-valence, triple-zeta) basis set[72-75] with MP2 theory. In order to best describe the multiple hydrogen-bonding interactions in the various conformers,[76] the basis set was augmented (aug-cc-pVTZ)[73,75] with diffuse functions in the geometry optimization of the twelve lowest-energy conformers. The quantum chemistry packages MOLPRO (2010.1),[77] CFour (v1.0),[78] MPQC (2.3),[79] PSI4,[80] and QChem (4.0)[81-82] were used in this study.

3.2.1. Geometry Optimizations

The side-chain hydroxyl group adds complexity to the conformational analysis of serine, since it can work as either a donor or acceptor in an intramolecular hydrogen bond. In order to fully probe the potential energy surface of serine conformations, six large-amplitude modes were simultaneously varied to generate a multidimensional grid of 15,552 starting structures. The variations included two-fold NH_2 inversion, twelve-fold

NH_2 rotation about the C_α–N_1 axis, three-fold rotation of the two OH moieties about the C_β–O_{11} and C_5–C_7 axes, six-fold rotation of the –COOH group about the C_α–C_5 axis, and twelve-fold rotation of the $–CH_2OH$ side chain about the C_α–C_β axis. The starting structures were then tightly optimized at the HF/6-31G* level. Redundant conformers were identified by checking that total energies, bond lengths, and all angles were equivalent within 10^{-8} hartree, 0.0001 Å, and 0.05°, respectively. Eighty-nine unique conformers were found at the RHF/6-31G* level. Frozen-core MP2/cc-pVTZ optimizations were then started at these RHF structures without any geometrical constraints, yielding a final set of 85 unique conformers based on the same redundancy criteria. Geometry optimizations were followed by vibrational frequency computations at the same level of theory to characterize the stationary points. The twelve MP2/cc-pVTZ conformers within 12 kJ mol^{-1} of the lowest-energy structure were chosen for a more detailed analysis. These structures were reoptimized at the frozen-core MP2/aug-cc-pVTZ level. See the Supporting Information for Cartesian coordinates and energies of all the MP2 structures found.

3.2.2. Relative Energies – Focal-Point Analysis (FPA)

The focal point analysis (FPA) approach[53-58] was utilized for obtaining the most accurate relative energies with the aug-cc-pV*n*Z (*n*=D, T, Q, 5) series of basis sets.[73,83] The 1s core orbitals of the heavy atoms were kept frozen (FC) in all correlation treatments unless otherwise stated. The twelve lowest-energy structures obtained at the MP2/aug-cc-pVTZ level were included in the FPA investigation. Coupled-cluster energy increments with the aug-cc-pVTZ basis set were incorporated additively since the higher-order electron correlation contributions to the conformational energies do not change

significantly with the size of the basis set. To account for core electron correlation, all-electron (AE) MP2/aug-cc-pCVTZ[72,75] computations were differenced from frozen-core (FC) ones. The relativistic and diagonal Born-Oppenheimer auxiliary corrections often included in FPA computations were deemed negligible and thus omitted here.

Zero-point vibrational energies (ZPVEs) were obtained as harmonic and anharmonic values at the MP2/cc-pVTZ and MP2/6-31G* levels, respectively. In order to account for anharmonicity in ZPVEs, many thermochemistry protocols rely on second-order vibrational perturbation theory (VPT2).[58, 84-87] The VPT2 expression for the anharmonic ZPVE of an asymmetric top is

$$E_0 = G_0 + \frac{1}{2}\sum_i \omega_i + \frac{1}{4}\sum_i \sum_{j \geq i} X_{ij}\,, \tag{3.1}$$

where the ω_i and X_{ij} terms are the usual harmonic frequencies and anharmonicity constants, respectively, for the normal modes. Inclusion of the G_0 term[88-92] in ZPVEs exactly eliminates all resonance denominators arising from the vibrational anharmonic constants (X_{ij}). The G_0 values utilized here were obtained from CFour and patched by hand to fix a known bug.[93] With roper inclusion of the G_0 term, anharmonic ZPVE values computed for H_2O and C_2H_4 with G09 and CFour agreed to better than 0.02 kJ mol^{-1}.[93]

3.2.3. Natural Bond Orbital Analysis

Stabilizing effects other than H-bonding interactions were evaluated by using the natural bond orbital (NBO) method.[94-96] The NBO scheme decomposes the one-particle density matrix to obtain formally occupied one-center core orbitals and lone pairs (n_x) and two-center bonding orbitals ($\sigma_{X\text{-}Y}$, $\pi_{X\text{-}Y}$). These NBOs allow the molecular orbital picture to be transformed into a localized description corresponding to traditional Lewis

diagrams.[97] The localized, Lewis density is transformed to the exact density through delocalizations into formally unoccupied two-center antibonding orbitals ($\sigma^*_{X\text{-}Y}$, $\pi^*_{X\text{-}Y}$) and unoccupied one-center Rydberg orbitals. These delocalizations can be interpreted physically as energy-stabilizing donor–acceptor interactions between localized orbitals, including conjugation ($\pi \rightarrow \pi^*$) or hyperconjugation ($\sigma \rightarrow \sigma^*$). The second-order energy correction arising from these donor–acceptor interactions is

$$E_2 = -\frac{F_{ij}^2}{\varepsilon_i - \varepsilon_{j*}} \tag{3.2}$$

where F_{ij} is the Fock matrix element between occupied orbital i and unoccupied orbital j^*, and ε_i and ε_{j*} are the corresponding diagonal Fock matrix elements. The E_2 values indicate the most important relaxation effects from an idealized, local density to the exact density.

3.2.4. Spectroscopic Parameters

For the twelve lowest-energy conformers of serine, equilibrium rotational constants and harmonic vibrational frequencies were determined at the MP2/aug-cc-pVTZ and MP2/cc-pVTZ levels of theory, respectively. For the same conformers, vibrational anharmonicities, vibration-rotation interaction constants (α_i), and quartic and sextic centrifugal distortion constants were computed at the MP2/6-31G* level using the VPT2[58,84-87] formalism. Vibrational corrections for the rotational constants were evaluated by taking one-half the sum of the α_i constants.

Blanco et al.[26] pointed out that for conformers with the same amino acid backbone but different intramolecular hydrogen bonds, the rotational constants are similar. Conclusive conformational evidence comes from the values of ^{14}N quadrupole coupling constants

because of their sensitivity towards the orientation of the $-NH_2$ group with respect to the principal inertial axis system. These quadrupole coupling constants were computed by evaluating electric field gradients at nitrogen using MP2 theory conjoined with a cc-pCV5Z basis on nitrogen and cc-pCVTZ functions on all other atoms.

3.3. Results and Discussion

3.3.1. Energies

The serine conformers are labeled according to their relative energy ordering at the MP2/cc-pVTZ level for all 85 conformers. Figure 3.2 depicts the twelve lowest-energy conformers of serine. Following earlier nomenclature,[16,98] a series of dihedral angles were chosen to uniquely identify each conformers: $\tau_1(H_8–O_7–C_5=O_6)$ specifies the carboxyl group as cis or trans, $\tau_2(N_1–C_\alpha–C_5=O_6)$ identifies the type of carboxyl amine–hydrogen bond, $\tau_3(N_1–C_\alpha–C_\beta–O_{11})$ defines the type of amine hydroxyl-side-chain hydrogen bond, $\tau_4(C_5–C_\alpha–C_\beta–O_{11})$ describes the interaction between the carboxyl and polar side chain, and $\tau_5(N_1–C_\alpha–O_{11}–H_{12})$ gives the orientation of the carboxyl hydrogen relative to the amine group. Consistent with the Klyne-Prelog specification,[99] and we use the terms C (cis, $-30° < \tau < +30°$), G^+ (gauche, $+30° < \tau < +90°$), G^- (gauche, $-90° < \tau < -30°$), A^+ (anticlinal, $+90° < +150°$), A^- (anticlinal, $-150° < -90°$), and T (trans, $-150° < +150°$) to describe the torsion-angles.[16] For some conformers, an extra indicator is added to indicate different nitrogen lone pair orientations relative to the $C_\alpha–C_\beta$ bond ($\tau_6(X_1–N_1–C_\alpha–C_\beta)$, see Appendix B). For example, global minimum **Ser-I** is $TTG^+G^-A^+$ (173.7°, –157.7°, 58.9°, –62.6°, 122.4°, –154.9° (T)), share the same labeling as the higher-lying counterpart with the set of dihedral angles of (178.5°, 172.9°, 60.7°, –66.8°, 131.2°, 66.9° (G^+)). The only difference between the two conformers is that the amine group of **Ser-I** is facing towards the $C_\alpha–C_\beta$ bond (the nitrogen lone pair is facing away from it), and the carboxylic hydrogen is acting as a donor forming a hydrogen bond with the amine nitrogen. The rotation of the amine group breaks this hydrogen bond and resulted in a higher lying conformer.

Because the relative energies of the serine conformers are controlled by nonbonded interactions within the molecule, Gronert et al.[12] used a cutoff distance 2.75 Å for near-atom interactions and defined eight bonding schemes. However this arbitrary criterion does not sufficiently describes the conformer structure preference. In order to ensure a more insightful analysis of the stabilization effect due to each hydrogen bond type and the inner relation between the bonding pattern and conformer structures, we proposed a categorizing scheme that's based on the different hydrogen bonds between the fundamental donor and acceptor fragments (see Table 3.1 and Figure 3.2) and the structure parameters (selected dihedral angles). The hydrogen bonds **a** ~ **d** are used to indicate the interaction between the carboxyl and amine group. In the case of serine, where the polar side chain CH_2OH could serves as a hydrogen donor, hence two extra hydrogen bonds **e** and **f** are added. Finally hydrogen bonds **g** ~ **i** could be formed when side chain serving as a donor. All serine conformers could then be categorized into six classes: $\tau_1\tau_2$ = **CC**, **CA**, **CT**, **TC**, **TA**, **TT**. The dihedral angle labels are correlated with the hydrogen bonding patterns and reflect the rotational degrees of freedom in serine, which would be discussed in next section.

Table 3.1. Labeling for the intramolecular hydrogen bondings of amino acid serine

Label	Donor	Acceptor
a	$O–H_{bb}$	C=O
b	$O–H_{bb}$	NH_2
c	NH_2	$O–H_{bb}$
d	NH_2	C=O
e	$O–H_{bb}$	CH_2OH
f	NH_2	CH_2OH
g	CH_2OH	$O–H_{bb}$
h	CH_2OH	C=O
i	CH_2OH	NH_2

The subscript bb indicates the backbone COOH group

Table 3.2 listed the FPA relative energies of the twelve lowest energy conformers of serine. SCF/CBS is unable to yield the correct relative energies of the conformers, as **Ser-II**, **Ser-IV**, **Ser-V**, and **Ser-X**, **Ser-XII** were lower in energy than the global minimum (see Table 2). The MP2 correlation energy generally destabilizes all the conformers except for conformers **Ser-III**, **Ser-VI** and **Ser-VII**, which is consistent with the case of cysteine.[16] The mean squared interatomic distances for the lowest twelve conformers are in the range of 7.8~8.7 $Å^2$ whereas all class **C** conformers' (**CT**, **CA**, and **CC**) are smaller than 8.3 $Å^2$. By this measure, the class **C** conformers are the most compact, and these are the conformers most stabilized by electron correlation. Compared to δ[MP2], the δ[CCSD] and δ[CCSD(T)] energy increments affect relative energies as much as 3.1 and 2.3 kJ mol^{-1}, and brings the energy range from 12 kJ mol^{-1} down to 10.25 kJ mol^{-1}. However, the relative energy ordering did not change much and agrees well with the MP2/cc-pVTZ ordering except for few higher lying conformers. Core correlation has a minimal affect on the relative energies, for even the largest change is smaller than 0.15 kJ mol^{-1}. This is in line with earlier work on the conformers of threonine,[60] proline,[62] and

cysteine.[16] Harmonic ZPVE correction is independent of the theory used,[15] and could change the relative energy on the order of 2.6 kJ mol^{-1}. Anharmonic ZPVE corrections were comparatively smaller, the largest was found to be 0.15 kJ mol^{-1}.

The FPA errors could be estimated based on the observed convergence to the basis set and correlation limits. There is virtually no basis set error in RHF relative energies as it converged within 0.05kJ mol^{-1} of the aug-cc-pV5Z basis. MP2 correlation increments match the extrapolated values within 0.05 kJ mol^{-1} for all conformers as well. aug-cc-pVDZ and aug-cc-pVTZ CCSD and CCSD(T) increments matches within 0.2 kJ mol^{-1}. Hence the basis set error in the coupled-cluster values should not be greater than 0.1 kJ mol^{-1}.

Since higher-order correlation corrections due to quadrupole and higher excitations are generally an order of magnitude less than CCSD(T) corrections. The neglect of higher excitations should introduce an error to the serine relative energies of at most 0.2 kJ mol^{-1}. With anharmonicity accounted, the zero-point error should not be greater than 0.3 kJ mol^{-1}.

Two recent studies reported relative energies for the lowest-energy conformers of serine as summarized in Table 3.2, along with the energy computed at varies level of theories in this study. The MP2/aug-cc-pVTZ single-point energies are quite accurate (MAD=0.51) because the CCSD and CCSD(T) increments usually of opposite and partially cancel (Table 3.3). In general, B3LYP performs reasonably well for establish the energy ordering when combined with a larger basis set (beyond 6-31G*), but underestimate the relative energy of **Ser-II**, and can be in error by as much as 2.5 kJ mol^{-1}, as seen in **Ser-VIII**.

By substituting one H of CH_2 by the CH_2OH of the well-studied glycine amino acid, lowest serine conformers could be successfully identified (see Figure 3.3). The two lowest conformers **Ser-I** and **Ser-III** derive from the parent glycine **IIn**, as well as the other type A conformers (**Ser-VI**, **VII**, and **IX**).[19, 59] **Ser-II**, which derives from the global minimum glycine **Ip**, is almost degenerate in energy to **Ser-I**. **Ser-V, Ser-VIII** and **Ser-XII** derive from **Gly-IIIp**. It can be observed that the most stable conformations of serine follow the same order observed for each glycine type.

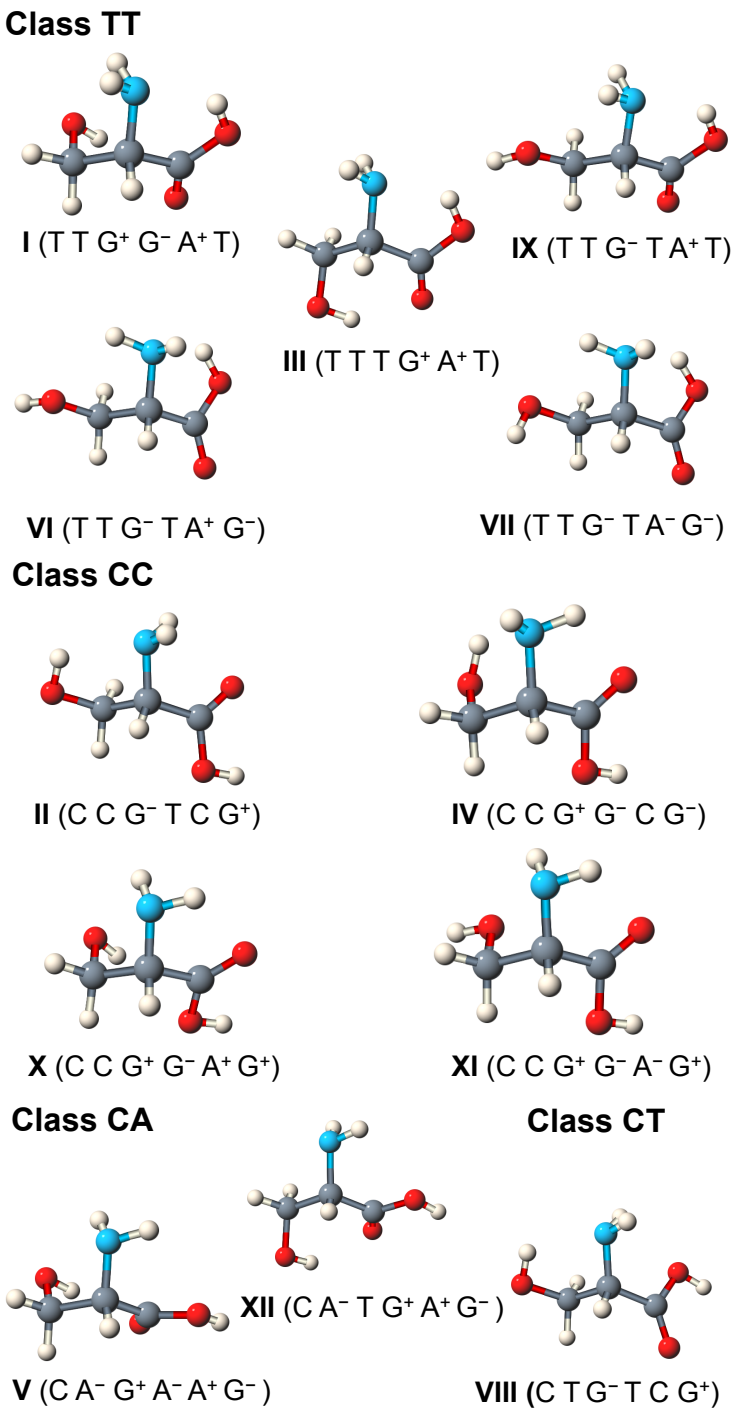


Figure 3.2. Depiction of the twelve lowest-energy conformers of serine, as optimized with MP2/aug-cc-pVTZ theory

The series of labels in parentheses identifies conformer as cis (C), gauche (G), trans (T), or anticlinal (A) with respect to the dihedral angles $\tau(H_8–O_7–C_5=O_6)$, $\tau(N_1–C_\alpha–C_5=O_6)$, $\tau(N_1–C_\alpha–C_\beta–O_{11})$, $\tau(C_5–C_\alpha–C_\beta–O_{11})$ and $\tau(N_1–C_\alpha–O_{11}–H_{12})$.

Wilke et al.[16] adopted the same geometry optimization scheme, and found 71 cysteine conformers. The 14 additional conformers of serine when compared with cysteine coincide with the original prediction of increased conformers. One thing worth mentioning is that the HF/3-21G* level also failed to distinguish conformers with different amino hydrogen that interacts with the OH of the carboxyl group. This also justified our choice of 12-degrees of freedom of the amine group rotation. The lowest five cysteine conformers **Ser-I**, **II**, **IV**, **V**, **VII**, **X**, and **XII** corresponding to **Cys-I**, **V**, **IV**, **VII**, **II**, **III**, and **X** respectively. Both **Ser-I** and **Cys-I** belong to class **b** with an extra H-bond between the side chain and the carboxyl oxygen. In general, when the side chain hydrogen is involved in a H-bond with either the NH_2 group (**Ser-II** and **Ser-IV**) or the carboxyl oxygen (**Ser-V** and **Ser-XII**), the cysteine analogous are much higher in energy, partly due to a much weaker H-bond of $CH_2SH\cdots NH_2$ or $CH_2SH\cdots O{=}C$ provides a much less stabilization effect. The analogous structure to **Ser-CCTG$^+$T** (see supporting information Table S2, serine geometry at MP2/cc-pVTZ level) has not been obtained for cysteine. The optimization of such a structure has collapsed to **Cys-X** involved a rotation of the carboxylic group. This carboxylic group rotation changed the hydrogen bond type from **d** to **c**.

Table 3.2 Comparison of Conformational Energies of Serine (kJ mol^{-1}) with different bonding schemes for Different Levels of Theory without Zero-Point Vibrational Correction

	CCSD(T)[a] CBS	MP2[b] ATZ	MP2[b] TZ	MP2[b] 6-31G*	RHF[c] 6-31G*	B3LYP[d] 6-31G*	B3LYP[d] 6-311+G**	B3LYP[e] 6-311++G**
Ser-I	0.00	0.00	0.00	0.00	0.00	0.00	0.00	0.00
Ser-II	2.09	2.46	2.66	2.90	−5.02	−2.84	0.84	0.05
Ser-III	2.68	3.47	2.85	4.36	3.77	−3.43	1.51	1.61
Ser-IV	3.56	3.69	4.24	4.33	−2.09	4.48	3.72	3.66
Ser-V	6.02	7.33	7.18	6.21	−1.67	7.20	6.53	6.72
Ser-VI	7.57	6.69	7.52	13.11	9.62	8.83	6.32	7.42
Ser-VIII	9.08	9.10	9.57	10.17	2.09	7.49	6.65	6.59
MAD		0.51	0.66	1.71	4.11	2.16	0.91	1.05

[a]CCSD(T)/CBS denotes the extrapolated value from the focal point analysis based on geometry optimized at MP2/aug-cc-pVTZ level.

ATZ=aug-cc-pVTZ, TZ=cc-pVTZ

[b]Computed at the MP2/aug-cc-pVTZ, MP2/cc-pVTZ, and MP2/6-31G* level reference geometries respectively.

[c]Computed at the RHF/6-31G* reference geometires.[12]

[d]Computed at the B3LYP/6-31G* reference.[14]

[e]Computed at the B3LYP/6-311++G** reference geometries.[15]

MAD = Mean Absolute Deviation from CCSD(T)/CBS values.

Table 3.3 Focal Point Analysis for the Relative Energies of the Twelve Lowest-Energy Conformers of Serine[a]

	Basis	I	II	III	IV	V	VI	VII	VIII	IX	X	XI	XII
ΔE_e(RHF)	ADZ	0.00	−5.52	3.68	−2.64	−2.18	7.03	8.12	2.09	6.19	1.21	−1.13	−1.67
	ATZ	0.00	−5.69	3.85	−2.97	−1.72	6.78	7.82	2.01	6.11	1.42	−1.38	−1.38
	AQZ	0.00	−5.82	3.72	−3.10	−1.76	6.74	7.78	1.88	6.02	1.42	−1.38	−1.42
	A5Z	0.00	−5.86	3.72	−3.10	−1.76	6.74	7.74	1.84	5.98	1.42	−1.46	−1.46
	CBS	0.00	−5.86	3.72	−3.14	−1.80	6.74	7.74	1.84	5.94	1.38	−1.46	−1.51
δ[MP2]	ADZ	+0.00	+7.32	+0.21	+6.40	+8.58	−0.59	−1.21	+6.07	+3.26	+8.74	+10.54	+11.46
	ATZ	+0.00	+8.16	−0.38	+6.65	+9.04	−0.08	−0.75	+7.11	+3.77	+9.33	+11.76	+12.22
	AQZ	+0.00	+8.08	−0.46	+6.61	+9.04	−0.08	−0.67	+7.20	+3.68	+9.54	+11.92	+12.22
	A5Z	+0.00	+8.08	−0.46	+6.57	+9.04	−0.04	−0.63	+7.20	+3.68	+9.54	+11.88	+12.22
	CBS	+0.00	+8.08	−0.46	+6.53	+9.00	−0.04	−0.59	+7.15	+3.68	+9.58	+11.88	+12.26
δ[CCSD]	ADZ	+0.00	−1.30	−0.21	−1.17	−2.30	+0.59	+0.67	−0.96	−0.84	−2.34	−2.26	−3.01
	ATZ	+0.00	−1.42	−0.13	−1.21	−2.43	+0.59	+0.71	−1.09	−0.92	−2.47	−2.47	−3.14
δ[CCSD(T)]	ADZ	+0.00	+1.13	−0.42	+1.26	+1.13	+0.25	−0.08	+1.05	+0.75	+1.59	+2.09	+1.55
	ATZ	+0.00	+1.30	−0.46	+1.38	+1.26	+0.29	−0.04	+1.17	+0.75	+1.67	+2.30	+1.76
ΔE_e(CCSD(T)/CBS)		0.00	2.09	2.68	3.56	6.02	7.57	7.82	9.08	9.46	10.17	10.25	9.37
Δ(core)		+0.00	−0.06	+0.02	−0.09	+0.13	−0.09	−0.01	+0.04	−0.07	+0.15	−0.01	+0.08
Δ(ZPVE, harm)		+0.00	−1.33	+0.38	−1.20	−0.43	−0.62	−0.34	−1.33	−1.58	−2.00	−2.55	−1.45
δ(anharm)		+0.00	+0.15	−0.01	+0.09	+0.08	+0.01	+0.00	+0.13	+0.07	+0.03	+0.18	+0.13
ΔE_0(FPA)		0.00	0.86	3.07	2.35	5.82	6.88	7.49	7.93	7.88	8.36	7.88	8.13

[a]All values given in kJ mol^{-1}. Basis set abbreviations: A*n*Z = aug-cc-pV*n*Z, *n*= D, T, Q, 5. ΔE_e denotes a vibrationless relative energy between conformers. δ denotes an increment with respect to the preceding level of theory in the hierarchy RHF → MP2 → CCSD → CCSD(T). Δ(core)= core electron correlation corrections; Δ(ZPVE, harm)= relative energy change due to harmonic ZPVE; δ(anharm) = anharmonicity correction to Δ(ZPVE, harm). ΔE_0(FPA) = ΔE_e(RHF,CBS) + δ(MP2,CBS) + δ(CCSD,ATZ) + δ(CCSD(T),ATZ) + Δ(core) + Δ(ZPVE, harm) + δ(anharm).

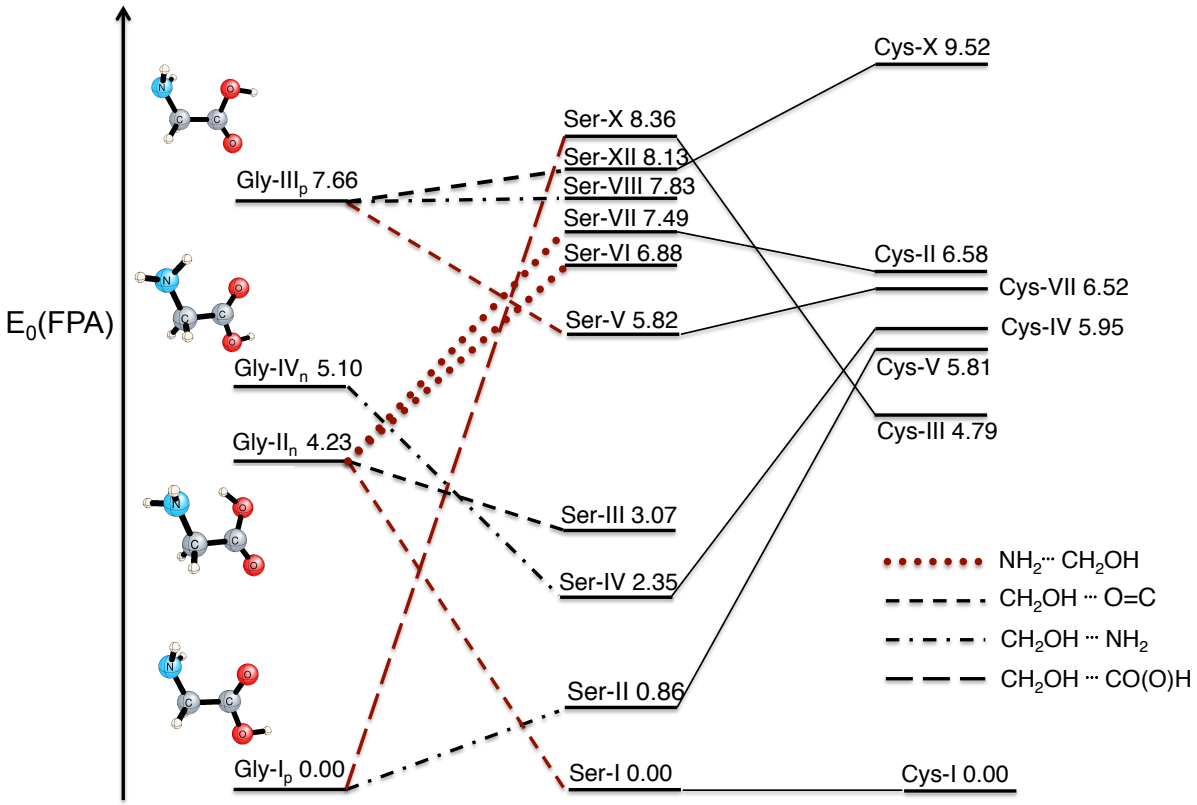


Figure 3.3 Structural relation between the parent glycine molecule and the polar side chain substituted serine and cysteine[16] with FPA relative energies in kJ mol^{-1}

3.3.2. Geometries and Structural Effects on Relative Energies

The CCSD(T)/CBS//B3LYP/aCCT relative energies of glycine conformers predicted that the N–H···O=C H-bonding interaction (**d** type) stabilizes the glycine conformer more so than the O–H···N–H (**b** type) and N–H···O–H (**c** type). Dokmaisrijan et al.[100] found that for valine, leucine and isoleucine, three of the more complicated non-polar amino acids, the global minimum conformer of each amino acid presents the N–H···O=C interaction, which is in agreement with prior theoretical studies. Moreover, the O–H···N–H (**b** type) interaction is observed in the second lowest energy conformer while the N–H···O–H (**c** type) interaction is less favorable. In addition, improvement of the relative energies of lowest conformers by adding the ΔE_{ZPE} values can change the stability order since the ΔE_{ZPE} can destabilize the conformational energies.

The parentage diagram of the possible H-bonding schemes in relation with the structure for serine is depicted in Figure 3.4. The general stability of the H-bonding schemes of serine were analyzed by compare the average energies of the conformers within each scheme with the overall mean energy. Each of the 78 of the 85 serine conformers contains at least one of **a** ~ **d** type hydrogen bonds when using the 2.75 Å criterion, shows the dominating interaction between the COOH and NH_2 groups. The possible values of $\tau_1(H_8–O_7–C_5=O_6)$ are only C (cis) and T (trans), corresponding to the *cis* or *trans* conformation of COOH group. Among 85 conformers, 50 are with a *cis* carboxylic group and forming a type **a** hydrogen bond with the interatomic distance ($H_8\cdots O_6$) between 2.26 ~ 2.28 Å, and were stabilized by 3.28 kJ mol^{-1}. In contrast the *trans* conformers were higher in energy by 4.69 kJ mol^{-1}. This preference for the *cis* arrangement around the C–O bond is commonly found for unsubstituted carboxylic

acids.[101-102] **b**, **c** and **d** type hydrogen bonds can be form depending on the different orientations of the carboxylic and amine groups about the C_5–C_α bond. The six degrees of freedom about the C_5–C_α bond are reflected by the values of $\tau_2(N_1–C_\alpha–C_5=O_6)$ (C, T, G^+, G^-, A^+, and A^-). When COOH is in cis conformation (τ_1=C), **d** type hydrogen bond ($NH_2\cdots O=C$) is most likely formed when τ_2 is G or C ($H_{2/3}\cdots O_6$ = 2.21 ~ 2.59 Å), whereas amine hydrogen will bond with carboxylic oxygen when τ_2 is equal to T, forming the strong **c** type hydrogen bond ($H_{2/3}\cdots O_7$ = 2.03 ~ 2.48 Å). A subset of conformers (τ_1=C, τ_2=A) shares the common feature of an approximate perpendicular relative orientation between the COOH plane and the N_1–C_α bond. Conformers within this group still maintain the type c hydrogen bonding but with an elongated interatomic distance ($H_{2/3}\cdots O_7$ = 2.21 ~ 3.37 Å) due to the rotation of the COOH group about the C_α–C_5. When COOH is in trans conformation (τ_1=T), a *trans* τ_2 usually facilitates the type **b** ($OH_{bb}\cdots NH_2$, subscript bb indicate the carboxylic oxygen in COOH group) hydrogen bond with a very short interatomic distance ($H_8\cdots N_1$ = 1.87 ~ 2.21 Å). When C=O bond is in *cis* position with N_1–C_α bond, **d** type hydrogen bond ($NH_2\cdots O=C$) is dominating with a short interatomic distance ($H_{2/3}\cdots O_6$ = 2.13 ~ 2.55 Å). Again, the COOH plane is approximately perpendicular to the N_1–C_α bond when τ_2=A, type **c** hydrogen bond still exists with an elongated interatomic distance ($H_{2/3}\cdots O_7$ = 2.60 ~ 3.37 Å) and the conformers co-stabilized with a weak type **d** hydrogen bond. Based on the combination of τ_1 and τ_2, conformers are divided into six classes (τ_1 τ_2 = CC, CA, CT, TC, TA, and TT) with the **a** ~ **d** type hydrogen bonds explicitly correlated with the COOH and NH_2 relative orientation.

At the next level, the sixth structure indicator $\tau_6(X–N_1–C_\alpha–C_\beta)$ indicates the orientation of the NH_2 about the $C_\alpha–C_\beta$ bond which changes the type of **c** and **d** hydrogen bonds. For example, **Ser-II**, **IV**, **X**, and **XI** all belong to CA class. In **Ser-IV**, $\tau_6 = G^-$ with only one of the amine hydrogen pointing towards the carbonyl oxygen ($H\cdots O_6$ = 2.21 Å). For the other three conformers the NH_2 is slightly rotated towards C=O bond and forming a bifurcated **c** hydrogen bond ($H\cdots O_6$ = 2.23 ~ 2.51 Å).

The type **f** and **i** hydrogen bonds demonstrate the interaction between amine and polar CH_2OH side, whereas type **e**, **g**, and **h** are characteristics of CH_2OH and COOH interaction. In general, each type of hydrogen bonds dictates several dihedral angles of the conformer structures. The different combination of dihedral angles and its inner correlation with the types of hydrogen bonds as well as interatomic distance ranges are given in Table 3.4. Since **g** and **h** type hydrogen bonds involve two atoms on the both ends of the $C_5–C_\alpha–C_\beta–O_{11}$ back bone chain, the occurrences are lower due to higher degrees of structure constraints, hence are excluded from Table 3.4.

Table 3.4 Structure Features and Hydrogen Bond Correlation with Interatomic Distance range in Å, Average Relative Energy in kJ mol^{-1} and occurrence

H-Bond	τ	τ	ΔE	Range	n
f	$\tau_4 = T$	$\tau_6 = G^-, T$	+0.06	2.26 ~ 3.04	43
i	$\tau_4 = G^-, T$	$\tau_5 = C$	–1.40	2.17 ~ 2.88	20
e	$\tau_4 = C, G^+, A^+$	$\tau_5 = A^+, T$	–0.90	1.76 ~ 1.82	8

Hydrogen bond notations see Table 3.1

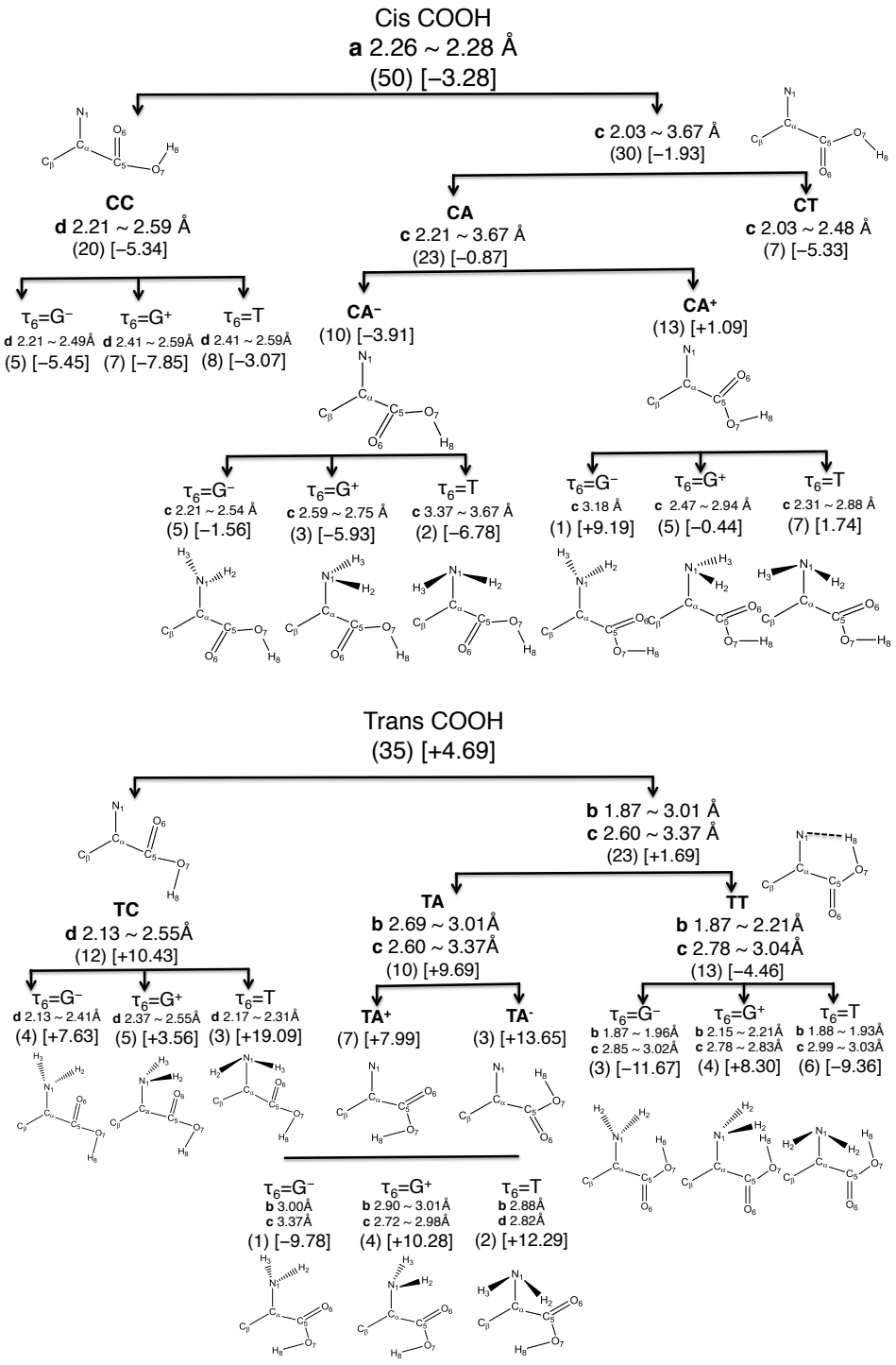


Figure 3.4 Relative Average Energy (in kJ mol^{-1}) of the Conformers of Serine classified according to $\tau_1\tau_2$ value.[a]

[a]Number in the parenthesis is the number conformers sharing the same structure feature. Number in the bracket is the relative average energy in in kJ mol^{-1}. Upper case letter is the class name ($\tau_1\tau_2$=CC, CA, CT, TC, TA, TT), lower case letter indicate hydrogen bond type (a, b, c, d).
All energies were calculated at MP2/cc-pVTZ level, without ZPVE corrections.

Ser-I (class **TT**), which is identified as the global minimum at CCSD(T)/CBS level, is the only conformer that has all three donors involved in the intramolecular bonding with three different acceptors (Figure 3.2). The two most stable conformers **Ser-I** and **Ser-II** are energetically comparable (in a range of 0.86 kJ mol^{-1}) but have quite different structures. **Ser-II** has a rather weak intramolecular H-bond between one of the H atoms of the amine group and the O atom of the carbonyl group, as well as a weak intramolecular hydrogen bond between the O–H group of the side chain and the N atom of the amino group. **Ser-I**, however, has a strong intramolecular H-bond between the O–H group of the carboxyl group and the N atom of the amino group, and a weaker H-bond between the amine H atoms and the O atom of the hydroxyl.

Bond lengths and bond angles change little among the low-lying conformers with few exceptions. O_7–H_8 bond distance has a standard deviation of 0.007 Å. A spread of the O_7–C_5–C_α angles is consistent with the trans angle rule.[103] If the carboxyl group assumes a *cis* conformation (O_7–H_8 bond trans to the C_5–C_α), essentially no hyperconjugative interactions exist between the carbonyl oxygen lone pair and C_5–C_α bond (see Appendix B 4.2). This results in a smaller O_7–C_5–C_α angle in average 111.5°. In the other case, when COOH assumes a *trans* conformation (O_7–H_8 bond cis to the C_5–C_α), the O_7–C_5–C_α angle is much larger between 113.6° and 114.3° for all class TT conformers. A longer O_7–H_8 is also observed for class TT conformers compare with other classes.

Even larger angle variations of the O_{11}–C_α–C_β and N_1–C–C (2.2° and 2.5°, respectively) are consistent with hyperconjugation from the oxygen and nitrogen lone pair to the C–C antibonding orbital ($n_O \rightarrow \sigma^*_{C-C}$, $n_N \rightarrow \sigma^*_{C-C}$). In general, if a C–C bond is trans to the X–H bond, the X–C–C angle will be smaller, because both reduced bond

repulsion relative to the gauche conformer and weaker hyperconjugation from the lone pair. For conformers **Ser-I**, **III**, and **IX**, the N–H bonds are gauche to the C_α–C_β bond, and the angles are in the range 114.4°–114.8°, whereas for the other conformers with a trans conformations, these angles are in the range 107°–109° (see Appendix B.5). In particular, for both C_α–C_β and C_5–C_α, large hyperconjugative interactions ($E_2 > 30$ kJ mol^{-1}) are observed with large C–C–N angles, while weaker interactions ($E_2 < 25$ kJ mol^{-1}) are observed with smaller C–C–N angles.

3.3.3. Vibrational Fundamentals

H-bond interactions play an important role in the conformational energy and harmonic vibrational frequencies. The presence of H-bonds of in the lower-energy conformers allows IR spectra of the most stable conformers to be distinguished. Many vibrational fundamentals are found to be characteristic for some of the conformers. Anharmonic vibrational frequencies in characteristic hydrogen bonding regions of the infrared spectra are given in Table 3 for the twelve lowest-energy conformers of serine.

Experimental studies on neutral amino acids are rather scarce, mainly because of the low thermal stability and low vapor pressure of these compounds. Since most amino acids decompose before melting, it is extremely difficult to obtain a concentration in the gas phase sufficient for infrared studies. Thus, Lambie et al.[27] investigated the conformational behavior of neutral serine isolated in low-temperature Ar matrices. The experimental infrared spectral characteristics of serine are evaluated using theoretically calculated data, and the theoretical rotamerization constants are compared with experimental values. The twelve most stable conformers of serine were selected from the work of Gronert and O'Hair[9] as the starting point of the geometry optimization at the B3LYP/6-31++G** level. Conformers typically have small energy differences, which make identification of these forms in the experimental spectrum difficult or even impossible. For this reason, only the four most stable conformers (**Ser-I, Ser-II**, **Ser-III**, and **Ser- IV**) with a relative energy difference smaller than 5 kJ mol^{-1} were further analyzed.

Jarmelo et al.[15] studied the conformational preferences of neutral serine starting by a full systematic investigation of its potential energy surface. 9 conformers lay within 7 kJ mol^{-1} were predicted to account for 93% of the total conformational population at room temperature. Theoretical calculations at both the MP2 and B3LYP levels of theory with the 6-311+G** basis set (scaled using a single factor of 0.978, except for νOH stretching modes two scaling factors were used depending on the strength of the H-bond interactions), together with temperature variation studies and in situ irradiation experiments were used to interpret the spectroscopic data obtained for the compounds isolated in low-temperature inert matrixes. The combination of MP2/cc-pVTZ harmonic frequencies (without scaling) and MP2/6-31G* anharmonic corrections employed here agree with attempted experimental assignments on average within 30 cm^{-1}, although some deviations may be substantially larger.

The most valuable information is contained in spectral region between 3650 and 1200 cm^{-1} of the experimental infrared spectrum. The backbone (bb) O–H works as a hydrogen bond donor to either form a intramolecular bond with the nitrogen in the amine group (class **TT**) or the C=O when it takes the cis-conformation of the carboxyl group (class **C**). For conformers with hydrogen bonding between the O–H group and the amino N atom, (class **TT**: **Ser-I**, **III**, **VI**, **VII**, and **IX**), the $\nu(OH)_{bb}$ mode is strongly red-shifted. The average H-bond distance is 1.891 Å and almost all modes are around 3234 cm^{-1} (from 3217–3254 cm^{-1}). The average difference between $\nu(OH)_{bb}$ mode of trans and cis COOH is around 300 cm^{-1} . The

side chain O–H stretch varies over a narrow range of 3535–3689 cm^{-1}. For class **TT** conformers with a free alcohol side chain group (**Ser-VI**, **VII**, and **IX**), side chain OH ($\nu(OH)_{sc}$) is predicted at frequencies above 3600 cm^{-1} . One exception is **Ser-III** where side chain OH is H-bonded to the carbonyl oxygen with a more red-shifted $\nu(OH)_{sc}$ mode (3535 cm^{-1}). In conformers belonging to type B and C, the $\nu(OH)_{bb}$ bands of **Ser-II**, **IV**, and **VIII** are predicted to occur at slightly higher frequencies than $\nu(OH)_{sc}$, since in these conformers the alcohol side chain group is H-bonded to the amine group. The other four conformers (**Ser-V**, **X**, **XI**, and **XII**) have a reversed predicted order of frequencies for the $\nu(OH)_{bb}$ and $\nu(OH)_{sc}$ mode, since in this case the H-bond involving the side chain group is established with the carbonyl oxygen atom, which is a weaker H-bond acceptor than the amine nitrogen. When the side chain oxygen served as an acceptor and forming a H-bond with amine group, this stretching mode is most blue shifted around 3685 cm^{-1} for all the conformers (**Ser-VI**, **Ser-VII**, **Ser-IX**, and **Ser-XI**).

The "free" $\nu(OH)_{sc}$ bands of class **TT** conformers **Ser-I**, **VI**, **VII**, and **IX** are observed at 3629, 3660, 3637, and 3664 cm^{-1}, respectively, matches with our predicted value within 24 cm^{-1}. Those corresponding to the H-bond OH_{sc} group in **Ser-V** and **Ser-II**, **IV**, **VIII** conformers appear at 3610 cm^{-1} and in 3560-3550 cm^{-1} region, respectively. The $\nu(OH)_{sc}$ band of **Ser-III** is observed at 3543 cm^{-1}. Compared to the narrow range of the S–H stretch in the cysteine side chain (2539-2560 cm^{-1}), the large discrepancy of the same of in serine (~120 cm^{-1}) could be consistently contributed to stronger hydrogen bonds. This increased H-bond

strength could be used to explain the increased number of conformers of serine compare to that of cysteine. In turn, the "free" The $\nu(OH)_{bb}$ vibrations in class **C** conformers give rise to the bands observed at 3592 (**Ser-IV**), 3585 (**Ser-VIII**), 3567 (**Ser-II**), and 3563 (**Ser-V**) cm^{-1}, whereas those originated in the strongly H-bonded carboxylic group of class **TT** conformers can be ascribed to the broad band centered around 3170 cm^{-1}.

The ν(NH) stretching (both symmetric and asymmetric) modes were found to be of low intensity and lie at nearly the same position, and does not help with distinguishing conformers. Another particular informative region is around 1800 cm^{-1} in the region of the intense C=O band. Statistically, there is a general preference towards cis-conformation of the carbonyl group, and seven among the total twelve lowest-energy conformers adapted this structure (class **C**). According to theoretical prediction, class **TT** conformers should give rise to νC=O bands appearing at higher frequencies than class **C** conformers, whereas conformers **Ser-V**, **X**, and **XII** should absorb at a considerably lower frequency than all of the other forms. Among all class **CC** conformers, **Ser-X** contains an extra H-bond between the side-chain O–H with the carboxyl OH. And in class **CA** conformers, **Ser-V** and **Ser-XII** both contain a H-bond between the side-chain O–H donor with the carboxyl oxygen acceptor. The C=O stretching frequencies of those three conformers are most red-shifted around 1762 cm^{-1}.

In conformers **Ser-VI**, **VII**, and **IX**, the carbonyl group is not participating in any H-bond, the νC=O modes are assigned to the two overlapping higher

frequency bands observed in this region at 1790 and 1788 cm^{-1}, whereas **Ser-I** gives rise to the band at 1778 cm^{-1}. The lowest frequency band at 1755 was assigned to **Ser-V**. Based on the changes of the band intensities upon UV irradiation and annealing of the matrix, the intense band at 1773 cm^{-1} was assigned to **Ser-III** and **Ser-IV**, 1771 cm^{-1} to **Ser-VIII**, where **Ser-II** contribute to both bands.

The δCOH bending vibrations are predicted to give rise to IR bands appearing in a relatively broad spectral range extending over 300 cm^{-1} (see Table 3 and supporting information). The general trend that the stronger a H-bond is, the higher the frequency of the δCOH vibration should be is valid for both alcohol side chain and carboxylic OH groups. The δCOH_{bb} modes in class **C** conformers (which have the cis-COOH group) are predicted by the calculations to give rise to low-intensity IR bands (5-51 km mol^{-1}) in the 1257 - 1348 cm^{-1} region, whereas for the H-bonded type A conformers, the δCOH_{bb} vibrations shall give rise to intense (310-471 km mol^{-1}) bands at 1337-1409 cm^{-1}. All δCOH_{sc} bands are predicted to have significantly lower intensities (<80 km mol^{-1}). For all type A conformers with an OH_{sc} serving as a H-bond acceptor (**Ser-I**, **VI**, **VII**, **IX**), the IR bands due to δCOH_{sc} vibrations are predicted to appear in the 1129 – 1221 cm^{-1} region. Once again as an exception among class **TT** conformers, the δCOH_{sc} band of **Ser-III** is predicted to appear at the highest frequency predicted at 1428 cm^{-1} with a stronger H-bond between OH_{sc} and carbonyl oxygen. Class **C** conformers with relatively weak H bonds involving the alcohol side chine group as a proton

donor are expected to absorb within the 1370-1420 cm^{-1} region. In summary, for class **C** conformers, the frequencies of the δCOH_{sc} vibrations are predicted to be higher than the frequencies of the δCOH_{bb} with the exception of **Ser-XI**, whereas for the class **TT** conformers (except for **Ser-III**) the reversed order of frequencies is expected.

The intense band at 1400 cm^{-1} is assigned to the δCOH_{bb} vibration of **Ser-I**. In the case of **Ser-III**, the assignment of 1376 cm^{-1} is confirmed by the increased intensity upon annealing. The δCOH_{sc} band due to class **C** conformers are observed as a shoulder at 1410 cm^{-1} with contribution from the δCOH_{sc} band of **Ser-III**.

The νC–O and νN–C single-bond stretching modes also provide some diagnostic through frequencies and are predicted by the computations to give rise to bands in the 850-1200 cm^{-1} region. In class **TT** conformers, $\nu C–O_{bb}$ is expected to originate low-intensity bands (<30 km mol^{-1}) at frequencies between 1150-1210 cm−1, whereas in class **C** conformers, this vibration shall give rise to more intense bands appearing at lower frequencies (1100-1150 cm^{-1}). This indicate that in the studied compounds the $C–O_{bb}$ bond is weaker for a *cis* carboxylic group than in a *trans* carboxylic group, correlating well with the longer $C–O_{bb}$ bond in class **C** conformers than in type A forms. The $\nu C–O_{sc}$ and νN–C vibrations are coupled with oscillations along other coordinates for most conformers. But in general, $\nu C–O_{sc}$ shall correspond to a relatively intense band and appearing between 970-

1060 cm^{-1}. On the other hand, νN–C is in general predicted to give rise to a weak band with exceptions for **Ser-I**, **II**, and **IV**.

As expected, bands due to $\nu C–O_{bb}$ of class **C** conformers (predicted to be intense) are clearly observed, whereas for class **TT** conformers, only the band due to **Ser-VI** could be experimentally identified at 1163 cm^{-1}. The most intense bands in this region at 1137, 1132, 1126, and 1123 cm^{-1} were assigned to **Ser-II**, **IV**, **VIII**, and **V**, respectively. In all cases agree with predicted values within 20 cm^{-1}. The relatively intense $\nu C–O_{sc}$ bands were also observed (**Ser-II**, **III**, **VIII** at 1065 cm^{-1}, **Ser-IV** at 1057 cm^{-1}, **Ser-VI**, **VII** at 1043 cm^{-1}, **Ser-IX** at 1010 cm^{-1}, and, finally, 975 cm^{-1} to **Ser-I**).

The most intense bands predicted by calculations below 950 cm^{-1} are due to τC–O torsional and ωNH_2 wagging modes. For class **TT** conformers, the $\tau C–O_{sc}$ bands are predicted at frequencies below 400 cm^{-1} except for **Ser-III**, where $\tau C–O_{sc}$ band was predicted to occur at 580 cm^{-1}. In general, $\tau C–O_{bb}$ for class **C** conformers, where the carboxyl group is in the *cis* form and not taking part in other H-bond are predicted to be lower in frequencies and are clearly observed experimentally. The band at 579 cm^{-1} is ascribed to the class **CA** conformer **Ser-V** (predicted frequency 589 cm^{-1}), whereas **Ser-II** and **VIII** give rise to the intense doublet at 568/566 cm^{-1} (predicted at 585 and 589 cm^{-1}).

Table 3.5 Anharmonic Vibrational Fundamentals Characteristic of Hydrogen Bonding in the Twelve Lowest-Energy Conformers of Serine[a]

	Class TT					Class CC				Class CA		Class CT
	Ser-I	**Ser-III**	**Ser-VI**	**Ser-VII**	**Ser-IX**	**Ser-II**	**Ser-IV**	**Ser-X**	**Ser-XI**	**Ser-V**	**Ser-XII**	**Ser-VIII**
ν(O–H)sc	3644(53)	3535(156)	3685(59)	3669(48)	3689(53)	3546(76)	3544(66)	3669(40)	3693(54)	3615(71)	3633(65)	3551(74)
ν(O–H)bb	3224(272)	3241(267)	3217(291)	3233(279)	3254(268)	3574(83)	3584(92)	3571(78)	3581(77)	3573(90)	3576(90)	3576(88)
$\nu^{as}(NH_2)$	3450(18)	3456(15)	3441(25)	3442(24)	3446(15)	3442(14)	3467(23)	3430(13)	3433(12)	3451(14)	3448(8)	3455(13)
$\nu^{s}(NH_2)$	3375(12)	3383(2)	3388(3)	3388(3)	3389(6)	3392(9)	3358(13)	3344(5)	3389(6)	3373(5)	3388(3)	3397(7)
$\nu^{as}(C_\beta H_2)$	3013(15)	2983(25)	2967(18)	3012(12)	2961(16)	3016(16)	3037(13)	3028(12)	3000(22)	3023(14)	3031(15)	3010(15)
$\nu^{s}(C_\beta H_2)$	2969(25)	2885(50)	2919(26)	2959(17)	2909(35)	2877(44)	2928(45)	2974(32)	2930(28)	2943(32)	2913(39)	2882(46)
$\nu(C_\alpha–H)$	2940(12)	2972(7)	2972(8)	2951(14)	2969(4)	2991(4)	2934(41)	2936(10)	2956(20)	2916(20)	2973(9)	
ν(C=O)	1804(244)	1795(236)	1810(263)	1811(260)	1799(252)	1787(225)	1799(220)	1749(228)	1800(229)	1769(218)	1768(218)	1786(220)
δ(COH)sc	1215(10)	1428(19)	1221(18)	1129(2)	1218(21)	1411(59)	1407(56)	1370(12)	1268(13)	1427(22)	1396(27)	1414(81)
δ(COH)bb	1409(310)	1391(471)	1384(381)	1337(350)	1374(383)	1348(51)	1310(27)	1257(10)	1279(12)	1258(6)	1288(12)	1290(44)
ν(C–O)bb	1195(15)	1190(20)	1159(13)	1205(11)	1194(13)	1151(51)	1130(140)	1108(223)	1106(241)	1123(253)	1134(197)	1143(168)
ν(C–O)sc	976(78)	1083(69)	1061(80)	1061(105)	1043(104)	1076(132)	1027(76)	998(103)	1037(49)	1047(5)	1078(94)	1073(121)
$\nu(N–C_\alpha)$	840(85)	1117(3)	1105(34)	1114(42)	1111(5)	1105(185)	1112(87)	899(35)	921(16)	1123(72)	1118(46)	1141(4)
$\rho_w(NH_2)$	923(70)	818(110)	949(65)	945(48)	950(50)	848(89)	898(83)	915(101)	895(131)	853(106)	840(161)	822(99)
$\rho_t(O–H)_{bb}$	876(46)	857(78)	840(71)	834(22)	825(56)	585(97)	657(70)	639(99)	603(91)	589(104)	603(87)	611(101)
$\rho_t(O–H)_{sc}$	415(103)	580(89)	229(102)	294(61)	225(103)	529(119)	570(155)	310(106)	203(52)	541(153)	474(178)	507(102)

[a] All frequencies in cm^{-1}; double-harmonic infrared intensities in km mol^{-1} given in parentheses. Harmonic frequencies and intensities were computed at the MP2/cc-pVTZ level. Anharmonic corrections were computed using MP2/6-31G*.

ν(O–H)sc: Stretching of the side chain O–H bond; ν(O–H)bb: Stretching of the back bone COOH group O–H bond; $\nu^{as}(NH_2)$: Asymmetric NH_2 stretching, $\nu^{s}(NH_2)$: Symmetric NH_2 stretching; δ(COH): bending of the side chain or back bone COH group; ν(C–O)sc: Stretching of the side chain C–O bond; ν(C–O)bb: Stretching of the back bone COOH group C–O bond; ϱ_w, ϱ_t: wagging and twisting.

3.3.4. Rotational Spectra

The super sonic jet of a LA-MB-FTMW spectrometer provides an environment where amino acids can be considered isolated, thus allowing the evaluation of the role of intramolecular interactions through the investigation of conformational preference in the gas phase. The two-body collisions with the carrier gas cool these stable conformers to very low temperatures, thereby trapping them in their energy minima. Alonso et al[26] reported the identification of six low-energy conformers of cysteine and seven low-energy conformers of serine. The seven conformers that have been identified correspond to **Ser-I – Ser-VI** and **Ser-XII**. Computed rotational constants, ^{14}N quadrupole coupling constants, centrifugal distortion constants, and dipole moments are reported in Table 4 along with experimental values,[26] where available.

The different orientations of the CH_2OH side chain to the skeleton carboxylic and amine group about the C_α–C_β bond have been indicated according to International Union of Pure and Applied Chemistry terminology.[104] Two dihedral angles were selected: $\tau(N_1–C_\alpha–C_\beta–O_{11})$ and $\tau(C_5–C_\alpha–C_\beta–O_{11})$. 12 conformers hence could be categorized into gauche/gauche, gauche/trans, and trans/gauche types (see Table 4 and supporting info Table S6). Except for **Ser-X** and **Ser-XI**, almost all conformers have substantial dipole moments along the principal axes, make the observation of the related rotational transitions possible. In gauche/trans conformers (**Ser-II**, **VI**, **VII**, **VIII**, and **IX**), the CH_2OH side chain is positioned antiperiplanar to the carboxyl group, the overall geometry is extended along the A axis, results in a much larger A_e rotational constants. When the CH_2OH side chain is gauche to the carboxyl group, the overall geometry is more compact about the B axis, which is reflected in the larger B_e rotational constants in

comparison to gauche/trans conformers (Table 3.6). Last but not least, the trans/gauche conformers have the smallest C_e rotational constants.

The ground state vibrational constants obtained by combining the MP2/aug-cc-pVTZ equilibrium rotational constants and MP2/6-31G* level vibrational corrections should be accurate enough to deduce the presence of conformers when interpreting experimental microwave spectra. The mean absolute deviations from experiment are only 11, 6, and 5 MHz for A_0, B_0, and C_0, respectively. In all cases, the zero-point vibrational corrections lower the rotational constant, zero-point vibrational corrections to the rotational constants improve agreement for A_0 and B_0, but lessen the agreement for C_0.

For conformers showing only slight geometry changes but different intramolecular H-bonds, the rotational constants are very similar and they do not allow discrimination. In these cases, ^{14}N nuclear quadrupole hyperfine structure identifies the observed lines belonging to different serine conformers. The presence of a single ^{14}N nucleus in serine splits each rotational transition into several close hyperfine components by the interaction of the ^{14}N nuclear electric quadrupole moment with the molecular electric field gradient at the nitrogen position.[26]

Quadrupole coupling constants ($\chi_{\alpha\alpha}$) of the nitrogen nucleus are given as[105]

$$\chi_{\alpha\alpha} = eq_{\alpha\alpha}Q \tag{3.3}$$

The electric-field gradient $q_{\alpha\alpha}$ along the α-axis at the nitrogen nucleus is obtained in a.u. (hartree/bohr^2), e is the fundamental charge, and Q is the nuclear quadrupole moment (typically given in mbarn=10^{-31} m^2) and can be taken from the compilations of P. Pyykkö.[106] The nitrogen quadrupole moment was 20.44 mb. Wilke et al.[16] used the combination of a cc-pCV5Z basis on nitrogen and cc-pVTZ basis on all other atoms, and

his results matches both the full cc-pCV5Z result and the experimental coupling constant for ammonia. The predicted quadrupole coupling constants for most of the cysteine amino acids are within 0.1 MHz of experiment with the largest deviation being 0.23 MHz. Thus we feel the combination of MP2 and the locally dense basis should offer the required accuracy and help to resolve the ambiguity in conformer assignment based on rotational constants. In deed, the average mean absolute deviation from experiment of serine conformers is only 0.11 MHz.

The ambiguity in assignment based on rotational constants is removed for some conformers. For example, **Ser-II** has a strong χ_{aa} quadrupole coupling comes from the strong H-bond between side chain hydrogen donor and nitrogen atom, while **Ser-VI** exhibits almost no χ_{aa} coupling. The same discrepancy also exists for **Ser-III** and **XII**, where there is a strong χ_{aa} coupling for **Ser-III** due to the H-bond between the carboxyl hydrogen and nitrogen, but non-exist for **Ser-XII** in the absence of this H-bond.

Table 3.6 Equilibrium {A_e, B_e, C_e5 and Ground-State Rotational Constants {A_0, B_0, C_0} , ^{14}N Nuclear Quadrupole Coupling Constants χ, Quartic Centrifugal Distortion Constants in the A-Reduced Representation, and Dipole Moments of the 12 Lowest-Energy Conformers of Serine.

	Gauche/Gauche					Gauche/Trans			Trans/Gauche			
	Ser-I	**Ser-IV**	**Se-V**	**Ser-X**	**Ser-XI**	**Ser-II**	**Ser-VI**	**Ser-VII**	**Ser-VIII**	**Ser-IX**	**Ser-III**	**Ser-XII**
A_e	3552	3545	3975	3458	3479	4498	4542	4497	4537	4647	3654	3493
B_e	2417	2339	2251	2396	2326	1833	1860	1843	1789	1875	2412	2340
C_e	1761	1824	1681	1763	1832	1464	1484	1479	1491	1397	1531	1614
A_0	3525(3557)	3504(3524)	3929(3932)	3407	3439	4452(4479)	4497(4517)	4455	4489	4602	3624(3639)	3462(3510)
B_0	2382(2380)	2313(2308)	2233(2243)	2363	2308	1822(1830)	1845(1847)	1830	1768	1859	2387(2388)	2311(2322)
C_0	1744(1741)	1813(1805)	1662(1665)	1757	1821	1449(1444)	1469(1464)	1464	1485	1385	1516(1519)	1602(1584)
χ_{aa}	–3.49	–0.80	–0.50	–1.21	–1.61	–4.31	–0.29	–0.27	–4.40	–2.71	–3.58	–0.81
χ_{bb}	2.04	2.42	–0.78	1.32	2.18	2.75	1.95	1.93	2.75	1.15	1.98	–0.83
χ_{cc}	1.46	–1.62	1.28	–0.11	–0.57	1.55	–1.66	–1.66	1.65	1.56	1.60	1.63
D_J	0.91	0.98	0.52	0.86	0.96	0.23	0.21	0.21	0.44	0.14	0.32	0.45
D_{JK}	0.15	–0.87	–0.85	–0.30	–0.64	1.38	1.19	1.11	4.07	0.84	–0.10	–0.33
D_K	0.52	1.56	2.94	1.60	1.20	0.19	0.40	0.59	–2.38	0.94	0.72	1.69
d_J	0.26	0.19	0.24	0.19	0.20	0.04	0.03	0.03	0.06	0.04	0.13	–0.01
d_K	0.79	1.10	0.79	1.38	1.64	2.84	1.93	1.80	11.41	0.61	0.35	–0.11
μ_a	2.04	0.71	2.83	1.45	0.52	2.33	4.45	3.75	2.44	4.24	0.77	3.40
μ_b	3.22	1.08	0.14	2.18	2.27	0.50	1.66	1.68	2.77	1.53	4.88	0.08
μ_c	1.50	2.77	0.31	0.80	0.77	0.67	0.24	2.15	0.39	0.67	0.28	0.81

Equilibrium rotational constants given in MHz and belong to the structures optimized at the MP2(FC)/aug-cc-pVTZ level.

Ground-state rotational constants are determined from MP2(FC)/aug-cc-pVTZ equilibrium structures with anharmonic MP2/6-31G* correction.

14N nuclear quadrupole coupling tensor from MP2/cc-pVTZ-LD in MHz

Quartic centrifugal distortion constants from MP2/cc-pVTZ in KHz

Dipole moments are given in Debye and computed at the MP2/cc-pVTZ level.

3.4. Conclusion

The detailed high-level ab initio structural investigation of serine allows us to draw the following conclusions about this neutral amino acid. Because of the added flexibility of the –OH side chain, serine exhibits 85 unique conformers (see Appendix Table B.1) and twelve conformers within 8 kJ mol^{-1} of the lowest minimum. Through the focal point approach, we have established definitive relative energies of the twelve lowest conformers to within a standard error of 0.3 kJ mol^{-1}. Harmonic frequencies were computed at the MP2/cc-pVTZ level with anharmonic corrections at the MP2/6-31G* level. The vibrational perturbation theory generally performs well (within 20 cm^{-1} of experiment), although it breaks down for a few large-amplitude motions with very low frequencies.

References:

1. Chyba, C. F.; Thomas, P. J.; Brookshaw, L.; Sagan, C., *Science* **1990,** *249*, 366-373.
2. Luscombe, N. M.; Laskowski, R. A.; Thornton, J. M., *Nucleic Acids Res.* **2001,** *29*, 2860-2874.
3. Berulis, I.; Winnewisser, G.; Krasnov, V.; Sorochenko, R., *Sov. Astron. Lett.* **1985,** *11*, 251.
4. Snyder, L. E., *Origins Life Evol. Biosphere* **1997,** *27*, 115-133.
5. Hughes, A. B., *Amino Acids, Peptides and Proteins in Organic Chemistry, Analysis and Function of Amino Acids and Peptides*. John Wiley & Sons: 2013; Vol. 5.
6. Barrientos, C.; Redondo, P.; Largo, L.; Rayón, V. M.; Largo, A., *Astrophys. J.* **2012,** *748*, 99.
7. Bada, J. L.; Glavin, D. P.; McDonald, G. D.; Becker, L., *Science* **1998,** *279*, 362-365.
8. Singh, A.; Gupta, V.; Misra, A.; Tandon, P., *Astron. Astrophys.* **2014,** *563*, 55.
9. Van Alsenoy, C.; Scarsdale, J.; Sellers, H.; Schäfer, L., *Chem. Phys. Lett.* **1981,** *80*, 124-126.
10. Van Alsenoy, C.; Kulp, S.; Siam, K.; Klimkowski, V. J.; Ewbank, J. D.; Schäfer, L., *J. Mol. Struct.- THEOCHEM* **1988,** *181*, 169-178.
11. Tarakeshwar, P.; Manogaran, S., *J. Mol. Struct.- THEOCHEM* **1994,** *305*, 205-224.
12. Gronert, S.; O'Hair, R. A., *J. Am. Chem. Soc.* **1995,** *117*, 2071-2081.
13. Noguera, M.; Rodrıguez-Santiago, L.; Sodupe, M.; Bertran, J., *J. Mol. Struct.-THEOCHEM* **2001,** *537*, 307-318.
14. Miao, R.; Jin, C.; Yang, G.; Hong, J.; Zhao, C.; Zhu, L., *J. Phys. Chem. A* **2005,** *109*, 2340-2349.
15. Jarmelo, S.; Lapinski, L.; Nowak, M.; Carey, P.; Fausto, R., *J. Phys. Chem. A* **2005,** *109*, 5689-5707.
16. Wilke, J. J.; Lind, M. C.; Schaefer III, H. F.; Császár, A. G.; Allen, W. D., *J. Chem. Theory Comput.* **2009,** *5*, 1511-1523.
17. Kasalová, V.; Allen, W. D.; Schaefer III, H. F.; Czinki, E.; Császár, A. G., *J. Comput. Chem.* **2007,** *28*, 1373-1383.
18. Császár, A. G., *J. Phys. Chem.* **1996,** *100*, 3541-3551.
19. Császár, A. G., *J. Am. Chem. Soc.* **1992,** *114*, 9568-9575.
20. Lovas, F.; Kawashima, Y.; Grabow, J.-U.; Suenram, R.; Fraser, G.; Hirota, E., *Astrophys. J. Lett.* **1995,** *455*, L201.
21. Stepanian, S.; Reva, I.; Radchenko, E.; Rosado, M.; Duarte, M.; Fausto, R.; Adamowicz, L., *J. Phys. Chem. A* **1998,** *102*, 1041-1054.
22. Stepanian, S.; Reva, I.; Radchenko, E.; Adamowicz, L., *J. Phys. Chem. A* **1998,** *102*, 4623-4629.
23. Stepanian, S.; Reva, I.; Radchenko, E.; Adamowicz, L., *J. Phys. Chem. A* **1999,** *103*, 4404-4412.
24. Stepanian, S.; Reva, I.; Radchenko, E.; Adamowicz, L., *J. Phys. Chem. A* **2001,** *105*, 10664-10672.

25. Lambie, B.; Ramaekers, R.; Maes, G., *Spectrochim. Acta, Part A* **2003,** *59*, 1387-1397.
26. Blanco, S.; Sanz, M. E.; López, J. C.; Alonso, J. L., *Proc. Natl. Acad. Sci. U. S. A.* **2007,** *104*, 20183-20188.
27. Lambie, B.; Ramaekers, R.; Maes, G., *J. Phys. Chem. A* **2004,** *108*, 10426-10433.
28. Suenram, R. D.; Lovas, F., *J. Mol. Spectrosc.* **1978,** *72*, 372-382.
29. Suenram, R.; Lovas, F., *J. Am. Chem. Soc.* **1980,** *102*, 7180-7184.
30. Godfrey, P. D.; Brown, R. D., *J. Am. Chem. Soc.* **1995,** *117*, 2019-2023.
31. McGlone, S. J.; Elmes, P. S.; Brown, R. D.; Godfrey, P. D., *Mol. Struct.* **1999,** *485*, 225-238.
32. Godfrey, P.; Firth, S.; Hatherley, L.; Brown, R.; Pierlot, A., *J. Am. Chem. Soc.* **1993,** *115*, 9687-9691.
33. Blanco, S.; Lesarri, A.; López, J. C.; Alonso, J. L., *J. Am. Chem. Soc.* **2004,** *126*, 11675-11683.
34. Lesarri, A.; Cocinero, E. J.; López, J. C.; Alonso, J. L., *Angew. Chem.* **2004,** *116*, 615-620.
35. Lesarri, A.; Sánchez, R.; Cocinero, E. J.; López, J. C.; Alonso, J. L., *J. Am. Chem. Soc.* **2005,** *127*, 12952-12956.
36. Cocinero, E. J.; Lesarri, A.; Grabow, J. U.; López, J. C.; Alonso, J. L., *ChemPhysChem* **2007,** *8*, 599-604.
37. Lesarri, A.; Mata, S.; Cocinero, E. J.; Blanco, S.; López, J. C.; Alonso, J. L., *Angew. Chem.* **2002,** *114*, 4867-4870.
38. Lesarri, A.; Cocinero, E. J.; López, J. C.; Alonso, J. L., *J. Am. Chem. Soc.* **2005,** *127*, 2572-2579.
39. Sanz, M. E.; Lesarri, A.; Peña, M. I.; Vaquero, V.; Cortijo, V.; López, J. C.; Alonso, J. L., *J. Am. Chem. Soc.* **2006,** *128*, 3812-3817.
40. Lesarri, A.; Cocinero, E. J.; López, J. C.; Alonso, J. L., *ChemPhysChem* **2005,** *6*, 1559-1566.
41. Cocinero, E. J.; Villanueva, P.; Lesarri, A.; Sanz, M. E.; Blanco, S.; Mata, S.; López, J. C.; Alonso, J. L., *Chem. Phys. Lett.* **2007,** *435*, 336-341.
42. Sanz, M. E.; Cortijo, V.; Caminati, W.; López, J. C.; Alonso, J. L., *Chem.–Eur. J.* **2006,** *12*, 2564-2570.
43. Stepanian, S. G.; Ivanov, A. Y.; Adamowicz, L., *Chem. Phys.* **2013,** *423*, 20-29.
44. Dobrowolski, J. C.; Jamróz, M. H.; Kołos, R.; Rode, J. E.; Cyrański, M. K.; Sadlej, J., *Phys. Chem. Chem. Phys.* **2010,** *12*, 10818-10830.
45. Boeckx, B.; Maes, G., *Spectrochim. Acta, Part A* **2012,** *86*, 366-374.
46. Boeckx, B.; Maes, G., *J. Phys. Chem. A* **2012,** *116*, 1956-1965.
47. Boeckx, B.; Ramaekers, R.; Maes, G., *Biophys. Chem.* **2011,** *159*, 247-256.
48. Boeckx, B.; Ramaekers, R.; Maes, G., *J. Mol. Spectrosc.* **2010,** *261*, 73-81.
49. Bazsó, G.; Magyarfalvi, G.; Tarczay, G., *J. Mol. Struct.* **2012,** *1025*, 33-42.
50. Bazsó, G.; Najbauer, E. E.; Magyarfalvi, G.; Tarczay, G., *J. Phys. Chem. A* **2013,** *117*, 1952-1962.
51. Stepanian, S. G.; Ivanov, A. Y.; Smyrnova, D. A.; Adamowicz, L., *J. Mol. Struct.* **2012,** *1025*, 6-19.
52. Najbauer, E. E.; Bazsó, G.; Góbi, S.; Magyarfalvi, G.; Tarczay, G., *J. Phys. Chem. B* **2014,** *118*, 2093-2103.

53. Allen, W. D.; East, A. L.; Császár, A. G., *Structures and conformations of non-rigid molecules*, Laane, J.; Dakkouri, M.; van der Veken, B.; Oberhammer, H., Eds. Springer: The Netherlands, **1993**; pp 343-373.
54. East, A. L.; Allen, W. D., *J. Chem. Phys.* **1993,** *99*, 4638-4650.
55. Császár, A. G.; Allen, W. D.; Schaefer III, H. F., *J. Chem. Phys.* **1998,** *108*, 9751-9764.
56. Császár, A. G.; Tarczay, G.; Leininger, M. L.; Polyansky, O. L.; Tennyson, J.; Allen, W. D., *Spectroscopy from Space*, Demaison, J.; Sarka, K.; Cohen, E. A., Eds. Springer: The Netherlands, **2001**; pp 317-339.
57. Wilke, J. J.; Allen, W. D.; Schaefer, H. F., *J. Chem. Phys.* **2008,** *128*, 74308-74500.
58. Simmonett, A. C.; Schaefer, H. F.; Allen, W. D., *J. Chem. Phys.* **2009,** *130*, 44301.
59. Császár, A. G., *J. Mol. Struct.* **1995,** *346*, 141-152.
60. Szidarovszky, T.; Czakó, G.; Császár, A. G., *Mol. Phys.* **2009,** *107*, 761-775.
61. Allen, W. D.; Czinki, E.; Császár, A. G., *Chem.–Eur. J.* **2004,** *10*, 4512-4517.
62. Czinki, E.; Császár, A. G., *Chem. Eur. J.* **2003,** *9*, 1008-1019.
63. Roothaan, C. C. J., *Rev. Mod. Phys.* **1951,** *23*, 69-89.
64. Krishnan, R.; Frisch, M.; Pople, J., *J. Chem. Phys.* **1980,** *72*, 4244-4245.
65. Čížek, J., *J. Chem. Phys.* **1966,** *45*, 4256-4266.
66. Crawford, T. D.; Schaefer III, H. F., *Rev. Comput. Chem.* **2000,** *14*, 33-136.
67. Purvis III, G. D.; Bartlett, R. J., *J. Chem. Phys.* **1982,** *76*, 1910-1918.
68. Raghavachari, K.; Trucks, G. W.; Pople, J. A.; Head-Gordon, M., *Chem. Phys. Lett.* **1989,** *157*, 479-483.
69. Jayatilaka, D.; Lee, T. J., *J. Chem. Phys.* **1993,** *98*, 9734-9747.
70. Lee, T. J.; Taylor, P. R., *Int. J. Quantum Chem.* **1989,** *36*, 199-207.
71. Hariharan, P. C.; Pople, J. A., *Theor. Chim. Acta* **1973,** *28*, 213-222.
72. Peterson, K. A.; Dunning Jr, T. H., *J. Chem. Phys.* **2002,** *117*, 10548-10560.
73. Kendall, R. A.; Dunning Jr, T. H.; Harrison, R. J., *J. Chem. Phys.* **1992,** *96*, 6796-6806.
74. Dunning Jr, T. H., *J. Chem. Phys.* **1989,** *90*, 1007-1023.
75. Woon, D. E.; Dunning Jr, T. H., *J. Chem. Phys.* **1995,** *103*, 4572-4585.
76. Frisch, M. J.; Pople, J. A.; Del Bene, J. E., *J. Phys. Chem.* **1985,** *89*, 3664-3669.
77. Werner, H.-J.; Knowles, P. J.; Knizia, G.; Manby, F. R.; Schütz, M.; Celani, P.; Korona, T.; Lindh, R.; Mitrushenkov, A.; Rauhut, G.; Shamasundar, K. R.; Adler, T. B.; Amos, R. D.; Bernhardsson, A.; Berning, A.; Cooper, D. L.; Deegan, M. J. O.; Dobbyn, A. J.; Eckert, F.; Goll, E.; Hampel, C.; Hesselmann, A.; Hetzer, G.; Hrenar, T.; Jansen, G.; Köppl, C.; Liu, Y.; Lloyd, A. W.; Mata, R. A.; May, A. J.; McNicholas, S. J.; Meyer, W.; Mura, M. E.; Nicklaß, A.; O'Neill, D. P.; Palmieri, P.; Peng, D.; Pflüger, K.; Pitzer, R.; Reiher, M.; Shiozaki, T.; Stoll, H.; Stone, A. J.; Tarroni, R.; Thorsteinsson, ; Wang, T. M., *MOLPRO*, version 2006.1; 2006. Version 2010.1.
78. Stanton, J.F.; Gauss, J.; Harding, M.E.; Szalay, P.G.; with contributions from Auer, A. A.; Bartlett, R. J.; Benedikt, U.; Berger, C.; Bernholdt , D. E.; Bomble, Y. J.; Cheng, L.; Christiansen, O.; Heckert, M.; Heun, O.; Huber, C.; Jagau, T.-C.; Jonsson, D.; Jusélius, J.; Klein, K.; Lauderdale, W. J.; Matthews, D. A.; Metzroth, T.; Mück, L. A.; O'Neill, D. P.; D.R. Price, E. Prochnow, C. Puzzarini, K. Ruud, F. Schiffmann, W. Schwalbach, C. Simmons, S. Stopkowicz, A. Tajti, J. Vázquez, F. Wang, J.D. Watts and

the integral packages MOLECULE (J. Almlöf and P.R. Taylor), PROPS (P.R. Taylor), ABACUS (T. Helgaker, H.J. Aa. Jensen, P. Jørgensen, and J. Olsen), and ECP routines by A. V. Mitin and C. van Wüllen. *CFOUR*, For the current version, see http://www.cfour.de. 2008.
79. Janssen, C. L.; Nielsen, I. B.; Leininger, M. L.; Valeev, E. F.; Kenny, J. P.; Seidl, E. T., *The Massively Parallel Quantum Chemistry Program (MPQC),* Version 2.3.1; Sandia National Laboratories, Livermore, CA, USA, 2008.
80. Turney, J. M.; Simmonett, A. C.; Parrish, R. M.; Hohenstein, E. G.; Evangelista, F. A.; Fermann, J. T.; Mintz, B. J.; Burns, L. A.; Wilke, J. J.; Abrams, M. L.; Russ, N. J.; Leininger, M. L.; Janssen, C. L.; Seidl, E. T.; Allen, W. D.; Schaefer, H. F.; King, R. A.; Valeev, E. F.; Sherrill, C. D.; Crawford, T. D., *WIREs Comput. Mol. Sci.* **2012,** *2*, 556-565.
81. Shao, Y.; Molnar, L. F.; Jung, Y.; Kussmann, J.; Ochsenfeld, C.; Brown, S. T.; Gilbert, A. T.; Slipchenko, L. V.; Levchenko, S. V.; O'Neill, D. P., *Phys. Chem. Chem. Phys.* **2006,** *8*, 3172-3191.
82. Krylov, A. I.; Gill, P. M., *WIREs Comput. Mol. Sci.* **2013,** *3*, 317-326.
83. Peterson, K. A.; Woon, D. E.; Dunning Jr, T. H., *J. Chem. Phys.* **1994,** *100*, 7410-7415.
84. Mills, I.; Rao, K. N.; Mathews, C. W., *Molecular spectroscopy: Modern research, Academic, New York* **1972,** 115-140.
85. Clabo, D. A.; Allen, W. D.; Remington, R. B.; Yamaguchi, Y.; Schaefer, H. F., *Chem. Phys.* **1988,** *123*, 187-239.
86. Allen, W. D.; Yamaguchi, Y.; Császár, A. G.; Clabo Jr., D. A.; Remington, R. B.; Schaefer, H. F., *Chem. Phys.* **1990,** *145*, 427-466.
87. Thiel, W.; Scuseria, G.; Schaefer III, H. F.; Allen, W. D., *J. Chem. Phys.* **1988,** *89*, 4965-4975.
88. Bomble, Y. J.; Vázquez, J.; Kállay, M.; Michauk, C.; Szalay, P. G.; Császár, A. G.; Gauss, J.; Stanton, J. F., *J. Chem. Phys.* **2006,** *125*, 064108.
89. Tajti, A.; Szalay, P. G.; Gauss, J., *J. Chem. Phys.* **2007,** *127*, 014102.
90. Barone, V., *J. Chem. Phys.* **2004,** *120*, 3059-3065.
91. Schuurman, M. S.; Allen, W. D.; Schaefer, H. F., *J. Comput. Chem.* **2005,** *26*, 1106-1112.
92. Tajti, A.; Szalay, P. G.; Császár, A. G.; Kállay, M.; Gauss, J.; Valeev, E. F.; Flowers, B. A.; Vázquez, J.; Stanton, J. F., *J. Chem. Phys.* **2004,** *121*, 11599-11613. See footnote 69 for the G_0 expression of asymmetric tops.
93. Pfeiffer, F.; Rauhut, G.; Feller, D.; Peterson, K. A., *J. Chem. Phys.* **2013,** *138*, 044311. See footnote 37. The G_0 formula implemented in CFour contains a bug that omits the contribution of the sum of rotational constants. This can be fixed by using a patch as described in https://lists.uni-mainz.de/sympa/arc/cfour/2012-08/thrd2.html.
94. Reed, A. E.; Curtiss, L. A.; Weinhold, F., *Chem. Rev.* **1988,** *88*, 899-926.
95. Reed, A. E.; Weinhold, F., *J. Chem. Phys.* **1983,** *78*, 4066-4073.
96. Reed, A. E.; Weinstock, R. B.; Weinhold, F., *J. Chem. Phys.* **1985,** *83*, 735-746.
97. Glendening, E. D.; Landis, C. R.; Weinhold, F., *WIREs Comput. Mol. Sci.* **2012,** *2*, 1-42.

98. Dobrowolski, J. C.; Rode, J. E.; Sadlej, J., *J. Mol. Struct.- THEOCHEM* **2007,** *810*, 129-134.
99. Eliel, E. L.; Wilen, S. H., *Stereochemistry of organic compounds*. John Wiley & Sons: New York, 2008.
100. Dokmaisrijan, S.; Lee, V. S.; Nimmanpipug, P., *J. Mol. Struct.- THEOCHEM* **2010,** *953*, 28-38.
101. Fausto, R.; de Carvalho, L. B.; Teixeira-Dias, J.; Ramos, M., *J. Chem. Soc., Perkin Trans. 2* **1989,** *85*, 1945-1962.
102. Fausto, R.; Teixeira-Dias, J., *J. Mol. Struct.- THEOCHEM* **1987,** *150*, 381-389.
103. Räsänen, M.; Aspiala, A.; Homanen, L.; Murto, J., *J. Mol. Struct.* **1983,** *96*, 81-100.
104. Moss, G., *Pure Appl. Chem.* **1996,** *68*, 2193-2222.
105. Hollas, J. M., *High resolution spectroscopy*. London, 2013; Vol. 1.
106. Polák, R.; Fišer, J., *Chem. Phys. Lett.* **2008,** *351*, 83-90.

CHAPTER 4

TRUNCATED COULOMB ANALYSIS*

* He, K; Allen, W. D. To be submitted to *Journal of Chemical Theory and Computation*

Abstract

In order to place the concept of intramolecular dispersion on a firm theoretical footing that does not involve artificial partitioning into molecular fragments, we have developed a new approach for dividing electron correlation energies given by general wave function methods into long-, medium-, and short-range components. By means of inverse error-function transforms, we show how the Coulomb operator within two-electron integrals can be split using arbitrary switching functions. An appealing form of the switching function is found that allows MP2, CCSD, and CCSD(T) correlation energies to be computed as a function of a sharp cutoff distance over which electrons are allowed to interact. The truncated Coulomb analysis presented here provides a better understanding of how the correlation energy varies with electron-electron interaction distance. The partition of the correlation energy is achieved based on the common features of the correlation energy dependence on the electron-electron interaction distance. Preliminary results are presented for the interaction energy of a series of noncovalently bonded complexes, as well as atomization energies. The common understanding of dispersion is challenged, but in a way supported by simple physical models.

4.1 Introduction

Van der Waals (also called dispersive) interactions between atoms and molecules play an important role in many chemical systems. They are delicately balanced with electrostatic and exchange/repulsion interactions,[1] and together they control, for example, the structure of DNA and proteins, the packing of crystals, the formation of aggregates, host-guest systems, and the orientation of molecules on surfaces or in molecular films.[2-7] It is generally believed that van der Waals effects are of major importance only for intermolecular situations (for example, weakly bonded complexes), but their importance has been demonstrated in numerous systems. A delicate balance between inter- and intramolecular dispersion effects is a quite general phenomenon for larger molecules. An analysis of the interaction energy in the water dimer and several alcohol dimers using symmetry-adapted perturbation theory shows that the size and shape of substituents strongly influence the stabilization of hydrogen-bonded complexes.[8] The larger and bulkier the substituents are, the more important the attractive dispersion interaction is, which eventually becomes of the same magnitude as the total stabilization energy. Electrostatics alone is a poor predictor of the hydrogen-bond stability trends in the sequence of dimers investigated, and in fact, dispersion interactions predict these trends better.

Recently synthesized diamondoid dimers such as 1-(1-diamantyl) diamantane and 2-(1-diamantyl) tetramantane exhibit the longest C–C covalent bonds ever observed, up to 1.71 Å in length.[9] These extraordinary long central C–C bonds appear to be stabilized by intramolecular van der Waals attractions, and despite severe steric crowding they are stable even at temperatures above 200 °C.[9-10] In the 1-(1-diamantyl) diamantane case,

intramolecular dispersion greatly stabilizes the central C–C bond by nearly 36 kcal mol^{-1} based on massive MP2, CCSD, and CCSD(T) wave function computations with large basis sets.[11]In comparison, DFT methods that incorporate dispersion yield a disturbing scatter of results.[9]

For larger systems, DFT is the preferred tool due to the skyrocketing cost of the more accurate *ab initio* methods. It is known that commonly used DFs do not describe the long-range dispersion interaction correctly.[12-15] It is clear that all semilocal DFs and conventional hybrid functionals asymptotically cannot provide the correct $-C_6/R^6$ dependence of the dispersion interaction energy with respect to the interatomic (molecular) distance R. The densities corresponding to the atomic or molecular 'virtual' electronic excitations states are not represented by conventional (hybrid) functionals that only consider electron exchange but do not employ virtual orbitals. Most of the current dispersion-corrected DFT approaches include in various ways empirical components, because dispersion is a troublesome kind of electron correlation operating merely on long-range scales. At short electron-electron distances, the standard functionals describe the corresponding effects rather well. Thus, any dispersion-including DFT approach is faced with the problem of merging in a seamless fashion the short- and long- range asymptotic regions.

One alternative approach to dispersion-corrected DFT is to preserve the form of common GGAs and hybrid functionals at short range while incorporating 100% Hartree-Fock exchange at long-range. Functionals along these lines are known variously as "Coulomb-attenuated" functionals, "range-separated" functionals, or "long-range-corrected" density functionals. These functionals are all based upon a partition of the

electron-electron Coulomb potential into long- and short- range components using the error (erf) function

$$\frac{1}{r_{12}} \equiv \frac{1-\mathrm{erf}(\omega r_{12})}{r_{12}} + \frac{\mathrm{erf}(\omega r_{12})}{r_{12}}, \tag{4.1}$$

The first term on the right of Eq. (4.1) is singular but short-range, and it decays to zero on a length scale of ~ 1/ω. The second term constitutes a non-singular, long-range background. The basic idea of long-range-corrected-DFT (LRC-DFT) is to utilize the short-range component of the Coulomb operator in conjunction with standard DFT exchange, while at the same time incorporating full Hartree-Fock exchange using the long-range part of the Coulomb operator. Evaluation of the short- and long-range Hartree-Fock exchange energies is straightforward,[16] so the crux of LRC-DFT rests upon the form of the short-range GGA exchange energy. Some examples of short-range GGA exchange functionals include short-range variants of B88 and PEB exchange described by Hirao and co-workers,[17-18] an alternative formulation of short-range PEB exchange proposed by Scuseria and co-workers,[19] and several short-range variants of B97 introduced by Chai and Head-Gordon.[20-22] These LRC-DFT functionals have been shown to remove the near-continuum of spurious charge-transfer excited states that appear in large-scale TDDFT calculations.[23] However, certain results depend sensitively upon the range-separation parameter ω,[23-26] and the results of LRC-DFT calculations must therefore be interpreted with caution, and probably for a range of ω values.

The non-relativistic electronic Schrödinger equation for an *N*-electron system has the form

$$\left[\sum_{i}^{N} \bar{h}\,(r_i) + \sum_{i<j}^{N} r_{ij}^{-1}\right]\Psi = E\Psi, \tag{4.2}$$

The Hamiltonian consists of two major parts, the trivial one-electron terms $\bar{h}$ and the troublesome two-electron terms. The most difficult terms in the equation are r_{ij}^{-1} which describe electron-electron interactions. Without these terms, the equation could be exactly solvable. Coulomb integrals express long-distance interaction between electrons in the molecule.

Why are the r_{ij}^{-1} terms so difficult? A theoretical answer is that the terms are responsible for the coupling of electron motion and create many body effects. A practical answer is the difficulty in dealing with four-center two-electron integrals. The integrals resulting from r_{ij}^{-1} are at the heart of virtually all QM methods. A simple way to eliminate the coupling effect that makes the terms difficult is to write r_{ij}^{-1} as a sum of products of one-particle functions, in other words, resolving them.

The first chemical interest in resolving two-particle functions was the work by Gilbert.[27] The aim was to achieve linear-scaling Coulomb energy calculations by resolving the long-range Ewald operator based on Coulomb orthonormal polynomials f_{lmn}. Another related work was by Gill in 1997,[28] wherein the Ewald operator was expanded in a Taylor series. The resolution of the Coulomb operator also results in a factorization of two-electron integrals and possibly linear-scaling computational methods. To accomplish linear scaling, one has to avoid the naïve pairwise summation over electron-electron interactions. Several clever techniques are available to achieve this goal. The KWIK algorithm[29] partitions the Coulomb energy into short- and long-range parts. The short-range one is treated analytically while the other is computed by Fourier summation. These spatial divisions of the Coulomb operator have made use of $\alpha(r) = \mathrm{erfc}(\omega r)$, where ω is an adjustable parameter. This is largely due to the fact that

the necessary integrals for using this attenuator are trivially related to those for the regular Coulomb potential. However, erf and erfc functions do not yield very fine control over the division of the Coulomb operator, and the short-range component never has the curvature of the Coulomb potential for any finite ω. These issues led to the development of the CASE[30] and CAP(m)[31] methods.

Dutoi and Head-Gordon[32] advanced a scheme by introducing an explicit cutoff radius r_0 for the Coulomb potential, by allowing $\alpha(r) = \text{terfc}(\omega r,\ \omega r_0)$ where

$$\text{terfc} = \frac{1}{2}[\text{erf}(x + y) + \text{erf}(x - y)] \tag{4.3}$$

and $\text{terfc} = 1 - \text{terf}$. The terf function is named for "two erfs", and it approaches zero linearly at the origin, hence only the short-range potential is singular. The terfc attenuator essentially turns off the Coulomb potential over a domain of size ~ 1/ω centered at r_0.

In this project, a new form of switching function is used to divide the Coulomb operator into the short- and long-range parts. A truncated Coulomb analysis of the CCSD(T) correlation energies as a function of a sharp cutoff distance over which electrons are allowed to interact is reported. Both the intra- and intermolecular interactions are considered through sampling a variety off non-covalent interaction and atomization energies. The truncated coulomb analysis presented here provides a better understanding of how the correlation energy varies with electron-electron interaction distance.

4.2 Computational Methods

4.2.1 Molecular Systems and Electronic Structure Computations

Electrostatic interactions dominate ionic and hydrogen-bonded systems. For some hydrogen-bonded systems, an electrostatic approximation was employed,[33] and it was found that the electrostatic energy agreed very well with the non-empirical SCF interaction energy in the entire range from large separation to the vdW minimum. The Hartree-Fock method completely misses the dispersion interaction, which involves electron correlation between electrons. In *ab initio* calculations, the total interaction energy can be divided into two parts: Hartree-Fock (ΔE_{HF}) and correlation energy (ΔE_{corr})

$$\Delta E_{int} = \Delta E_{HF} + \Delta E_{corr}. \quad (4.4)$$

The term ΔE_{corr} contains both the nondynamical and dynamical correlation energy, and dispersion is a part of the dynamical correlation energy.

For the total interaction energy, most correlation energy can be recovered by using the CCSD(T) method. In this study, CCSD level of theory is used for this qualitative analysis study for efficiency reasons. Correlation energies of all dimers/complexes and monomers are obtained at CCSD/aug-cc-pVTZ employing the truncated Coulomb integral implemented in PSI4.[34] Large basis sets which contain polarization and diffuse functions must be used for reliable results of post-Hartree Fock methods. Among all sorts of basis sets, Dunning's correlation-consistent basis set aug-cc-pVTZ.[35-36]

A total of 24 systems are selected from several databases developed by Zhao and Truhlar:[37-38] HB6/04,[38] CT7/04,[38] DI6/O4,[38] WI7/05,[37] PPS5/05[37] for various kinds of noncovalent interactions. The types of interaction studied include: hydrogen bonded

dimers, charge transfer complexes, dipole interaction complexes, weak interaction complexes, and π-π stacking complexes. These dimer/complex structures are optimized at the CCSD/cc-pVTZ level in CFour.[39] Monomer geometries are taken from the optimized dimer/complex CCSD/cc-pVTZ structures.

4.2.2 Truncated Coulomb Integral and Correlation Energies

The coupled cluster singles and doubles correlation energy in the atomic orbital (AO) representation is

$$\varepsilon_{\mathrm{CCSD}} = \sum_{\mu\nu} t_{\mu\nu} h_{\mu\nu} + \frac{1}{2} \sum_{\mu\nu\lambda\sigma} (\mu\nu|\lambda\sigma) \left[t_{\mu\nu\lambda\sigma} + t_{\mu\nu}(t_{\lambda\sigma} + 2P_{\lambda\sigma}) - t_{\mu\lambda}(t_{\nu\sigma} + 2P_{\nu\sigma}) \right]. \quad (4.5)$$

The $\varepsilon_{\mathrm{CCSD}}$ can be divided into long- and short-range component by dividing the two-electron integrals using the switching function $f(r_{12})$. Indices μ, ν, λ, σ indicate atomic orbitals. The cluster amplitudes are back-transformed from the molecular orbital (MO) to the AO basis set as follows:

$$t_{\mu\nu} = \sum_{ia} t_i^a \, C_{\mu i} C_{\nu a}, \quad (4.6a)$$

$$t_{\mu\nu\lambda\sigma} = \sum_{ijab} t_{ij}^{ab} \, C_{\mu i} C_{\nu a} C_{\lambda j} C_{\sigma b}, \quad (4.6b)$$

where t_i^a and t_{ij}^{ab} are the initially computed MO amplitudes. Indices (i, j) and (a, b) indicate occupied and virtual orbitals, respectively. The division of the two-electron integrals is

$$(\mu\nu|\lambda\sigma) = (\mu\nu|r_{12}^{-1}[1 - f(r_{12})]|\lambda\sigma)_{r_{12}<r_x} + (\mu\nu|r_{12}^{-1} f(r_{12})|\lambda\sigma)_{r_{12}>r_x}, \quad (4.7)$$

where the first term is the short-range part ($r_{12} < r_x$) and the second term is the long-range part ($r_{12} > r_x$). The cutoff r_x is the distance within which electrons are allowed to interact.

When computing the truncated correlation energy, only the short-range portion is included, where the long-range CCSD correlation energy is

$$\varepsilon_{long}^{CCSD} = \frac{1}{2}\sum_{\mu\nu\lambda\sigma}(\mu\nu|\lambda\sigma)_{r_{12}>r_x}\left[t_{\mu\nu\lambda\sigma} + t_{\mu\nu}(t_{\lambda\sigma} + 2P_{\lambda\sigma}) - t_{\mu\lambda}(t_{\nu\sigma} + 2P_{\nu\sigma})\right]. \quad (4.8)$$

Several candidate $f(r_{12})$ functions could be used to facilitate this correlation energy division. These include

$$f_1(r, r_x) = \mathrm{erf}\left[\frac{r}{r_x}\alpha(r_x)\right], \quad (4.9a)$$

the $\mathrm{erf}\,(\mathrm{r}, r_x)$ function that has a non-zero long-range part;

$$f_2(r, r_x) = \mathrm{terf}[r, r_x, \alpha(r_x)] \equiv \frac{1}{2}\mathrm{erf}[\alpha(r_x)(r + r_x)] + \frac{1}{2}\mathrm{erf}[\alpha(r_x)(r - r_x)], \quad (4.9b)$$

the $\mathrm{terf}\,(\mathrm{r}, r_x)$ function that turns off short-range correlation over a domain whose sharpness is determined by $\alpha(r_x)$; and the switching function $f_3(r, r_x)$ containing the product of the hyperbolic function $\tanh(r)$ and the $\mathrm{terf}(r, r_x)$ function,

$$f_3(r, r_x) = \tanh(r)\,\mathrm{terf}[r, r_x, \alpha(r_x)]. \quad (4.9c)$$

The switching function we eventually settled on is

$$f_4(r, r_x) = \frac{1 - H(r_x)}{r} = \begin{cases} \frac{1}{r}, r < r_x, \\ 0, r > r_x \end{cases} \quad (4.9d)$$

where $H(r, r_x)$ is the Heaviside step function.

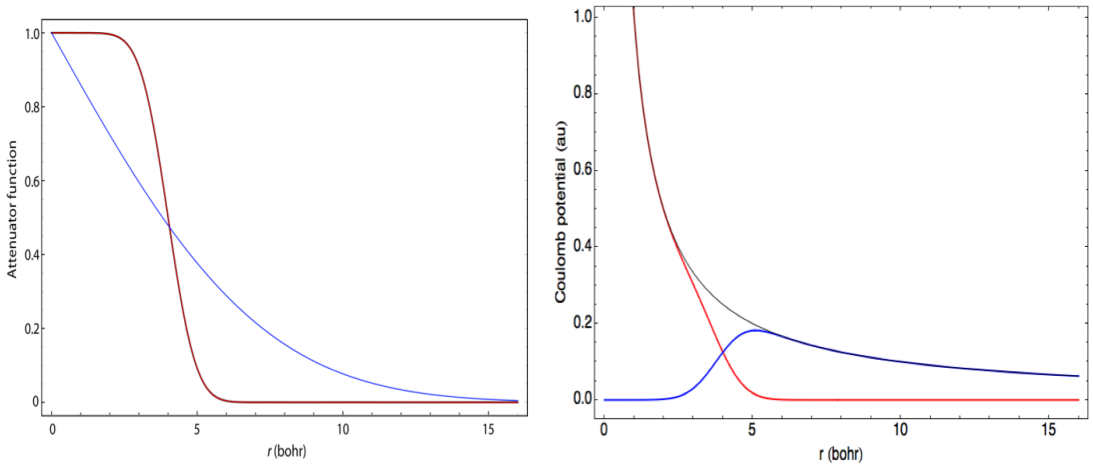


Figure 4.1 Coulomb Truncation Function $f_3(r, r_x)$

The left panel shows the representation of the complementary switching function $1 - f_3(r, r_x)$ (Eq. 4.9c) (red) and the corresponding error function $\mathrm{erfc}(r/8)$ (blue) vs. electron-electron distance (in bohr) for r_x=4. The right panel compares the short-range (red), long-range (blue), and total (black) electron-electron Coulombic potential derived from the switching function $f_3(r, r_x)$ with r_x=4.

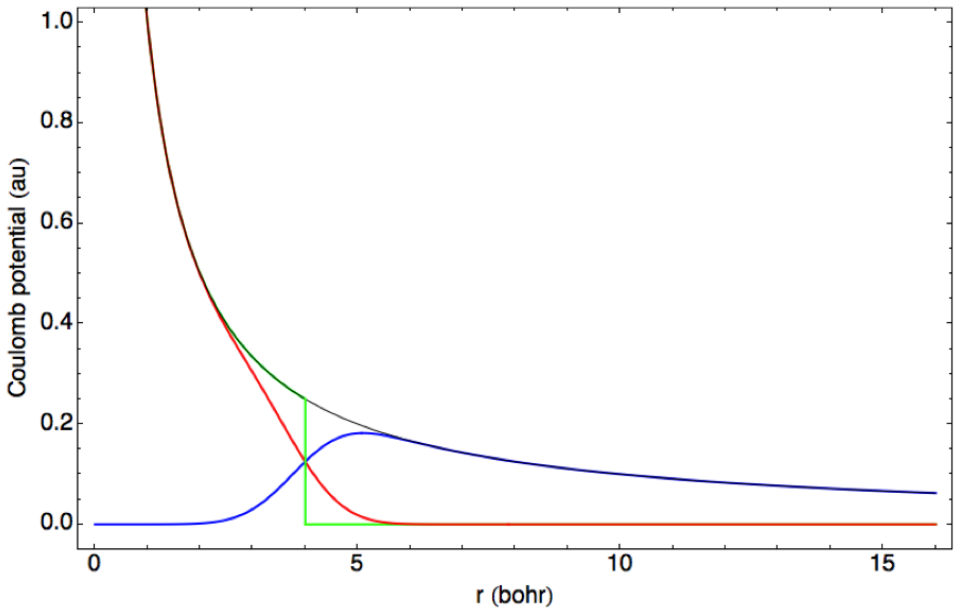


Figure 4.2 Exact Step-Function

Comparison of the short-range (green) Coulomb potential derived from the step function (Eq. 4.9d) versus the short-range (red), and long-range (blue) counterparts derived from $f_3(r, r_x)$. The total electron-electron Coulombic potential is shown in black.

4.3 Results and Discussion

4.3.1 Correlation Energy Truncation Performance

Atomization energies are computed for a series of compounds containing of first- and second-row atoms, represented by the equation

$$X + nH \rightarrow X\text{–}H_n, \tag{4.10a}$$

where X = Be – F or Al – Cl. Once the truncated correlation energy is computed for both the products and reactants, the correlation energy contribution to the atomization energy ΔE_{corr} is computed as the difference between that of the product and reactants:

$$\Delta E_{corr}^{CCSD} = \varepsilon_{X-H_n}^{CCSD} - \varepsilon_{X}^{CCSD}. \tag{4.10b}$$

The interaction energies for the non-covalent complexes are defined in a similar fashion:

$$A + B \rightarrow A\cdots B, \tag{4.11a}$$

$$\Delta E_{corr}^{CCSD} = \varepsilon_{A\cdots B}^{CCSD} - \varepsilon_{A\,+\,B}^{CCSD}, \tag{4.11b}$$

where A⋯B denotes a complex taken from aforementioned databases, while A and B are the monomers. For geometries of all the noncovalent complexes, see Appendix C.1.

In order to ensure a consistent discussion, a set of notations is defined: ε_R^{CCSD} is the correlation energy of the product (X-H molecule or A ⋯ B complex, R stands for 'right-hand-side') and ε_L^{CCSD} is the correlation energy of the reactants (A, B or X, L stands for 'left-hand-side'). Thus the interaction energy and atomization energy are defined as

$$\Delta E_{corr}^{CCSD} = \varepsilon_R^{CCSD} - \varepsilon_L^{CCSD}, \tag{4.12}$$

where ΔE_{corr}^{CCSD} is the correlation energy contribution to the total intermolecular interaction energy or atomization energy. When the full potential energy surface (PES) is of interest, the molecular fragments or monomers are pulled apart from each other in 0.5 Å

increments, and one-dimensional dissociation curves are obtained for each r_x cutoff value.

The performance of the electron-electron interaction truncation is demonstrated in Figure 4.3 using argon dimer as an example. Since the potential of the dominating dispersion interaction falls off with distance as $-1/R^6$ at long-range region, we performed a least-squares fit of the tail of the PES for the argon dimer using the equation $E_{int} = -B/R^6$, where B is a fitting parameter. We included points with R as small as ~ 0.5 Å beyond equilibrium. We have fitted the CCSD/aug-cc-pVTZ curve from R = 3.8 - 7.3 Å and obtained a B value of 667.3 kcal mol^{-1} Å^6. It can be seen from Figure 4.3 that between R = 4.0 and 7.0 Å, the fitted curve deviates from the full CCSD/aug-cc-pVTZ interaction energy curve and probably would be much better if fit did not included small R. The imperfect $-1/R^6$ fit results from the fact that higher order dispersion coefficients are neglected in this simple fitting and in addition to dispersion other energy components also contribute to the overall binding energy (such as exchange-repulsion), especially at the shorter intermonomer distances.

As for the potential energy curves obtained for each r_x cutoff value, the energy decays to zero much more rapidly and at a smaller distance. When increasing the r_x cutoff values, more electron correlation energy is recovered, and the curve eventually converges to the full PES (usually when $r_x > 10$ bohr).

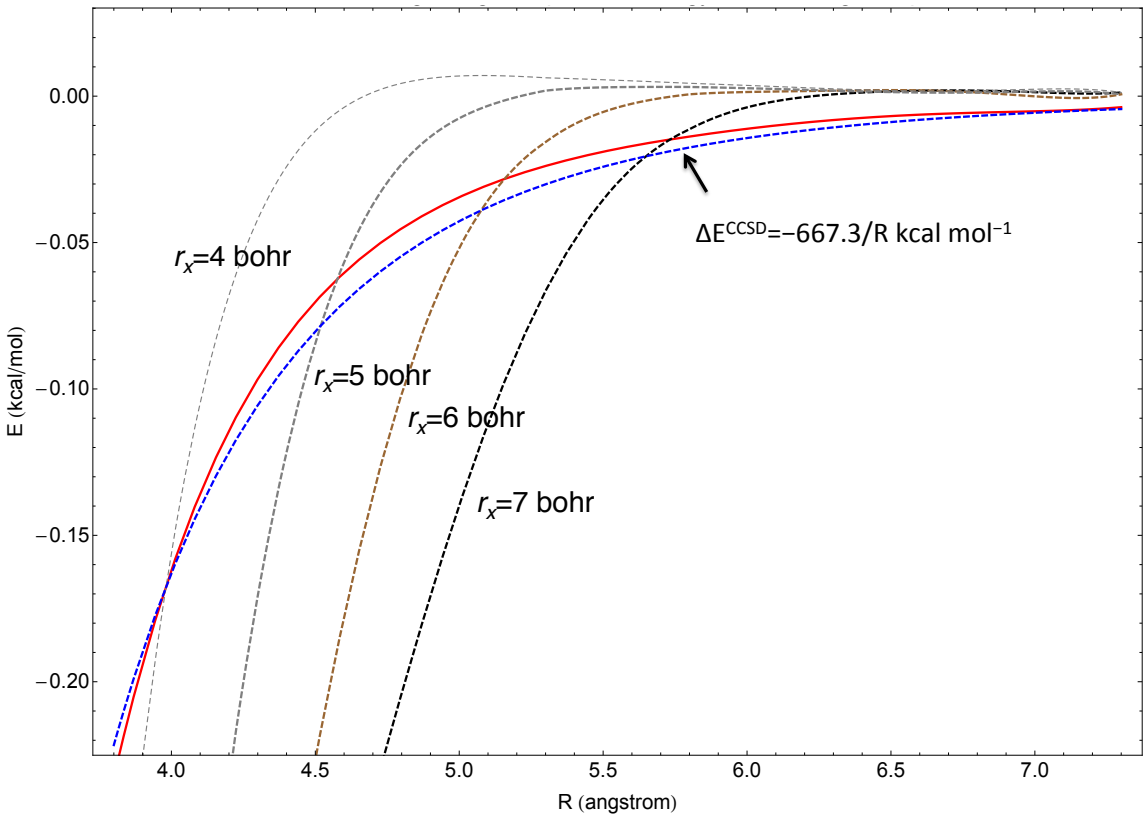


Figure 4.3 Ar dimer long-range correlation energy contribution to the binding energy

The red curve is the full CCSD/aug-cc-pVTZ urves of the Ar dimer. The Ar atoms are displaced at an increasing interatomic separation distance (R in Å). Dashed curves are the PESs for various r_x cutoff value (r_x= 4, 5, 6, and 7 bohr). The blue dashed line is the least-squares fitted long-range interaction energy curve.

4.3.2 Correlation Energy Dependence on the Electron-electron Distance

The correlation energies of each complex, monomer, and atom are plotted against the r_x cutoff values in Figures 4.4 and 4.5. Common features of the correlation energy dependence on the electron-electron interaction distance (r_x) can be observed from these curves. As expected, the correlation energy increases rapidly in magnitude as the distance over which electrons are allowed to interact increases at short-range; however, it eventually reaches a minimum point (most negative value). Beyond the minimum point, the correlation energy starts to decrease gradually in magnitude and eventually levels off to a constant value. This shape is universal for all the systems included in this study and is expected to be characteristic for the correlation energy dependence on the electron-electron interaction distance in general.

The correlation contribution to the atomization energies generally reaches its maximum magnitude when r_x is half of the atomic van der Waals radius, for example, the oxygen's van der Waal's radii is 1.595 Å. For interaction energies, this r_x values are proportional to the total CCSD correlation energies hence also proportional to the overall size of the complexes.

When gradually decreasing the allowed electron-electron interaction distances, the correlation energies actually decrease instead of increase. A subtle but non-negligible maximum point (less negative value) appears. This feature is demonstrated by the expanded view of the correlation energy curves for argon and argon dimer in Figure 4.5a. Despite this common feature, the atomization energy and interaction energy curves behave qualitatively different from each other.

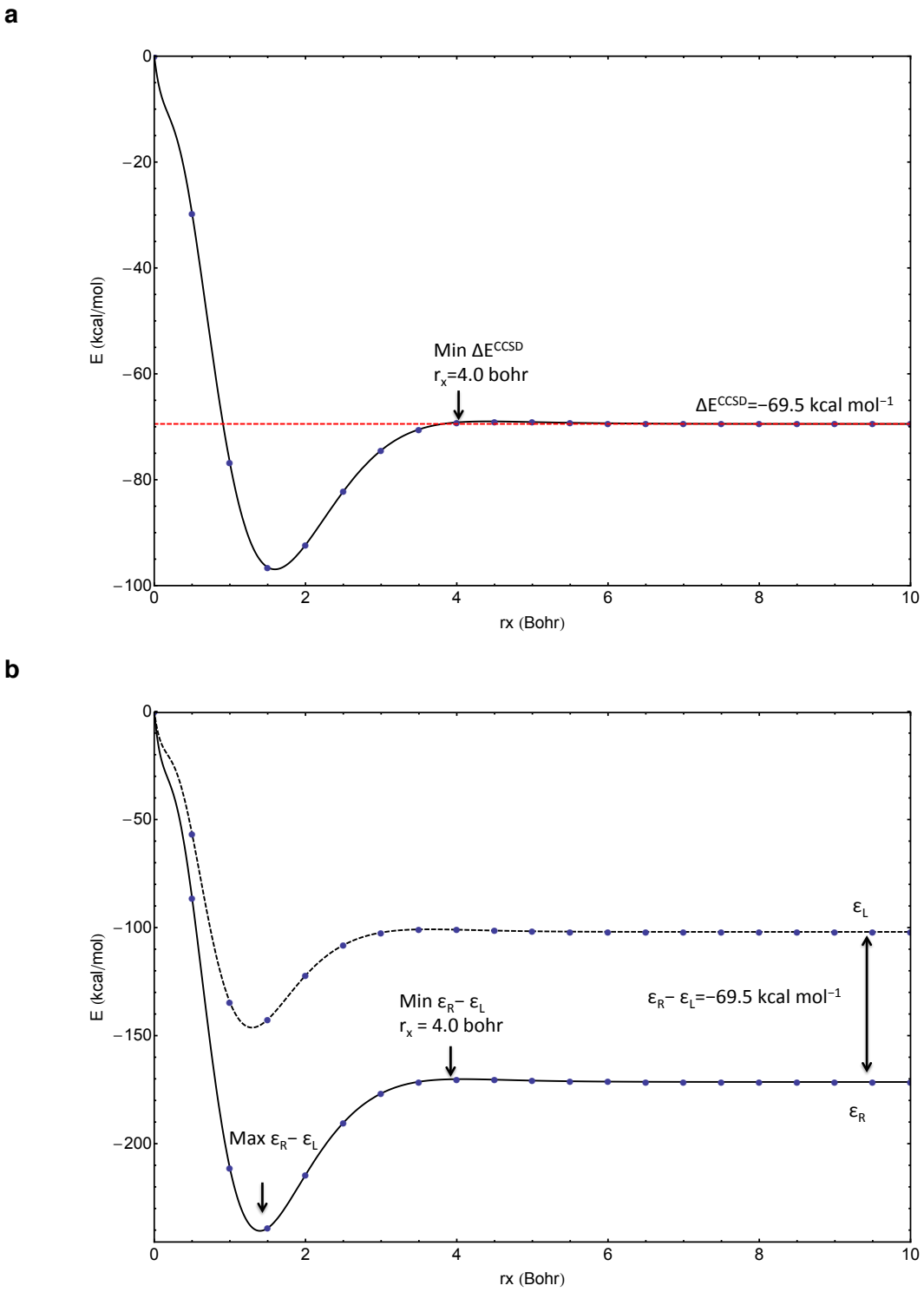
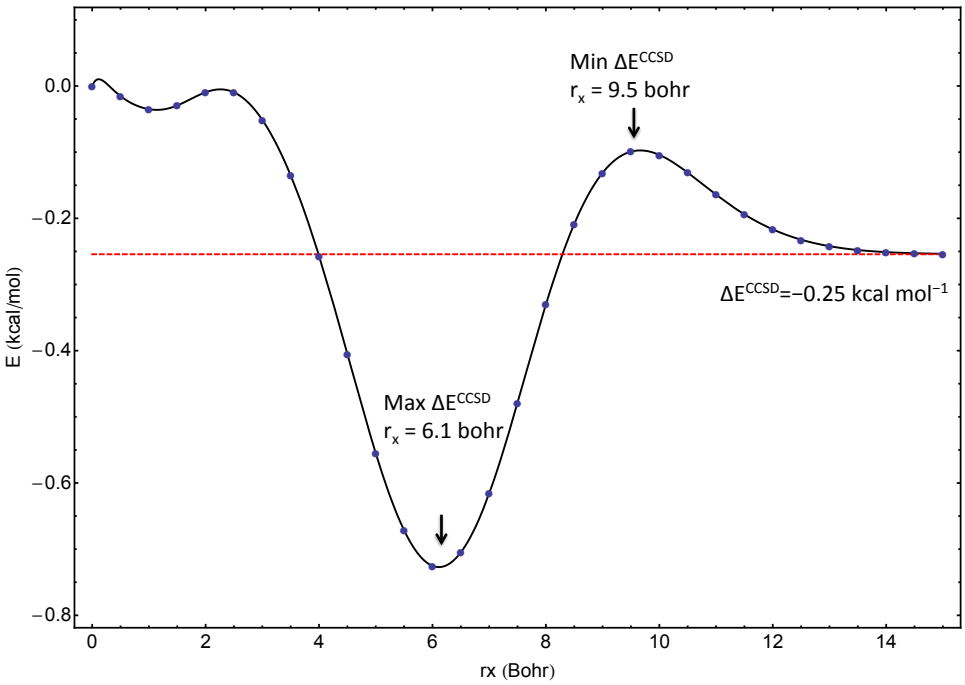


Figure 4.4 Electron-electron distance (r_x in bohr) dependence of the CCSD/aug-cc-pVTZ atomization energy of H_2O

Red line in **a** is the correlation contribution to the atomization energy, dashed line in **b** is the oxygen correlation energy; and solid line is the H_2O molecular correlation energy.

a



b A

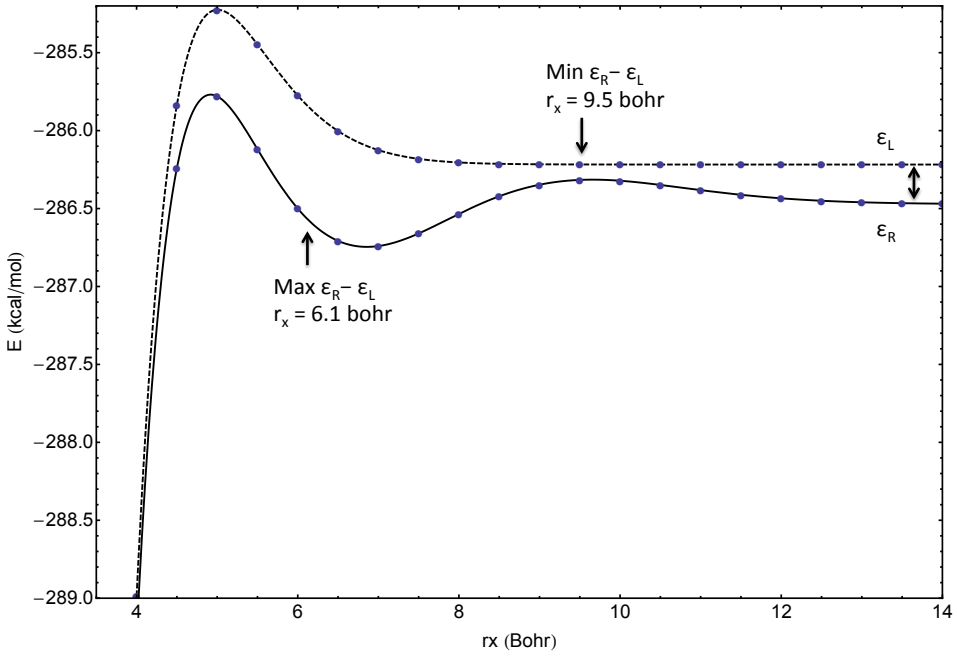


Figure 4.5 Electron-electron distance (r_x in bohr) dependence of the CCSD/aug-cc-pVTZ correlation energy of argon dimer at equilibrium interatomic separation (4.1 Å)

Red line in **a** is the correlation energy contribution to the binding energy; dashed line in **b** is the correlation energy of two argon atoms, and solid line is argon dimer correlation energy.

The value of ΔE^{CCSD} corresponds to the difference between ε_R and ε_L (Eq. 4.12), which are superimposed upon each other in Figure 4.4b and 4.5b. The atomization energy dependence on the electron-electron correlation energy is similar to that of the total correlation energy. But the interaction energy reaches another maximum point (less negative value) in the longer-range region around 9.5 bohr.

4.3.3 Partition of the Correlation Energy

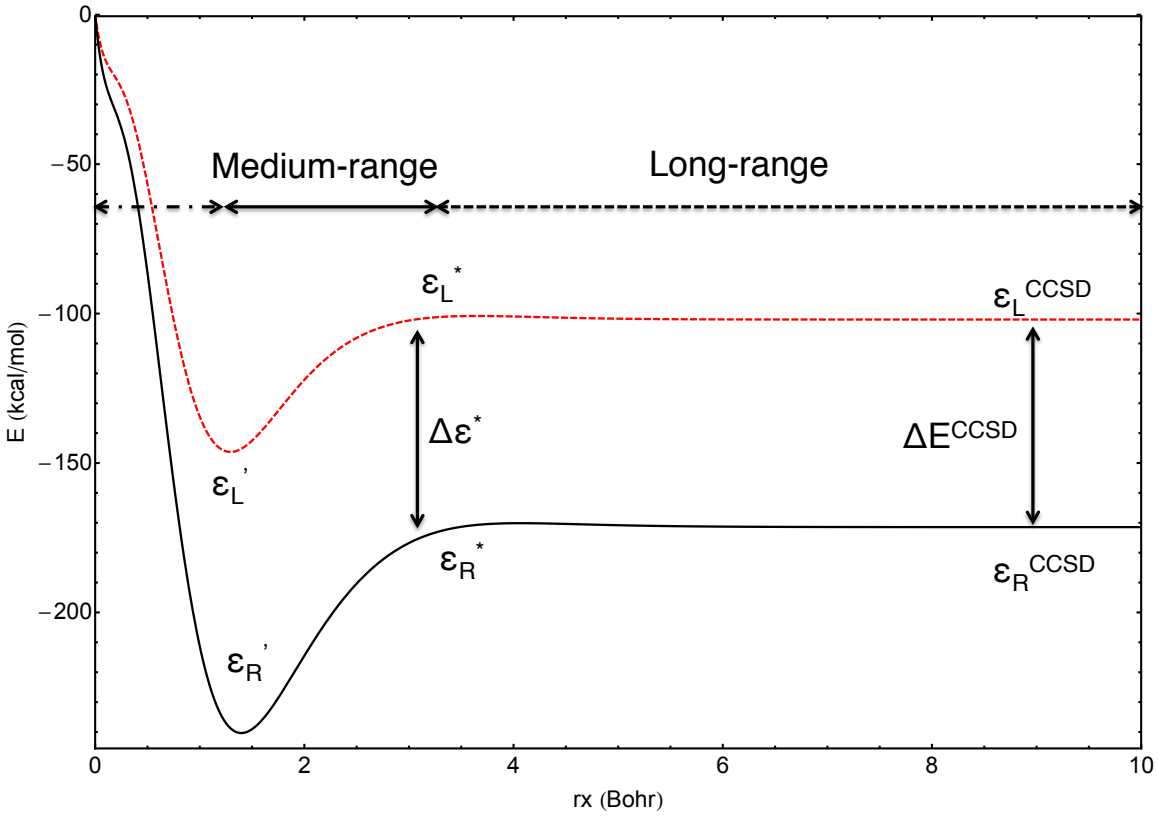


Figure 4.6 Partition of the Correlation Energy for a generic reaction

Labeling: ε' denotes the minimum (the maximum correlation energy), ε^* denotes the maximum peak (the minimum correlation energy); ε^{CCSD} is the full CCSD/aug-cc-pVTZ correlation energy. Subscript R and L indicate the correlation energy of the complex (molecular) and monomer (atomic) correlation energy, respectively (see Eq. 4.12).

Figure 4.6 shows the superimposed correlation energy curves. The peak lowering effect is quantified by $\Delta\varepsilon^*$, a quantity equal to the difference between the maximum peaks of two curves

$$\Delta\varepsilon^* = \varepsilon_R^* - \varepsilon_L^*. \tag{4.13}$$

The maximum peak ε^* is used to indicate the starting point of the long-range electron interaction. The relationship of ε^* with the full correlation energy contribution ΔE^{CCSD} is represented by the almost linear dependence in Figure 4.7. The data for both atomization

energies and complexation energies are fitted by a least-squares regression line, where the slope gives the ratio between $\Delta\varepsilon^*$ and ΔE^{CCSD}. For the atomization energy, the peak difference $\Delta\varepsilon^*$ is close to but slightly smaller than ΔE^{CCSD}, whereas in the cases of intermolecular interaction energies, the slope is 1.26. Could this be a quantitative distinction between the intra- and intermolecular dispersion? Here we draw a tentative conclusion from a further decomposition of the total correlation energy based on a partition of the electron-electron interaction distance into three ranges.

Based on the common features of the correlation energy curves, we propose to partition the total correlation energy contribution to the interaction energy into short-range (ΔE_{sr}), medium-range (ΔE_{mr}), and long-range (ΔE_{lr}) components according to

$$\Delta E_{sr}^{CCSD} = \varepsilon_R' - \varepsilon_L', \tag{4.14a}$$

$$\Delta E_{mr}^{CCSD} = (\varepsilon_R^* - \varepsilon_R') - (\varepsilon_L^* - \varepsilon_L'), \tag{4.14b}$$

$$\Delta E_{lr}^{CCSD} = (\varepsilon_R^{CCSD} - \varepsilon_R^*) - (\varepsilon_L^{CCSD} - \varepsilon_L^*). \tag{4.14c}$$

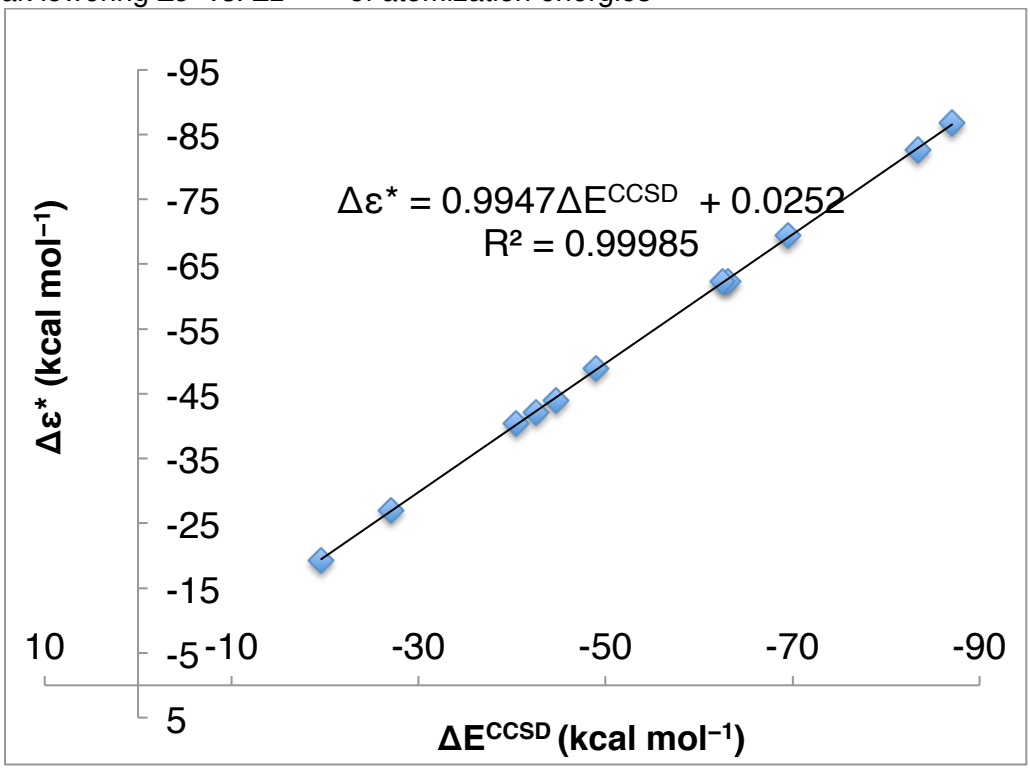
Hence at 'infinite' electron-electron distance (when r_x > 10 bohr for all sampled cases), the energy difference between two curves equals to the correlation energy contribution to the interaction (or atomization) energy

$$\Delta E^{CCSD} = \varepsilon_R^{CCSD} - \varepsilon_L^{CCSD} = \Delta E_{sr}^{CCSD} + \Delta E_{mr}^{CCSD} + \Delta E_{lr}^{CCSD}, \tag{4.15}$$

and

$$\Delta\varepsilon^* = \varepsilon_R^* - \varepsilon_L^* = \Delta E_{sr}^{CCSD} + \Delta E_{mr}^{CCSD}. \tag{4.16}$$

a Peak lowering $\Delta\varepsilon^*$ vs. ΔE^{CCSD} of atomization energies



b Peak lowering $\Delta\varepsilon^*$ vs. ΔE^{CCSD} for intermolecular interaction energies

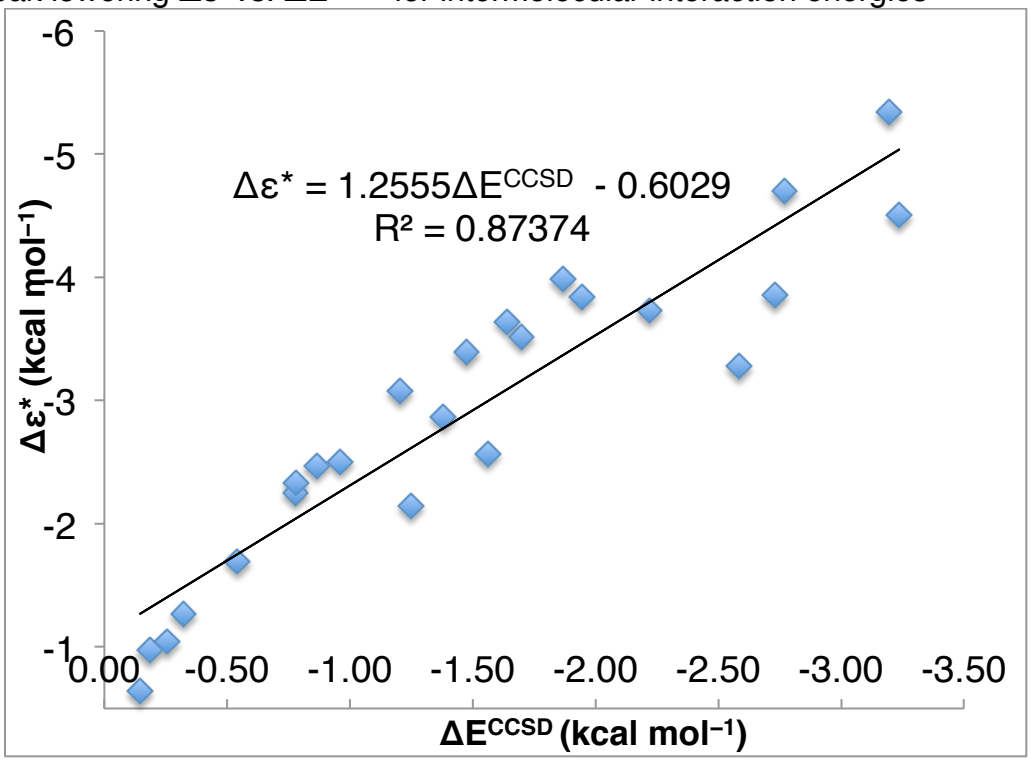


Figure 4.7 Relationships between $\Delta\boldsymbol{\varepsilon}^*$ and E^{CCSD} for atomization and intermolecular interaction energies in kcal mol^{-1}.

Table 4.1 Decomposition of the Atomization Energy in kcal mol^{-1}

	ΔE_{int}	ΔE^{CCSD}	$\Delta\varepsilon^*$	ΔE_{sr}^{CCSD}	ΔE_{mr}^{CCSD}	ΔE_{lr}^{CCSD}
BeH_2	–144.7	–19.60	–19.34	–24.34	+5.00	–0.26
BH_3	–276.1	–44.71	–44.03	–59.29	+15.25	–0.68
CH_4	–411.3	–83.41	–82.57	–133.95	+31.28	–0.83
NH_3	–287.6	–87.06	–86.73	–117.95	+31.23	–0.33
H_2O	–225.0	–69.46	–69.33	–94.07	+24.74	–0.13
HF	–137.3	–40.46	–40.46	–54.01	+13.55	+0.01
AlH_3	–209.4	–42.48	–42.10	–53.47	+11.37	–0.48
SiH_4	–317.2	–63.08	–62.29	–79.92	+17.63	–0.79
PH_3	–233.1	–62.48	–62.31	–79.50	+17.19	–0.17
H_2S	–175.7	–48.98	–48.97	–63.81	+14.84	–0.01
HCl	–103.4	–27.03	–27.05	–35.66	+8.62	+0.01

ΔE_{int} is the total atomization energy, ΔE^{CCSD} is the CCSD/aug-cc-pVTZ correlation energy contribution to the atomization energy, $\Delta\varepsilon^*$ is the peak energy difference which equals to the sum of short-range (ΔE_{sr}^{CCSD}) and medium-range (ΔE_{mr}^{CCSD}) components (see Eq 4.16), and ΔE_{lr}^{CCSD} is the long-range component.

Table 4.2 Decomposition of the Interaction Energy in kcal mol^{-1}

		ΔE_{int}	ΔE^{CCSD}	$\Delta\varepsilon^*$	ΔE_{sr}^{CCSD}	ΔE_{mr}^{CCSD}	ΔE_{lr}^{CCSD}
Hydrogen Bond	$(NH_3)_2$	–2.9	–1.47	–2.89	–0.53	–2.36	+1.46
	$(HF)_2$	–4.6	–0.86	–1.97	–0.41	–1.56	+1.10
	$(H_2O)_2$	–4.9	–1.20	–2.58	–0.56	–2.01	+1.37
	$NH_3\cdots H_2O$	–6.2	–1.64	–3.13	–0.94	–2.19	+1.49
	$(HCONH_2)_2$	–15.4	–3.19	–4.84	–0.32	–4.52	+1.65
	$(HCOOH)_2$	–17.8	–2.77	–4.20	–0.38	–3.82	+1.43
Dispersion Interaction	Ne_2	–0.1	–0.15	–0.14	–0.05	–0.08	–0.01
	NeAr	–0.1	–0.18	–0.47	–0.03	–0.44	+0.29
	$CH_4\cdots Ne$	–0.2	–0.32	–0.77	–0.08	–0.68	+0.44
	$CH_4\cdots Ar$	–0.4	–0.54	–1.19	–0.11	–1.08	+0.65
	$(CH_4)_2$	–0.5	–0.78	–1.75	–0.14	–1.61	+0.97
	Ar_2	–0.2	–0.25	–0.54	–0.02	–0.52	+0.29
	$C_2H_4\cdots C_2H_2$	–1.6	–0.96	–2.00	–0.21	–1.80	+1.04
π–π Stacking	$(C_2H_2)_2$	–1.3	–0.78	–1.83	+0.06	–1.89	+1.05
	$(C_2H_4)_2$	–1.4	–1.87	–3.48	–0.50	–2.98	+1.61

ΔE_{int} is the total atomization energy, ΔE^{CCSD} is the CCSD/aug-cc-pVTZ correlation energy contribution to the interaction energy, $\Delta\varepsilon^*$ is the peak energy difference which equals to the sum of short-range (ΔE_{sr}^{CCSD}) and medium-range (ΔE_{mr}^{CCSD}) components (see Eq 4.16), and ΔE_{lr}^{CCSD} is the long-range component.

The values of each energy component are listed in Tables 4.1 and 4.2. The different $\Delta\varepsilon^*/\Delta E^{CCSD}$ ratios between the intra- and intermolecular interaction can be explained by the differences of three components. The biggest contribution to the atomization energy, which contains both dynamical and nondynamical electron correlation energies, comes from the short-range region. The medium-range components are destabilizing (indicated by the positive values). The long-range electron-electron interaction only contributes a small amount to correlation energy effect. Also the magnitudes of the correlation energies are proportional to the numbers of bonds broken in each reaction.

In contrast, for the intermolecular interactions, the short-range components are quite small, less than 50% generally of the total CCSD correlation energy contribution for all types of systems. The biggest contribution comes from the medium-range, and the long-range electron-electron correlation effect is actually repulsive.

In summary, based on our observations and the three-region partitioning of the correlation energy, atomization energies of small molecules are mostly influenced by short-range electron correlation. Consistent with common intuition, intermolecular electron correlation is longer range in character and recovered by the contributions from both short- and medium-range components in our analysis. What is particularly interesting is the alternating pattern between the attractive and repulsive regions of the electron correlation effect, which indicates that in order for the electron-electron interaction to be stabilizing at certain range, a price has to be paid at the next longer-range region. This conclusion is in contrast to prevailing understanding of the correlation energy as being attractive at all ranges.

4.4 Conclusion

The Coulomb operator within two-electron integrals can be split using arbitrary switching functions by the mathematical methods employed here. Correlation energies can be computed as a function of a sharp cutoff distance over which electrons are allowed to interact. The characteristics of the correlation energies with respect to the cutoff distance appear universal for different types of systems. A division of the correlation energies based on common features of the uniformly shaped curves is proposed. A key conclusion from this work is that dispersion cannot be simplistically understood as long-range electron correlation, a key realization in devising approaches to quantify intramolecular dispersion effects.

Reference

1. Stone, A., *The theory of intermolecular forces*. Oxford University Press: Oxford, 2013.
2. Lehn, J.-M., *Supramolecular chemistry*. VCH: Weinheim, 1995.
3. Meyer, E. A.; Castellano, R. K.; Diederich, F., *Angew. Chem.* **2003,** *115*, 1244-1287.
4. Meyer, E. A.; Castellano, R. K.; Diederich, F., *Angew. Chem. Int. Ed.* **2003,** *42*, 1210-1250.
5. Kannan, N.; Vishveshwara, S., *Protein Eng.* **2000,** *13*, 753-761.
6. Hobza, P.; Šponer, J., *Chem. Rev.* **1999,** *99*, 3247-3276.
7. Dąbkowska, I.; Gonzalez, H. V.; Jurečka, P.; Hobza, P., *J. Phys. Chem. A* **2005,** *109*, 1131-1136.
8. Hoja, J.; Sax, A. F.; Szalewicz, K., *Chem. Eur. J.* **2014,** *20*, 2292-2300.
9. Fokin, A. A.; Chernish, L. V.; Gunchenko, P. A.; Tikhonchuk, E. Y.; Hausmann, H.; Serafin, M.; Dahl, J. E.; Carlson, R. M.; Schreiner, P. R., *J. Am. Chem. Soc.* **2012,** *134*, 13641-13650.
10. Schreiner, P. R.; Chernish, L. V.; Gunchenko, P. A.; Tikhonchuk, E. Y.; Hausmann, H.; Serafin, M.; Schlecht, S.; Dahl, J. E.; Carlson, R. M.; Fokin, A. A., *Nature* **2011,** *477*, 308-311.
11. Magers, D. B. Overcoming Three Theoretical Challenges in High Accuracy Ab Initio Electronic Structure Theory. University of Georgia, 2014.
12. Kristyán, S.; Pulay, P., *Chem. Phys. Lett.* **1994,** *229*, 175-180.
13. Hobza, P.; Reschel, T., *J. Comput. Chem.* **1995,** *16*, 1315-1325.
14. Pérez-Jordá, J.; Becke, A. D., *Chem. Phys. Lett.* **1995,** *233*, 134-137.
15. Pérez-Jordá, J. M.; San-Fabián, E.; Pérez-Jiménez, A. J., *J. Chem. Phys.* **1999,** *110*, 1916-1920.
16. Adamson, R. D.; Dombroski, J. P.; Gill, P. M., *J. Comput. Chem.* **1999,** *20*, 921-927.
17. Iikura, H.; Tsuneda, T.; Yanai, T.; Hirao, K., *J. Chem. Phys.* **2001,** *115*, 3540-3544.
18. Song, J.-W.; Hirosawa, T.; Tsuneda, T.; Hirao, K., *J. Chem. Phys.* **2007,** *126*, 154105.
19. Henderson, T. M.; Janesko, B. G.; Scuseria, G. E., *J. Chem. Phys.* **2008,** *128*, 194105.
20. Chai, J.-D.; Head-Gordon, M., *J. Chem. Phys.* **2008,** *128*, 084106.
21. Chai, J.-D.; Head-Gordon, M., *Phys. Chem. Chem. Phys.* **2008,** *10*, 6615-6620.
22. Chai, J.-D.; Head-Gordon, M., *Chem. Phys. Lett.* **2008,** *467*, 176-178.
23. Tsuneda, T.; Suzumura, T.; Hirao, K., *J. Chem. Phys.* **1999,** *110*, 10664-10678.
24. Hamprecht, F. A.; Cohen, A. J.; Tozer, D. J.; Handy, N. C., *J. Chem. Phys.* **1998,** *109*, 6264-6271.
25. Rohrdanz, M. A.; Herbert, J. M., *J. Chem. Phys.* **2008,** *129*, 034107.
26. Rohrdanz, M. A.; Martins, K. M.; Herbert, J. M., *J. Chem. Phys.* **2009,** *130*, 054112.
27. Gilbert, A., *BSc.(Hons) thesis, Massey University, Masset, New Zealand* **1996**.

28. Gill, P. M. W., *Chem. Phys. Lett.* **1997,** *270*, 193-195.
29. Dombroski, J. P.; Taylor, S. W.; Gill, P. M., *J. Phys. Chem.* **1996,** *100*, 6272-6276.
30. Adamson, R. D.; Dombroski, J. P.; Gill, P. M., *Chem. Phys. Lett.* **1996,** *254*, 329-336.
31. Gill, P. M.; Adamson, R. D., *Chem. Phys. Lett.* **1996,** *261*, 105-110.
32. Dutoi, A. D.; Head-Gordon, M., *J. Phys. Chem. A* **2008,** *112*, 2110-2119.
33. Alagona, G.; Tani, A., *J. Chem. Phys.* **1981,** *74*, 3980-3988.
34. Turney, J. M.; Simmonett, A. C.; Parrish, R. M.; Hohenstein, E. G.; Evangelista, F. A.; Fermann, J. T.; Mintz, B. J.; Burns, L. A.; Wilke, J. J.; Abrams, M. L.; Russ, N. J.; Leininger, M. L.; Janssen, C. L.; Seidl, E. T.; Allen, W. D.; Schaefer, H. F.; King, R. A.; Valeev, E. F.; Sherrill, C. D.; Crawford, T. D., *WIREs Comput. Mol. Sci.* **2012,** *2*, 556-565.
35. Dunning Jr, T. H., *J. Chem. Phys.* **1989,** *90*, 1007-1023.
36. Woon, D. E.; Dunning Jr, T. H., *J. Chem. Phys.* **1993,** *98*, 1358-1371.
37. Zhao, Y.; Truhlar, D. G., *J. Phys. Chem. A* **2005,** *109*, 5656-5667.
38. Zhao, Y.; Truhlar, D. G., *J. Chem. Theory Comput.* **2005,** *1*, 415-432.
39. Stanton, J.F.; Gauss, J.; Harding, M.E.; Szalay, P.G.; with contributions from Auer, A. A.; Bartlett, R. J.; Benedikt, U.; Berger, C.; Bernholdt , D. E.; Bomble, Y. J.; Cheng, L.; Christiansen, O.; Heckert, M.; Heun, O.; Huber, C.; Jagau, T.-C.; Jonsson, D.; Jusélius, J.; Klein, K.; Lauderdale, W. J.; Matthews, D. A.; Metzroth, T.; Mück, L. A.; O'Neill, D. P.; D.R. Price, E. Prochnow, C. Puzzarini, K. Ruud, F. Schiffmann, W. Schwalbach, C. Simmons, S. Stopkowicz, A. Tajti, J. Vázquez, F. Wang, J.D. Watts and the integral packages MOLECULE (J. Almlöf and P.R. Taylor), PROPS (P.R. Taylor), ABACUS (T. Helgaker, H.J. Aa. Jensen, P. Jørgensen, and J. Olsen), and ECP routines by A. V. Mitin and C. van Wüllen. *CFOUR*, For the current version, see http://www.cfour.de. 2008.

APPENDIX A

SUPPORTING INFORMATION FOR CHAPTER 2

Table A.1 Glycine conformers MP2/aug-cc-pVTZ level Cartesian geometries (in Å) and MP2/cc-pVTZ vibrational frequencies (in cm^{-1}) and intensities (in km mol^{-1} and %)

Ip

C	-0.4981111579	-0.0866092185	-0.0021413235
C	0.7673387252	0.7445304131	-0.0004838655
N	2.0027667970	-0.0071703503	0.0054393012
O	-1.5985079914	0.7035109642	-0.0079516854
O	-0.5498176952	-1.2952487332	0.0012069129
H	-2.3615796720	0.1046247567	-0.0086354469
H	0.7260260323	1.4022359184	0.8686082686
H	0.7314739005	1.3974691475	-0.8734004035
H	2.0325034487	-0.6218263621	-0.7991771675
H	2.0273224321	-0.6176309599	0.8134185030

IIn

C	-0.6113003292	-0.0482781526	-0.0269935025
C	0.7072342276	-0.8140027166	-0.1050697522
N	1.8496282234	0.0818382595	0.0844833380
O	-0.4625551037	1.2842603679	-0.0340328688
O	-1.6854030541	-0.5976215324	0.0155687581
H	0.5116591105	1.4180327370	-0.0580844677
H	0.6551328437	-1.6326493744	0.6115275001
H	0.7452206244	-1.2572936718	-1.0993354906
H	2.1991654772	0.0421208677	1.0326194058
H	2.6159009991	-0.1488935153	-0.5318051439

IVn

C	-0.4867843726	-0.0809652958	-0.0235208225
C	0.7561149266	0.7598092485	-0.1313926361
N	1.9243239852	-0.0507909218	0.1625044213
O	-1.5945331697	0.6872366551	0.0813469330
O	-0.5166693546	-1.2898589046	-0.0605660266
H	-2.3459014165	0.0738884038	0.0978509201
H	0.6712766510	1.5886742489	0.5705870921
H	0.7332382788	1.1914144539	-1.1399684490
H	1.7866093761	-0.9838081599	-0.2086706183
H	2.7519688358	0.3395725435	-0.2664324875

IIIp

C	-0.5840938710	0.0833057169	-0.0037515032
C	0.7685011309	0.7717073646	-0.0060604057
N	1.9665182180	-0.0418590523	0.0034750774
O	-0.4899761347	-1.2687543595	0.0086058616
O	-1.6433606349	0.6681941627	-0.0118914012
H	-1.4055439038	-1.5911359629	0.0089990773
H	0.7729049164	1.4221369385	-0.8810809327
H	0.7686691903	1.4362122866	0.8583431911
H	1.9791345630	-0.6423417601	0.8178254225
H	1.9831979543	-0.6553382082	-0.8010564007

Vn

C	-0.5639013387	-0.0966983847	-0.0357901864
C	0.7884372541	-0.6978084122	-0.3174609679
N	1.8603806336	0.0806269096	0.2908978862
O	-0.5253330240	1.2575680740	-0.0784212199
O	-1.5820311980	-0.7204732602	0.1543681609
H	-1.4341891477	1.5545753835	0.0851234800
H	0.7798291943	-1.7014751172	0.0992781320
H	0.8518722485	-0.7919385164	-1.4096939284
H	2.7571461722	-0.3233592355	0.0525422992
H	1.8511788461	1.0277336235	-0.0666009290

VIp

C	-0.5096607019	-0.1027985950	0.0002285669
C	0.7510532882	0.7510063896	0.0000832681
N	1.9962200654	0.0184236898	-0.0000391297
O	-1.6781038971	0.5943454793	-0.0003379688
O	-0.5188949795	-1.3065193656	0.0014742951
H	-1.4886011889	1.5416792756	-0.0014956318
H	0.7140030982	1.4041463038	0.8754848141
H	0.7139058358	1.4041578288	-0.8753025592
H	2.0253622957	-0.5951749769	-0.8058611449
H	2.0250254724	-0.5960140546	0.8051708169

VIIp

C	-0.6113375907	-0.0604116504	0.0000000000
C	0.7398524156	-0.7752735859	0.0000000000
N	1.9525275328	0.0119508169	0.0000000000
O	-0.5693446076	1.2917932474	0.0000000000
O	-1.6583527010	-0.6570158507	0.0000000000
H	0.3660069502	1.5460546236	0.0000000000
H	0.7349603014	-1.4302312962	0.8705189155
H	0.7349603014	-1.4302312962	-0.8705189155
H	2.1190991799	0.5508218214	0.8357209071
H	2.1190991799	0.5508218214	-0.8357209071

VIIIn

C	-0.4941627052	-0.0953510739	-0.0207753268
C	0.7441122785	0.7720795917	-0.1148699610
N	1.9280314955	-0.0216392105	0.1492767514
O	-1.6703779835	0.5752179280	0.0620608601
O	-0.4777268095	-1.2990854927	-0.0500100010
H	-1.4973654097	1.5241375671	0.1094075381
H	0.6591152355	1.5851799323	0.6112494738
H	0.7166099959	1.2268492123	-1.1132551111
H	1.7360472322	-0.9846741547	-0.1052913211
H	2.7156108757	0.2999989134	-0.3954047869

Table A.2 Glycine transition states MP2/aug-cc-pVTZ level Cartesian geometries (in Å).

TS-1

C	-0.5154686827	0.0973136123	-0.1317176553
C	0.8789294828	-0.1811361201	-0.6450124275
N	1.8909841090	-0.0121134534	0.3966310250
O	-1.1869010837	-1.0431359815	0.1653880856
O	-0.9774391036	1.2004400745	0.0615084285
H	-2.0389013118	-0.7633159923	0.5372089953
H	1.0843614614	0.5237511656	-1.4475539815
H	0.9387220581	-1.1931470476	-1.0367373448
H	1.8190745451	0.9171427656	0.7951208446
H	1.7327021787	-0.6719741945	1.1490085610

TS-2

C	-0.5004576881	0.1112629090	0.0093308034
C	0.7479875380	-0.7458453935	-0.0034160149
N	2.0080263156	-0.0371493075	0.0047112756
O	-1.6675609671	-0.6382903742	-0.0569022983
O	-0.5144060500	1.3123338832	-0.0019046797
H	-1.9460215428	-0.8977051532	0.8292938311
H	0.6814879908	-1.3864607853	-0.8841787271
H	0.6935045734	-1.4209617946	0.8536875019
H	2.0622469559	0.5692856497	-0.8050403085
H	2.0506451806	0.5789239451	0.8076620502

TS-3

C	-0.5441891045	-0.1070495576	-0.0918725273
C	0.8496781538	-0.3903424765	-0.6019888841
N	1.7891450173	0.0804180565	0.4207207557
O	-0.8384042384	1.2422098533	-0.0641776081
O	-1.3373751097	-0.9497595257	0.2387248269
H	-0.6398206243	1.5939254814	0.8117758557
H	1.0007153593	0.1931656967	-1.5083434545
H	0.9284807300	-1.4523163588	-0.8361781506
H	1.9140583379	-0.6303000548	1.1308030694
H	2.6985574451	0.2576597090	0.0161050902

TS-4

C	-0.5604149312	0.0991847034	-0.0734285251
C	0.8250388461	0.5073009887	-0.5244473240
N	1.8838708052	-0.0593213827	0.3303025835
O	-0.7711787619	-1.2503366806	-0.0578052086
O	-1.4335135381	0.8492690100	0.2781084925
H	-0.0109032350	-1.7023321107	-0.4476393372
H	0.9644629863	0.1675829934	-1.5545935541
H	0.8616301562	1.5923805589	-0.5245636027
H	2.3075625025	0.6735505915	0.8828540874
H	1.5030100738	-0.7223988799	0.9942092627

TS-5

C	-0.5600270312	0.1098436410	-0.0591355090
C	0.8081418612	0.6143679162	-0.4486353857
N	1.8246396305	-0.0454215112	0.3637211584
O	-0.6371494060	-1.2810707854	-0.0305840121
O	-1.4963893620	0.7968506902	0.2412830191
H	-0.8144056083	-1.6107849274	-0.9202039433
H	0.8295186469	1.6852973255	-0.2657453609
H	0.9117406664	0.4502168372	-1.5310897459
H	1.7752419433	-1.0481616606	0.2345112985
H	2.7486877288	0.2574947785	0.0841862970

TS-6

C	-0.5747109734	0.0842040955	-0.0057364016
C	0.7871496982	0.7207812416	-0.2166468170
N	1.9152920044	-0.0693220849	0.1505948512
O	-0.5347535169	-1.2652837875	-0.0796669637
O	-1.6020075543	0.7057941133	0.1541021520
H	-1.4546493784	-1.5575370419	0.0192486104
H	0.7792346908	1.6469040538	0.3534375592
H	0.8045315992	1.0150795645	-1.2724086955
H	2.1920753766	-0.8586552172	-0.3953296419
H	2.4987694945	0.2040365402	0.9122345178

TS-7

C	-0.5789248156	0.1002271165	-0.0136978973
C	0.7856571054	0.6859848004	-0.3230802288
N	1.9387192210	-0.0163775519	0.2145900916
O	-0.6369586006	-1.2823596449	-0.1532679979
O	-1.5607102102	0.7488252859	0.2326765307
H	-0.3876703955	-1.7097726212	0.6745745481
H	0.8691721974	0.7050731552	-1.4123809725
H	0.7868133441	1.7175977764	0.0213326206
H	1.9282136378	-0.0240404659	1.2264825558
H	1.9607647065	-0.9748997568	-0.1084068957

TS-8

C	-0.5581114205	0.1101136265	-0.0837101927
C	0.8352345584	0.5082723557	-0.5220156770
N	1.8921870710	-0.0313308441	0.3267624673
O	-0.7283412536	-1.2722449499	-0.0094112206
O	-1.4236901717	0.8663879039	0.2673691943
H	-1.0061553668	-1.6099379080	-0.8695475934
H	0.9918078545	0.1493488514	-1.5410245978
H	0.8918905482	1.5936968646	-0.5301902560
H	1.8079418664	0.3443055443	1.2639039634
H	1.7897060633	-1.0363066871	0.4041663870

TS-9

C	-0.5640634350	0.0957773762	-0.0868739169
C	0.8467704356	0.4323163213	-0.5459214265
N	1.9144056162	-0.0133675611	0.3439937611
O	-0.8618636063	-1.2325305764	-0.0078505833
O	-1.3929442978	0.9138494107	0.2229441286
H	-0.1095270156	-1.7525193085	-0.3161133566
H	1.0151882560	0.0010367633	-1.5345206565
H	0.8939846733	1.5137481574	-0.6409525285
H	1.7606352185	0.3279077972	1.2850047751
H	1.9794738028	-1.0217588094	0.3957683311

TS-10

C	-0.4877818674	0.1032221507	-0.0121404591
C	0.7355718377	-0.7721167282	-0.0596829494
N	1.9435846507	0.0148288541	0.0937266748
O	-1.6678392850	-0.6171304787	0.0791321997
O	-0.4707424901	1.3047752274	0.0010089182
H	-1.9641529741	-0.8782232855	-0.8007503789
H	0.6684459695	-1.3373213023	-0.9993514131
H	0.6363743508	-1.5031230295	0.7449425673
H	1.8052253824	0.9324269825	-0.2942724035
H	2.7233287993	-0.4126589205	-0.3760618363

Table A.3 Focal point energy table for all glycine conformers (all energies in hartree)

Ip	HF	MP2	CCSD	CCSD(T)
DZ	-282.88442460	-283.73558951	-283.76441596	-283.79565265
TZ	-282.95138497	-283.98150979	-283.99782491	-284.04292074
QZ	-282.96935371	-284.06232927	-284.06847922	-284.11677061
5Z	-282.97346836	-284.09121926		
IIn				
DZ	-282.87899501	-283.73474784	-283.76247353	-283.79439446
TZ	-282.94614588	-283.98099434	-283.99611493	-284.04195802
QZ	-282.96411344	-284.06180639	-284.06670717	-284.11575815
5Z	-282.96820962	-284.09065503		
IVn				
DZ	-282.88181111	-283.73356207	-283.76223352	-283.79349766
TZ	-282.94890388	-283.97968896	-283.99581348	-284.04095386
QZ	-282.96687046	-284.06052151	-284.06647147	-284.11480794
5Z	-282.97098873	-284.08939973		
IIIp				
DZ	-282.88104750	-283.73305618	-283.76164663	-283.79302383
TZ	-282.94800167	-283.97890310	-283.99498353	-284.04021723
QZ	-282.96595902	-284.05969455	-284.06559641	-284.11402608
5Z	-282.97006756	-284.08856522		
Vn				
DZ	-282.87989738	-283.73171772	-283.76046965	-283.79173569
TZ	-282.94684060	-283.97750488	-283.99371586	-284.03883334
QZ	-282.96479695	-284.05824735	-284.06427734	-284.11258439
5Z	-282.96891124	-284.08711803		
VIp				
DZ	-282.87529329	-283.72782850	-283.75671156	-283.78814893
TZ	-282.94240842	-283.97374480	-283.99002268	-284.03533046
QZ	-282.96042231	-284.05456232	-284.06065219	-284.10916281
5Z	-282.96453534	-284.08341526		
VIIp				
DZ	-282.87171209	-283.72591289	-283.75405768	-283.78579628
TZ	-282.93917071	-283.97232362	-283.98784752	-284.03350332
QZ	-282.95719686	-284.05319305	-284.05851544	-284.10737712
5Z	-282.96130196	-284.08207361		
VIIIn				
DZ	-282.87246322	-283.72557601	-283.75429326	-283.78576927
TZ	-282.93977456	-283.97184269	-283.98791749	-284.03329091
QZ	-282.95779780	-284.05268429	-284.05856204	-284.10713874
5Z	-282.96191473	-284.08153975		

Table A.4 Focal point energy table for all glycine transition states (all energies in hartree)

TS-1	HF	MP2	CCSD	CCSD(T)
DZ	-282.87962216	-283.73223755	-283.76079012	-283.79232590
TZ	-282.94663294	-283.97793081	-283.99389479	-284.03926892
QZ	-282.96457665	-284.05869420	-284.06445452	-284.11302521
5Z	-282.96868553	-284.08756340		
TS-2				
DZ	-282.87513076	-283.72646288	-283.75480512	-283.78587297
TZ	-282.94275541	-283.97279483	-283.98861105	-284.03356218
QZ	-282.96080545	-284.05387270	-284.05955341	-284.10769605
5Z	-282.96492966	-284.08282277		
TS-3				
DZ	-282.86508804	-283.71596521	-283.74561635	-283.77675476
TZ	-282.93215870	-283.96185317	-283.97889089	-284.02387323
QZ	-282.95010883	-284.04254337	-284.04938366	-284.09756415
5Z	-282.95421333	-284.07136802		
TS-4				
DZ	-282.86212058	-283.71264098	-283.74253623	-283.77356540
TZ	-282.92931868	-283.95848944	-283.97574031	-284.02057652
QZ	-282.94726160	-284.03913670	-284.04616992	-284.09419541
5Z	-282.95137133	-284.06794216		
TS-5				
DZ	-282.85914967	-283.71075793	-283.74050881	-283.77166559
TZ	-282.92618771	-283.95653245	-283.97359608	-284.01860045
QZ	-282.94411260	-284.03707913	-284.04391644	-284.09211289
5Z	-282.94821567	-284.06587430		
TS-6				
DZ	-282.86603987	-283.71967909	-283.74859385	-283.78015790
TZ	-282.93331602	-283.96573197	-283.98195451	-284.02740504
QZ	-282.95128300	-284.04640603	-284.05240387	-284.10105246
5Z	-282.95539217	-284.07522493		
TS-7				
DZ	-282.87309742	-283.72425708	-283.75257375	-283.78364928
TZ	-282.94082403	-283.97058154	-283.98642624	-284.03135313
QZ	-282.95888101	-284.05165521	-284.05735848	-284.10547407
5Z	-282.96300102	-284.08061405		
GT-8				
DZ	-282.86089135	-283.71247012	-283.74210013	-283.77335605
TZ	-282.92799934	-283.95835336	-283.97531574	-284.02043237
QZ	-282.94594567	-284.03900549	-284.04574934	-284.09406550
5Z	-282.95004678	-284.06783093		

TS-9

DZ	-282.86087165	-283.71266863	-283.74227530	-283.77356499
TZ	-282.92789866	-283.95844306	-283.97536885	-284.02051105
QZ	-282.94582476	-284.03904275	-284.04574093	-284.09408168
5Z	-282.94992523	-284.06785412		

TS-10

DZ	-282.86209974	-283.71364534	-283.74325727	-283.77443275
TZ	-282.92914307	-283.95947577	-283.97641633	-284.02145818
QZ	-282.94708699	-284.04012762	-284.04686182	-284.09510165
5Z	-282.95119320	-284.0689305 0		

Table A.5 Vibrational Frequency with anharm correction and TED analysis.

Anharmonicities computed by means of second-order vibrational perturbation theory (VPT2) with a resonance cutoff of 80 cm^{-1}. Absolute infrared intensities from the double-harmonic approximation are given in km/mol.

The internal coordinates are defined as :
$S_1=r(C_1-C_2)$, $S_2=r(C_1-N_3)$, $S_3=\theta(C_1-C_2-N_3)$, $S_4=r(C_1-O_4)$, $S_5=\theta(O_4-C_1-C_2)$, $S_6=\tau(O_4-C_1-C_2-N_3)$, $S_7=r(C_1=O_5)$, $S_8=\theta(O_5=C_1-C_2)$, $S_9=\tau(O_5=C_1-C_2-N_3)$, $S_{10}=r(O_4-H_6)$, $S_{11}=\theta(C_1-O_4-H_6)$, $S_{12}=\tau(H_6-O_4-C_1-C_2)$, $S_{13}=r(C_2-H_7)$, $S_{14}=\theta(C_1-C_2-H_7)$, $S_{15}=\tau(H_7-C_2-C_1-O_4)$, $S_{16}=r(C_2-H_8)$, $S_{17}=\theta(C_1-C_2-H_8)$, $S_{18}=\tau(H_8-C_2-C_1-O_4)$, $S_{19}=r(N_3-H_9)$, $S_{20}=\theta(C_2-N_3-H_9)$, $S_{21}=\tau(C_1-C_2-N_3-H_9)$, $S_{22}=r(N_3-H_{10})$, $S_{23}=\theta(C_2-C_3-H_{10})$, $S_{24}=\tau(C_1-C_2-N_3-H_{10})$.

Ip

Mode	Total Energy Distribution	ω_i (cm^{-1})	$v_i - \omega_i$ (cm^{-1})	v_i (cm^{-1})	Intensity (km mol^{-1})
v_1	$S_6(38) + S_9(34)$	65	+8	73	6
v_2	$S_{21}(42) + S_{23}(42) - S_6(11)$	218	−12	206	45
v_3	$S_3(50) + S_8(28) - S_5(18)$	260	1	261	9
v_4	$S_5(67) + S_1(15) + S_3(15)$	468	−6	462	31
v_5	$S_{12}(39) - S_6(23) + S_9(21)$	515	−12	503	31
v_6	$S_8(61) - S_3(16) - S_4(15)$	639	−3	636	7
v_7	$S_{12}(61) + S_6(20) - S_9(14)$	657	−29	628	89
v_8	$S_1(46)$	843	−21	822	77
v_9	$S_{18}(28) + S_{15}(28) - S_9(24)$	926	−10	916	2
v_{10}	$S_{24}(17) - S_{21}(17) - S_{23}(13) - S_{20}(13)$	956	−52	904	132
v_{11}	$S_4(39) - S_{11}(26) - S_2(26)$	1142	−34	1108	224
v_{12}	$S_2(47) - S_3(11) - S_{11}(11)$	1181	−35	1146	60
v_{13}	$S_{14}(31) - S_{17}(31) - S_{23}(16) + S_{20}(16)$	1195	−29	1166	1
v_{14}	$S_{11}(37) - S_{14}(16) - S_{17}(16)$	1317	−38	1280	16
v_{15}	$S_{23}(23) - S_{20}(23) - S_{17}(11) + S_{14}(11)$	1399	−36	1363	0
v_{16}	$S_{14}(21) + S_{17}(21) + S_4(15) - S_1(14)$	1421	−72	1349	29
v_{17}	$S_{15}(45) - S_{18}(45)$	1473	−34	1439	13
v_{18}	$S_{20}(26) + S_{23}(26) - S_{21}(24) - S_{24}(24)$	1677	−57	1621	17
v_{19}	$S_7(84)$	1827	−135	1692	231
v_{20}	$S_{16}(50) + S_{13}(50)$	3100	−115	2985	14
v_{21}	$S_{13}(50) - S_{16}(50)$	3148	−150	2999	4
v_{22}	$S_{22}(50) + S_{19}(50)$	3537	−175	3363	3
v_{23}	$S_{19}(50) - S_{22}(50)$	3622	−177	3446	7
v_{24}	$S_{10}(100)$	3770	−186	3584	75

IIn

Mode	Total Energy Distribution	ω_i (cm^{-1})	$\nu_i - \omega_i$ (cm^{-1})	ν_i (cm^{-1})	Intensity (km mol^{-1})
ν_1	$S_9(43) + S_6(21) + S_{18}(10) + S_{15}(10)$	95	−26	70	3
ν_2	$S_{21}(39) + S_{24}(38) + S_6(12)$	268	−28	241	16
ν_3	$S_3(49) + S_5(37)$	327	−15	312	20
ν_4	$S_8(55) + S_1(17) + S_3(14)$	511	−5	506	22
ν_5	$S_9(34) - S_{15}(11)$	559	−20	539	5
ν_6	$S_5(49) - S_3(25)$	658	+44	701	7
ν_7	$S_1(29) + S_{34}(14) + S_{24}(12)$	840	−26	813	28
ν_8	$S_{12}(72)$	870	−43	827	82
ν_9	$S_6(24) + S_{12}(18) + S_{20}(14)$	903	−29	874	60
ν_{10}	$S_6(24) + S_{23}(21) - S_{21}(14) - S_4(10)$	961	−48	912	63
ν_{11}	$S_2(79)$	1094	−25	1069	10
ν_{12}	$S_{17}(38) + S_{20}(20) - S_{23}(19) - S_{14}(15)$	1173	−28	1145	2
ν_{13}	$S_4(44) - S_1(19) + S_{11}(18)$	1247	−35	1212	18
ν_{14}	$S_{14}(54) - S_{15}(16) + S_{20}(11)$	1333	−32	1300	9
ν_{15}	$S_{17}(44) + S_{23}(13) - S_{20}(10)$	1378	−45	1333	5
ν_{16}	$S_{11}(68) - S_4(10)$	1438	−49	1389	374
ν_{17}	$S_{18}(47) - S_{15}(46)$	1484	−45	1439	5
ν_{18}	$S_{20}(28) + S_{23}(27) - S_{24}(22) + S_{21}(21)$	1662	−32	1630	33
ν_{19}	$S_7(83)$	1855	−35	1820	283
ν_{20}	$S_{13}(57) + S_{16}(43)$	3106	−136	2970	10
ν_{21}	$S_{16}(57) - S_{13}(43)$	3164	−145	3019	5
ν_{22}	$S_{10}(97)$	3499	−244	3255	292
ν_{23}	$S_{19}(59) + S_{22}(39)$	3562	−145	3417	1
ν_{24}	$S_{22}(59) - S_{19}(40)$	3657	−174	3482	18

IIIp

Mode	Total Energy Distribution	ω_i (cm^{-1})	$\nu_i - \omega_i$ (cm^{-1})	ν_i (cm^{-1})	Intensity (km mol^{-1})
ν_1	$S_9(46) + S_6(32) + S_{15}(10) + S_{18}(10)$	16	+17	33	0
ν_2	$S_{24}(47) + S_{21}(47)$	261	+1	262	44
ν_3	$S_3(50) + S_5(36) - S_8(11)$	269	−12	257	3
ν_4	$S_8(57) + S_1(20) + S_3(15)$	504	−15	489	12
ν_5	$S_{12}(30) + S_9(25) - S_{18}(14) - S_{15}(13)$	523	+177	700	22
ν_6	$S_5(63) - S_3(18)$	597	+12	609	51
ν_7	$S_{12}(68) - S_9(14)$	692	−32	660	102
ν_8	$S_1(36) + S_4(30)$	821	−20	801	70
ν_9	$S_6(53) - S_{15}(11) - S_{18}(11)$	917	−10	907	2
ν_{10}	$S_{24}(19) - S_{21}(18) + S_{23}(14) + S_{20}(13)$	930	−53	878	159
ν_{11}	$S_2(74)$	1163	−36	1127	22
ν_{12}	$S_{11}(49) - S_4(28)$	1180	−50	1130	204
ν_{13}	$S_{17}(29) - S_{14}(29) + S_{23}(19) - S_{20}(18)$	1200	−72	1128	2
ν_{14}	$S_{14}(35) + S_{17}(35)$	1362	−48	1314	21
ν_{15}	$S_{11}(26) + S_4(21) - S_1(17) + S_8(11)$	1378	−40	1339	55
ν_{16}	$S_{23}(22) - S_{20}(22) + S_{14}(15) - S_{17}(14)$	1399	−68	1331	0
ν_{17}	$S_{18}(44) - S_{15}(44)$	1471	−32	1440	2
ν_{18}	$S_{23}(26) + S_{20}(26) - S_{24}(23) + S_{21}(23)$	1676	−74	1602	26
ν_{19}	$S_7(85)$	1824	−30	1794	231
ν_{20}	$S_{13}(53) + S_{16}(47)$	3104	−134	2970	12
ν_{21}	$S_{16}(53) - S_{13}(47)$	3152	−137	3015	3
ν_{22}	$S_{19}(50) + S_{22}(50)$	3548	−130	3418	3
ν_{23}	$S_{22}(50) - S_{19}(50)$	3637	−175	3462	7
ν_{24}	$S_{10}(100)$	3762	−185	3577	79

IVn

Mode	Total Energy Distribution	ω_i (cm^{-1})	$\nu_i - \omega_i$ (cm^{-1})	ν_i (cm^{-1})	Intensity (km mol^{-1})
ν_1	$S_6(48) + S_9(33)$	99	−2	97	3
ν_2	$S_{24}(49) + S_{21}(48)$	196	−31	166	51
ν_3	$S_3(52) + S_8(25) - S_5(17)$	285	−17	268	1
ν_4	$S_5(62) + S_3(17)$	469	0	469	13
ν_5	$S_{12}(39) + S_9(17) - S_6(16)$	528	−11	517	26
ν_6	$S_8(49) - S_{12}(20) - S_3(12)$	630	+2	633	38
ν_7	$S_{12}(40) + S_6(23) - S_9(21)$	672	−33	639	78
ν_8	$S_1(54) + S_4(15)$	860	−20	840	7
ν_9	$S_{21}(23) - S_{24}(21) - S_{20}(21) - S_{23}(17)$	872	−53	819	160
ν_{10}	$S_{18}(23) - S_9(20) + S_{15}(20) - S_{14}(11)$	1040	−40	1000	8
ν_{11}	$S_2(63) - S_{23}(11)$	1129	−26	1102	41
ν_{12}	$S_4(32) - S_{11}(30) - S_{14}(12)$	1158	−30	1128	205
ν_{13}	$S_{14}(27) + S_{20}(17) - S_{11}(13) - S_{23}(11)$	1233	−38	1195	40
ν_{14}	$S_{17}(32) - S_{18}(16) + S_{20}(12) + S_6(10)$	1277	−41	1236	1
ν_{15}	$S_{11}(34) + S_4(17) + S_8(11)$	1344	−28	1316	36
ν_{16}	$S_{14}(24) + S_{17}(16) - S_1(15) + S_{23}(11)$	1467	−51	1416	34
ν_{17}	$S_{15}(48) - S_{18}(42)$	1511	−44	1467	11
ν_{18}	$S_{20}(31) + S_{23}(24) - S_{24}(22) + S_{21}(21)$	1642	−87	1555	55
ν_{19}	$S_7(82)$	1831	−29	1801	223
ν_{20}	$S_{16}(96)$	3031	−147	2884	34
ν_{21}	$S_{13}(96)$	3134	−151	2983	10
ν_{22}	$S_{19}(64) + S_{22}(36)$	3541	−156	3385	6
ν_{23}	$S_{22}(64) - S_{19}(36)$	3645	−176	3469	13
ν_{24}	$S_{10}(100)$	3771	−184	3586	81

Vn

Mode	Total Energy Distribution	ω_i (cm^{-1})	$\nu_i - \omega_i$ (cm^{-1})	ν_i (cm^{-1})	Intensity (km mol^{-1})
ν_1	$S_9(53) + S_6(31)$	65	−3	62	2
ν_2	$S_{24}(40) + S_{21}(39) - S_3(10)$	239	−8	231	31
ν_3	$S_3(46) + S_5(21) + S_{21}(13)$	290	−13	277	15
ν_4	$S_8(26) - S_5(24) + S_3(13)$	454	1	452	5
ν_5	$S_8(40) + S_{12}(17) + S_1(16) + S_5(13)$	551	−8	543	29
ν_6	$S_{12}(58) - S_5(21)$	602	−24	578	64
ν_7	$S_9(31) - S_{12}(18) - S_6(16)$	707	−21	685	76
ν_8	$S_1(40) + S_4(28) + S_{20}(11)$	849	−21	827	27
ν_9	$S_{23}(25) + S_{24}(18) - S_{21}(15)$	868	−41	827	118
ν_{10}	$S_6(37) + S_{17}(11)$	1037	−38	999	21
ν_{11}	$S_2(42) + S_{20}(21) - S_4(12)$	1096	−30	1066	41
ν_{12}	$S_2(30) - S_{11}(24) + S_4(16)$	1148	−30	1118	138
ν_{13}	$S_{11}(31) + S_{14}(29)$	1236	−36	1200	57
ν_{14}	$S_{17}(40) + S_{18}(24) + S_{23}(14)$	1307	−45	1262	5
ν_{15}	$S_{11}(24) - S_{14}(23) + S_4(21) + S_8(14)$	1367	−30	1337	44
ν_{16}	$S_{17}(22) + S_{14}(16) - S_1(13) + S_{20}(11)$	1443	−34	1409	46
ν_{17}	$S_{15}(49) - S_{18}(41)$	1509	−41	1468	3
ν_{18}	$S_{23}(28) + S_{20}(26) + S_{21}(23) - S_{24}(23)$	1653	−94	1559	33
ν_{19}	$S_7(84)$	1834	−33	1801	248
ν_{20}	$S_{16}(97)$	3020	−157	2863	39
ν_{21}	$S_{13}(97)$	3168	−140	3028	6
ν_{22}	$S_{19}(51) + S_{22}(49)$	3543	−146	3397	2
ν_{23}	$S_{22}(51) - S_{19}(49)$	3640	−175	3464	8
ν_{24}	$S_{10}(100)$	3771	−186	3586	81

VIp

Mode	Total Energy Distribution	ω_i (cm^{-1})	$\nu_i - \omega_i$ (cm^{-1})	ν_i (cm^{-1})	Intensity (km mol^{-1})
ν_1	$S_6(38) + S_9(34)$	78	+4	82	8
ν_2	$S_{21}(42) + S_{24}(42) - S_6(11)$	207	−13	194	57
ν_3	$S_3(52) + S_8(27) - S_5(17)$	263	+2	265	27
ν_4	$S_{12}(88)$	463	−19	444	79
ν_5	$S_5(63) + S_1(17) + S_3(13)$	472	−6	465	1
ν_6	$S_6(35) - S_9(35) + S_{12}(13)$	571	−10	561	12
ν_7	$S_8(64) - S_3(15) - S_4(13)$	652	−22	630	14
ν_8	$S_1(44) + S_3(13) - S_5(11)$	850	−21	828	23
ν_9	$S_{15}(28) + S_{18}(28) - S_9(24)$	929	+6	935	1
ν_{10}	$S_{21}(17) - S_{24}(17) + S_2(15) - S_{20}(14)$	956	−52	904	181
ν_{11}	$S_4(41) - S_2(25) + S_{11}(21)$	1152	−29	1123	27
ν_{12}	$S_2(48) - S_3(12) + S_{11}(11)$	1185	−34	1151	5
ν_{13}	$S_{17}(30) - S_{14}(30) - S_{20}(18) + S_{23}(18)$	1193	−27	1166	1
ν_{14}	$S_{11}(57) - S_4(11)$	1296	−39	1258	338
ν_{15}	$S_{17}(32) + S_{14}(32) - S_1(11)$	1395	−49	1345	44
ν_{16}	$S_{20}(23) - S_{23}(23) - S_{14}(12) + S_{15}(11)$	1407	−38	1369	0
ν_{17}	$S_{15}(47) - S_{18}(47)$	1478	−10	1468	7
ν_{18}	$S_{20}(25) + S_{23}(25) - S_{24}(24) + S_{21}(24)$	1678	−55	1623	20
ν_{19}	$S_7(85)$	1854	−33	1821	187
ν_{20}	$S_{16}(50) + S_{13}(50)$	3073	−138	2935	22
ν_{21}	$S_{13}(50) - S_{16}(50)$	3122	−149	2973	8
ν_{22}	$S_{19}(50) + S_{22}(50)$	3536	−175	3361	5
ν_{23}	$S_{22}(50) - S_{19}(50)$	3620	−177	3443	9
ν_{24}	$S_{10}(100)$	3823	−183	3640	60

VIIp

Mode	Total Energy Distribution	ω_i (cm^{-1})	$\nu_i - \omega_i$ (cm^{-1})	ν_i (cm^{-1})	Intensity (km mol^{-1})
ν_1	$S_9(51) + S_6(29) + S_{18}(12) + S_{15}(12)$	76	+1	77	5
ν_2	$S_3(48) + S_5(41)$	290	−20	270	21
ν_3	$S_{21}(42) + S_{24}(42) - S_{12}(13)$	368	+20	388	85
ν_4	$S_8(59) + S_1(25) + S_3(13)$	506	−17	489	3
ν_5	$S_{21}(21) - S_{24}(21) + S_5(18) - S_3(14)$	539	−185	354	130
ν_6	$S_9(33) - S_{15}(18) - S_{18}(18)$	544	−15	529	3
ν_7	$S_{12}(78)$	658	−41	617	24
ν_8	$S_5(37) + S_{24}(14) - S_{21}(14)$	682	−161	520	132
ν_9	$S_1(43) + S_4(38)$	855	−23	832	40
ν_{10}	$S_6(45) + S_{20}(12) - S_{23}(12)$	907	−19	888	4
ν_{11}	$S_2(68)$	1133	−43	1090	11
ν_{12}	$S_{17}(25) - S_{14}(25) - S_{20}(22) + S_{23}(22)$	1169	−34	1135	1
ν_{13}	$S_{11}(39) + S_4(25) + S_2(16) - S_1(14)$	1207	+6	1213	5
ν_{14}	$S_{11}(39) - S_4(20) - S_8(13)$	1348	−24	1324	283
ν_{15}	$S_{14}(34) + S_{17}(34)$	1360	−19	1341	87
ν_{16}	$S_{17}(19) - S_{14}(19) + S_{20}(16) - S_{23}(16)$	1377	−44	1333	0
ν_{17}	$S_{18}(46) - S_{15}(46)$	1467	−35	1431	4
ν_{18}	$S_{23}(35) + S_{20}(35) + S_{21}(15) - S_{24}(15)$	1651	−42	1609	22
ν_{19}	$S_7(85)$	1853	−33	1819	221
ν_{20}	$S_{16}(50) + S_{13}(50)$	3113	−121	2992	9
ν_{21}	$S_{13}(50) - S_{16}(50)$	3165	−152	3013	2
ν_{22}	$S_{22}(50) + S_{19}(50)$	3576	−132	3444	11
ν_{23}	$S_{19}(50) - S_{22}(50)$	3692	−156	3536	16
ν_{24}	$S_{10}(100)$	3759	−213	3546	96

VIIIn

Mode	Total Energy Distribution	ω_i (cm^{-1})	$\nu_i - \omega_i$ (cm^{-1})	ν_i (cm^{-1})	Intensity (km mol^{-1})
ν_1	$S_6(42) + S_9(29)$	94	−11	82	7
ν_2	$S_{21}(45) + S_{24}(45)$	176	−60	116	45
ν_3	$S_5(45) + S_8(25) - S_5(17)$	293	+2	295	12
ν_4	$S_{12}(73) - S_5(11)$	465	−15	449	69
ν_5	$S_5(50) + S_{12}(20) + S_3(14) + S_1(10)$	481	−9	471	25
ν_6	$S_9(34) - S_6(31)$	576	−35	541	7
ν_7	$S_8(55) - S_3(14) - S_4(11)$	654	−25	629	8
ν_8	$S_1(52) + S_4(16)$	863	−21	842	9
ν_9	$S_{21}(25) - S_{23}(22) - S_{24}(21) - S_{20}(17)$	878	−60	818	154
ν_{10}	$S_{18}(23) - S_9(21) + S_{15}(19) - S_{14}(14)$	1031	−46	985	10
ν_{11}	$S_2(61) - S_{17}(14) + S_{23}(12)$	1138	−+201	1339	17
ν_{12}	$S_4(33) + S_{11}(31)$	1170	−27	1143	7
ν_{13}	$S_{20}(31) - S_{23}(17) + S_{11}(12) + S_2(12)$	1245	−8	1237	9
ν_{14}	$S_{17}(30) - S_{14}(19) - S_{18}(17) - S_{15}(12)$	1273	−42	1231	23
ν_{15}	$S_{11}(45) - S_4(18) - S_8(10)$	1314	−47	1267	353
ν_{16}	$S_{14}(30) + S_{17}(22) + S_{23}(15) - S_1(12)$	1445	−69	1376	37
ν_{17}	$S_{15}(49) - S_{18}(45)$	1511	−38	1473	8
ν_{18}	$S_{20}(31) + S_{23}(23) - S_{24}(22) + S_{21}(21)$	1643	−73	1570	55
ν_{19}	$S_7(83)$	1855	−33	1822	180
ν_{20}	$S_{16}(88) + S_{13}(12)$	3028	−128	2900	39
ν_{21}	$S_{13}(88) - S_{16}(12)$	3084	−152	2932	22
ν_{22}	$S_{19}(72) + S_{22}(28)$	3534	−156	3378	12
ν_{23}	$S_{22}(72) - S_{19}(28)$	3645	−176	3469	17
ν_{24}	$S_{10}(100)$	3829	−188	3641	63

[a] The percentage contribution of each internal coordinates S_i to the total energy of each mode is listed in parentheses. The components with contribution ≥10% are listed. The sign preceding each S_i denotes the relative phase of the internal coordinates in the normal-mode eigenvector.

Table A.6 Rotational Isomerization Pathways Tunneling Parameters

The frozen-core MP2/cc-pVTZ method was employed to map out the IRP to high precision and to obtain harmonic vibrational frequencies along the path by projection onto a space of natural internal coordinates. The final potential energy function V along the isomerization IRP was then constructed from all-electron CCSD(T)/cc-pCVTZ energy points. A nearly exact Fourier fit of these points was used to represent V in terms of the arc length s (atomic units) in mass-weighted coordinates along the IRP, as well as to ensure that V(s) extended smoothly all the way to the reactant minimum.

	TS-1 **IIIp -> Ip**	**TS-2** **IVn -> Ip**
Collision energy (ε) (kcal mol^{-1})	0.05	0.56
Collision frequency (ω_0) (cm^{-1})	16	196
Barrier[a] (kcal mol^{-1})	0.77	5.10
Turning points (s_1, s_2) (u$^{1/2}$bohr)	(−9.52, 3.62)	(−1.34, 3.62)
Effective barrier frequency (cm^{-1})	54	702
Barrier penetration integral (θ)	19	9
Half-life $t_{1/2}$ (s)	8.97×10^{4}	1.16×10^{-5}

	TS-3 **VIp -> Ip**	**TS-4** **IVn -> IIn**
Collision energy (ε) (kcal mol^{-1})	1.32	1.72
Collision frequency (ω_0) (cm^{-1})	463	600
Barrier[a] (kcal mol^{-1})	7.38	13.14
Turning points (s_1, s_2) (u$^{1/2}$bohr)	(−1.96, 1.47)	(−10.59, 5.09)
Effective barrier frequency (cm^{-1})	556	610
Barrier penetration integral (θ)	16	59
Half-life $t_{1/2}$ (s)	1.67	1.47×10^{38}

	TS-5 **Vn -> IIn**	**TS-6** **VIp -> IIn**
Collision energy (ε) (kcal mol^{-1})	1.72	0.59
Collision frequency (ω_0) (cm^{-1})	526	301
Barrier[a] (kcal mol^{-1})	12.96	5.29
Turning points (s_1, s_2) (u$^{1/2}$bohr)	(−2.43, 6.40)	(−14.25, 2.38))
Effective barrier frequency (cm^{-1})	526	301
Barrier penetration integral (θ)	51	61
Half-life $t_{1/2}$ (s)	4.87×10^{30}	8.79×10^{39}

	TS-7 **Vn -> IIIp**	**TS-8** **VIIp -> IIIp**
Collision energy (ε) (kcal mol^{-1})	0.68	1.88
Collision frequency (ω_0) (cm^{-1})	239	658
Barrier[a] (kcal mol^{-1})	5.14	8.38
Turning points (s_1, s_2) ($u^{1/2}$bohr)	(−2.26, 1.06))	(−2.50, 1.57)
Effective barrier frequency (cm^{-1})	715	545
Barrier penetration integral (θ)	11	18
Half-life $t_{1/2}$ (s)	2.55×10^{-4}	2.25×10^{2}

	TS-9 **VIIp -> IIIp**	**TS-10** **VIIIn -> IVn**
Collision energy (ε) (kcal mol^{-1})	1.88	1.33
Collision frequency (ω_0) (cm^{-1})	658	465
Barrier[a] (kcal mol^{-1})	8.35	7.59
Turning points (s_1, s_2) ($u^{1/2}$bohr)	(−6.47, 1.59)	(−2.03, 1.49)
Effective barrier frequency (cm^{-1})	526	558
Barrier penetration integral (θ)	28	16
Half-life $t_{1/2}$ (s)	8.94×10^{10}	4.96

APPENDIX B

SUPPORTING INFORMATION FOR CHAPTER 3

Table B.1 85 unique conformers located at MP2/cc-pVTZ level in Å (energy in hartree)

1 T T G^+ G^- A^+:T ENERGY=-398.30296920

N	-0.2712068583	-0.9659532185	1.3285844128
H	-0.6529128337	-0.9588047238	2.2646125936
C	-0.2561337648	0.3815663565	0.7567444255
H	0.0373640659	1.0882575367	1.5361578523
C	-1.5761856843	0.8162199795	0.1408169557
C	0.8406821086	0.4395196416	-0.3117025477
H	-1.4964184798	1.8393394360	-0.2247693888
H	-2.3626648953	0.7694748636	0.8920566247
O	-1.9517223544	-0.0815635579	-0.8940151454
O	0.8450333802	1.2527400186	-1.2073056071
H	-1.4173928090	0.1528433348	-1.6613301227
O	1.7897241200	-0.4867874144	-0.1560460162
H	1.4490285652	-1.0427758827	0.5805388884
H	-0.8790915602	-1.5453293700	0.7573200749

2 C C G^+ T C ENERGY=-398.30195692

N	-0.7237535484	-1.5759263866	0.5715728037
H	-0.4073234184	-1.9551210793	1.4543060460
C	-0.3369208746	-0.1781451837	0.4545511253
H	-0.4967279487	0.3245332111	1.4071466445
C	-1.2633171276	0.4750300417	-0.5788891802
C	1.0991098233	0.0101632927	0.0253948342
H	-1.0394620404	0.0468222780	-1.5641151697
H	-1.0892128405	1.5472481950	-0.6217410742
O	-2.6052441487	0.2609214890	-0.2150999798
O	1.7960745897	-0.8513642052	-0.4606234811
H	-2.6229655751	-0.6649963430	0.0696199333
O	1.5081895235	1.2855625130	0.1999735392
H	2.4131361752	1.3240685196	-0.1456513062
H	-0.2367195892	-2.1028843425	-0.1465857350

3 T T T G^- A^- ENERGY=-398.30188250

N	-0.3371005685	1.7046072713	-0.6122503343
H	-0.1956520205	2.5910925589	-0.1478437243
C	0.1917083492	0.6005356395	0.1911860550
H	0.0042194856	0.8183021102	1.2440040735
C	1.6885624183	0.3464518027	0.0200801988
C	-0.6035060188	-0.6661902805	-0.1257504857
H	2.2240580371	1.2766552577	0.2072374009
H	1.8763627466	0.0567737693	-1.0224499371
O	2.1785519649	-0.6082868158	0.9279552756
O	-0.2037468901	-1.7823597439	0.1314951417
H	1.6033477388	-1.3802373595	0.8154342140
O	-1.7854247585	-0.4382664027	-0.6993740845
H	-1.7947985607	0.5358541999	-0.8331118856
H	0.1460040767	1.7548179929	-1.5026299080

4 C C G^- G^+ C ENERGY=-398.30135554

N	0.5591518505	-1.5994007812	0.1587723703
H	0.8084043912	-2.3091004316	-0.5153518052
C	0.1021161334	-0.3859791664	-0.5071010980
H	-0.3425962720	-0.5549122856	-1.4936569404
C	1.2958115733	0.5575618061	-0.6453483348
C	-0.9728872080	0.2476284695	0.3479027179
H	0.9864342439	1.5164620802	-1.0515401461
H	2.0160812040	0.1011118096	-1.3325241993
O	1.8636068309	0.7867084753	0.6246683617
O	-1.4752225778	-0.2632352610	1.3221252113
H	1.9037308505	-0.0960628039	1.0227506435
O	-1.3358671005	1.4556688745	-0.1262430411
H	-2.0191001122	1.7804917618	0.4791099877
H	-0.1823608073	-1.9608385473	0.7461652722

5 C A^+ G^- G^- A^+ ENERGY=-398.30023342

N	0.5704411887	-1.5520491139	-0.5891485026
H	-0.2623507529	-2.1028579481	-0.7536196692
C	0.2909053007	-0.1307693011	-0.7734735061
H	0.1436166396	0.0613864436	-1.8377513485
C	1.4790597135	0.6744272892	-0.2734481881
C	-0.9706069094	0.2989159574	-0.0493779753
H	1.3122015381	1.7374395025	-0.4608749570
H	2.3624559081	0.3550338203	-0.8206355780
O	1.7366462255	0.4243443652	1.0978062949
O	-1.0292661396	1.0183212269	0.9276267329
H	0.9821693764	0.7999363759	1.5685824688
O	-2.0706714140	-0.2597925397	-0.5998549664
H	-2.8168359162	0.0259658322	-0.0505856799
H	0.8516552415	-1.6929409104	0.3747608745

6 T T G^- T A^+:G^+ ENERGY=-398.30010629

N	0.1899101928	-1.3097630468	0.8853012159
H	-0.1920952330	-2.2087945654	0.6196507795
C	0.1087394819	-0.3673148449	-0.2299481745
H	0.1822485865	-0.8359040800	-1.2118979767
C	1.2271322742	0.6517182036	-0.1007427416
C	-1.2079918700	0.4050165480	-0.1725117618
H	1.1091822363	1.1934842242	0.8427161573
H	1.1539005815	1.3569662963	-0.9282886058
O	2.4495727756	-0.0754554409	-0.1216849157
O	-1.6121283573	1.0800437318	-1.0878420672
H	3.1677330930	0.5466253249	0.0231511042
O	-1.8341499530	0.3005359073	1.0069106372
H	-1.2622861257	-0.3174596577	1.5168157980
H	1.1665293173	-1.4623766002	1.1097325511

7 T T G^- T A^-:G^+ ENERGY=-398.30008361

N	0.0381178604	1.3434873503	-0.7244744840
H	-0.3836541470	2.1768708273	-0.3349753569
C	0.0791880739	0.2657409298	0.2597910766
H	0.1703824212	0.6084815739	1.2928302795

C	1.2586400341	-0.6481540721	-0.0658270968
C	-1.1841444101	-0.5857956012	0.1701270282
H	1.1311929066	-1.0452400463	-1.0723730637
H	1.2721933416	-1.4802021782	0.6373199736
O	2.4853253535	0.0669903377	-0.0839682685
O	-1.4961191046	-1.3838860311	1.0205082312
H	2.7385184916	0.2368160181	0.8283769410
O	-1.8695962367	-0.4028592383	-0.9658068482
H	-1.3739404816	0.3138466519	-1.4223317328
H	0.9878608971	1.5842774780	-0.9854186792

8 C T G^- T G^- ENERGY=-398.29932600

N	-0.7196200942	1.4717264889	0.3976495477
H	-0.3402545745	1.3102732977	1.3232289460
C	-0.3555639958	0.3669166861	-0.4790513831
H	-0.5333072694	0.6620812115	-1.5113524328
C	-1.2981565666	-0.7998492275	-0.1629726392
C	1.0682759814	-0.1362348623	-0.3992320506
H	-1.0760982852	-1.1648600539	0.8477934533
H	-1.1334387652	-1.6127567078	-0.8662238985
O	-2.6358875339	-0.3790891911	-0.2782343572
O	1.6287483600	-0.7543978864	-1.2735703085
H	-2.6411066163	0.5030768149	0.1212757423
O	1.6418510432	0.1269262900	0.8014059706
H	2.5180348736	-0.2861743813	0.7634478394
H	-0.3157465569	2.3384075213	0.0684775706

9 T T G^- T A^+:T ENERGY=-398.29879438

N	-0.1253056844	1.1064316220	1.0640373268
H	-0.4578478415	0.5216001978	1.8239008930
C	-0.1014905894	0.3283163167	-0.1754516045
H	-0.1148654316	1.0378910404	-1.0052189934
C	-1.2685866041	-0.6202365064	-0.3514128111
C	1.2242152137	-0.4247402278	-0.2807317618
H	-1.2592534197	-1.3579903226	0.4585125061
H	-1.1612736734	-1.1507931255	-1.2965320676
O	-2.4441172903	0.1787839629	-0.3091022099
O	1.3949845199	-1.3661885038	-1.0173879144
H	-3.1941304487	-0.3894722964	-0.5029368252
O	2.1848664874	0.0796973687	0.5039153197
H	1.7305758067	0.7953615474	1.0007722882
H	-0.7970950447	1.8581309267	0.9806038541

10 C C G^+ G^- A^+:G^+ ENERGY=-398.29864110

N	-1.0694225774	-1.6598836014	0.0123572161
H	-1.2945498294	-1.3729497406	-0.9346751109
C	-0.4472404231	-0.5278809975	0.6706413435
H	-0.3658128514	-0.7315904011	1.7430130280
C	-1.3199676807	0.7069328492	0.4943011805
C	0.9707340103	-0.2706375890	0.1854999531
H	-0.9778597063	1.5144146123	1.1397082792
H	-2.3368628717	0.4384146036	0.7692305032

O	-1.3646042767	1.1131090823	-0.8684243644
O	1.6565067178	-1.0615708443	-0.4162271755
H	-0.5689292563	1.6279340631	-1.0339628055
O	1.4133735618	0.9693610035	0.5249039494
H	2.3323000281	1.0076843254	0.2176141973
H	-0.3862188450	-2.4019443655	-0.0852051938

11 C C G^+ G^- A^-:G^+ ENERGY=-398.29848811

N	-1.0125746800	-1.6916058167	0.0411622082
H	-0.3177086831	-2.4287318951	0.0435206088
C	-0.4602466507	-0.5203006991	0.6899263710
H	-0.4316713293	-0.6778225586	1.7707876962
C	-1.3581874863	0.6737613873	0.4262935402
C	0.9644735959	-0.2034598776	0.2604125131
H	-1.0057639261	1.5370491983	0.9905613045
H	-2.3698421095	0.4137336136	0.7418533263
O	-1.2987724714	0.9119840019	-0.9765012301
O	1.6277496771	-0.8641867502	-0.5020789636
H	-1.9180392988	1.6149246179	-1.1885922792
O	1.4337222902	0.9096487170	0.8739590410
H	2.3398621390	1.0209808024	0.5495847752
H	-1.1485690670	-1.4583257410	-0.9363589118

12 C A^- T G^+ A^+:G^+ ENERGY=-398.29840641

N	-0.1263783761	-2.0205328094	0.3161373534
H	-1.0646698840	-2.3086547024	0.0690538459
C	0.1708988224	-0.7203989291	-0.2772674748
H	0.0817192061	-0.8094120099	-1.3605986578
C	1.5993198941	-0.3263786181	0.0642331035
C	-0.7914321450	0.3648704891	0.1659858396
H	2.2620782192	-1.1010352683	-0.3114782136
H	1.7069665872	-0.2870027458	1.1533612614
O	1.9828980791	0.8908481937	-0.5397963829
O	-0.4967320191	1.3814513832	0.7608133411
H	1.4554039982	1.5713241895	-0.1058603286
O	-2.0677894241	0.0592360616	-0.1540795396
H	-2.6073855372	0.7927776287	0.1783529460
H	-0.1050204208	-1.9458328629	1.3268719064

13 C T G^+ G^- C:G^- ENERGY=-398.29812659

N	0.8233231766	1.6615994225	-0.0925285020
H	0.0378487428	2.2424923954	-0.3505313539
C	0.3866870478	0.4988177318	0.6760094313
H	0.2032213592	0.7023563710	1.7361413797
C	1.4734032755	-0.5673361899	0.5538254389
C	-0.9049237726	-0.0904578054	0.1496930889
H	1.1438604677	-1.4888484074	1.0261884754
H	2.3736232841	-0.2089295777	1.0651363170
O	1.7222661293	-0.8373746464	-0.8078417517
O	-1.4031157215	-1.0996965406	0.5861743672
H	1.7392183307	0.0383433764	-1.2218718443
O	-1.4627819858	0.6398566511	-0.8420663087

H	-2.2726062098	0.1646782635	-1.0831188059
H	1.4510578759	2.2246939557	0.4665630680

14 C A^- G^+ G^- A^+ ENERGY=-398.29802004

N	-0.3555160073	1.6179447904	0.8131896400
H	-0.9416004714	1.1446530958	1.4937441556
C	-0.2493532280	0.7381259549	-0.3516249305
H	0.0668453749	1.3301519263	-1.2093867242
C	-1.5377721029	-0.0140159866	-0.6784667135
C	0.8560831187	-0.2488642532	-0.0397731871
H	-1.3704366864	-0.6999471239	-1.5150410478
H	-2.2988817559	0.7053409935	-0.9776152909
O	-2.0459466737	-0.6918050015	0.4552200051
O	0.6868322723	-1.3363139239	0.4778921967
H	-1.3523984113	-1.3172465018	0.7068955139
O	2.0710140754	0.2120251760	-0.3765090806
H	2.7015167915	-0.4643357239	-0.0838633240
H	-0.8528702958	2.4587085780	0.5474487872

15 T G^+ G^+ G^- C ENERGY=-398.29797489

N	-0.5365821641	-1.3552670370	-0.6469216737
H	-1.2024387606	-2.0686939811	-0.3718610856
C	-0.1565078478	-0.5597517677	0.5311548806
H	0.0367103998	-1.1616650883	1.4213453910
C	-1.3017843945	0.4066239002	0.7944880247
C	1.1684350024	0.1311501930	0.1996369078
H	-1.0504886628	1.1148249452	1.5809386988
H	-2.1902338114	-0.1502080570	1.1024535085
O	-1.5717716196	1.1650503105	-0.3846063248
O	2.2254910626	-0.4191099531	0.3985942242
H	-1.5883473997	0.4947463725	-1.0884081468
O	1.0924639952	1.3523427543	-0.3459184272
H	0.1438198430	1.5595032112	-0.4921355969
H	0.2750843576	-1.8473558028	-1.0021623803

16 C A^- T G^+ A^+:G^- ENERGY=-398.29790774

N	0.2178583358	-2.0043705973	-0.3021432599
H	-0.3344769069	-2.7779204696	0.0465183255
C	-0.2597178897	-0.7664268617	0.3054883108
H	-0.2976716958	-0.7810998064	1.4030658182
C	-1.6610902013	-0.4569693208	-0.2052461892
C	0.6768832574	0.3630442322	-0.0551144441
H	-2.3033558161	-1.3100760931	0.0097419773
H	-1.6176886214	-0.3339776295	-1.2898892654
O	-2.2356723253	0.6590139153	0.4399650124
O	0.3401032548	1.4696891574	-0.4188759550
H	-1.6906528752	1.4105187087	0.1774020945
O	1.9707842268	0.0163968422	0.1062069477
H	2.4872677937	0.8009109717	-0.1336792992
H	1.1747084629	-2.1795710492	-0.0238820737

17 T T G^- T A^-:T ENERGY=-398.29763325

N	-0.1561979158	-1.2540280834	-0.9737547345
H	-0.8222431453	-1.9777594832	-0.7385788102
C	-0.1170133257	-0.2471981707	0.0881546811
H	-0.1352717094	-0.7773462160	1.0435805452
C	-1.2712426976	0.7440739641	0.0573805232
C	1.2239556746	0.4874816972	0.0507757432
H	-1.2682942827	1.2638157549	-0.9016237929
H	-1.1380126396	1.4902526669	0.8388508184
O	-2.5237620148	0.0780618908	0.1475127061
O	1.4194639689	1.5301579593	0.6279763741
H	-2.7067604434	-0.0718234123	1.0788694958
O	2.1630741170	-0.1483676113	-0.6605871470
H	1.6950100364	-0.9360809383	-1.0156001921
H	-0.5040716226	-0.8289780180	-1.8273312105

18 T C T A^+ C ENERGY=-398.29721060

N	-0.1264336723	2.0295144869	-0.2575972479
H	0.1927557720	2.6863962109	0.4397869510
C	0.1436420007	0.6653396913	0.1590027592
H	0.3374256295	0.5622175205	1.2334440958
C	1.3838461026	0.1712054224	-0.5748227585
C	-1.0823229328	-0.2020639697	-0.1268513971
H	2.1845771273	0.8955546196	-0.4288565516
H	1.1685769891	0.0975181689	-1.6420333098
O	1.7489458209	-1.1025954381	-0.0225338554
O	-2.1730682047	0.2677622631	-0.3478020995
H	2.4305874514	-1.4937604436	-0.5765973755
O	-0.8772848542	-1.5259290618	-0.0894007747
H	0.0817905297	-1.6785009962	0.0325248664
H	-1.1325797590	2.1308925258	-0.3377033024

19 C C T G^+ T ENERGY=-398.29704936

N	0.2255830387	2.0479034498	-0.0942266937
H	0.4330669705	2.2242537908	0.8828120074
C	-0.1208007138	0.6484082448	-0.2502998018
H	-0.1912947288	0.4039431217	-1.3104162053
C	-1.5106616894	0.4063535748	0.3582003624
C	0.8890198678	-0.2849413187	0.3883077798
H	-2.1514446830	1.2062442217	-0.0014787473
H	-1.4424818452	0.4943939584	1.4495239511
O	-2.1067084521	-0.8105541545	-0.0336648660
O	1.8165544137	0.0485870487	1.0859232988
H	-1.4746154241	-1.5130576184	0.1510955877
O	0.6123969614	-1.5927052954	0.1222937123
H	1.2841077855	-2.1046424929	0.5994374099
H	1.0945874986	2.2357514692	-0.5790217952

20 C T G^+ G^- A^-:G^+ ENERGY=-398.29700669

N	0.5956852655	1.7351557574	0.2750806287
H	-0.2163898631	2.3370137826	0.3105939388
C	0.2435604173	0.3995145105	0.7126420982
H	0.0606431880	0.4067191213	1.7889817826

C	1.4108705733	-0.5350069846	0.4567207902
C	-0.9961496193	-0.2386363249	0.0955697712
H	1.1680239561	-1.5282788882	0.8343089656
H	2.2890280271	-0.1414350340	0.9706527746
O	1.6003547878	-0.5474566405	-0.9553304012
O	-1.4019205638	-1.3407593894	0.3847809378
H	2.3324242650	-1.1363604523	-1.1546365858
O	-1.6173516966	0.5622292271	-0.7978490661
H	-2.3766275231	0.0466498050	-1.1102037240
H	0.8674667858	1.6847275100	-0.6994419106

21 C C T G^+ A^+ ENERGY=-398.29688078

N	0.1336712117	-2.0288705011	-0.1575775608
H	-0.3111629985	-2.7324451863	0.4151703738
C	-0.2655317324	-0.7014217178	0.2774918875
H	-0.4378145723	-0.6029952066	1.3572369158
C	-1.5743117852	-0.3163631833	-0.4209929331
C	0.8596985342	0.2527698425	-0.0439491868
H	-2.2480622190	-1.1658216226	-0.3317110231
H	-1.3770940679	-0.1653503167	-1.4859826789
O	-2.2359057402	0.7829425263	0.1680650003
O	1.9993915245	-0.0616940542	-0.2894264788
H	-1.6413655271	1.5356942187	0.0911435045
O	0.4557373032	1.5502452212	-0.0118300280
H	1.2444467452	2.0753328857	-0.2169464848
H	1.1355933238	-2.1297819059	-0.0537523075

22 C A^+ G^+ G^- A^+:G^+ ENERGY=-398.29675512

N	0.5531389704	1.7173312537	-0.4573972958
H	-0.2541208079	2.2216900660	-0.7993682817
C	0.1693514308	0.7025564367	0.5078480960
H	-0.1346275198	1.1778969599	1.4396002919
C	1.3891863743	-0.1736568020	0.7985307642
C	-1.0056068183	-0.1657829926	0.1019375461
H	1.1207506902	-0.9517891551	1.5185985154
H	2.1536931945	0.4614253503	1.2393280114
O	1.9638851707	-0.7194617499	-0.3754213593
O	-2.0168452246	-0.3364387987	0.7401543294
H	1.2813570285	-1.2414825501	-0.8116925036
O	-0.7971494658	-0.7786054485	-1.1013715895
H	-1.5939269124	-1.3082890041	-1.2601079239
H	0.9946658893	1.2658084343	-1.2487896006

23 C A^+ G^+ G^- A^+:G^+ ENERGY=-398.29675512

N	0.5531389704	1.7173312537	-0.4573972958
H	-0.2541208079	2.2216900660	-0.7993682817
C	0.1693514308	0.7025564367	0.5078480960
H	-0.1346275198	1.1778969599	1.4396002919
C	1.3891863743	-0.1736568020	0.7985307642
C	-1.0056068183	-0.1657829926	0.1019375461
H	1.1207506902	-0.9517891551	1.5185985154
H	2.1536931945	0.4614253503	1.2393280114

O	1.9638851707	-0.7194617499	-0.3754213593
O	-2.0168452246	-0.3364387987	0.7401543294
H	1.2813570285	-1.2414825501	-0.8116925036
O	-0.7971494658	-0.7786054485	-1.1013715895
H	-1.5939269124	-1.3082890041	-1.2601079239
H	0.9946658893	1.2658084343	-1.2487896006

24 C C G^- T A^- ENERGY=-398.29664346

N	-0.5149053071	1.6005311348	-0.3768074612
H	-1.5119837253	1.7146610181	-0.2383156209
C	-0.2180048629	0.1819857203	-0.3967846509
H	-0.3323815742	-0.2082720778	-1.4107368547
C	-1.1141294643	-0.6468104403	0.5350320987
C	1.2102792022	-0.0382103299	0.0273260448
H	-0.9646039526	-0.3094177991	1.5601656137
H	-0.8562553792	-1.7063345729	0.4716877483
O	-2.4860094128	-0.4224083460	0.2483740895
O	1.8469825517	0.7083656477	0.7336394366
H	-2.6856742250	-0.8654175998	-0.5819666802
O	1.6882193849	-1.2192182207	-0.4250612895
H	2.5822366853	-1.2974246229	-0.0584836455
H	-0.0433569206	2.0142634885	0.4195421713

25 T C T G^+ A^-:G^- ENERGY=-398.29640250

N	-0.0327530479	-1.7016174718	-1.0922597080
H	-0.3945801311	-2.6161932276	-0.8633961654
C	-0.1220375319	-0.8070258972	0.0463552450
H	-0.1937497671	-1.3298658551	1.0102725940
C	-1.3665096351	0.0651470829	-0.1120224509
C	1.1580119981	0.0255820448	0.1304551961
H	-2.2334484867	-0.5728602178	-0.2796314741
H	-1.2506024765	0.7100729211	-0.9794766001
O	-1.5776209896	0.9303799309	1.0142859042
O	2.1805453992	-0.3031841365	-0.4220188647
H	-1.9559429484	0.4062195359	1.7273209446
O	1.0836838500	1.1316304988	0.8828200835
H	0.1527070683	1.2464177379	1.1655020350
H	0.9488106988	-1.8066819463	-1.3255457391

26 T T G^- T C:T ENERGY=-398.29630965

N	-0.0534122402	1.5233879176	-0.1859995174
H	0.5881215209	2.1952931130	0.2110436877
C	0.0984734156	0.2071051725	0.4388638195
H	0.2949600357	0.3716197127	1.4996889502
C	1.2295068001	-0.6431005010	-0.1198055729
C	-1.2266357722	-0.5534455084	0.3630401507
H	1.0455936144	-0.8418145134	-1.1811646061
H	1.2470061022	-1.5976357697	0.3960451927
O	2.4947180163	-0.0353348113	0.0851052940
O	-1.3117036680	-1.7441689362	0.5412155125
H	2.5703505295	0.7004669188	-0.5279759042
O	-2.2846563231	0.2275466395	0.1041771486

H	-1.8971537191	1.1203291967	-0.0163398864
H	0.1254526879	1.4751313691	-1.1828792690

27 C C G^- T A^+:T ENERGY=-398.29629756

N	-0.8463339454	-1.5829040388	-0.6750309470
H	-1.8574013621	-1.5820469465	-0.6220012024
C	-0.3396722274	-0.5994598730	0.2613923549
H	-0.3124729758	-1.0247540895	1.2648530745
C	-1.1685525562	0.6831801051	0.3290365271
C	1.0623888084	-0.2160131612	-0.1366083346
H	-1.1631276526	1.1590049095	-0.6566197168
H	-0.7385402581	1.3700919039	1.0618205849
O	-2.4801308061	0.2815323492	0.7004875593
O	1.5022657443	-0.2711549343	-1.2614156521
H	-3.0520994190	1.0519724553	0.6517921915
O	1.7687214970	0.2617430889	0.9121299717
H	2.6282119481	0.5250029636	0.5492469229
H	-0.5819017951	-1.3025017323	-1.6124323339

28 C G^- T G^+ A^-:G^+ ENERGY=-398.29622425

N	0.2591933669	2.0162003677	0.3089190321
H	-0.2864610367	2.1877285724	-0.5295083418
C	0.4192141852	0.5780586373	0.4514387526
H	0.7705763306	0.3519847134	1.4578254927
C	1.4664897467	0.1240290625	-0.5670446402
C	-0.8549441329	-0.1985414783	0.1897890906
H	2.4080855731	0.6219149915	-0.3300942551
H	1.1453841725	0.4536849950	-1.5543256218
O	1.5985514970	-1.2829227340	-0.6509650321
O	-1.6550688539	0.0849336908	-0.6722236085
H	1.8849470826	-1.6057440452	0.2086164986
O	-0.9965028511	-1.2554033022	1.0180228826
H	-1.8010878810	-1.7118100567	0.7267964820
H	-0.2930991989	2.3790735858	1.0758362679

29 C C G^+ G^- C ENERGY=-398.29606412

N	-0.4713510126	-1.6731330001	-1.0828108382
H	-1.4495173034	-1.9124509859	-1.1641249282
C	-0.1875888127	-0.9664862346	0.1526670709
H	0.0733435565	-1.6732877212	0.9433685415
C	-1.3426876237	-0.1020700318	0.6644515080
C	1.0059589759	-0.0704220175	-0.0790498427
H	-1.0829284210	0.3381820720	1.6241264543
H	-2.2148043727	-0.7494305860	0.8068976163
O	-1.6323877168	0.9753593009	-0.2054520465
O	1.4402613487	0.2425340425	-1.1624479282
H	-1.7305173667	0.6065352200	-1.0899645455
O	1.5178048896	0.3756121964	1.0866566776
H	2.2349657143	0.9805063984	0.8443182587
H	-0.1851678554	-1.1149336532	-1.8766739981

30 T C T G^+ A^-:G^+ ENERGY=-398.29605370

N	-0.1084723783	2.0417367690	0.1818035761
H	-0.9112117784	2.3353478204	0.7269769148
C	0.1388571311	0.6402680289	0.4663062541
H	0.4307847348	0.5540902904	1.5178335113
C	1.3243302427	0.1766013101	-0.3758995639
C	-1.0991136113	-0.2483966439	0.2879409414
H	2.1321309464	0.8978024872	-0.2675067094
H	1.0453902847	0.1303320869	-1.4279777376
O	1.7568123264	-1.1453355160	-0.0283401159
O	-2.2136249103	0.2077499416	0.2033480121
H	2.2944200547	-1.0794184342	0.7672917058
O	-0.8731369784	-1.5730501628	0.2627164091
H	0.0950268254	-1.7138943760	0.2525502256
H	-0.4262028894	2.1206823984	-0.7790324236

31 C C A^- G^+ T ENERGY=-398.29601944

N	-0.0766696061	1.9309548226	-0.2647216131
H	0.5256678102	2.0903089544	0.5334407525
C	-0.3160009833	0.5085360528	-0.4097563247
H	-0.6108797552	0.2707974398	-1.4326830633
C	-1.4116873954	-0.0411237143	0.5244941857
C	0.9699212816	-0.2143945643	-0.1038164161
H	-2.2804924918	0.6081346303	0.4246531999
H	-1.0597081111	0.0298317127	1.5604556668
O	-1.8507802785	-1.3412392836	0.1962018631
O	1.9079485484	0.2414243071	0.5041466256
H	-1.0673286583	-1.8921576956	0.0930828239
O	0.9314848191	-1.5055566922	-0.5315250195
H	1.7691028987	-1.9003507829	-0.2423769671
H	-0.9473390783	2.4201758133	-0.1058307134

32 T T G^+ G^- CENERGY=-398.29589590

N	0.6061369509	1.2295312606	-0.6039360014
H	0.0018677063	2.0303173057	-0.7475753633
C	0.1525595954	0.4421079830	0.5469954202
H	-0.1011354009	1.0368940982	1.4267241578
C	1.2524928231	-0.5393541733	0.9344314464
C	-1.0961962070	-0.3557559165	0.1794376208
H	0.9064915894	-1.1445561681	1.7679793536
H	2.1330777368	0.0269149390	1.2594923841
O	1.5698986845	-1.4329813081	-0.1140504690
O	-1.8058877963	-0.8591815382	1.0129064337
H	1.7736306279	-0.9020503218	-0.8909793577
O	-1.3263402449	-0.4632881016	-1.1392610881
H	-0.5835285932	0.0012147398	-1.5673618778
H	1.5318245280	1.6031342013	-0.4270146593

33 C A^- G^- T A^+:G^- ENERGY=-398.29581779

N	0.2449137843	1.5701417123	-0.3789088615
H	1.1708606421	1.9590371122	-0.2462547423
C	0.2064223998	0.2879519927	0.3176769074
H	0.3310731949	0.3730391560	1.4057092532

C	1.3152372679	-0.5935330675	-0.2095308388
C	-1.1337002256	-0.3647687070	0.0814650933
H	1.2024831713	-0.6907954852	-1.2905185733
H	1.2508730663	-1.5821312741	0.2451096989
O	2.5316052206	0.0650655190	0.1324849929
O	-1.3180384981	-1.4915034673	-0.3156660895
H	3.2496428538	-0.3960944596	-0.3079162649
O	-2.1439142459	0.4780327396	0.3981836397
H	-2.9595921414	-0.0111541200	0.2130397869
H	-0.4167584900	2.2098233490	0.0414589980

34 C T T A^+ T ENERGY=-398.29576011

N	-0.2071525472	1.6674360922	-0.7121370503
H	0.5630681895	2.3071986746	-0.8615046481
C	0.2212486704	0.6002969644	0.1732795718
H	0.3995942004	1.0086875259	1.1688708266
C	1.5154850657	-0.1173971537	-0.2568194675
C	-0.8356919580	-0.4630948795	0.3335386107
H	2.2658071225	0.6465353152	-0.4577407238
H	1.3256323091	-0.6518150067	-1.1967922956
O	2.0424165807	-0.9633511330	0.7371602013
O	-0.7296209881	-1.3979008509	1.1040998879
H	1.2983398961	-1.4766470545	1.0812573694
O	-1.8755272619	-0.3351280778	-0.5084612820
H	-2.4406377109	-1.1046944332	-0.3366749200
H	-0.4640735682	1.2931230170	-1.6167200804

35 C A^- T G^+ A^+:T ENERGY=-398.29564341

N	0.0387225048	-1.8862217969	-0.3025228619
H	-0.0031361559	-1.8223751051	-1.3135584815
C	-0.3243875386	-0.5988177638	0.2826506307
H	-0.4457611804	-0.7374642874	1.3574993598
C	-1.5954194493	0.0145745878	-0.2927814074
C	0.8340331794	0.3622375247	0.0980276767
H	-2.4239340638	-0.6658887709	-0.1013897464
H	-1.4797845901	0.1092078603	-1.3772427165
O	-1.9306679647	1.2492980538	0.3059950722
O	0.7906690987	1.3721960686	-0.5767734928
H	-1.2581843763	1.8705472523	0.0037952775
O	1.9312226077	-0.0178320175	0.7699482155
H	2.6020641223	0.6555957719	0.5791824181
H	-0.6430371938	-2.5831393779	-0.0309469441

36 C G^- T G^+ C:G^+ ENERGY=-398.29563393

N	-0.1032479826	1.7982473995	0.8530160052
H	0.2445102094	1.4020025887	1.7201330494
C	-0.2752665592	0.7120315967	-0.1039083964
H	-0.4050970062	1.1216075174	-1.1028338327
C	-1.5232668128	-0.0608953954	0.2840482110
C	0.8939036983	-0.2538818466	-0.1015358801
H	-2.3728739221	0.6224237574	0.2506065260
H	-1.3964212707	-0.4191369956	1.3097145059

O	-1.6599337304	-1.1374992448	-0.6310600460
O	1.3537790986	-0.7423784705	0.9071391862
H	-2.3641166062	-1.7084034421	-0.3140403965
O	1.3830537761	-0.4972114498	-1.3325134531
H	2.0999916369	-1.1381157345	-1.2066965408
H	0.6161544707	2.4313077198	0.5266980619

37 C C G^- T A^+:G^- ENERGY=-398.29550649

N	-0.7355551648	-1.4691175096	-0.5466483951
H	-0.0768405986	-2.2244322030	-0.4099427810
C	-0.3275783658	-0.3144318755	0.2297309938
H	-0.3947167886	-0.4521782240	1.3192140108
C	-1.2226838000	0.8596739138	-0.1173238469
C	1.1310296310	-0.0399915732	-0.0470559810
H	-1.1781038944	1.0237088351	-1.1962637822
H	-0.8910324342	1.7570870970	0.4041796894
O	-2.5310043239	0.4755901974	0.2936935561
O	1.9121693068	-0.8446226630	-0.4955055872
H	-3.1516997137	1.1180064267	-0.0590735575
O	1.4941225759	1.2128317248	0.3169090385
H	2.4463958166	1.2628919761	0.1432612349
H	-1.6466742465	-1.7701391227	-0.2288865926

38 C G^+ T G^+ A^+ ENERGY=-398.29532066

N	-0.0119908947	1.8999693206	0.4423748999
H	0.2557435579	1.6585702462	1.3898673300
C	-0.3006078247	0.6822846588	-0.3138492623
H	-0.4711675610	0.9569032946	-1.3527657897
C	-1.5569170552	0.0422302388	0.2541638990
C	0.8895373432	-0.2552350089	-0.3163276994
H	-2.3903415829	0.7161647727	0.0749291255
H	-1.4468495634	-0.0765043623	1.3352395503
O	-1.8663597578	-1.1875597389	-0.3763993321
O	1.8179944952	-0.2051251618	-1.0870763083
H	-1.2597071734	-1.8411397147	-0.0156978853
O	0.8515497920	-1.1410975267	0.7208357747
H	1.6834895298	-1.6363882427	0.6651407360
H	0.7748726949	2.3859672241	0.0297119617

39 C A^+ G^+ G^- A^+:T ENERGY=-398.29523193

N	-0.4905323129	-1.6619917254	-0.3651944719
H	-1.1281708372	-2.2789139397	0.1237682444
C	-0.1735029172	-0.5345301791	0.5051683212
H	0.1278254749	-0.9098632742	1.4810470120
C	-1.3284423442	0.4594955753	0.6944012680
C	1.0410396304	0.1808752863	-0.0392153519
H	-0.9870912589	1.3236589040	1.2737855175
H	-2.1156715459	-0.0353973672	1.2611192886
O	-1.9197146385	0.8495604194	-0.5313313684
O	2.0771039854	0.3798901337	0.5447644172
H	-1.2228105210	1.2407118791	-1.0704030916
O	0.8172846988	0.6377251321	-1.3056832793

H	1.6417245783	1.0715032870	-1.5748921035
H	-1.0047489919	-1.3067271313	-1.1640034021

40 T A^+ G^+ G^- C:G^+ NERGY=-398.29522664

N	0.2748871150	-1.4923991861	0.7607900122
H	-0.3897627388	-2.2561522215	0.7696857865
C	0.0909221475	-0.7047386650	-0.4702341849
H	-0.1356255540	-1.3858032111	-1.2871680068
C	1.3983423880	0.0122611741	-0.7703385177
C	-1.0932709382	0.2470709596	-0.3470693854
H	1.2896976565	0.7026599958	-1.6042343111
H	2.1633873598	-0.7242668306	-1.0134053258
O	1.8088236234	0.8023628114	0.3528575290
O	-2.1864586273	0.0115073225	-0.8000631790
H	2.0849593157	0.1725652711	1.0295950121
O	-0.8522795834	1.3618815861	0.3776713970
H	0.1051476118	1.3947133695	0.5767279955
H	0.0360802239	-0.9234093759	1.5654731783

41 C A^- G^- T C ENERGY=-398.29522335

N	0.3387357319	1.6010727543	-0.1948153638
H	1.0046746598	2.1377488240	0.3457327985
C	0.2189381898	0.2702108199	0.3989977039
H	0.3064646398	0.2860534181	1.4927251159
C	1.3231551621	-0.6214698245	-0.1575667258
C	-1.1241267665	-0.3544735581	0.1109675603
H	1.1131542370	-0.8282184449	-1.2090303489
H	1.3553514915	-1.5650286893	0.3785767953
O	2.5874447852	-0.0019047004	0.0047976566
O	-1.3150640375	-1.5369647407	-0.0484771292
H	2.5977002887	0.7360636534	-0.6133468553
O	-2.1251190177	0.5587400988	0.0893248916
H	-2.9335984990	0.0515165982	-0.0796407559
H	-0.5447438652	2.0884537910	-0.1245303434

42 C A^+ T G^+ A^- ENERGY=-398.29519168

N	0.2030928327	1.8568046319	0.5597511649
H	0.4001290779	1.5622845048	1.5090333367
C	-0.1508844771	0.6903195715	-0.2379157186
H	-0.1962082330	0.9843562975	-1.2861470220
C	-1.5239096290	0.2006992316	0.2129920715
C	0.8338484111	-0.4586812957	-0.1684806989
H	-2.2508833944	0.9912009565	0.0190801508
H	-1.4976641736	0.0174719254	1.2858173489
O	-1.8862012494	-1.0324619510	-0.3820793601
O	1.3565997195	-1.0004601698	-1.1136536605
H	-1.9372959392	-0.8991953407	-1.3334811656
O	1.0746584826	-0.8173749821	1.1168787560
H	1.6857492380	-1.5675066557	1.0687519300
H	1.0541393339	2.2763362758	0.2073048669

43 C C G^- T C ENERGY=-398.29494606

N	-0.7563000881	-1.4431316384	0.6369498296
H	-1.7544152252	-1.4442491834	0.7993275975
C	-0.2690536793	-0.0785800432	0.5942633182
H	-0.2772421809	0.3385055508	1.6005095391
C	-1.0715479358	0.8664905803	-0.3140496246
C	1.1456833735	-0.0905507646	0.0782171153
H	-0.9675475279	0.5374987417	-1.3520952855
H	-0.6799949432	1.8788798629	-0.2305829021
O	-2.4342710308	0.9172969259	0.0765714224
O	1.5943369471	-0.9144347247	-0.6850223839
H	-2.8916487142	0.2001321134	-0.3687204000
O	1.8459602951	0.9819190663	0.5083718561
H	2.7119909103	0.9192718763	0.0770675900
H	-0.5659192003	-1.8996473633	-0.2471126722

44 C A^- G^- T A^- ENERGY=-398.29480285

N	-0.2427202350	1.6844611586	0.2831570203
H	-1.1870312754	2.0264556930	0.1500084943
C	-0.1979124922	0.3100424408	-0.1991313244
H	-0.3255442422	0.2181027957	-1.2888174391
C	-1.3001148212	-0.4817587005	0.4814084648
C	1.1522807126	-0.2860329077	0.1208861005
H	-1.1820703472	-0.3934183147	1.5583427833
H	-1.2331022596	-1.5350099689	0.2114274649
O	-2.5764381789	0.0682095840	0.1711073798
O	1.3493354510	-1.3352735354	0.6877516927
H	-2.8061335679	-0.2158565206	-0.7181218283
O	2.1515738473	0.5035224250	-0.3365384099
H	2.9739717790	0.0572865340	-0.0842291175
H	0.3785596296	2.2693503167	-0.2598812815

45 C C G^+ G^- A^-:T ENERGY=-398.29475480

N	-0.7300247551	-1.6984883344	0.3156881559
H	-1.7082245633	-1.7991153043	0.5554626710
C	-0.2648450461	-0.3850150140	0.7173931859
H	-0.0232212837	-0.3861159399	1.7823238504
C	-1.2479943560	0.7577081444	0.4778871666
C	1.0115009379	-0.0804030596	-0.0351655249
H	-0.8320095929	1.6868451343	0.8731311973
H	-2.1748151316	0.5316525969	1.0145862499
O	-1.4670681469	0.8349797352	-0.9223697030
O	1.4250916497	-0.6840993174	-0.9935010581
H	-2.0411698858	1.5858455617	-1.0936349565
O	1.6411442413	0.9971986982	0.4930784085
H	2.4178531110	1.1404906299	-0.0679648346
H	-0.6637761785	-1.7630025311	-0.6931738081

46 T A^+ A^+ A^- A^- ENERGY=-398.29473976

N	-0.2054423254	1.5717915081	0.8298058211
H	0.6798055415	2.0153726303	1.0444059838
C	-0.0455720485	0.7156076259	-0.3456715473
H	0.1979291531	1.3505044048	-1.1957945963

C	-1.3693927479	0.0395892292	-0.6364955225
C	1.1337926200	-0.2487367706	-0.2003782526
H	-1.2921046143	-0.5768852190	-1.5340020550
H	-2.1260468805	0.8100962524	-0.7807274167
O	-1.6991331760	-0.7691593949	0.5042658872
O	2.2393576287	0.0263846892	-0.6016537902
H	-2.5300258108	-1.2218039684	0.3349073094
O	0.8957568747	-1.3948125036	0.4692284844
H	-0.0584154162	-1.4335653181	0.6706885179
H	-0.4501227984	1.0006158347	1.6301021766

47 C G^- T G^+ A^-:T ENERGY=-398.29467769

N	0.0099983362	-2.0996590219	-0.5029753747
H	-0.8450795776	-2.6393617477	-0.4466057570
C	-0.1450724852	-0.8467938512	0.2207949581
H	-0.0686563263	-1.0326384126	1.2925876345
C	-1.4671808097	-0.1328526444	-0.0821544711
C	0.9806152824	0.0695635453	-0.1932883336
H	-2.2890989310	-0.7979232436	0.2030937157
H	-1.5253857979	0.0381824725	-1.1561630783
O	-1.5824980169	1.1393188916	0.5269170290
O	1.3513305050	0.2040291440	-1.3366385455
H	-1.4837415348	1.0243607371	1.4770121237
O	1.5050663183	0.7466348336	0.8463850785
H	2.1679343667	1.3421946678	0.4637949086
H	0.1672226710	-1.8827303705	-1.4810468879

48 C C A^- T A^- ENERGY=-398.29463001

N	-0.4730756216	1.4959418577	0.6543456618
H	-1.3931830361	1.8557604465	0.4406592083
C	-0.2130437969	0.3396162682	-0.1759288966
H	-0.3046166263	0.5209780039	-1.2594971372
C	-1.2104813508	-0.7556873399	0.1839962281
C	1.2209291771	-0.0918602959	0.0229980981
H	-1.1442824060	-0.9467804333	1.2529289737
H	-0.9879080728	-1.6729516427	-0.3593777207
O	-2.5410608222	-0.3124654729	-0.0560396138
O	2.0902539900	0.5830788928	0.5189449085
H	-2.6999087542	-0.3797658052	-1.0019070091
O	1.4442306159	-1.3324933811	-0.4750410523
H	2.3896130379	-1.4970151866	-0.3388093272
H	0.2125056660	2.2185340885	0.4816556784

49 C A^+ G^- T A^- ENERGY=-398.29461103

N	0.2787924577	1.4475112680	-0.7042041919
H	1.2611878505	1.6796416998	-0.8014102974
C	0.1745156804	0.4151156834	0.3142456703
H	0.2896476176	0.8738629196	1.2971717755
C	1.2274480177	-0.6945172297	0.1831470858
C	-1.1813311127	-0.2426364111	0.3239052279
H	1.1114423273	-1.1856592370	-0.7823397984
H	1.0941475073	-1.4378792501	0.9728732938

O	2.5378607748	-0.1488803783	0.1906321139
O	-1.7286467534	-0.6840875563	1.3069829476
H	2.7427264607	0.0995409905	1.0970866944
O	-1.6944422859	-0.3646507130	-0.9232527644
H	-2.5366024015	-0.8315072148	-0.8130158119
H	-0.0150061405	1.0649664290	-1.5950779453

50 C A^+ T G^+ C:G^+ ENERGY=-398.29436849

N	-0.3898208656	-1.9001343359	0.3353950676
H	-0.5162788635	-1.6234547915	1.3020847413
C	0.0487913648	-0.7439022744	-0.4420860532
H	0.0025433945	-0.9912065895	-1.5001150134
C	1.4828775414	-0.4273854047	-0.0677001050
C	-0.8357997497	0.4706340950	-0.2476674468
H	2.0972905572	-1.2954164466	-0.3119435750
H	1.5382855175	-0.2495430933	1.0093946726
O	1.8598189542	0.7243973212	-0.8065085501
O	-1.5578710845	0.9655440335	-1.0794412903
H	2.7317071102	0.9969292485	-0.5102363577
O	-0.7727164199	0.9202091407	1.0337334773
H	-1.3820686751	1.6721953318	1.0722460456
H	-1.2941627815	-2.2133402347	0.0054193873

51 C A^+ G^- T A^+:T ENERGY=-398.29427632

N	-0.1991044316	-1.7623124623	-0.3657247102
H	-1.1388502369	-2.1274082350	-0.2631405260
C	-0.1728988652	-0.4438848725	0.2462426867
H	-0.2299634976	-0.5561449350	1.3277929079
C	-1.3206673905	0.4710476738	-0.1793347641
C	1.1186165642	0.2811924211	-0.0386564446
H	-1.2645515247	0.6391774588	-1.2593809439
H	-1.2379123456	1.4308896992	0.3367950560
O	-2.5153022846	-0.2109645623	0.1757175974
O	1.6574565367	1.0601375017	0.7116034728
H	-3.2598456023	0.3126113178	-0.1316650382
O	1.5829292365	0.0176249427	-1.2836850315
H	2.3878515909	0.5492151235	-1.3768522152
H	-0.0281047493	-1.6731590715	-1.3602180472

52 C G^- T G^+ C:T ENERGY=-398.29397350

N	0.2855047952	2.0098816704	0.6196559301
H	-0.4404467934	2.7128178223	0.5559344679
C	-0.0794932757	0.8461583547	-0.1793571217
H	-0.0280511472	1.0964651386	-1.2365491178
C	-1.4623163186	0.2975215608	0.1435659916
C	0.9346083732	-0.2329370617	0.1268023330
H	-2.2000048474	1.0866772159	-0.0319454089
H	-1.4818166292	0.0266402874	1.2028100379
O	-1.6885616103	-0.8261480186	-0.6926200908
O	1.1740781058	-0.6162969627	1.2501189951
H	-2.4889419267	-1.2654703829	-0.3940681132
O	1.5384997999	-0.7191606475	-0.9704763971

H	2.1430622307	-1.4073195616	-0.6519766446
H	0.3473712437	1.7265405849	1.5912101385

53 C T G^+ G^- A^-:T ENERGY=-398.29381843

N	-0.4454767164	-1.4269805662	-0.9326528329
H	-0.7186198590	-0.7483984557	-1.6334310983
C	-0.2260835228	-0.7336090584	0.3245116880
H	0.0605743369	-1.4608601980	1.0851541972
C	-1.4284909761	0.0397992152	0.8563521073
C	0.9265029224	0.2486095451	0.2432184770
H	-1.1630076300	0.5124725199	1.8036836819
H	-2.2534616568	-0.6595922039	1.0213666128
O	-1.7608908918	1.0025249731	-0.1356957523
O	1.3996012410	0.7943573041	1.2145490027
H	-2.4265545894	1.5906815336	0.2295287193
O	1.3485754947	0.4812375477	-1.0127449251
H	2.0462362592	1.1482811428	-0.9234208593
H	-1.2309804120	-2.0575492991	-0.8244650183

54 T C G^- T C ENERGY=-398.29378630

N	0.6551670434	1.4141952545	-0.8703699530
H	0.2936306050	2.3406975436	-0.6839927852
C	0.1938729573	0.4816992124	0.1454574961
H	0.2695226392	0.9617801221	1.1229624461
C	1.1553216452	-0.7138504656	0.1326320301
C	-1.2254889144	-0.0083425953	-0.0885224715
H	1.0387319830	-1.2352480935	-0.8248369320
H	0.9225256051	-1.4191829825	0.9291589048
O	2.4737785683	-0.2666979064	0.3283592375
O	-1.7986028967	0.0911871286	-1.1433281598
H	2.5406830265	0.5130635271	-0.2429333813
O	-1.8130716985	-0.6352741779	0.9606386428
H	-1.2211773374	-0.5980207561	1.7214232374
H	0.2443667741	1.1338061887	-1.7562943121

55 C A^+ T A^+ A^- ENERGY=-398.29330597

N	0.1771962442	-1.9388652124	-0.4826681145
H	-0.5753131359	-2.6167443767	-0.4708742964
C	-0.2419560406	-0.7328586184	0.2219981704
H	-0.3953137755	-0.9796125688	1.2723998858
C	-1.5125123874	-0.0956304718	-0.3457365799
C	0.8726762531	0.2855669896	0.1975302241
H	-2.3339503268	-0.8121993442	-0.2410337299
H	-1.3650614370	0.0971531335	-1.4070470116
O	-1.8224400773	1.1553988484	0.2394301793
O	1.3262361185	0.8598425142	1.1567529804
H	-1.8819925668	1.0333940738	1.1921971854
O	1.2939654316	0.5063775267	-1.0711932115
H	1.9869206953	1.1800993565	-1.0045110146
H	0.3574180045	-1.7129498504	-1.4536826671

56 C C G^+ G^- A^+:G^- ENERGY=-398.29325341

N	1.0279966441	1.6205943704	-0.1962792387
H	1.7768801492	2.0770330853	0.3058648681
C	0.4849821210	0.5325284858	0.5962622577
H	0.4339349378	0.7465409085	1.6751232134
C	1.3108182436	-0.7432918848	0.4325541514
C	-0.9524922884	0.3208560892	0.1808141241
H	1.0604655771	-1.4438270511	1.2319776152
H	2.3605441722	-0.4732742259	0.5339236377
O	1.1716418318	-1.3405224972	-0.8411692066
O	-1.6529211033	1.1435609921	-0.3569529578
H	0.3296288262	-1.8052998576	-0.8338366916
O	-1.4018529350	-0.9162475334	0.5165342356
H	-2.3357540662	-0.9288205893	0.2564172657
H	0.3036668899	2.3082247080	-0.3620282742

57 C T G^+ G^- C:T ENERGY=-398.29318949

N	0.6004228801	1.5680320932	-0.5318783102
H	1.4885831086	2.0081530087	-0.3282845134
C	0.2203717019	0.6627996348	0.5413705125
H	-0.1090641017	1.2488182115	1.4004799447
C	1.3319531619	-0.2731740676	1.0257769803
C	-0.9586870049	-0.2021317952	0.1552733351
H	0.9561319744	-0.8961867525	1.8342573211
H	2.1558463761	0.3370410814	1.4102506074
O	1.7715545472	-1.1573118452	0.0109307695
O	-1.6396990275	-0.8003124974	0.9542682026
H	2.1258777922	-0.6183261819	-0.7030410531
O	-1.1432579881	-0.2809025164	-1.1798276677
H	-1.8804976373	-0.8984478643	-1.2999838317
H	0.6759672170	1.0755564907	-1.4112202972

58 C A^+ G^- T C ENERGY=-398.29309100

N	-0.3233570914	-1.4183078292	-0.7347685218
H	-1.2449684954	-1.8316470262	-0.6749569038
C	-0.1784478829	-0.4183882467	0.3112459278
H	-0.2730450587	-0.9123667990	1.2761714813
C	-1.2056284625	0.7221698211	0.2638226144
C	1.1909025630	0.2113675539	0.2788682382
H	-1.0541378018	1.3080360424	-0.6478027746
H	-1.0633172968	1.3766034111	1.1220517037
O	-2.5309223237	0.2259162377	0.3442523611
O	1.8047787943	0.5928952243	1.2470079205
H	-2.7776807687	-0.0814284519	-0.5317225271
O	1.6317476672	0.3865766629	-0.9906493346
H	2.4890750921	0.8308902205	-0.9080384631
H	-0.2254639345	-0.9930398211	-1.6484717220

59 C C A^- T G^+ ENERGY=-398.29268376

N	-0.4526842632	1.7101111829	-0.3380658951
H	0.0614424242	2.0807719363	0.4543959690
C	-0.2392372887	0.2760097060	-0.3788252584
H	-0.4169942310	-0.0971799946	-1.3868386281

C	-1.2335904237	-0.4366459994	0.5329714528
C	1.1613856615	-0.1267204378	0.0413305659
H	-1.2440514706	0.0835272236	1.4953016404
H	-0.9109964811	-1.4684231347	0.6939768774
O	-2.4968043097	-0.3908742263	-0.1036418033
O	1.9097157926	0.5586367399	0.7005935131
H	-3.1654792178	-0.6062775406	0.5512142517
O	1.4796298177	-1.3727252468	-0.3769175045
H	2.3669396583	-1.5484874925	-0.0283261666
H	-0.0367496686	2.1395882841	-1.1545180145

60 T C G^+ G^- C:G^- ENERGY=-398.29255024

N	0.8341836442	-1.4076839312	-0.4773201174
H	1.2146837402	-1.7521227076	-1.3476230136
C	0.1362943271	-0.1448649517	-0.6747895616
H	-0.3012263139	-0.0299858838	-1.6746433379
C	1.1483715981	0.9722082660	-0.4321908387
C	-1.0328871036	-0.1052751694	0.3060258565
H	0.7104556090	1.9682299820	-0.5233236742
H	1.9227377252	0.9009475395	-1.2033489421
O	1.6858382564	0.8612731574	0.8625792738
O	-1.4572562677	-1.0877169691	0.8596776010
H	1.8748888812	-0.0855347214	0.9532844410
O	-1.6279109461	1.0920559009	0.4809410929
H	-1.1046712912	1.7732784878	0.0439807305
H	0.1755061411	-2.0904489994	-0.1207025103

61 C A^+ T G^+ A^+ ENERGY=-398.29246365

N	0.2539989533	-1.9649391694	-0.3380155989
H	-0.3838231544	-2.7134668615	-0.0969961701
C	-0.1710598939	-0.7300780891	0.3188123340
H	-0.2049205007	-0.8980037509	1.3925497741
C	-1.5242275578	-0.2133549120	-0.1676663683
C	0.9110070483	0.3012399978	0.0950634599
H	-2.2921456405	-0.9248687603	0.1335182361
H	-1.5145339511	-0.1689701367	-1.2595627098
O	-1.8792776453	1.0332709879	0.4050933952
O	1.6745842086	0.7361117281	0.9192777863
H	-1.4005994055	1.7174084545	-0.0719698259
O	0.9280223254	0.7004575442	-1.2085576676
H	1.6764150397	1.3120513826	-1.2820006753
H	0.2029681739	-1.8464584151	-1.3433089697

62 C A^+ T G^+ C:T ENERGY=-398.29214416

N	0.3198395281	1.9338139137	0.4113699565
H	-0.2930377464	2.7088595419	0.1906188686
C	-0.1171055195	0.7412557639	-0.3088499002
H	-0.0535987193	0.9291020046	-1.3781035755
C	-1.5301803704	0.2985382518	0.0422598444
C	0.8642466025	-0.3721244915	-0.0188636397
H	-2.2190854035	1.1083229930	-0.2179501033
H	-1.5866525636	0.1267775355	1.1203632605

O	-1.8052346530	-0.8822632820	-0.6932571124
O	1.5598123022	-0.9409411152	-0.8213099100
H	-2.6540104139	-1.2265146030	-0.4036821206
O	0.8789652728	-0.6572248428	1.3103882300
H	1.5387975874	-1.3584016971	1.4164502692
H	0.2480320966	1.7706040271	1.4085619326

63 T T G^+ G^- A^+:G^+ ENERGY=-398.29192453

N	-0.1701638376	1.6916113709	-0.4101173358
H	-0.5251669753	1.7999675576	0.5296238849
C	-0.1203132466	0.3068291581	-0.8244794647
H	0.0069819186	0.2512462943	-1.9059535077
C	-1.4539258230	-0.3435282693	-0.4695898109
C	0.9804001572	-0.5730019467	-0.2230882270
H	-1.4723945435	-1.3668628273	-0.8410575298
H	-2.2539047381	0.2288366502	-0.9322181307
O	-1.6774937101	-0.2862976106	0.9357728824
O	1.1827284924	-1.7017311591	-0.5977349143
H	-1.2314519301	-1.0399402331	1.3345000486
O	1.6863072203	-0.0269420007	0.7883268073
H	1.3259778991	0.8634649804	0.9147640252
H	0.6764851167	2.2180270354	-0.5603237277

64 T T G^+ G^- A^- ENERGY=-398.29137959

N	-0.7087155707	1.6059616181	-0.4703845071
H	-1.1407494084	1.6534945058	0.4417414808
C	-0.2148235698	0.2772880122	-0.7681800390
H	-0.0260842834	2.3385019859	-0.5931860213
H	-0.0127764860	0.1951774140	-1.8359026292
C	1.0743045064	-0.1808067786	-0.0732098399
C	-1.2993043596	-0.7257984937	-0.4221787888
O	1.6752899769	-1.1641721997	-0.4262159867
H	-0.9425771800	-1.7295932428	-0.6523156850
H	-2.1915786136	-0.5010832651	-1.0089429531
O	-1.5468110958	-0.5626791970	0.9725201046
O	1.4984212067	0.5773263224	0.9571380183
H	-2.1995560178	-1.2135283280	1.2426499586
H	0.8345558951	1.2703506466	1.0791178878

65 T A^- G^+ G^- A^+ ENERGY=-398.29129525

N	0.4832667465	-1.5777825532	0.6391572477
H	-0.3317979373	-1.9417406625	1.1171598526
C	0.1137872188	-0.6662113782	-0.4432382129
H	-0.2427745777	-1.2529745933	-1.2949760097
C	1.3585248771	0.1004794412	-0.8706979090
C	-0.9794165339	0.3047658830	-0.0166778589
H	1.1102026339	0.7690965292	-1.6986260908
H	2.1034508491	-0.6160862167	-1.2088556080
O	1.9311922281	0.8042768007	0.2142607392
O	-0.7873163634	1.4379170905	0.3608128563
H	1.2600464621	1.4497502534	0.4757170998
O	-2.2401593401	-0.1965693991	-0.0095814415

H	-2.2275214315	-1.0779471423	-0.4011079278
H	1.0151831684	-1.0417160529	1.3168962628

66 C A^- G^- T A^+:G^+ ENERGY=-398.29088576

N	0.4276608952	-1.5913417483	0.5635236945
H	0.2342885089	-1.3629801586	1.5325094074
C	0.2696865311	-0.3897561368	-0.2561501073
H	0.3944923285	-0.6782648381	-1.2989157970
C	1.3269862061	0.6373663992	0.0914861593
C	-1.1076135465	0.2077714967	-0.0699900697
H	1.3239727996	0.8005297958	1.1727549648
H	1.0708227658	1.5856865516	-0.3869427654
O	2.5705093418	0.1398690228	-0.3684950716
O	-1.3856986332	1.1360420040	0.6564800842
H	3.2531225771	0.7485296117	-0.0752638868
O	-2.0430372960	-0.4811783891	-0.7676048660
H	-2.8925006676	-0.0775247765	-0.5325363436
H	-0.2527018110	-2.2881968345	0.2856235973

67 C A^+ T G^+ A^- ENERGY=-398.29075104

N	0.1184047024	-1.8250233560	-0.5856527773
H	-0.6302533847	-2.5057372980	-0.5321882629
C	-0.2140724321	-0.6856161776	0.2627899096
H	-0.3252134651	-0.9290032383	1.3250166982
C	-1.5119566293	-0.0704654883	-0.2470916631
C	0.8846134102	0.3549554020	0.2132885488
H	-2.3114611583	-0.8139227843	-0.1611574500
H	-1.3895695617	0.1807515093	-1.2967981238
O	-1.8389330912	1.1324235838	0.4232115961
O	1.4733689423	0.7705697329	1.1854046048
H	-1.9360216060	0.9348297478	1.3597144328
O	1.1283169824	0.7832234317	-1.0403108916
H	1.8129476422	1.4630204695	-0.9501612644
H	0.9468616489	-2.2907875344	-0.2361643573

68 T T T G^+ A^+ ENERGY=-398.29067039

N	-0.2332048684	1.7658125891	-0.6419353867
H	-1.0676508732	2.2622985043	-0.3732959330
C	0.1532073945	0.6690427722	0.2215468015
H	0.0773779105	1.0045306236	1.2567751912
C	1.6263838017	0.3189986355	-0.0241682631
C	-0.6835714576	-0.6093294115	0.1215835458
H	2.1916618912	1.2468978996	0.0026743864
H	1.7242289025	-0.1071357269	-1.0314436932
O	2.1560825280	-0.5346230716	0.9588405593
O	-0.3491440781	-1.6583697445	0.6262332360
H	1.5335516787	-1.2728415801	1.0287810809
O	-1.8327415984	-0.5157823385	-0.5712886359
H	-1.8719548297	0.3928468567	-0.9048651994
H	-0.2222854018	1.5547199920	-1.6283376898

69 C A^- T G^+ A^- ENERGY==-398.29047647

N	0.0530442134	-1.8410502743	-0.6353547860
H	-0.6900409189	-2.5215381444	-0.5323205555
C	-0.2801170181	-0.6419298128	0.1360742750
H	-0.4477384831	-0.8348403986	1.2035589617
C	-1.5193595231	0.0093565518	-0.4492468365
C	0.9114827032	0.2871406887	0.0268579800
H	-2.2881054892	-0.7568611649	-0.5885884535
H	-1.2743930005	0.4288085046	-1.4204252220
O	-1.9883455561	1.0803596135	0.3510125514
O	0.9866078299	1.2897553350	-0.6365456530
H	-2.3596659524	0.7042430370	1.1537609960
O	1.9461342967	-0.1934606037	0.7655375206
H	2.6831147914	0.4160224426	0.6084035631
H	0.8888251068	-2.2670217744	-0.2538533413

70 C A^+ G^- T A^+:G^+ ENERGY=-398.29046016

N	0.3153139190	-1.6206840647	0.6425632749
H	-0.3401173534	-2.3323068279	0.3448334647
C	0.2072601749	-0.4517900046	-0.2184407086
H	0.3150641821	-0.7635642108	-1.2551433046
C	1.3265835232	0.5339250006	0.0858853647
C	-1.1170089512	0.2784869874	-0.1212961639
H	1.3643809232	0.6980238220	1.1667236065
H	1.1030724060	1.4901575948	-0.3982205169
O	2.5299113749	-0.0216541349	-0.4078869899
O	-1.8323114794	0.5892028321	-1.0444490510
H	3.2554607353	0.5255360627	-0.0964653316
O	-1.4208133990	0.5712179385	1.1713272632
H	-2.2679155521	1.0406957078	1.1384255847
H	0.0550234964	-1.3651967029	1.5875975078

71 T T G^- T C:G^+ ENERGY=-398.29038799

N	0.3744744868	-1.1537104343	0.7879187091
H	-0.1917634271	-1.9873718887	0.7468683121
C	0.1120803996	-0.1759766699	-0.2575759484
H	0.0431400091	-0.7162867789	-1.2025153368
C	1.3226199464	0.7497867870	-0.3500096869
C	-1.1592310532	0.6659152665	-0.1459051506
H	1.4016058262	1.3187724257	0.5855334581
H	1.1800733919	1.4558971726	-1.1614407609
O	2.4945773090	0.0107767033	-0.6067643338
O	-1.3885835601	1.5900259865	-0.8834151746
H	2.4411032694	-0.7566602575	-0.0227784651
O	-2.0262173995	0.3144773612	0.8310738519
H	-1.6435733149	-0.4492686927	1.2833802982
H	0.3815491165	-0.7643179809	1.7209222278

72 T A^+ G^+ G^- A^- ENERGY=-398.29013958

N	0.1597704446	1.6405973737	-0.6038191274
H	0.8333377952	2.3440255542	-0.3253646185
C	0.0126186974	0.6571017845	0.4667803235
H	-0.2438944361	1.1849391930	1.3825841806

C	1.2663589818	-0.1719228025	0.7252780483
C	-1.2046278500	-0.2108183502	0.1482993357
H	1.0718408769	-0.9360178030	1.4813535977
H	2.0639819992	0.4843609897	1.0792144544
O	1.6440995083	-0.7738589719	-0.5214029601
O	-2.2714946710	-0.0741177101	0.6896837988
H	2.3419787814	-1.4141052242	-0.3567196197
O	-1.0142754826	-1.1407229556	-0.8132415999
H	-0.0610295879	-1.1774549783	-1.0114431157
H	0.5417109428	1.1905789006	-1.4270926976

73 T T T G^+ G^- ENERGY=-398.28930219

N	-0.4501546691	-1.7516907193	-0.0924704636
H	-0.4727327500	-1.9271615905	0.9062897426
C	0.1416973338	-0.4377117245	-0.3635377526
H	0.3669329788	-0.4022297608	-1.4329451025
C	1.4293654068	-0.1407678197	0.4067502016
C	-0.9322389490	0.6298558357	-0.1279228622
H	2.0048692905	-1.0702582610	0.4701565880
H	1.1822741702	0.1740301462	1.4194532650
O	2.1968277636	0.9047688530	-0.1508067055
O	-0.6973967830	1.7606896197	0.2103756773
H	2.5606481122	0.5906257670	-0.9833041155
O	-2.1807758213	0.1807151097	-0.3580761781
H	-2.0741320404	-0.7818427199	-0.4923988218
H	0.1032499569	-2.4893197356	-0.5078784726

74 T A^- T G^+ A^+:G^+ ENERGY=-398.28927644

N	-0.3760950871	-1.7316528169	0.5483276769
H	-1.2592072063	-2.0642690392	0.1818089333
C	0.1361992227	-0.6036782918	-0.2290078373
H	0.2463677379	-0.9203980227	-1.2683089499
C	1.5052845419	-0.2220777594	0.3104887960
C	-0.7906347721	0.6021147281	-0.1610428738
H	2.1836997982	-1.0558208525	0.1508651321
H	1.4215410053	-0.0493219210	1.3868517842
O	2.0425467485	0.9005104877	-0.3576356767
O	-0.6429196656	1.5214463822	0.6089719114
H	1.5435099675	1.6613049795	-0.0399614094
O	-1.8725022305	0.5698886308	-0.9783367601
H	-1.7916954697	-0.1873524043	-1.5699952768
H	-0.5540785907	-1.4280591005	1.4993595498

75 T A^+ G^+ G^- C:T ENERGY=-398.28899770

N	0.3403735348	1.5563367531	-0.7990077156
H	1.1187809256	2.1848155355	-0.6440285831
C	0.0750007195	0.7455425356	0.3869876320
H	0.5545395818	0.9767402433	-1.6000368738
H	-0.2540554146	1.4091147887	1.1847500844
C	-1.1207248034	-0.1520711161	0.0734605699
C	1.2787299523	-0.0533067421	0.8866708500
O	-2.2424186777	0.0834151045	0.4406301749

H	0.9988805020	-0.6954929752	1.7200466713
H	2.0565167473	0.6321601232	1.2284514331
O	1.7987477927	-0.9270067338	-0.1252836244
O	-0.8336712708	-1.2339800090	-0.6843386656
H	2.3095896426	-0.3885176477	-0.7377688999
H	0.1378647680	-1.3219658600	-0.7326570531

76 T C G^+ G^- A^-:G^+ ENERGY=-398.28884530

N	0.5572460856	-1.8000459148	0.0838397709
H	-0.2587795523	-2.3893261424	0.2007865268
C	0.1564176903	-0.5836701436	-0.5911010140
H	-0.0219851038	-0.8029599810	-1.6484689692
C	1.2986902405	0.4153502303	-0.5146348717
C	-1.1389508112	0.0178238717	-0.0357948663
H	1.0997235116	1.2967538817	-1.1332849962
H	2.1963611082	-0.0739686430	-0.8955147026
O	1.4334099322	0.7706580551	0.8520049146
O	-1.7790572204	-0.4782835734	0.8524716702
H	2.2507352982	1.2638760412	0.9608353445
O	-1.5738171942	1.1520691363	-0.6453661500
H	-0.9388757356	1.4096693893	-1.3229259575
H	0.8270037509	-1.5417792073	1.0271033005

77 T G^- G^- T A^+ ENERGY=-398.28832435

N	0.3868796963	1.5386322642	0.5828776293
H	1.3846496623	1.7098511540	0.5968893696
C	0.1630208216	0.1166403728	0.4308558844
H	0.2402416913	-0.3638123234	1.4105921717
C	1.1620628223	-0.5722569183	-0.4986476228
C	-1.2208802668	-0.1078797095	-0.1480645147
H	1.0853556921	-0.1136330586	-1.4882689733
H	0.9340734112	-1.6391999345	-0.5866189650
O	2.4437780482	-0.3658271888	0.0768173987
O	-1.7484918714	0.6572446949	-0.9133110605
H	3.1064208146	-0.6407392788	-0.5625022254
O	-1.8202793570	-1.2774041647	0.1841479055
H	-1.2859310134	-1.7193993926	0.8541772870
H	-0.0046671512	2.0073724834	-0.2265002843

78 T A^+ G^- T C ENERGY=-398.28764218

N	0.4693716017	1.6591230329	-0.2135269973
H	-0.0310113549	2.3621041309	0.3163871834
C	0.2040220409	0.3254706366	0.3410104372
H	0.3601718483	0.3826756546	1.4156315910
C	1.2488465904	-0.6192495630	-0.2400927626
C	-1.2401391390	-0.1067654943	0.1424267430
H	1.1135932609	-0.7103731652	-1.3299399888
H	1.1500778593	-1.6147400025	0.1893336958
O	2.5406204477	-0.1446354714	0.0488218417
O	-2.0922483196	0.0158878526	0.9839302569
H	2.4774087341	0.8135083145	-0.0774215366
O	-1.5619275853	-0.5847689208	-1.0913576342

H	-0.7573394845	-0.6876588620	-1.6133964823
H	0.1299044999	1.7204908570	-1.1675823473

79 ENERGY=-398.28764093

N	-0.5733047286	1.5710584019	-0.3551050190
H	-1.5722206882	1.6226559355	-0.1945522609
C	-0.1919489050	0.1779506830	-0.4468209383
H	-0.2762721556	-0.1521124481	-1.4891755193
C	-1.0574846825	-0.7481125886	0.4207667970
C	1.2443979992	0.0183967743	0.0136370503
H	-0.9304033499	-0.4624901812	1.4638541749
H	-0.7483529940	-1.7917732417	0.3088381427
O	-2.4358978780	-0.5794763457	0.1331965827
O	1.7551331761	0.7271699712	0.8418385192
H	-2.6096939280	-0.9728630517	-0.7273523276
O	1.9196397361	-1.0373681393	-0.5037506578
H	1.3836868726	-1.4402469673	-1.1964402369
H	-0.1062574741	1.9690411978	0.4524686931

80 T C G^+ G^- C:T ENERGY=-398.28688322

N	-0.8009727022	-1.7012152341	0.0379826809
H	-1.8091517046	-1.7196581633	-0.0195040524
C	-0.3052111468	-0.4725196214	0.6232227193
H	-0.1403350460	-0.6106297030	1.6976866071
C	-1.2527414221	0.7176359847	0.4450701750
C	1.0285068797	-0.1391860305	-0.0290504804
H	-0.8879192278	1.5907821030	0.9860564223
H	-2.2218723483	0.4433624615	0.8766126587
O	-1.3749009263	1.1128689038	-0.9039376000
O	1.3996148722	-0.6189455917	-1.0687004477
H	-1.4938727518	0.3119990914	-1.4268448250
O	1.7839416435	0.7757016731	0.6196077756
H	1.3461524864	1.0214203968	1.4428164858
H	-0.3949636058	-1.8302832705	-0.8803671190

81 T A^- T G^+ A^+:G^- ENERGY=-398.28658213

N	-0.1310842353	-1.9513199289	0.3301039713
H	-1.1130332754	-2.1855151931	0.2677687297
C	0.1766819406	-0.6712583500	-0.3108473988
H	0.1006757155	-0.6822882991	-1.4070079743
C	1.5944272034	-0.2642829803	0.0598661290
C	-0.8016478326	0.3769638817	0.1924379315
H	2.2841500455	-1.0287515927	-0.2961750461
H	1.6640951813	-0.2213149334	1.1477472578
O	1.9730959115	0.9492129446	-0.5541360215
O	-0.4996164985	1.3310430492	0.8642336486
H	1.4686989949	1.6334555023	-0.0991712435
O	-2.0974036148	0.1820981455	-0.1635933464
H	-2.1456587787	-0.5524910131	-0.7866971472
H	0.3765292425	-2.6952982328	-0.1317704902

82 T C G^- T G^+ ENERGY=-398.28618946

N	-0.6173287376	-1.6064213674	0.1131007636
H	-1.4939759449	-1.8139358027	0.5699921942
C	-0.2011647867	-0.2623696653	0.4490125649
H	-0.3057325864	-0.0083591535	1.5150860749
C	-1.0731256585	0.7137288907	-0.3260226194
C	1.2738629287	-0.1035549013	0.1204830598
H	-1.0213351734	0.4467165714	-1.3827758084
H	-0.7347439061	1.7479303424	-0.2037093951
O	-2.3866422062	0.5605005769	0.1921702127
O	1.9826045097	-0.9998216462	-0.2531201014
H	-3.0058381933	0.9040525045	-0.4568944419
O	1.7847166370	1.1403814012	0.3145975918
H	1.0906949198	1.7176166432	0.6530708307
H	0.0828351979	-2.2710823938	0.4137460735

83 T C G^+ G^- A^-:G^+ ENERGY=-398.28506558

N	-0.5000721010	-1.8436750948	-0.2346149726
H	-1.4866477436	-1.9772796611	-0.4132549333
C	-0.2919605900	-0.6238564093	0.5175841510
H	-0.2464795808	-0.8510409114	1.5888658507
C	-1.3811794853	0.4304068888	0.3306408221
C	1.0490653928	-0.0264995593	0.1099795230
H	-1.1956896896	1.2867782764	0.9882402798
H	-2.3385925145	-0.0132567019	0.6228923551
O	-1.3755422093	0.8106470269	-1.0314197670
O	1.6528985667	-0.3387838581	-0.8804423001
H	-2.0455501211	1.4875490831	-1.1586379811
O	1.5326227840	0.9318991718	0.9415980345
H	0.9495810293	1.0081262647	1.7053605103
H	-0.0458607377	-1.7305145158	-1.1340185725

84 T G^+ G^- T A^- ENERGY=-398.28437446

N	0.3799941393	1.6966406568	0.2624678445
H	1.2714667745	1.9395868777	0.6702093623
C	0.1183973414	0.2885158613	0.4465363501
H	0.2289436550	-0.0672260682	1.4860285100
C	1.1119866724	-0.4907083364	-0.4125334661
C	-1.3319025421	0.0097828124	0.0799717993
H	1.0280232754	-0.1391924293	-1.4381140939
H	0.9150186907	-1.5677196525	-0.3964247984
O	2.4459419041	-0.2235166160	-0.0100316407
O	-2.1462144564	0.8659534275	-0.1390200223
H	2.5949038988	-0.6721483480	0.8278268888
O	-1.6919293110	-1.3005539214	0.0592118961
H	-0.9244799041	-1.8450274241	0.2668799347
H	-0.3512531380	2.2514131601	0.6853834355

85 T A^+ T G^+ A^+ ENERGY=-398.28373883

N	-0.0539952921	1.9282654784	-0.3938181866
H	-0.7623470454	2.4385050878	0.1195018081
C	0.2765292822	0.6909034707	0.3110691907
H	0.5605002201	0.9423260527	1.3301110440

C	1.4647494156	0.0393615600	-0.3813301071
C	-0.9123390106	-0.2526949489	0.4348278996
H	2.3104046161	0.7176170914	-0.3113780877
H	1.2575361855	-0.0847755432	-1.4548359274
O	1.8589423437	-1.1758489464	0.2213033212
O	-1.5872751745	-0.3716146337	1.4230689395
H	1.1589437005	-1.8243751771	0.0946745289
O	-1.2240045382	-0.9639584564	-0.6921953954
H	-0.6045593153	-0.7322606305	-1.3951613727
H	-0.4491273875	1.7284965951	-1.3055896552

Table B.2 12 lowest-energy conformers at MP2/aug-cc-pVTZ level in Å, energy in hartree

Ser-I MP2/aug-cc-pVTZ=-398.33774407

N	-0.3449572828	-1.6845075551	0.3514066685
H	-0.1193685239	-2.5974856819	-0.0211372926
C	0.0521393763	-0.6200999488	-0.5710006967
H	-0.1361737952	-0.9537736785	-1.5948198715
C	1.5036946734	-0.1850766705	-0.4398856598
C	-0.8578294265	0.5920548071	-0.3418790622
H	1.7290139520	0.5844955294	-1.1781761745
H	2.1577350850	-1.0405176221	-0.6039426564
O	1.7613054194	0.2711999604	0.8833940545
O	-0.5576975572	1.7146208265	-0.6828602844
H	1.4198218112	1.1723576298	0.9399968012
O	-2.0119345428	0.2955398683	0.2627707301
H	-1.9225954468	-0.6584625256	0.4907507814
H	0.1676022578	-1.5706339387	1.2215996625

Ser-II MP2/aug-cc-pVTZ=-398.33680539

N	0.6956944492	1.5368261187	0.2915869887
H	0.3859244803	2.0952598619	1.0769736292
C	0.2354617841	0.1638233058	0.4225482041
H	0.3445780853	-0.1606162672	1.4572006414
C	1.1438359910	-0.7202620510	-0.4420591766
C	-1.1989910834	-0.0347866387	-0.0118954258
H	0.9822873331	-0.4610024725	-1.4961754359
H	0.9019341587	-1.7711321925	-0.2992162017
O	2.4899971818	-0.5297350575	-0.0691885743
O	-1.8392801745	0.7479138873	-0.6783583282
H	2.5790345908	0.4299886796	0.0388805899
O	-1.6777220859	-1.2328071958	0.3926022563
H	-2.5769694374	-1.3027255652	0.0337647622
H	0.2723837269	1.9487205872	-0.5350879294

Ser-III MP2/aug-cc-pVTZ=-398.33642376

N	-0.5020816632	1.6751264906	-0.1644517281
H	-0.5385562808	1.6189561088	-1.1771936803
C	0.2188587587	0.5283472001	0.3913631717
H	0.6323328260	0.8132430582	1.3613173714
C	1.3661583514	0.0188271904	-0.4817094168
C	-0.7764052592	-0.5987753535	0.6698456752
H	2.0315548077	0.8527154997	-0.7058396514
H	0.9502375004	-0.3480561566	-1.4298860941
O	2.1386766389	-0.9663919728	0.1635933084
O	-0.4409456669	-1.7536097086	0.8367183552
H	1.5068744857	-1.6436844745	0.4540228815
O	-2.0507781506	-0.2059927198	0.7257523099
H	-2.0182719882	0.7509714868	0.4980654530
H	-0.0451813600	2.5458773511	0.0724330444

Ser-IV MP2/aug-cc-pVTZ=-398.33634024

N	-0.8654717133	1.4143560919	-0.3892569388
H	-1.2586556888	1.7936643430	-1.2398384465
C	-0.1718591947	0.1580941857	-0.6416158880
H	0.2367315123	0.0682364138	-1.6550021594
C	-1.1507994935	-0.9893759858	-0.3969236320
C	1.0031211899	0.0594967166	0.3058640257
H	-0.6552428397	-1.9514314039	-0.5006401171
H	-1.9518952707	-0.9212983252	-1.1408981509
O	-1.6622317405	-0.9088504307	0.9175110158
O	1.3907788794	0.9510543634	1.0269585937
H	-1.9018935180	0.0243716108	1.0297213526
O	1.5990158118	-1.1481512965	0.2305144605
H	2.3327405680	-1.1261556976	0.8647790799
H	-0.2239795021	2.0930484145	0.0050848043

Ser-V MP2/aug-cc-pVTZ=-398.33495212

N	-0.0866336919	-1.6446003810	0.7549802486
H	-1.0678636905	-1.8837087824	0.8289827990
C	0.1605423323	-0.7947482405	-0.4055660605
H	0.0269859084	-1.3926452999	-1.3103128546
C	1.5900255093	-0.2807525264	-0.3521929898
C	-0.8099730691	0.3699672380	-0.4792900161
H	1.8039988524	0.3136669564	-1.2436035247
H	2.2613251656	-1.1363601143	-0.3253135323
O	1.8338474446	0.4634263465	0.8325635467
O	-0.5342842918	1.5445744545	-0.3324921706
H	1.3196114034	1.2767903968	0.7410224141
O	-2.0749699075	-0.0550512202	-0.6975964309
H	-2.6358923073	0.7370949834	-0.6849271527
H	0.1813573424	-1.1370528108	1.5919347235

Ser-VI MP2/aug-cc-pVTZ=-398.33519496

N	0.0724906569	0.9753281088	-1.0527354512
H	-0.3271530308	1.9039218164	-0.9870744276
C	0.0996397382	0.3269501517	0.2576996200
H	0.2147047351	1.0214216001	1.0919875682
C	1.2458228386	-0.6689906513	0.3016075756
C	-1.1871819072	-0.4661267046	0.4827637217
H	1.1013356588	-1.4212567321	-0.4804752878
H	1.2484737017	-1.1575694787	1.2763031747
O	2.4421692925	0.0723343492	0.0738326654
O	-1.5017952232	-0.9142684889	1.5599796810
H	3.1825661517	-0.5426979885	0.0598474569
O	-1.9023742163	-0.6578580760	-0.6345180483
H	-1.3984509014	-0.1713986285	-1.3273824759
H	1.0236285054	1.0863397223	-1.3878497727

Ser-VII MP2/aug-cc-pVTZ=-398.33505696

N	0.0787518695	1.1185847133	-0.9577082680
H	-0.3106151093	2.0351055723	-0.7730198704
C	0.0789412649	0.2889927719	0.2438007169

H	0.1811352762	0.8534507450	1.1742966526
C	1.2222571981	-0.7197341294	0.1480754586
C	-1.2163332356	-0.5134837146	0.3399808208
H	1.0935243501	-1.3209740658	-0.7522720401
H	1.1956293077	-1.3773818270	1.0169139555
O	2.4793523810	-0.0698006468	0.0018862439
O	-1.5544199087	-1.0923227260	1.3457512602
H	2.7466032988	0.2656584248	0.8643334653
O	-1.9068758786	-0.5607678199	-0.8076683125
H	-1.3939902087	0.0139236291	-1.4209566358
H	1.0345933945	1.2552600732	-1.2701864471

Ser-VIII MP2/aug-cc-pVTZ=-398.33427894

N	0.5082012792	1.3140195124	-0.7710944107
H	0.0398932295	2.1992395386	-0.6254894501
C	0.2132082137	0.3799606625	0.3063285489
H	0.3325470852	0.8903198040	1.2611130638
C	1.2555938266	-0.7431245117	0.2460660242
C	-1.1611273285	-0.2532598822	0.3099247861
H	1.1085567513	-1.3119309156	-0.6808154427
H	1.1304128153	-1.4155319402	1.0924650144
O	2.5542294739	-0.1974787751	0.3101232562
O	-1.7077683117	-0.7069861194	1.2894611623
H	2.5231185286	0.5830679480	-0.2641208510
O	-1.7012361579	-0.3186773746	-0.9333791035
H	-2.5440665458	-0.7892440412	-0.8313953877
H	0.1739191402	0.9439580942	-1.6540852103

Ser-IX MP2/aug-cc-pVTZ=-398.33399322

N	-0.0627305916	1.5617039242	-0.1619442425
H	0.0946948079	1.4689982379	-1.1608104757
C	0.0877558327	0.2596917746	0.4888719970
H	0.3288559182	0.4419674799	1.5388279366
C	1.1745620638	-0.6193180782	-0.0965268312
C	-1.2512494026	-0.4794571529	0.4805729193
H	0.9460492546	-0.8289142948	-1.1476979737
H	1.2067105109	-1.5638796151	0.4458841179
O	2.3922354769	0.1111552209	0.0260804364
O	-1.3550505151	-1.6656293983	0.6896559759
H	3.1160180099	-0.4585273480	-0.2525792748
O	-2.3015745858	0.3175622200	0.2433227247
H	-1.9025947228	1.2024603057	0.0815069695
H	0.6449279431	2.2017037243	0.1759437208

Ser-X MP2/aug-cc-pVTZ=-398.33366289

N	0.8258213133	-1.8156225739	-0.0936444384
H	1.0060582923	-1.6170965894	0.8858378619
C	0.3684872310	-0.5936839062	-0.7228737735
H	0.3521675925	-0.7289265958	-1.8098971984
C	1.3408928934	0.5372166861	-0.4139453218
C	-1.0513561245	-0.2145507370	-0.3292263640
H	1.1166690682	1.4127890020	-1.0219564446

H	2.3449143653	0.1876841572	-0.6445530447
O	1.3351595279	0.8555454962	0.9753649176
O	-1.8501639029	-0.9462717978	0.2063408758
H	0.5971467315	1.4540963648	1.1344262893
O	-1.3488747878	1.0681084206	-0.6727936331
H	-2.2813423077	1.1962708853	-0.4346301582
H	0.0836121072	-2.5062848122	-0.1065775679

Ser-XI MP2/aug-cc-pVTZ=-398.33378908

N	0.4974343619	-1.8623424067	0.1944512451
H	-0.3461908692	-2.4225833263	0.1520107655
C	0.3092703885	-0.6400751519	-0.5579996846
H	0.2938125533	-0.8669594463	-1.6275986800
C	1.4783326185	0.2954058576	-0.3106563231
C	-0.9995824233	0.0736980160	-0.2483204417
H	1.3945146094	1.1765803861	-0.9476032944
H	2.4000865321	-0.2433267198	-0.5381026877
O	1.4179060099	0.6512213322	1.0699639656
O	-1.8525759382	-0.3229732055	0.5101424127
H	2.1864996546	1.1894040078	1.2827142535
O	-1.1219927334	1.2167965815	-0.9678888903
H	-1.9793756661	1.5966210657	-0.7193355020
H	0.6149479018	-1.6152809907	1.1718218613

Ser-XII MP2/aug-cc-pVTZ=-398.33361156

N	-0.1335405177	1.7162824848	-0.6516793111
H	-0.9347275642	2.1923673459	-0.2548629063
C	0.2823131995	0.6071371405	0.2026176151
H	0.4970248230	1.0011816014	1.1968063591
C	1.5445044468	-0.0181215328	-0.3696066753
C	-0.8023269826	-0.4428152466	0.3478868422
H	2.3214098761	0.7422297848	-0.3914806172
H	1.3509169299	-0.3418433141	-1.3975857860
O	2.0216982914	-1.0875870640	0.4258231552
O	-0.7631449901	-1.5721467363	-0.0986368774
H	1.3918750670	-1.8102737792	0.3112559458
O	-1.8750804188	0.0396065638	1.0139278207
H	-2.5301280624	-0.6763960248	1.0332888633
H	-0.4118930977	1.3706447765	-1.5639414281

Table B.3 Focal Point Energy of the Lowest-twelve Energy Conformers(in hartree)

Ser-I	HF	MP2	CCSD	CCSD(T)
DZ	-396.79148354	-397.99381748	-398.03256995	-398.07730909
TZ	-396.88387854	-398.33774403	-398.35875621	-398.42289587
QZ	-396.90883269	-398.45062265		
5Z	-396.91455778	-398.49091693		
Ser-II				
DZ	-396.79358375	-397.99313065	-398.03237700	-398.07668004
TZ	-396.88604298	-398.33680539	-398.35836371	-398.42201060
QZ	-396.91104600	-398.44975243		
5Z	-396.91678782	-398.49006821		
Ser-III				
DZ	-396.79008302	-397.99233839	-398.03117458	-398.07606957
TZ	-396.88241551	-398.33642376	-398.35748782	-398.42181039
QZ	-396.90741971	-398.44938663		
5Z	-396.91314379	-398.48968200		
Ser-IV				
DZ	-396.79248915	-397.99238947	-398.03159044	-398.07584701
TZ	-396.88501567	-398.33634024	-398.35781872	-398.42143894
QZ	-396.91000442	-398.44927329		
5Z	-396.91574388	-398.48959518		
Ser-V				
DZ	-396.79230785	-397.99137997	-398.03101175	-398.07531981
TZ	-396.88453095	-398.33495210	-398.35688482	-398.42054290
QZ	-396.90949617	-398.44783690		
5Z	-396.91523214	-398.48815686		
Ser-VI				
DZ	-396.78879922	-397.99135024	-398.02987775	-398.07452463
TZ	-396.88129491	-398.33519497	-398.35597879	-398.42001270
QZ	-396.90625923	-398.44808039		
5Z	-396.91199244	-398.48837157		
Ser-VII				
DZ	-396.78839710	-397.99118937	-398.02968694	-398.07445007
TZ	-396.88090455	-398.33505696	-398.35580455	-398.41996268
QZ	-396.90587608	-398.44791878		
5Z	-396.91160764	-398.48820651		
Ser-VIII				
DZ	-396.79068975	-397.99071276	-398.02982676	-398.07417492
TZ	-396.88311758	-398.33427893	-398.35570041	-398.41939271
QZ	-396.90810874	-398.44716100		
5Z	-396.91384901	-398.48747363		

Ser-IX

DZ	-396.78911742	-397.99020665	-398.02928334	-398.07373783
TZ	-396.88155748	-398.33399321	-398.35535692	-398.41920699
QZ	-396.90654555	-398.44693994		
5Z	-396.91228389	-398.48724222		

Ser-X

DZ	-396.79101626	-397.99001289	-398.02965605	-398.07379599
TZ	-396.88334453	-398.33366288	-398.35560776	-398.41910573
QZ	-396.90828461	-398.44644136		
5Z	-396.91402000	-398.48674158		

Ser-XI

DZ	-396.79190828	-397.99023345	-398.02984285	-398.07378382
TZ	-396.88440571	-398.33378886	-398.35574873	-398.41900688
QZ	-396.90936212	-398.44661565		
5Z	-396.91510853	-398.48693707		

Ser-XII

DZ	-396.79212633	-397.99008824	-398.02998036	-398.07413078
TZ	-396.88439682	-398.33361156	-398.35581253	-398.41928339
QZ	-396.90937768	-398.44651487		
5Z	-396.91511720	-398.48681664		

Table B.4 Vibrational Frequency with anharm correction and TED analysis.

Anharmonicities computed by means of second-order vibrational perturbation theory (VPT2) with a resonance cutoff of 80 cm^{-1}. Absolute infrared intensities from the double-harmonic approximation are given in km/mol.

The internal coordinates are defined as (atom numbers correspond to Fig 3.2): $S_1=r(N_1–H_2)$, $S_2=r(N_1–C_\alpha)$, $S_3=\theta(C_\alpha–N_1–H_2)$, $S_4=r(C_\alpha–H_4)$, $S_5=\theta(N_1–C_\alpha–H_4)$, $S_6=\tau(H_2–N_1–C_\alpha–H_4)$, $S_7=r(C_\alpha–C_\beta)$, $S_8=\theta(N_1–C_\alpha–C_\beta)$, $S_9=\tau(H_2–N_1–C_\alpha–C_\beta)$, $S_{10}=r(C_\alpha–C_5)$, $S_{11}=\theta(N_1–C_\alpha–C_5)$, $S_{12}=\tau(H_2–N_1–C_\alpha–C_5)$, $S_{13}=r(C_\beta–H_{10})$, $S_{14}=\theta(C_\alpha–C_\beta–H_{10})$, $S_{15}=\tau(N_1–C_\alpha–C_\beta–H_{10})$, $S_{16}=r(C_\beta–H_9)$, $S_{17}=\theta(C_\alpha–C_\beta–H_9)$, $S_{18}=\tau(N_1–C_\alpha–C_\beta–H_9)$, $S_{19}=r(C_\beta–O_{11})$, $S_{20}=\theta(C_\alpha–C_\beta–O_{11})$, $S_{21}=\tau(N_1–C_\alpha–C_\beta–O_{11})$, $S_{22}=r(C_5=O_6)$, $S_{23}=\theta(C_\alpha–C_5=O_6)$, $S_{24}=\tau(N_1–C_\alpha–C_5=O_6)$, $S_{25}=r(O_{11}–H_{12})$, $S_{26}=\theta(C_\beta–O_{11}–H_{12})$, $S_{27}=\tau(C_\alpha–C_\beta–O_{11}–H_{12})$, $S_{28}=r(C_5–O_7)$, $S_{29}=\theta(C_\alpha–C_5–O_7)$, $S_{30}=\tau(O_7–C_5–C_\alpha–O_6)$, $S_{31}=r(O_7–H_8)$, $S_{32}=\theta(C_5–O_7–H_8)$, $S_{33}=\tau(C_\alpha–C_5–O_7–H_8)$, $S_{34}=r(N_1–H_3)$, $S_{35}=\theta(C_\alpha–N_1–H_3)$, $S_{36}=\tau(C_5–C_\alpha–N_1–H_3)$.

Ser-I

Mode	Total Energy Distribution	ω_i (cm^{-1})	$\nu_i - \omega_i$ (cm^{-1})	ν_i (cm^{-1})	Intensity (km mol^{-1})
ν_1	$S_{24}(81) - S_9(19) - S_{12}(15)$	69	–6	63	5
ν_2	$S_{21}(66) - S_{12}(14)$	114	–7	107	8
ν_3	$S_{20}(35) - S_{12}(34) + S_{24}(13)$	223	–4	218	4
ν_4	$S_{11}(37) + S_8(21) + S_{29}(18) - S_{23}(14)$	301	+14	316	22
ν_5	$S_{36}(24) + S_{12}(23) + S_8(15) - S_{11}(11)$	354	–9	345	27
ν_6	$S_9(52) - S_{12}(20) + S_{29}(17) - S_{18}(17)$	375	–17	357	19
ν_7	$S_{27}(42) + S_{29}(16) + S_{30}(12)$	450	–35	415	103
ν_8	$S_{27}(42) + S_{23}(22)$	517	–34	483	3
ν_9	$S_{23}(32) - S_{27}(15) + S_{10}(15) + S_{30}(12)$	565	–23	542	7
ν_{10}	$S_{20}(25) + S_{11}(21) - S_{29}(19) + S_{30}(13)$	609	–13	597	5
ν_{11}	$S_{10}(19) - S_{23}(14) + S_{30}(13) + S_{28}(12)$	778	–13	765	6
ν_{12}	$S_{33}(28) + S_{12}(15) + S_{10}(11) + S_7(10)$	832	–22	810	15
ν_{13}	$S_{33}(61) + S_{30}(20)$	885	–45	840	85
ν_{14}	$S_2(28) + S_7(23) + S_{14}(11)$	902	–26	876	46
ν_{15}	$S_3(18) + S_{36}(14)$	951	–28	923	70
ν_{16}	$S_{19}(36) - S_{12}(11)$	1006	–30	976	78
ν_{17}	$S_3(19) + S_2(15)$	1100	+7	1107	21
ν_{18}	$S_{19}(42) - S_7(19) + S_2(11)$	1130	–31	1099	56
ν_{19}	$S_{35}(19) - S_5(13) - S_3(11) - S_{26}(10)$	1186	–24	1162	5
ν_{20}	$S_{28}(45) + S_{32}(12) + S_6(12)$	1237	–42	1195	15
ν_{21}	$S_2(18) + S_{17}(17) + S_{35}(15) - S_{14}(11)$	1251	–36	1215	10
ν_{22}	$S_6(47) - S_7(11) - S_{32}(11)$	1323	–50	1272	8
ν_{23}	$S_{26}(36) - S_5(18) - S_{21}(14)$	1389	–41	1348	14
ν_{24}	$S_{14}(43) + S_{17}(20) + S_5(17)$	1404	–35	1369	7
ν_{25}	$S_{32}(23) - S_5(23) - S_{26}(14) + S_{17}(12)$	1416	–32	1384	112
ν_{26}	$S_{32}(40) - S_{28}(12)$	1445	–37	1409	310
ν_{27}	$S_{18}(43) - S_{15}(42)$	1506	–42	1464	8
ν_{28}	$S_{12}(28) - S_{36}(27) + S_{35}(25) + S_3(21)$	1650	–73	1576	34
ν_{29}	$S_{22}(81)$	1833	–29	1804	244
ν_{30}	$S_4(86)$	3093	–153	2940	12
ν_{31}	$S_{13}(54) + S_{16}(32) + S_4(14)$	3103	–134	2969	25
ν_{32}	$S_{16}(63) - S_{13}(37)$	3159	–146	3013	15
ν_{33}	$S_{31}(98)$	3476	–252	3224	272
ν_{34}	$S_{34}(71) + S_1(28)$	3517	–142	3375	12
ν_{35}	$S_1(72) - S_{34}(28)$	3627	–176	3450	18
ν_{36}	$S_{25}(100)$	3825	–181	3644	53

Ser-II

Mode	Total Energy Distribution	ω_i (cm^{-1})	$\nu_i - \omega_i$ (cm^{-1})	ν_i (cm^{-1})	Intensity (km mol^{-1})
ν_1	$S_{24}(95)$	57	–4	53	2
ν_2	$S_{21}(67) - S_{12}(29) - S_9(20)$	130	–3	127	9
ν_3	$S_{12}(40) + S_{11}(16) + S_8(15) - S_{30}(14)$	187	–3	184	4
ν_4	$S_9(94)$	245	–17	228	10
ν_5	$S_{11}(26) + S_{23}(21) - S_{29}(17) + S_9(11)$	287	–5	282	6
ν_6	$S_{20}(33) + S_8(22)$	342	–6	337	1
ν_7	$S_{29}(26) - S_8(21) + S_{10}(21)$	413	–5	408	27
ν_8	$S_{29}(31) + S_8(23) + S_{11}(13)$	531	–2	529	7
ν_9	$S_{27}(89)$	588	–58	529	119
ν_{10}	$S_{33}(66)$	605	–20	585	97
ν_{11}	$S_{23}(42) - S_{33}(15) - S_{28}(14)$	657	–13	643	17
ν_{12}	$S_{30}(53) + S_{33}(13) - S_7(10)$	746	–19	728	27
ν_{13}	$S_2(24) + S_{10}(17) - S_9(11)$	867	–19	848	89
ν_{14}	$S_7(32) - S_{10}(11) + S_6(11) + S_{17}(10)$	922	–25	898	33
ν_{15}	$S_{12}(29) + S_3(27)$	975	–36	939	66
ν_{16}	$S_{35}(15) - S_7(12) - S_5(10)$	1036	–26	1010	12
ν_{17}	$S_{19}(81)$	1108	–32	1076	132
ν_{18}	$S_{28}(35) - S_{32}(26) - S_2(16)$	1143	–38	1105	185
ν_{19}	$S_5(18) + S_3(14) + S_2(13) - S_7(12)$	1182	–31	1151	11
ν_{20}	$S_2(14)$	1199	+7	1206	56
ν_{21}	$S_6(58) + S_{32}(19)$	1263	–35	1229	5
ν_{22}	$S_{17}(36) - S_{35}(14)$	1303	0	1303	11
ν_{23}	$S_{32}(20) + S_{28}(14) + S_5(11) + S_{14}(10)$	1357	–9	1348	51
ν_{24}	$S_{14}(40) + S_{15}(13) + S_6(13) + S_{26}(11)$	1388	–29	1359	3
ν_{25}	$S_5(49)$	1440	–37	1403	36
ν_{26}	$S_{26}(51) - S_{17}(17) + S_{18}(14)$	1448	–37	1411	59
ν_{27}	$S_{18}(43) - S_{15}(41)$	1528	–33	1495	1
ν_{28}	$S_{35}(27) + S_{36}(26) - S_{12}(25) + S_3(21)$	1664	–71	1593	29
ν_{29}	$S_{22}(83)$	1815	–28	1787	225
ν_{30}	$S_{13}(96)$	3023	–146	2877	44
ν_{31}	$S_4(98)$	3133	–142	2991	4
ν_{32}	$S_{16}(95)$	3161	–145	3016	16
ν_{33}	$S_{34}(67) + S_1(33)$	3521	–129	3392	9
ν_{34}	$S_1(67) - S_{34}(33)$	3619	–177	3442	14
ν_{35}	$S_{25}(100)$	3737	–191	3546	76
ν_{36}	$S_{31}(100)$	3760	–186	3574	83

Ser-III

Mode	Total Energy Distribution	ω_i (cm^{-1})	$\nu_i - \omega_i$ (cm^{-1})	ν_i (cm^{-1})	Intensity (km mol^{-1})
ν_1	$S_{24}(84) - S_9(22) - S_{12}(18)$	71	–6	65	2
ν_2	$S_{21}(87)$	172	–5	167	6
ν_3	$S_8(45) - S_9(27) - S_{20}(25) - S_{12}(13)$	235	–8	227	11
ν_4	$S_{12}(100)$	295	–6	289	16
ν_5	$S_9(27) - S_{11}(23) - S_{29}(22) - S_{20}(14)$	334	–7	327	19
ν_6	$S_9(68)$	358	–20	338	17
ν_7	$S_8(28) + S_{20}(18) + S_7(17) - S_{11}(11)$	423	–5	418	4
ν_8	$S_{23}(43) + S_{10}(24) + S_{29}(12)$	557	–8	549	4
ν_9	$S_{29}(22) - S_{11}(20) - S_{27}(17) - S_{20}(16)$	597	–15	582	27
ν_{10}	$S_{27}(83)$	624	–44	580	89
ν_{11}	$S_{30}(40)$	743	–9	734	7
ν_{12}	$S_{10}(31) + S_{28}(13)$	821	–15	806	13
ν_{13}	$S_{33}(79)$	870	–52	818	110
ν_{14}	$S_{12}(27) + S_3(17) + S_{35}(16) - S_{36}(12)$	902	–45	857	78
ν_{15}	$S_{15}(15) + S_{18}(14)$	1004	–16	988	12
ν_{16}	$S_7(16) + S_{35}(15) - S_{28}(14) + S_{19}(14)$	1083	–36	1047	92
ν_{17}	$S_{19}(74)$	1115	–32	1083	69
ν_{18}	$S_2(37) - S_7(26)$	1147	–30	1117	3
ν_{19}	$S_3(27) + S_2(14) - S_{35}(10)$	1196	–29	1166	3
ν_{20}	$S_6(19) + S_{14}(17) - S_{17}(13) + S_{26}(11)$	1232	–125	1108	20
ν_{21}	$S_{28}(40) + S_{32}(17) - S_{10}(12)$	1254	–46	1208	4
ν_{22}	$S_6(27) - S_{14}(21) - S_5(17)$	1324	–41	1284	4
ν_{23}	$S_{17}(45)$	1386	–43	1344	14
ν_{24}	$S_5(42) - S_{26}(14)$	1400	–43	1357	9
ν_{25}	$S_{32}(50)$	1434	–43	1391	471
ν_{26}	$S_{26}(41) - S_{14}(18) - S_{15}(12)$	1468	–40	1428	19
ν_{27}	$S_{15}(43) - S_{18}(39)$	1524	–25	1500	1
ν_{28}	$S_3(26) + S_{36}(25) + S_{35}(24) - S_{12}(23)$	1654	–70	1584	34
ν_{29}	$S_{22}(80)$	1821	–26	1795	236
ν_{30}	$S_{16}(94)$	3014	–129	2885	50
ν_{31}	$S_4(98)$	3107	–136	2972	7
ν_{32}	$S_{13}(92)$	3128	–145	2983	25
ν_{33}	$S_{31}(100)$	3485	–245	3241	267
ν_{34}	$S_1(70) + S_{34}(29)$	3528	–145	3383	2
ν_{35}	$S_{34}(71) - S_1(30)$	3633	–177	3456	15
ν_{36}	$S_{25}(100)$	3724	–189	3535	156

Ser-IV

Mode	Total Energy Distribution	ω_i (cm^{-1})	$\nu_i - \omega_i$ (cm^{-1})	ν_i (cm^{-1})	Intensity (km mol^{-1})
ν_1	$S_{24}(97)$	75	–8	67	1
ν_2	$S_{12}(50) - S_{21}(50)$	111	–7	104	5
ν_3	$S_9(100)$	236	–19	217	15
ν_4	$S_{12}(61)$	239	–13	227	4
ν_5	$S_{11}(42) - S_{29}(26) + S_{23}(21)$	285	–5	281	5
ν_6	$S_8(42) + S_{12}(14)$	372	–7	366	2
ν_7	$S_{29}(48) + S_{11}(16)$	488	0	488	28
ν_8	$S_{33}(31) - S_{30}(21) - S_8(18) + S_{20}(13)$	534	–11	523	24
ν_9	$S_{23}(47) - S_{27}(15)$	583	–13	570	8
ν_{10}	$S_{27}(78)$	618	–48	570	155
ν_{11}	$S_{33}(60) + S_{30}(17)$	648	+10	657	70
ν_{12}	$S_{10}(22) - S_{30}(16) + S_7(10)$	765	–15	750	33
ν_{13}	$S_{12}(24) + S_{30}(18) + S_{10}(13) + S_3(11)$	837	–24	814	43
ν_{14}	$S_7(38) - S_{10}(12)$	922	–24	898	83
ν_{15}	$S_{36}(25) - S_9(22) - S_{35}(17) - S_3(10)$	935	–56	878	25
ν_{16}	$S_{17}(16) - S_2(14)$	1017	–20	997	1
ν_{17}	$S_{19}(49) - S_2(12)$	1098	–70	1027	76
ν_{18}	$S_2(29) + S_{19}(18) - S_{28}(10)$	1143	–31	1112	87
ν_{19}	$S_{32}(30) - S_{28}(25)$	1168	–38	1130	140
ν_{20}	$S_{14}(20) - S_{35}(12)$	1220	–33	1187	46
ν_{21}	$S_6(17) - S_{14}(11)$	1238	–31	1206	17
ν_{22}	$S_6(26) + S_{35}(14) - S_7(11)$	1317	–28	1289	4
ν_{23}	$S_{32}(29) + S_5(24) + S_{28}(13) - S_{17}(11)$	1342	–32	1310	27
ν_{24}	$S_5(23) + S_{17}(19) + S_{14}(14) + S_{26}(14)$	1380	–48	1332	6
ν_{25}	$S_{26}(46) - S_{14}(22) - S_{15}(14)$	1442	–36	1407	56
ν_{26}	$S_{17}(16) - S_{10}(14) - S_6(11) + S_{28}(11)$	1453	–28	1425	37
ν_{27}	$S_{15}(42) - S_{18}(38) - S_{17}(12)$	1526	–45	1481	3
ν_{28}	$S_{35}(29) + S_3(24) - S_{12}(23) + S_{36}(21)$	1629	–67	1562	61
ν_{29}	$S_{22}(82)$	1822	–22	1799	220
ν_{30}	$S_4(66) - S_{16}(33)$	3041	–114	2928	45
ν_{31}	$S_{16}(63) + S_4(34)$	3056	–122	2934	41
ν_{32}	$S_{13}(96)$	3170	–133	3037	13
ν_{33}	$S_{34}(57) + S_1(43)$	3539	–181	3358	13
ν_{34}	$S_1(57) - S_{34}(43)$	3646	–179	3467	23
ν_{35}	$S_{25}(100)$	3735	–191	3544	66
ν_{36}	$S_{31}(100)$	3770	–185	3584	92

Ser-V

Mode	Total Energy Distribution	ω_i (cm^{-1})	$\nu_i - \omega_i$ (cm^{-1})	ν_i (cm^{-1})	Intensity (km mol^{-1})
ν_1	$S_{24}(100)$	45	−10	35	1
ν_2	$S_{21}(85)$	171	−12	159	9
ν_3	$S_9(31) - S_{11}(25) + S_{20}(14) - S_{29}(13)$	222	−7	215	1
ν_4	$S_{11}(39) + S_9(30) - S_{30}(19) + S_{20}(17)$	261	−9	252	4
ν_5	$S_8(27) + S_{12}(26) - S_{23}(18)$	325	−3	322	10
ν_6	$S_9(69) + S_{36}(37)$	360	−11	349	31
ν_7	$S_{29}(40) - S_8(26) + S_{20}(10)$	389	−4	385	6
ν_8	$S_{27}(26) + S_{23}(22) + S_{29}(16) - S_{10}(12)$	541	−21	520	45
ν_9	$S_{27}(73) - S_{23}(13)$	582	−41	541	153
ν_{10}	$S_3(78)$	617	−28	589	104
ν_{11}	$S_{20}(20) + S_{30}(18) + S_{23}(13) + S_{33}(13)$	711	−22	689	20
ν_{12}	$S_{30}(26) + S_{10}(22) + S_{28}(11)$	763	−44	719	34
ν_{13}	$S_{30}(21) - S_7(14)$	849	−17	831	18
ν_{14}	$S_2(27) + S_{36}(13) - S_3(11)$	898	−46	853	106
ν_{15}	$S_7(32) + S_6(15)$	942	−30	912	18
ν_{16}	$S_{12}(20) + S_{21}(15) - S_{19}(14)$	1027	−137	890	69
ν_{17}	$S_{19}(43) - S_2(13) - S_3(10)$	1078	−31	1047	5
ν_{18}	$S_2(23) + S_{19}(20) - S_7(11)$	1151	−28	1123	72
ν_{19}	$S_{32}(39) + S_{28}(34)$	1162	−39	1123	253
ν_{20}	$S_{35}(20) + S_{15}(11) - S_5(10)$	1204	−31	1173	1
ν_{21}	$S_{17}(25) + S_2(16) + S_{26}(14) - S_{14}(13)$	1261	−29	1232	6
ν_{22}	$S_{32}(32) + S_6(21) + S_5(13) + S_{28}(12)$	1317	−58	1258	6
ν_{23}	$S_5(51) - S_3(11)$	1390	−18	1373	23
ν_{24}	$S_{14}(47) + S_{15}(15) + S_{26}(15)$	1403	−34	1369	5
ν_{25}	$S_6(28) + S_{10}(11) - S_7(10)$	1422	−35	1387	61
ν_{26}	$S_{26}(34) - S_{17}(27) + S_{18}(15)$	1444	−17	1427	22
ν_{27}	$S_{18}(46) - S_{15}(41)$	1509	−39	1470	4
ν_{28}	$S_{35}(28) - S_{12}(25) + S_3(24) + S_{36}(23)$	1642	−30	1612	35
ν_{29}	$S_{22}(82)$	1796	−26	1769	218
ν_{30}	$S_{13}(85) + S_{16}(11)$	3076	−132	2943	32
ν_{31}	$S_4(95)$	3101	−185	2916	20
ν_{32}	$S_{16}(89) - S_{13}(11)$	3165	−142	3023	14
ν_{33}	$S_{34}(57) + S_1(43)$	3524	−151	3373	5
ν_{34}	$S_1(57) - S_{34}(43)$	3628	−177	3451	14
ν_{35}	$S_{31}(100)$	3758	−185	3573	90
ν_{36}	$S_{25}(100)$	3798	−183	3615	71

Ser-VI

Mode	Total Energy Distribution	ω_i (cm^{-1})	$\nu_i - \omega_i$ (cm^{-1})	ν_i (cm^{-1})	Intensity (km mol^{-1})
ν_1	$S_{24}(79) + S_9(28)$	83	−6	77	0
ν_2	$S_{21}(68) - S_{12}(21) - S_9(14)$	141	−4	137	9
ν_3	$S_{12}(38) + S_8(15) + S_{30}(14) + S_{11}(10)$	194	−1	193	12
ν_4	$S_{27}(95)$	267	−38	229	102
ν_5	$S_{20}(34) - S_{11}(23) + S_8(18) - S_{12}(11)$	327	−9	318	3
ν_6	$S_{29}(28) - S_{36}(22) + S_{11}(14) - S_{12}(13)$	345	−23	322	37
ν_7	$S_9(65) + S_{12}(33)$	362	−15	347	6
ν_8	$S_8(27) - S_{23}(18) - S_{10}(18) - S_{20}(14)$	430	−16	414	9
ν_9	$S_{23}(37) + S_8(18) - S_{20}(11) + S_{11}(30)$	565	−9	556	7
ν_{10}	$S_{29}(40) - S_{11}(22) + S_{30}(17)$	662	−12	650	11
ν_{11}	$S_{30}(45) + S_7(10) - S_{12}(10)$	739	+20	759	11
ν_{12}	$S_{10}(27) + S_{28}(16)$	879	−17	863	12
ν_{13}	$S_{33}(86)$	891	−51	840	71
ν_{14}	$S_2(22) + S_7(20) + S_6(13) + S_{17}(11)$	917	−31	887	59
ν_{15}	$S_3(30) + S_7(23) - S_{12}(11)$	979	−31	949	65
ν_{16}	$S_{12}(28) - S_{35}(24)$	1040	−31	1009	39
ν_{17}	$S_{19}(84)$	1093	−32	1061	80
ν_{18}	$S_2(48) - S_{26}(14) + S_5(11)$	1135	−30	1105	34
ν_{19}	$S_6(13) - S_{15}(13) - S_{28}(13) - S_3(12)$	1204	−45	1159	13
ν_{20}	$S_{26}(27) - S_{17}(23) + S_{18}(16)$	1248	−26	1221	18
ν_{21}	$S_{28}(27) + S_6(14)$	1258	−37	1221	8
ν_{22}	$S_6(27) + S_{14}(27)$	1307	−29	1277	4
ν_{23}	$S_6(28) - S_{35}(21) + S_3(13)$	1340	−46	1294	3
ν_{24}	$S_5(65) + S_{17}(15)$	1382	−39	1343	16
ν_{25}	$S_{32}(67)$	1440	−56	1384	381
ν_{26}	$S_{14}(33) + S_{17}(22) + S_{26}(15)$	1459	−46	1413	3
ν_{27}	$S_{15}(46) - S_{18}(44)$	1533	−45	1488	5
ν_{28}	$S_{36}(28) - S_{12}(27) - S_{35}(25) - S_3(22)$	1658	−60	1599	37
ν_{29}	$S_{22}(81)$	1844	−34	1810	263
ν_{30}	$S_{13}(81) + S_{16}(18)$	3053	−134	2919	26
ν_{31}	$S_4(95)$	3106	−134	2972	8
ν_{32}	$S_{16}(78) - S_{13}(19)$	3135	−168	2967	18
ν_{33}	$S_{31}(99)$	3463	−246	3217	291
ν_{34}	$S_{34}(52) + S_1(47)$	3531	−144	3388	3
ν_{35}	$S_1(53) - S_{34}(47)$	3619	−179	3441	25
ν_{36}	$S_{25}(100)$	3865	−181	3685	59

Ser-VII

Mode	Total Energy Distribution	ω_i (cm^{-1})	$v_i - \omega_i$ (cm^{-1})	v_i (cm^{-1})	Intensity (km mol^{-1})
v_1	$S_{24}(78)$ S	85	–5	80	3
v_2	$S_{21}(69) - S_{12}(18) - S_9(13)$	139	–4	135	12
v_3	$S_{12}(41) + S_8(14) + S_{30}(14)$	189	0	188	8
v_4	$S_{20}(30) - S_{11}(28) + S_8(12)$	318	–8	310	18
v_5	$S_{27}(49) - S_9(18) - S_8(15)$	323	–29	294	61
v_6	$S_{29}(37) + S_{11}(14) - S_{12}(12) + S_{27}(11)$	348	–17	331	17
v_7	$S_9(50) + S_{36}(23)$	377	–27	350	47
v_8	$S_8(18) - S_{23}(18) - S_{10}(14) - S_{20}(13)$	440	–19	421	25
v_9	$S_{23}(35) + S_8(18) - S_{20}(11)$	568	–10	559	6
v_{10}	$S_{29}(31) - S_{11}(22) + S_{30}(17)$	666	–12	654	6
v_{11}	$S_{30}(46) + S_7(12) - S_{12}(10)$	735	+3	738	11
v_{12}	$S_{10}(28) + S_{28}(17)$	879	–24	856	51
v_{13}	$S_{33}(82)$	884	–50	834	22
v_{14}	$S_2(22) + S_7(14) + S_{17}(12)$	906	–27	879	69
v_{15}	$S_7(32) + S_3(25)$	971	–26	945	48
v_{16}	$S_{12}(33) - S_{35}(18) + S_{21}(12)$	1014	–30	984	46
v_{17}	$S_{19}(81)$	1092	–31	1061	105
v_{18}	$S_2(19) - S_{26}(18)$	1141	–27	1114	42
v_{19}	$S_2(32) + S_5(19) - S_7(11)$	1154	–25	1129	2
v_{20}	$S_{28}(34) + S_{32}(14) - S_{10}(14)$	1248	–43	1205	11
v_{21}	$S_6(47) - S_{17}(18)$	1294	–34	1261	9
v_{22}	$S_{35}(24) - S_3(18) - S_6(15)$	1314	–46	1268	3
v_{23}	$S_5(62) + S_{17}(11)$	1374	–36	1338	16
v_{24}	$S_{26}(31) + S_{17}(25) - S_{18}(13)$	1397	–38	1359	8
v_{25}	$S_{14}(50) + S_{15}(14) + S_{17}(11)$	1422	–37	1385	53
v_{26}	$S_{32}(67)$	1436	–99	1337	350
v_{27}	$S_{15}(46) - S_{18}(44)$	1516	–41	1475	3
v_{28}	$S_{36}(27) - S_{12}(26) - S_{35}(26) - S_3(22)$	1659	–63	1596	35
v_{29}	$S_{22}(81)$	1842	–31	1811	260
v_{30}	$S_4(99)$	3083	–131	2951	14
v_{31}	$S_{16}(68) + S_{13}(32)$	3095	–136	2959	17
v_{32}	$S_{13}(67) - S_{16}(32)$	3160	–148	3012	12
v_{33}	$S_{31}(98)$	3475	–242	3233	279
v_{34}	$S_{34}(58) + S_1(41)$	3529	–141	3388	3
v_{35}	$S_1(59) - S_{34}(41)$	3620	–178	3442	24
v_{36}	$S_{25}(100)$	3851	–183	3669	48

Ser-VIII

Mode	Total Energy Distribution	ω_i (cm^{-1})	$\nu_i - \omega_i$ (cm^{-1})	ν_i (cm^{-1})	Intensity (km mol^{-1})
ν_1	$S_{24}(90)$	35	−7	28	1
ν_2	$S_{21}(69) - S_{12}(19) - S_9(10)$	137	−4	133	5
ν_3	$S_{12}(40) + S_{11}(17) + S_8(15) + S_{30}(12)$	185	−2	183	2
ν_4	$S_9(97)$	274	−9	264	14
ν_5	$S_{11}(27) + S_{29}(21) - S_{36}(16)$	289	−10	279	3
ν_6	$S_{20}(35) + S_8(18) - S_{12}(13) + S_{29}(11)$	334	−7	327	2
ν_7	$S_8(29) - S_{10}(22) - S_{23}(20) - S_{20}(11)$	419	−6	412	13
ν_8	$S_{23}(24) + S_{11}(20) + S_8(12)$	545	−9	536	14
ν_9	$S_{27}(84)$	574	−66	507	102
ν_{10}	$S_{33}(24) - S_{29}(20) + S_{20}(12) - S_{23}(11)$	611	0	611	101
ν_{11}	$S_{33}(50) + S_{29}(18)$	638	−22	616	52
ν_{12}	$S_{30}(54) + S_{33}(19)$	753	−19	734	27
ν_{13}	$S_{10}(18) + S_2(18) + S_{28}(16) - S_9(11)$	846	−24	822	99
ν_{14}	$S_7(34) + S_{17}(13) + S_2(10)$	920	−25	896	12
ν_{15}	$S_{12}(34) + S_3(25) - S_{36}(12)$	950	−43	907	105
ν_{16}	$S_{35}(17) - S_7(13) - S_{14}(11) - S_5(11)$	1023	−21	1002	9
ν_{17}	$S_{19}(79)$	1107	−35	1073	121
ν_{18}	$S_2(38) - S_{32}(20) - S_7(10)$	1168	−27	1141	4
ν_{19}	$S_{32}(14) + S_3(11)$	1173	−31	1143	168
ν_{20}	$S_{32}(21)$	1200	−31	1168	40
ν_{21}	$S_6(71)$	1281	−29	1251	1
ν_{22}	$S_{17}(35) - S_{35}(13)$	1300	−32	1268	26
ν_{23}	$S_{32}(29) + S_{28}(25) + S_{23}(15) - S_{10}(15)$	1373	−83	1290	44
ν_{24}	$S_{14}(46) + S_{15}(20) + S_{26}(18) + S_6(11)$	1383	−33	1350	13
ν_{25}	$S_5(65) - S_3(12)$	1413	−39	1374	15
ν_{26}	$S_{26}(50) - S_{17}(19) + S_{18}(12) - S_{14}(11)$	1446	−32	1414	81
ν_{27}	$S_{18}(44) - S_{15}(41)$	1529	−43	1486	1
ν_{28}	$S_{35}(27) + S_{36}(25) - S_{12}(24) + S_3(23)$	1660	−88	1572	34
ν_{29}	$S_{22}(84)$	1819	−33	1786	220
ν_{30}	$S_{13}(96)$	3023	−141	2882	46
ν_{31}	$S_4(98)$	3140	−352	2788	3
ν_{32}	$S_{16}(95)$	3158	−148	3010	15
ν_{33}	$S_{34}(58) + S_1(42)$	3537	−140	3397	7
ν_{34}	$S_1(58) - S_{34}(42)$	3632	−177	3455	13
ν_{35}	$S_{25}(100)$	3743	−192	3551	74
ν_{36}	$S_{31}(100)$	3761	−186	3576	88

Ser-IX

Mode	Total Energy Distribution	ω_i (cm^{-1})	$\nu_i - \omega_i$ (cm^{-1})	ν_i (cm^{-1})	Intensity (km mol^{-1})
ν_1	$S_{24}(82)$	72	−9	63	1
ν_2	$S_{21}(73)$	122	−2	121	13
ν_3	$S_8(27) - S_9(22) + S_{20}(17) + S_{12}(11)$	198	−4	193	21
ν_4	$S_{27}(83) + S_{12}(16)$	258	−33	225	103
ν_5	$S_{12}(37) + S_{36}(31) - S_{27}(15)$	284	−23	262	25
ν_6	$S_{11}(39) - S_{20}(27) - S_{23}(11)$	325	−6	319	4
ν_7	$S_9(37) + S_{29}(20) - S_{12}(20) + S_{20}(11)$	376	−16	360	13
ν_8	$S_8(46)$	430	−7	424	11
ν_9	$S_{23}(31) + S_{11}(26) - S_{29}(16)$	531	−1	530	1
ν_{10}	$S_{23}(20) + S_{30}(19) - S_{20}(18) + S_{29}(17)$	616	+22	639	20
ν_{11}	$S_{30}(32) - S_{29}(14) - S_{23}(12)$	738	−11	728	9
ν_{12}	$S_{33}(68)$	864	−39	825	56
ν_{13}	$S_{23}(23) + S_{30}(22) - S_{10}(13)$	877	−28	849	40
ν_{14}	$S_2(20) + S_7(18) - S_{10}(14) - S_{12}(14)$	910	−33	877	67
ν_{15}	$S_3(24) + S_6(15) + S_{17}(12) - S_{14}(11)$	977	−27	950	50
ν_{16}	$S_{19}(74)$	1075	−32	1043	104
ν_{17}	$S_{35}(20) - S_{19}(14) - S_{28}(12)$	1113	−32	1081	17
ν_{18}	$S_2(34) - S_7(25) - S_{26}(23)$	1142	−32	1111	50
ν_{19}	$S_3(19) - S_{18}(16) + S_{21}(15) - S_{15}(11)$	1195	−32	1163	4
ν_{20}	$S_{28}(32) + S_6(25)$	1232	−38	1194	13
ν_{21}	$S_{26}(39) - S_{14}(12) - S_{17}(11)$	1253	−35	1218	21
ν_{22}	$S_{17}(17) - S_{14}(16) - S_3(13)$	1290	−37	1254	2
ν_{23}	$S_6(34) - S_{26}(12)$	1326	−39	1287	13
ν_{24}	$S_5(56) - S_{32}(16) - S_{35}(10)$	1408	−53	1356	20
ν_{25}	$S_{32}(47) - S_{28}(11) + S_5(10)$	1438	−65	1374	383
ν_{26}	$S_{14}(28) + S_{17}(20) + S_{26}(16)$	1459	−50	1409	6
ν_{27}	$S_{18}(42) - S_{15}(40)$	1534	−53	1481	2
ν_{28}	$S_{36}(28) - S_{12}(26) + S_3(24) + S_{35}(23)$	1662	−65	1597	34
ν_{29}	$S_{22}(82)$	1840	−42	1799	252
ν_{30}	$S_{13}(89) + S_{16}(10)$	3040	−130	2909	35
ν_{31}	$S_4(96)$	3101	−132	2969	4
ν_{32}	$S_{16}(86) - S_{13}(11)$	3137	−176	2961	16
ν_{33}	$S_{31}(98)$	3495	−240	3254	268
ν_{34}	$S_1(72) + S_{34}(26)$	3524	−135	3389	6
ν_{35}	$S_{34}(73) - S_1(27)$	3622	−176	3446	15
ν_{36}	$S_{25}(100)$	3869	−180	3689	53

Ser-X

Mode	Total Energy Distribution	ω_i (cm^{-1})	$\nu_i - \omega_i$ (cm^{-1})	ν_i (cm^{-1})	Intensity (km mol^{-1})
ν_1	$S_{24}(94)$	44	−10	34	0
ν_2	$S_{21}(71) - S_{12}(29)$	105	−16	88	4
ν_3	$S_9(34) + S_{20}(33)$	214	−10	203	1
ν_4	$S_{11}(48) + S_{23}(22) - S_{29}(21)$	271	−2	269	18
ν_5	$S_9(51) + S_{36}(46)$	292	−28	264	20
ν_6	$S_8(50) - S_9(16)$	351	−8	342	47
ν_7	$S_{27}(91)$	381	−71	310	106
ν_8	$S_{29}(36) + S_8(20) + S_{11}(13)$	483	−2	481	12
ν_9	$S_{30}(20) - S_{33}(18) - S_{20}(17) - S_{29}(17)$	516	−18	497	16
ν_{10}	$S_{23}(45) - S_{11}(17) - S_{20}(11)$	597	−12	585	20
ν_{11}	$S_{33}(76)$	669	−31	639	99
ν_{12}	$S_{10}(27) + S_{28}(14) - S_{30}(14)$	752	−13	738	25
ν_{13}	$S_{30}(27) + S_{12}(18) + S_7(13) + S_{19}(11)$	849	−18	831	8
ν_{14}	$S_2(28) + S_{14}(15) + S_7(11)$	919	−20	899	35
ν_{15}	$S_7(22) - S_{12}(19) + S_{35}(17) + S_{36}(10)$	951	−36	915	101
ν_{16}	$S_{19}(13) - S_{21}(11)$	1025	−28	998	103
ν_{17}	$S_{19}(50)$	1078	−27	1051	29
ν_{18}	$S_{28}(41) - S_{32}(34)$	1144	−36	1108	223
ν_{19}	$S_6(27) - S_2(23)$	1160	−36	1124	59
ν_{20}	$S_3(15) - S_{26}(14) - S_5(14) + S_{14}(10)$	1197	−18	1178	7
ν_{21}	$S_2(22) + S_{17}(13) - S_{32}(11) + S_3(11)$	1280	−37	1243	2
ν_{22}	$S_6(28) + S_{32}(26) + S_5(12)$	1308	−51	1257	10
ν_{23}	$S_3(28) + S_{14}(23) + S_{10}(11)$	1379	−28	1350	17
ν_{24}	$S_{26}(35) + S_{15}(12) + S_{14}(10)$	1398	0	1399	5
ν_{25}	$S_5(22) - S_{35}(15) + S_{26}(10)$	1406	−36	1370	12
ν_{26}	$S_{17}(39) + S_{14}(20) - S_{18}(12)$	1422	−37	1385	19
ν_{27}	$S_{18}(45) - S_{15}(42)$	1511	−38	1473	5
ν_{28}	$S_{36}(27) - S_{12}(25) - S_3(24) - S_{35}(22)$	1668	−63	1604	28
ν_{29}	$S_{22}(84)$	1822	−73	1749	228
ν_{30}	$S_4(99)$	3068	−132	2936	10
ν_{31}	$S_{13}(76) + S_{16}(22)$	3107	−133	2974	32
ν_{32}	$S_{16}(77) - S_{13}(23)$	3174	−146	3028	12
ν_{33}	$S_1(57) + S_{34}(43)$	3518	−173	3344	5
ν_{34}	$S_{34}(57) - S_1(43)$	3606	−176	3430	13
ν_{35}	$S_{31}(100)$	3755	−184	3571	78
ν_{36}	$S_{25}(100)$	3850	−182	3669	40

Ser-XI

Mode	Total Energy Distribution	ω_i (cm^{-1})	$\nu_i - \omega_i$ (cm^{-1})	ν_i (cm^{-1})	Intensity (km mol^{-1})
ν_1	$S_{24}(97)$	64	−6	58	1
ν_2	$S_{21}(59) - S_{12}(35)$	110	−7	103	0
ν_3	$S_9(44) + S_{20}(21)$	217	−12	205	53
ν_4	$S_{27}(74) + S_9(11)$	240	−37	203	52
ν_5	$S_{11}(25) + S_9(18) - S_{29}(13) + S_{23}(13)$	255	−9	246	48
ν_6	$S_{36}(32) + S_9(25) - S_{11}(14)$	277	−7	269	14
ν_7	$S_8(46) - S_9(18) - S_{12}(12) - S_{10}(11)$	362	−8	354	8
ν_8	$S_{29}(40) + S_{20}(15) + S_{11}(12) - S_{30}(12)$	479	−10	469	17
ν_9	$S_8(23) - S_{33}(18) + S_{29}(16) - S_{20}(15)$	518	−6	511	12
ν_{10}	$S_{23}(47) - S_{11}(17) + S_{33}(10)$	593	−6	587	51
ν_{11}	$S_{33}(61) + S_{30}(11)$	646	−43	603	91
ν_{12}	$S_{10}(23) - S_{30}(20) + S_{28}(11)$	755	−13	742	22
ν_{13}	$S_{30}(24) + S_{10}(12)$	850	−17	833	14
ν_{14}	$S_7(29) + S_2(19) + S_{14}(13) - S_{10}(11)$	944	−23	921	16
ν_{15}	$S_3(19) - S_2(15) - S_{36}(14)$	952	−57	895	131
ν_{16}	$S_{19}(60) - S_3(14)$	1066	−29	1037	49
ν_{17}	$S_{12}(16) + S_{35}(15) + S_{21}(14)$	1078	−32	1046	49
ν_{18}	$S_{28}(40) - S_{32}(32)$	1142	−37	1106	241
ν_{19}	$S_{19}(16) - S_6(16) + S_5(12) + S_3(11)$	1173	−25	1148	4
ν_{20}	$S_{26}(35) - S_2(19)$	1207	−34	1174	52
ν_{21}	$S_{18}(23) + S_{15}(17) - S_{17}(13)$	1253	−28	1225	14
ν_{22}	$S_{32}(32) - S_{17}(12)$	1312	−44	1268	13
ν_{23}	$S_6(31) + S_{26}(15) - S_{14}(13) + S_{35}(12)$	1319	−41	1279	12
ν_{24}	$S_6(21) + S_{10}(15) - S_{28}(15) - S_{32}(11)$	1400	−8	1392	13
ν_{25}	$S_5(47) - S_3(17) + S_{35}(11)$	1402	−37	1365	10
ν_{26}	$S_{17}(26) + S_{14}(25) + S_{26}(15)$	1458	−42	1416	3
ν_{27}	$S_{18}(45) - S_{15}(44)$	1528	−43	1485	7
ν_{28}	$S_{12}(27) - S_{36}(26) - S_{35}(25) - S_3(23)$	1667	−53	1613	28
ν_{29}	$S_{22}(84)$	1825	−25	1800	229
ν_{30}	$S_{16}(53) + S_{13}(35) - S_4(13)$	3075	−145	2930	28
ν_{31}	$S_4(87)$	3092	−136	2956	20
ν_{32}	$S_{13}(62) - S_{16}(38)$	3138	−138	3000	22
ν_{33}	$S_{34}(51) + S_1(49)$	3527	−138	3389	6
ν_{34}	$S_1(51) - S_{34}(49)$	3612	−179	3433	12
ν_{35}	$S_{31}(100)$	3767	−186	3581	77
ν_{36}	$S_{25}(100)$	3872	−180	3693	54

Ser-XII

Mode	Total Energy Distribution	ω_i (cm^{-1})	$v_i - \omega_i$ (cm^{-1})	v_i (cm^{-1})	Intensity (km mol^{-1})
v_1	$S_{24}(100)$	38	−4	35	1
v_2	$S_{21}(90)$	164	−5	159	4
v_3	$S_{12}(36) + S_8(31) + S_{11}(30)$	211	−12	198	2
v_4	$S_9(62) + S_{12}(38)$	269	−8	261	15
v_5	$S_{12}(59) + S_9(32)$	286	−10	276	24
v_6	$S_9(95)$	293	+23	317	5
v_7	$S_8(29) - S_{12}(17) + S_{20}(16) + S_7(16)$	454	−7	447	8
v_8	$S_{29}(41) + S_{10}(13) - S_{20}(11)$	511	−11	500	13
v_9	$S_{27}(95)$	532	−57	474	178
v_{10}	$S_{23}(36) + S_{20}(14) + S_2(11)$	593	−9	584	15
v_{11}	$S_{33}(77)$	628	−25	603	87
v_{12}	$S_{30}(33) + S_{10}(17)$	751	−19	733	20
v_{13}	$S_{30}(26) - S_{10}(18) - S_{28}(10)$	825	−22	803	23
v_{14}	$S_3(20) - S_{36}(18) + S_{12}(15) + S_{36}(14)$	890	−50	840	161
v_{15}	$S_3(18) + S_7(16)$	1008	−19	989	1
v_{16}	$S_{15}(13) + S_{12}(12) + S_{18}(11)$	1043	−25	1018	47
v_{17}	$S_{19}(79)$	1110	−31	1078	94
v_{18}	$S_2(35) - S_7(13) - S_{32}(10)$	1150	−32	1118	46
v_{19}	$S_{32}(29) - S_{28}(20) - S_6(14)$	1165	−32	1134	197
v_{20}	$S_{35}(20) + S_2(19)$	1196	−35	1161	2
v_{21}	$S_{14}(25) + S_5(18) - S_{17}(14) + S_{26}(11)$	1254	−29	1225	12
v_{22}	$S_6(33) + S_{32}(27) - S_{14}(13) + S_{28}(12)$	1323	−35	1288	12
v_{23}	$S_{17}(20) + S_5(15) - S_3(13) + S_{35}(12)$	1387	−31	1355	5
v_{24}	$S_5(33) - S_{26}(23)$	1400	−30	1371	50
v_{25}	$S_{17}(30) + S_6(24)$	1417	−39	1378	29
v_{26}	$S_{26}(33) - S_{14}(23) - S_{15}(12)$	1437	−41	1396	27
v_{27}	$S_{15}(45) - S_{18}(39)$	1516	−41	1475	4
v_{28}	$S_{35}(26) - S_{12}(26) + S_3(25) + S_{36}(23)$	1656	−83	1574	32
v_{29}	$S_{22}(83)$	1789	−29	1768	218
v_{30}	$S_{16}(94)$	3048	−135	2913	39
v_{31}	$S_4(99)$	3112	−139	2973	9
v_{32}	$S_{13}(94)$	3168	−137	3031	15
v_{33}	$S_{34}(64) + S_1(36)$	3524	−137	3388	3
v_{34}	$S_1(64) - S_{34}(36)$	3623	−175	3448	8
v_{35}	$S_{31}(100)$	3761	−185	3576	90
v_{36}	$S_{25}(100)$	3816	−183	3633	65

Table B.5 N–C–C angle and hyperconjugation changes due to amine rotation

Conformer	Bond	N−H/C-C Orientation	N−C−C Angle (degree)	$E_2(n_N \rightarrow \sigma^*_{C-C})$ (kJ mol^{-1})
	$C_\alpha-C_5$	Trans	108.3	23.2
Ser-I	$C_\alpha-C_\beta$	Gauche	114.4	35.6
	$C_\alpha-C_5$	Gauche	113.3	45.7
Ser-II	$C_\alpha-C_\beta$	Trans	107.6	14.0
	$C_\alpha-C_5$	Trans	108.9	23.9
Ser-III	$C_\alpha-C_\beta$	Gauche	114.7	33.0
	$C_\alpha-C_5$	Trans	108.3	0.0
Ser-IV	$C_\alpha-C_\beta$	Trans	108.1	19.3
	$C_\alpha-C_5$	Gauche	112.0	51.4
Ser-V	$C_\alpha-C_\beta$	Trans	108.9	0.0
	$C_\alpha-C_5$	Trans	110.2	23.5
Ser-VI	$C_\alpha-C_\beta$	Trans	109.1	0.0
	$C_\alpha-C_5$	Trans	110.4	24.4
Ser-VII	$C_\alpha-C_\beta$	Trans	108.6	0.0
	$C_\alpha-C_5$	Gauche	117.1	55.2
Ser-VIII	$C_\alpha-C_\beta$	Trans	107.4	11.9
	$C_\alpha-C_5$	Trans	109.5	20.7
Ser-IX	$C_\alpha-C_\beta$	Gauche	114.8	38.2
	$C_\alpha-C_5$	Gauche	112.8	54.5
Ser-X	$C_\alpha-C_\beta$	Trans	109.6	0.0
	$C_\alpha-C_5$	Gauche	113.5	56.4
Ser-XI	$C_\alpha-C_\beta$	Trans	109.4	0.0
	$C_\alpha-C_5$	Gauche	112.9	51.0
Ser-XII	$C_\alpha-C_\beta$	Trans	109.3	6.1

Table B.6 O–C–C angle and hyperconjugation changes

Conformer	O_7–H_8 Bond (Å)	O_7–H_8/C_5-C_α Orientation	O_7– C_5-C_α Angle (degree)	$E_2(n_O \rightarrow \sigma^*_{C–C})$ (kJ mol^{-1})
Ser-I	0.985	Cis	113.9	37.2
Ser-II	0.971	Trans	111.5	0.0
Ser-III	0.984	Cis	114.3	37.3
Ser-IV	0.970	Trans	111.5	0.0
Ser-V	0.971	Trans	111.4	0.0
Ser-VI	0.985	Cis	113.6	36.1
Ser-VII	0.985	Cis	113.7	36.2
Ser-VIII	0.971	Trans	112.3	0.0
Ser-IX	0.984	Cis	113.6	36.0
Ser-X	0.971	Trans	111.9	0.0
Ser-XI	0.970	Trans	111.4	0.0
Ser-XII	0.971	Trans	111.6	0.0

Conformer	O_{11}–H_{12}Bond (Å)	O_{11}–H_{12}/C_α-C_β Orientation	O_{11}– C_β-C_α Angle (degree)	$E_2(n_O \rightarrow \sigma^*_{C–C})$ (kJ mol^{-1})
Ser-I	0.965	Gauche	110.2	43.0
Ser-II	0.970	Gauche	109.8	61.9
Ser-III	0.971	Gauche	112.5	45.3
Ser-IV	0.970	Gauche	109.8	38.5
Ser-V	0.967	Gauche	111.6	46.7
Ser-VI	0.963	Trans	106.7	5.3
Ser-VII	0.963	Gauche	111.5	45.7
Ser-VIII	0.970	Gauche	109.9	367
Ser-IX	0.962	Trans	106.4	5.0
Ser-X	0.963	Gauche	111.2	44.6
Ser-XI	0.962	Trans	106.2	5.7
Ser-XII	0.965	Gauche	112.3	47.6

Table B.7 Summary of hyperconjugative interactions in kJ mol^{-1} for varying conformations about the C_α–C_β bond.

	X−C−C−Y	τ(X−C−C−Y)	E $\sigma_{X-C} \rightarrow \sigma^*_{C-Y}$	E $\sigma_{Y-C} \rightarrow \sigma^*_{C-X}$	∠X-C-C	∠C-C-Y
			Gauche/Gauche			
Ser-I	C_5-C_α-C_β-H_{10}	179.5	9.2	16.9	109.2	109.6
	H_4-C_α-C_β-O_{11}	178.8	17.8	6.0	109.7	110.1
	N_1-C_α-C_β-H_9	177.7	4.6	21.8	114.4	109.9
Ser-IV	C_5-C_α-C_β-H_{10}	−175.6	7.8	18.1	110.3	108.3
	H_4-C_α-C_β-O_{11}	179.5	15.7	5.8	109.3	109.5
	N_1-C_α-C_β-H_9	−174.6	6.2	16.4	108.1	110.9
Ser-V	C_5-C_α-C_β-H_{10}	−179.1	7.7	18.0	110.1	108.3
	H_4-C_α-C_β-O_{11}	178.1	18.5	5.5	109.5	109.9
	N_1-C_α-C_β-H_9	176.5	5.9	18.0	108.9	109.9
Ser-X	C_5-C_α-C_β-H_{10}	174.8	6.9	18.6	111.1	107.9
	H_4-C_α-C_β-O_{11}	174.2	20.2	5.1	107.9	111.1
	N_1-C_α-C_β-H_9	168.8	5.8	16.3	109.6	110.7
Ser-XI	C_5-C_α-C_β-H_{10}	179.9	8.2	17.3	110.0	108.1
	H_4-C_α-C_β-O_{11}	175.9	18.0	6.0	107.5	106.1
	N_1-C_α-C_β-H_9	174.4	5.9	16.8	109.4	110.0
			Gauche/Trans			
Ser-II	C_5-C_α-C_β-O_{11}	177.8	10.4	6.4	109.2	109.7
	H_4-C_α-C_β-H_9	174.4	12.0	13.3	107.7	108.4
	N_1-C_α-C_β-H_{10}	173.6	5.8	15.8	107.6	110.5
Ser-VI	C_5-C_α-C_β-O_{11}	178.6	14.2	6.2	107.0	106.8
	H_4-C_α-C_β-H_9	174.9	12.8	12.8	108.4	109.0
	N_1-C_α-C_β-H_{10}	−179.4	5.2	18.2	109.1	108.7
Ser-VII	C_5-C_α-C_β-O_{11}	176.7	15.6	5.4	107.0	111.6
	H_4-C_α-C_β-H_9	176.5	12.0	13.7	109.0	108.9
	N_1-C_α-C_β-H_{10}	−177.6	5.3	17.3	108.6	109.2
Ser-VIII	C_5-C_α-C_β-O_{11}	−177.8	11.0	6.3	108.4	109.9
	H_4-C_α-C_β-H_9	175.4	12.5	13.1	107.6	108.6
	N_1-C_α-C_β-H_{10}	174.0	5.6	16.2	107.4	110.0
Ser-IX	C_5-C_α-C_β-O_{11}	−177.0	11.6	7.3	110.6	106.4
	H_4-C_α-C_β-H_9	178.6	13.5	14.2	108.0	109.2
	N_1-C_α-C_β-H_{10}	−180.0	4.5	22.3	114.8	109.3

			Trans/Gauche			
Ser-III	C_5-C_α-C_β-H_9	177.4	8.2	17.4	110.4	108.7
	H_4-C_α-C_β-H_{10}	176.0	12.4	14.3	108.0	108.5
	N_1-C_α-C_β-O_{11}	172.7	6.5	8.5	114.7	112.5
Ser-XII	C_5-C_α-C_β-H_9	−177.2	7.3	17.7	110.2	108.1
	H_4-C_α-C_β-H_{10}	−177.1	12.5	14.1	108.7	109.0
	N_1-C_α-C_β-O_{11}	176.7	8.6	7.2	109.3	112.5

APPENDIX C

SUPPORTING INFORMATION FOR CHAPTER 4

Table C.1 All complexes geometry optimized at CCSD/cc-pVTZ level in Å

HB6/04

Hydrogen bond database that consists of the equilibrium binding energies of six hydrogen-bonded dimers.

$(NH_3)_2$

```
CCSD/CC-PVTZ  ENERGY=-112.93679159
N       -1.5873845261      -0.0490654510     0.0000000000
H       -2.1660595600       0.1398621436    -0.8081621289
H       -2.1660595600       0.1398621436     0.8081621289
H       -0.8573467973       0.6534271547     0.0000000000
N        1.5873845261       0.0490654510     0.0000000000
H        2.1660595600      -0.1398621436    -0.8081621289
H        0.8573467973      -0.6534271547     0.0000000000
H        2.1660595600      -0.1398621436     0.8081621289
```

$(HF)_2$

```
CCSD/CC-PVTZ  ENERGY= -200.67226663153167
H       -1.63263125      0.82371313          0.00000000
F       -1.33692798     -0.04587949          0.00000000
F        1.39751099      0.00984779          0.00000000
H        0.49058737     -0.14448325          0.00000000
```

$(H_2O)_2$

```
CCSD/CC-PVTZ  ENERGY=-152.65805757
O       -1.5645464593      -0.1139530973     0.0000000000
H       -1.9332021587       0.7684641652     0.0000000000
H       -0.6134865762       0.0309990263     0.0000000000
O        1.3618505981       0.1147005210     0.0000000000
H        1.6879312981      -0.3737643077    -0.7571186263
H        1.6879312981      -0.3737643077     0.7571186263
```

$NH_3\cdots H_2O$

```
CCSD/CC-PVTZ  ENERGY=-132.80076026
N       -1.3930847541      -0.0169512863     0.0039336919
H       -1.6519436805       0.9571881027    -0.0882034578
H       -1.8436726674      -0.5055346988    -0.7588294366
H       -1.8265203483      -0.3482464483     0.8559477637
O        1.5828736499       0.0972269040    -0.0386899557
H        0.6213692568       0.0036588712    -0.0194162122
H        1.9050185436      -0.7991984446     0.0450026067
```

$(HCONH_2)_2$

CCSD/CC-PVTZ ENERGY=-339.25481487

C	-2.0294665789	0.0453875617	0.0000000000
O	-1.4620160755	1.1277322242	0.0000000000
N	-1.4252657247	-1.1495943294	0.0000000000
H	-1.9814821805	-1.9814922680	0.0000000000
H	-0.4097682188	-1.2173715935	0.0000000000
H	-3.1260158447	-0.0163906721	0.0000000000
C	2.0294665789	-0.0453875617	0.0000000000
O	1.4620160755	-1.1277322242	0.0000000000
N	1.4252657247	1.1495943294	0.0000000000
H	1.9814821805	1.9814922680	0.0000000000
H	0.4097682188	1.2173715935	0.0000000000
H	3.1260158447	0.0163906721	0.0000000000

$(HCOOH)_2$

CCSD/CC-PVTZ ENERGY=-378.97675227

C	-1.8989245740	-0.1761945549	0.0000000000
O	-1.5088831619	1.0749966687	0.0000000000
O	-1.1793296957	-1.1531082008	0.0000000000
H	-2.9873192890	-0.2587489733	0.0000000000
H	-0.5221187678	1.1150921831	0.0000000000
C	1.8989245740	0.1761945549	0.0000000000
O	1.5088831619	-1.0749966687	0.0000000000
O	1.1793296957	1.1531082008	0.0000000000
H	2.9873192890	0.2587489733	0.0000000000
H	0.5221187678	-1.1150921831	0.0000000000

CT7/04

Six charge transfer complexes

$NH_3\cdots F_2$

```
CCSD/CC-PVTZ  ENERGY=-255.74603109
N         0.0000000000       0.0000137248    -2.1784888767
H         0.0000000000       0.9337325052    -2.5682663069
H         0.8086362889      -0.4668929793    -2.5680832881
H        -0.8086362889      -0.4668929793    -2.5680832881
F         0.0000000000       0.0000212194     0.6229524911
F         0.0000000000       0.0000185091     2.0237922687
```

$C_2H_2\cdots ClF$

```
CCSD/CC-PVTZ  ENERGY=-636.53859712
H         0.0000000000       1.6647539419    -2.2787701026
C         0.0000000000       0.6021258316    -2.2711062383
C         0.0000000000      -0.6021258316    -2.2711062383
H         0.0000000000      -1.6647539419    -2.2787701026
Cl        0.0000000000       0.0000000000     0.7584039345
F         0.0000000000       0.0000000000     2.3976517474
```

$HCN\cdots ClF$

```
CCSD/CC-PVTZ  ENERGY=-652.62693538
F         0.0000000000       0.0000000000     2.4962774365
Cl        0.0000000000       0.0000000000     0.8547520055
N         0.0000000000       0.0000000000    -1.8959556791
C         0.0000000000       0.0000000000    -3.0471705467
H         0.0000000000       0.0000000000    -4.1126852162
```

$NH_3\cdots Cl_2$

```
CCSD/CC-PVTZ  ENERGY=-975.88148556
N         0.0000000000      -0.0000028933    -2.8619765064
H         0.0000000000       0.9371814364    -3.2426717703
H         0.8116039233      -0.4685848844    -3.2426262356
H        -0.8116039233      -0.4685848844    -3.2426262356
Cl        0.0000000000       0.0000013193    -0.0930896788
Cl        0.0000000000      -0.0000090935     1.9345854266
```

$H_2O\cdots ClF$

```
CCSD/CC-PVTZ  ENERGY=-635.69599036
O         2.2660070820       0.0000521467    -0.0860283697
H         2.6228336447       0.7574972112     0.3796871099
H         2.6228595198      -0.7572830814     0.3798458816
Cl       -0.3579262941       0.0000132845    -0.0284228032
F        -2.0001569524      -0.0000085610     0.0305921815
```

$NH_3\cdots ClF$

```
CCSD/CC-PVTZ  ENERGY=-615.84223262
N         0.0000000000      -0.0000066699    -2.0962626609
H         0.0000000000       0.9408952617    -2.4665672605
H         0.8148197027      -0.4704411734    -2.4665365111
H        -0.8148197027      -0.4704411734    -2.4665365111
Cl        0.0000000000      -0.0000020299     0.3589830779
F         0.0000000000      -0.0000052152     2.0242148657
```

DI6/04

Three dipole interaction complexes

$(HCl)_2$

```
CCSD/CC-PVTZ  ENERGY=-920.66155489076721
H        -0.70935790       0.19834357          0.00000000
CL       -1.97136690      -0.00387558          0.00000000
CL        1.93599714       0.03397944          0.00000000
H         1.93659488      -1.24286790          0.00000000
```

$CH_3Cl\cdots HCl$

```
CCSD/CC-PVTZ  ENERGY=-959.88478673
C        -1.5297819785       1.1405468326     0.0000024775
Cl       -1.4231122374      -0.6472868341     0.0001408115
H        -0.5227306004       1.5427223289    -0.0011970370
H        -2.0632802683       1.4468363331     0.8923465088
H        -2.0653041000       1.4465699153    -0.8912194841
Cl        2.2259128771      -0.0115573080    -0.0001520103
H         1.0598123074      -0.5428852679     0.0000737337
```

$CH_3SH\cdots HCl$

```
CCSD/CC-PVTZ  ENERGY=-898.48932910
C        -1.4790359368       1.1675930725     0.0308949478
S        -1.4050632785      -0.6511754063    -0.0523035449
H        -1.4341404742       1.5208469045    -0.9963048292
H        -0.6309071749       1.5678201362     0.5788709596
H        -2.4124018415       1.4956639623     0.4781979943
H        -1.4549953129      -0.8781711719     1.2667932779
Cl        2.2370281708      -0.0282383919    -0.0705705625
H         1.0244218482      -0.4601971054    -0.1254912429
```

WI7/05

Seven weak interaction complexes

Ne_2

CCSD/CC-PVTZ ENERGY=-257.59656787392186

Ne	0.0000000000	0.0000000000	1.50030837
Ne	0.0000000000	0.0000000000	-1.50030837

Ne···Ar

CCSD/CC-PVTZ ENERGY=-655.83493279330230

Ar	0.0000000000	0.0000000000	1.18642244
Ne	0.0000000000	0.0000000000	-2.37151040

Ar_2

CCSD/CC-PVTZ ENERGY=-1054.07333182429466

Ar	0.0000000000	0.0000000000	2.05977306
Ar	0.0000000000	0.00000000 00	-2.05977306

CH_4···Ne

CCSD/CC-PVTZ ENERGY=-169.23050719

Ne	0.0007304365	-0.0345414812	-1.6996097640
C	-0.0007026551	0.0349621775	1.7344625299
H	-0.0010797525	0.0570264645	2.8219229954
H	-0.0211986781	1.0523345911	1.3504499276
H	-0.8779341281	-0.5026616357	1.3817033789
H	0.8973637773	-0.4669271162	1.3816009322

CH_4···Ar

CCSD/CC-PVTZ ENERGY=-567.46877198

Ar	0.0008458347	-0.0416748925	-2.0613064241
C	-0.0007412809	0.0363858135	1.8066998451
H	-0.0011710045	0.0583986128	2.8942184110
H	-0.0212150622	1.0539036773	1.4228845655
H	-0.8780286638	-0.5012647063	1.4540309557
H	0.8974891767	-0.4655555047	1.4540026467

CH_4···CH_4

CCSD/CC-PVTZ ENERGY=-80.86418689

C	0.0000000000	-0.0000126148	1.8870287850
H	-0.8877983994	0.5125522758	1.5233234016
H	0.8877983994	0.5125522758	1.5233234016
H	0.0000000000	-1.0251732912	1.5233295580
H	0.0000000000	-0.0000072795	2.9748314152
C	0.0000000000	0.0000126148	-1.8870287850
H	0.0000000000	0.0000072795	-2.9748314152
H	-0.8877983994	-0.5125522758	-1.5233234016
H	0.8877983994	-0.5125522758	-1.5233234016

H	0.0000000000	1.0251732912	-1.5233295580

$C_2H_4\cdots C_2H_2$

CCSD/CC-PVTZ ENERGY=-155.59713397

C	0.0000000000	-0.6660420162	-2.1507767857
C	0.0000000000	0.6660420162	-2.1507767857
H	0.9222674472	-1.2313345510	-2.1525092196
H	-0.9222674472	-1.2313345510	-2.1525092196
H	-0.9222674472	1.2313345510	-2.1525092196
H	0.9222674472	1.2313345510	-2.1525092196
C	0.0000000000	0.0000000000	2.9380457935
C	0.0000000000	0.0000000000	1.7342034547
H	0.0000000000	0.0000000000	0.6703118417
H	0.0000000000	0.0000000000	3.9999953597

PPS5/05

Two p-p stacking complexes

$C_2H_2\cdots C_2H_2$

CCSD/CC-PVTZ ENERGY=-154.34417596

C	-0.4018873953	1.7270227861	0.0000000000
C	0.4126599231	2.6132154979	0.0000000000
H	-1.1140824626	0.9382355090	0.0000000000
H	1.1264909025	3.3996959060	0.0000000000
C	0.4018873953	-1.7270227861	0.0000000000
C	-0.4126599231	-2.6132154979	0.0000000000
H	1.1140824626	-0.9382355090	0.0000000000
H	-1.1264909025	-3.3996959060	0.0000000000

$C_2H_4\cdots C_2H_4$

CCSD/CC-PVTZ ENERGY=-156.84942680

C	-0.4708262902	-0.4708293043	-1.9082457736
C	0.4708262902	0.4708293043	-1.9082457736
H	-0.8716306396	-0.8716394482	-0.9868142871
H	0.8716306396	0.8716394482	-0.9868142871
H	-0.8698841664	-0.8698925301	-2.8309716801
H	0.8698841664	0.8698925301	-2.8309716801
C	-0.4708262902	0.4708293043	1.9082457736
C	0.4708262902	-0.4708293043	1.9082457736
H	-0.8716306396	0.8716394482	0.9868142871
H	0.8716306396	-0.8716394482	0.9868142871
H	-0.8698841664	0.8698925301	2.8309716801
H	0.8698841664	-0.8698925301	2.8309716801

Table C.2 Interaction Energy in kcal mol^{-1}

		ΔE_{int}	ΔE^{CCSD}	$\Delta\varepsilon^{*}$	ΔE_{sr}^{CCSD}	ΔE_{mr}^{CCSD}	ΔE_{lr}^{CCSD}
Hydrogen	$(NH_3)_2$	−2.9	−1.47	−2.89	−0.53	−2.36	1.46
Bond	$(HF)_2$	−4.6	−0.86	−1.97	−0.41	−1.56	1.10
	$(H_2O)_2$	−4.9	−1.20	−2.58	−0.56	−2.01	1.37
	$NH_3\cdots H_2O$	−6.2	−1.64	−3.13	−0.94	−2.19	1.49
	$(HCONH_2)2$	−15.4	−3.19	−4.84	−0.32	−4.52	1.65
	(HCOOH)2	−17.8	−2.77	−4.20	−0.38	−3.82	1.43
Charge	$NH_3\cdots F_2$	−1.5	−1.38	−2.37	−0.67	−1.69	0.99
Transfer	$C_2H_2\cdots ClF$	−3.1	−1.94	−3.34	0.06	−3.40	1.40
	$HCN\cdots ClF$	−4.4	−1.70	−3.02	−0.22	−2.80	1.32
	$NH_3\cdots Cl_2$	−4.2	−2.58	−2.77	−0.90	−1.88	0.19
	$H_2O\cdots ClF$	−4.7	−1.56	−2.07	0.03	−2.10	0.51
	$NH_3\cdots ClF$	−8.8	−3.24	−4.00	−0.68	−3.32	0.77
Dipole	$(HCl)_2$	−1.9	−1.25	−1.65	−0.59	−1.06	0.40
Interaction	$CH_3Cl\cdots HCl$	−3.3	−2.22	−3.23	−1.01	−2.22	1.01
	$CH_3SH\cdots HCl$	−4.5	−2.73	−3.35	−1.63	−1.73	0.62
Weak	Ne_2	−0.1	−0.15	−0.14	−0.05	−0.08	−0.01
Interaction	NeAr	−0.1	−0.18	−0.47	−0.03	−0.44	0.29
	$CH_4\cdots Ne$	0.2	−0.32	−0.77	−0.08	−0.68	0.44
	$CH_4\cdots Ar$	−0.4	−0.54	−1.19	−0.11	−1.08	0.65
	$(CH_4)_2$	−0.5	−0.78	−1.75	−0.14	−1.61	0.97
	Ar_2	−0.2	−0.25	−0.54	−0.02	−0.52	0.29
	$C_2H_4\cdots C_2H_2$	−1.6	−0.96	−2.00	−0.21	−1.80	1.04
P-P	$(C_2H_2)_2$	−1.3	−0.78	−1.83	0.06	−1.89	1.05
Stacking	$(C_2H_4)_2$	−1.4	−1.87	−3.48	−0.50	−2.98	1.61

Table C.3 The turning point r_x cutoff values of the atomization energies and minimum point r_x cutoff values of the molecular correlation energies in Bohr

	r_x^1	r_x'
BeH_2	0.712	1.526
BH_3	0.885	1.593
CH_4	0.980	1.748
NH_3	0.947	1.693
H_2O	0.909	1.595
HF	0.837	1.461
AlH_3	0.904	1.726
SiH_4	0.952	1.724
PH_3	1.056	1.842
H_2S	1.153	2.106
HCl	1.187	2.187

Parameter r_x^1 is the r_x cutoff values at which the molecular correlation energy equals to the full CCSD correlation energy, r_x' is the r_x cutoff values at which the molecular correlation energy reaches it's maximum absolute value.

Table C.4 The turning point r_x cutoff values of the interaction energies and minimum point r_x cutoff values of the complexes correlation energies in Bohr

	r_x^1	r_x'
$(NH_3)_2$	2.737	4.617
$(HF)_2$	2.494	3.443
$(H_2O)_2$	2.688	4.049
$NH_3\cdots F_2$	2.541	4.434
$C_2H_2\cdots ClF$	2.853	6.300
$HCN\cdots ClF$	2.764	5.816
$CH_4\cdots Ne$	3.230	4.920
$CH_4\cdots Ar$	3.654	4.922
$(CH_4)_2$	3.533	4.934
$(C_2H_2)_2$	3.471	5.755
$(C_2H_4)_2$	3.297	5.895

Parameter r_x^1 is the r_x cutoff values at which the complex correlation energy equals to the full CCSD correlation energy, r_x' is the r_x cutoff values at which the complex correlation energy reaches it's maximum absolute value.